CHARACTERIZATION OF BACTERIA HAVING HEAVY METAL REMEDIATION POTENTIAL FROM CONTAMINATED SOIL OF CHANGKI, NAGALAND

THESIS SUBMITTED IN PARTIAL FULFILMENT
OF THE REQUIREMENTS FOR THE DEGREE OF
DOCTOR OF PHILOSOPHY

By

Mr. Bhagyudoy Gogoi

Ph.D. Regd. No. Ph.D./EVS/00356 w.e.f. 30/08/2019

Department of Environmental Science
School of Sciences, Nagaland University
Lumami-798627
Nagaland, India

February, 2026

CHARACTERIZATION OF BACTERIA HAVING HEAVY METAL REMEDIATION POTENTIAL FROM CONTAMINATED SOIL OF CHANGKI, NAGALAND

BY

Mr. Bhagyudoy Gogoi

and

Dr. Pranjal Bharali

(Supervisor)

Submitted

In Partial Fulfilment of the Requirements for the Degree of

Doctor of Philosophy

In

ENVIRONMENTAL SCIENCE

Of

NAGALAND UNIVERSITY

Dedication

*This thesis is dedicated to my Dear Father **Late P. K. Gogoi**, my beloved Mother **Mrs. Janoki Saikia Gogoi**, caring sister **Mrs. Sangeeta Gogoi Gohain**, my brother **Mr. Ved Prakash Gogoi** and my beloved wife **Mrs. Pritishmrita Gogoi**, along with my both nephew **Ayan** and **Aryan** and entire family for their love, endless support and encouragement.*

"Thank you, father, for always believing in me and mother for always supporting me".

नागालैण्डविश्वविद्यालय
NAGALAND UNIVERSITY
(संसदद्वारापारितअधिनियम1989, क्रमांक35केअंतर्गतस्थापितकेंद्रीयविश्वविद्यालय)
(A Central University established by an Act of Parliament No.35 of 1989)
मुख्यालय : लुमामी, जिला : जुन्हेबोटो (नागालैण्ड), पिनकोड –798627
Hqrs: Lumami, Dist. Zunheboto (Nagaland), Pin Code – 798627
वेबसाइट / Website : www.nagalanduniversity.ac.in

Dr. Pranjal Bharali
Assistant Professor
Department of Environmental Science
e-mail: bharalip@nagalanduniversity.ac.in

CERTIFICATE

This is to certify that the thesis entitled **"*Characterization of Bacteria having Heavy Metal Remediation Potential from Contaminated Soil of Changki, Nagaland*"** is an original research work carried out by Mr. Bhagyudoy Gogoi under my supervision. This thesis is being submitted to the School of Sciences, Nagaland University, in partial fulfilment of the requirements for the award of degree of Doctor of Philosophy in Environmental Science. The matter embodied in this thesis has not been previously submitted to any University/Institution for any other degree or diploma.

All assistance and help received during the entire course of doctoral research has been duly acknowledged.

Date:
Place: Lumami, Nagaland

(Dr. Pranjal Bharali)
Supervisor

नागालैण्ड विश्वविद्यालय
NAGALAND UNIVERSITY
(संसद द्वारा पारित अधिनियम 1989, क्रमांक 35 के अंतर्गत स्थापित केंद्रीय विश्वविद्यालय)
(A Central University established by an Act of Parliament No.35 of 1989)
मुख्यालय : लुमामी, जिला : जुन्हेबोटो (नागालैण्ड), पिनकोड – 798627
Hqrs: Lumami, Dist. Zunheboto (Nagaland), Pin Code – 798627
वेबसाइट / Website : www.nagalanduniversity.ac.in
DEPARTMENT OF ENVIRONMENTAL SCIENCE

DECLARATION

I, **Mr. Bhagyudoy Gogoi**, bearing Ph.D. Registration No. Ph.D./EVS/00356 with effect from 30th August, 2019 hereby declare that the work presented in this thesis entitled **"*Characterization of Bacteria having Heavy Metal Remediation Potential from Contaminated Soil of Changki, Nagaland*"** in partial fulfilment of the requirement for the award of the degree of Doctor of Philosophy in Environmental Science, submitted to School of Sciences, Nagaland University, Lumami, Nagaland is an authentic record of my research work under the supervision of Dr. Pranjal Bharali, Department of Environmental Science, Nagaland University.

I also declare that the work embodied in the present thesis is my original work and has not been submitted to any other University/Institute for any other degree or diploma.

Date:
Place: Lumami, Nagaland

(Bhagyudoy Gogoi)
Candidate

(Assoc. Prof. Latonglila Jamir)
Head
Department of Environmental Science
Nagaland University

(Dr. Pranjal Bharali)
Supervisor

नागालैण्ड विश्वविद्यालय
NAGALAND UNIVERSITY
(संसद द्वारा पारित अधिनियम 1989, क्रमांक 35 के अंतर्गत स्थापित केंद्रीय विश्वविद्यालय)
(A Central University established by an Act of Parliament No.35 of 1989)
मुख्यालय : लुमामी, जिला : जुन्हेबोटो (नागालैण्ड), पिनकोड – 798627
Hqrs: Lumami, Dist. Zunheboto (Nagaland), Pin Code – 798627
वेबसाइट / Website : www.nagalanduniversity.ac.in
DEPARTMENT OF ENVIRONMENTAL SCIENCE

COURSE WORK COMPLETION CERTIFICATE

This is to certify that Mr. Bhagyudoy Gogoi, a registered Research Scholar for a Ph.D. (Science) degree in Environmental Science under Nagaland University, bearing Registration No. Ph.D./EVS/00356 has satisfactorily completed all the courses offered in the Pre-Ph.D. Coursework Programme in the Department of Environmental Science, Nagaland University, Hqrs. Lumami.

The course includes:

ESP01 Research Methodology

ESP02 Literature Review and Report Writing

ESP05 Environmental Biology

(Assoc. Prof. Latonglila Jamir)
Head
Department of Environmental Science
Nagaland University

Sl. No. : 20- 9706

NAGALAND UNIVERSITY

STATEMENT OF MARKS

Ph. D COURSE WORK EXAMINATION 2021

DEPARTMENT OF ENVIRONMENTAL SCIENCE

The following are the marks secured by ***Bhagyudoy Gogoi***
Roll No . **04** *of Ph.D Course Work Examination held in* **2021**

Subject(s)/Paper(s)	Max. Marks	Minimum Qualifying Marks	Marks Secured
Paper No. ESP01	100	35	**62**
Paper No. ESP02	100	35	**75**
Paper No. ESP05	100	35	**72**
Total Aggregate Marks			**209**
Average Pass Mark – 55 %			

Result	Division	Percentage
Passed	**I Division**	**69.66%**

Marks compared by

NAGALAND UNIVERSITY HQRS : LUMAMI

COE/Asstt. Reg.(AR (Exams)

Asstt. Registrar (Exams)
Nagaland University
Hqrs. Lumami

NAGALAND UNIVERSITY

HEAD QUARTERS : LUMAMI

Ph. D COURSE WORK EXAMINATION

This is to certify that Mr/Ms BHAGYUDOY GOGOI

of Nagaland University bearing Roll No. 04 *is qualified in the Ph.D Course Work Examination*

in the Department of ENVIRONMENTAL SCIENCE *Nagaland University held in the Year* 2021

विभागाध्यक्ष / Head
पर्यावरण विज्ञान विभाग
Department of Environmental science
नागालैण्ड विश्वविद्यालय / Nagaland University
लुमामी / Lumami- 798 627
Head of Department

Dean
School of Sciences
Nagaland University
Hqrs. Lumami Nagaland

Sl.no. 00356

NAGALAND UNIVERSITY
नागालैण्ड विश्वविद्यालय

(A Central University Established by the Act of Parliament of India 1989)
Headquarters: Lumami मुख्यालय: लुमामी

Ph.D. Admission cum Registration Certificate

This is to certify that

Mr. /Mrs. /Ms. Bhagyudoy Gogoi *has been registered for research works leading to the Degree of Doctorate of Philosophy in Nagaland University*

Under the Supervision of Prof. / Dr. Pranjal Bharali

Co- Supervisor Prof. / Dr. _____

Department of Environmental Science

His / Her Registration number is PhD/EVS/00356

With effect from 30/8/2019

Date 19/5/2022

NAGALAND UNIVERSITY H.Q. LUMAMI

Dy. / Asst. Registrar (Acad)

Deputy Registrar (Acad)
Nagaland University
Headquarters : Lumami

नागालैण्ड विश्वविद्यालय
NAGALAND UNIVERSITY
(संसद द्वारा पारित अधिनियम 1989, क्रमांक 35 के अंतर्गत स्थापित केंद्रीय विश्वविद्यालय)
(A Central University established by an Act of Parliament No.35 of 1989)
मुख्यालय : लुमामी, जिला : जुन्हेबोटो (नागालैण्ड), पिनकोड – 798627
Hqrs: Lumami, Dist. Zunheboto (Nagaland), Pin Code – 798627
वेबसाइट / Website : www.nagalanduniversity.ac.in
DEPARTMENT OF ENVIRONMENTAL SCIENCE

Plagiarism Self Declaration Certificate

Name of the Research Scholar	Mr. Bhagyudoy Gogoi
Ph.D. Registration Number	Ph.D./EVS/00356 with effect from 30/08/2019
Title of the Ph.D. thesis	Characterization of Bacteria having Heavy Metal Remediation Potential from Contaminated Soil of Changki, Nagaland
Name and Institutional address of the supervisor	Dr. Pranjal Bharali Department of Environmental Science, Nagaland University, Lumami
Name of the Department and School	Department of Environmental Science, School of Sciences
Date of submission	09-02-2026
Date of Plagiarism check	05-02-2026
Percentage of similarity detected by the DRILLBIT software	3 %

I hereby declare/certify that the Ph.D. Thesis submitted by me is complete in all respect, as per the guidelines of the UGC/NU for this purpose. I also certify that the thesis has been checked for plagiarism using DrillBit similarity check software. It is also certified that the contents of the electronic version of the thesis are the same as the final hardcopy of the thesis. Copy of the Report generated by the software is also enclosed.

Date: **Bhagyudoy Gogoi**

Place: Lumami, Nagaland Name and Signature of the Scholar

DrillBit

The Report is Generated by DrillBit Plagiarism Detection Software

Submission Information

Author Name	Bhagyudoy Gogoi
Title	CHARACTERIZATION OF BACTERIA HAVING HEAVY METAL REMEDIATION POTENTIAL FROM CONTAMINATED SOIL OF CHANGKI, NAGALAND
Paper/Submission ID	5229802
Submitted by	bharalip@nagalanduniversity.ac.in
Submission Date	2026-02-05 16:18:56
Total Pages, Total Words	161, 42902
Document type	Thesis

Result Information

Similarity **3 %**

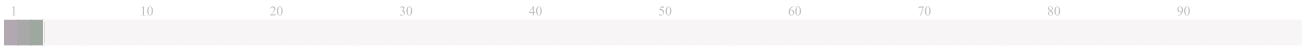

Sources Type

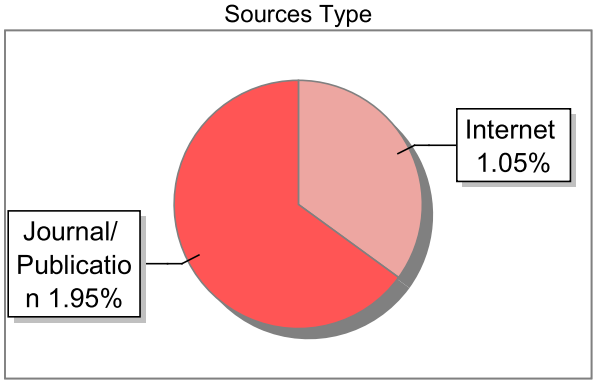

Report Content

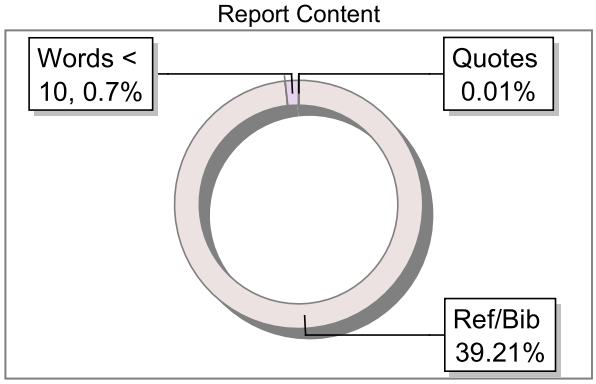

Exclude Information

Quotes	Excluded
References/Bibliography	Excluded
Source: Excluded < 10 Words	Excluded
Excluded Source	**0 %**
Excluded Phrases	Not Excluded

Database Selection

Language	English
Student Papers	Yes
Journals & publishers	Yes
Internet or Web	Yes
Institution Repository	Yes

A Unique QR Code use to View/Download/Share Pdf File

DrillBit

DrillBit Similarity Report

3	39	A
SIMILARITY %	MATCHED SOURCES	GRADE

A-Satisfactory (0-10%)
B-Upgrade (11-40%)
C-Poor (41-60%)
D-Unacceptable (61-100%)

LOCATION	MATCHED DOMAIN	%	SOURCE TYPE
1	biomedcentral.com	<1	Internet Data
2	academicjournals.org	<1	Publication
4	moam.info	<1	Internet Data
5	Grafted thermo-responsive gelatin microspheres as delivery systems in by Manuel-2010	<1	Publication
7	Thesis Submitted to Shodhganga Repository	<1	Publication
8	Isolation of Cr(VI) reducing bacteria from industrial effluents and their potent by Ahme-2009	<1	Publication
9	researchspace.ukzn.ac.za	<1	Publication
12	independent.academia.edu	<1	Internet Data
13	moam.info	<1	Internet Data
14	Enhanced fermentative lactic acid production from source-sorted organic household waste Focusing o, by Zhang, Zengshuai, Yr-2022	<1	Publication
19	www.dx.doi.org	<1	Publication
21	Thesis Submitted to Shodhganga Repository	<1	Publication

23	SAMHD1 controls innate immunity by regulating condensation of immunogenic self RNA, by Maharana, Shovamayee, Yr-2022	<1	Publication
24	scholarworks.umass.edu	<1	Publication
25	Thesis submitted to shodhganga - shodhganga.inflibnet.ac.in	<1	Publication
28	Evaluation of released malathion and spinosad from chitosanalginategelatin cap by Taktak-2016	<1	Publication
30	bmcmicrobiol.biomedcentral.com	<1	Publication
31	Enhancement of nutritional value and storage stability of silver carp surimi in, by Ferdous, Mst Jannatul, Yr-2025	<1	Publication
32	moam.info	<1	Internet Data
36	Optimization of Lactobacillus fermentum DSM 20049 Growth on Whey and L by Hanoune-2015	<1	Publication
37	Polarization-dependent laser autofluorescence of the polycrystalline networks of by Prysyazhnyuk-2016	<1	Publication
38	springeropen.com	<1	Internet Data
40	www.ncbi.nlm.nih.gov	<1	Internet Data
41	www.science.gov	<1	Internet Data
42	epubs.icar.org.in	<1	Publication
44	www.mdpi.com	<1	Publication
45	ejbpc.springeropen.com	<1	Publication
46	Thesis submitted to shodhganga - shodhganga.inflibnet.ac.in	<1	Publication
47	www.ncbi.nlm.nih.gov	<1	Internet Data

48	Effect of Helicobacter pylori biofilm formation on susceptibility to amoxicillin by Yonezawa-2019	<1	Publication
49	ijpsr.com	<1	Publication
50	moam.info	<1	Internet Data
51	Possible Participation of Superoxide Anion in the Intestinal Tryptophan 2,3-Dio, by Hirata, Fusao, Yr-1971	<1	Publication
52	Thesis Submitted to Shodhganga Repository	<1	Publication
53	bjid.org.br	<1	Internet Data
54	Conversion of post consumer polyethylene to the biodegradable polymer polyhydrox by Guzik-2014	<1	Publication
55	e-algae.org	<1	Internet Data
57	Thesis Submitted to Shodhganga Repository	<1	Publication
58	www.emerald.com	<1	Internet Data

ACKOWLEDGEMENT

First and foremost, I am grateful to my Father **Late Mr. Purna Kanta Gogoi** and **Mrs. Janoki Gogoi** for bringing me to this world and my Family for being my strength. Next, I thank God for your constant support and blessings in every walk of life. I also wholeheartedly thank my Supervisor **Dr. Pranjal Bharali** for his guidance, constant feedbacks and motivation. Further, I would like to thank the former, Head of Department, **Prof. Asthutosh Tripathi** for his guidance and motivation. I would also like to thank **Assoc. Prof. Latonglila Jamir (HOD)** for her motivation and support.

I am also grateful to the all the faculty members of **Department of Environmental Science**, **Nagaland University**, for providing the necessary facilities and resources and insightful suggestions. My two friends (**Shiva** and **Samson**) for your constant support through the PhD tenure. My sincere thanks to my lab mates and fellow research scholars for their support, insightful discussions, and cooperation.

I would like to express my gratitude to the

1. Nagaland University, Lumami
2. Department of Chemistry, Nagaland University
3. Department of Botany, Nagaland University
4. Department of Zoology, Nagaland University
5. Department of Chemical Science and Department of Molecular Biology and Biotechnology, Tezpur University
6. CSIR-North East Institute of Science and Technology (NEIST), Jorhat, Assam
7. Department of Environmental Science, Bharathiar University, Coimbatore.
8. Centre for Nanoscience & Nanotechnology, International Research Centre Sathyabama Institute of Science and Technology, Chennai
9. NERIWALM, Tezpur
10. AIIMS, Delhi

I would like to thank the UGC, Govt of India, for providing fellowship during this work.

Date

(Bhagyudoy Gogoi)
Department of
Environmental Science
Nagaland University

CONTENTS

Chapter 3

3. Materials and Methods

Chapter 4

4. Results

Chapter 5

5. Discussions

Chapter 6

LIST OF FIGURES

LIST OF TABLES

ABSTRACT

of

CHARACTERIZATION OF BACTERIA HAVING HEAVY METAL REMEDIATION POTENTIAL FROM CONTAMINATED SOIL OF CHANGKI, NAGALAND

Thesis submitted in partial fulfillment of the requirements for the award of Degree of Doctor of Philosophy in Environmental Science

Submitted by

Bhagyudoy Gogoi

Ph.D. Regd. No. Ph.D./EVS/00356 w.e.f. 30/08/2019

DEPARTMENT OF ENVIRONMENTAL SCIENCE

SCHOOL OF SCIENCES, NAGALAND UNIVERSITY

LUMAMI-798627, NAGALAND

INDIA

2026

ABSTRACT

Currently, the seriousness of heavy metal (HM) pollution has spanned globally, causing serious health hazards in all living organisms, whether of anthropogenic release or natural origin. Through the advent of industrialization, modern machinery has released loads of HMs such as arsenic (As), cadmium (Cd), lead (Pb), mercury (Hg), and chromium (Cr) into the various environmental matrices through different industrial effluents. Prolonged exposure to contaminated water, soil, and even air imparts detrimental effects on a wide array of flora and fauna, including humans and even microorganisms. These toxic HMs further reduce soil fertility, alter the physical and chemical properties of the environmental matrices, and affect the microbial balance and biodiversity. There is ample data on the extent of HM pollution in India. However, HM contamination in Nagaland's different environmental matrices, particularly for surface water, has been documented in a limited number of research studies that are now being published. Being persistent, non-biodegradable, and capable of transport and bioaccumulation, they have been prevalent in almost every environmental matrix and are found to be globally affecting living populations, leading to huge annual losses. Hence, remediation or control of HM pollution becomes a prerequisite for the safeguarding of the environment and achieving progressive growth and sustainable development. At present, several physicochemical-based remediation technologies are available to deal with the HM pollution. However, most of these technologies are associated with various limitations. With the advances in the understanding of bacterial systems, especially those of the HM-resistant or tolerant species, which eradicate HM pollutants in an eco-friendly manner, they have become a more promising alternative option. Additionally, bacterial-based remediation offers several advantages over conventional remediation technologies, specifically their sustainable and greener features, categorizing them as a dynamic component of current remediation technologies to combat HM pollution and safeguard the environment and public health. Most of the bacterial-based remediation techniques, however, are still in the early stages of development. In India, research on possible bacterial species with HM remediation potential is still underway, and there is a dearth of data in this field with regard to Nagaland state.

Therefore, the present study focused on exploring As HM-resistant bacteria from acid mine tailings of Changki, Nagaland, India, with the intention of studying their bioremediation potential. Based on MTC and MIC values for As HM, three potential bacterial species were selected. Two were identified as *Lysinibacillus* sp. strain AS3 and *Lysinibacillus* sp. strain AS4 through 16S rRNA sequencing, while the third was identified as *Staphylococcus equorum* strain AS11 through whole genome sequencing. As^{3+} and As^{5+} HM ions could be tolerated by strain AS3 up to concentrations of 781.25 ppm and 62,500 ppm, respectively, while strain AS4 could withstand concentrations of 1562.50 ppm and 15,625 ppm. Additionally, 781.25 ppm and 125,000 ppm of As^{3+} and As^{5+} HM ion concentrations were found to be tolerated by the AS11 strain. Further, the strains were also found to be tolerant to other HMs, Pb^{2+} and Cd^{2+} HM ions. Strain AS3 was able to tolerate Pb^{2+} and Cd^{2+} HM ions up to a concentration of 6250 ppm and 1562.50 ppm, respectively. Likewise, strain AS4 tolerates Pb^{2+} and Cd^{2+} HM ions up to 1562.50 ppm and 6250 ppm, respectively. Further, strain AS11 could tolerate up to 6250 ppm of Pb^{2+} HM ions and 48.82 ppm of Cd^{2+} HM ions. The growth kinetic studies of the bacterial strains indicate the diverse growth patterns in the presence and absence of selected HM ions. In both AS3 and AS4, an elongated lag phase was observed in the presence of As^{3+} HM ions. However, AS4 showed a similar growth pattern of As^{5+} to that of the control, unlike AS3, where As^{5+} treatment showed late exponential growth. Further, in both AS3 and AS4, an early exponential phase was observed in the presence of Pb^{2+} and Cd^{2+} HM ions. In the case of the AS11 strain, a prolonged lag phase was observed in the presence of As^{5+} and Cd^{2+} HM ions. While in the presence of As^{3+} and Pb^{2+}, the growth was not marked with a prolonged lag phase, unlike the other two strains. Further, an antibiotic susceptibility study indicated that the strain AS3 exhibited resistance to eight major antibiotics while remaining susceptible to the remaining six, whereas strains AS4 and AS11 demonstrated resistance to six antibiotics each and susceptibility to the remaining eight.

The biochemical profiling revealed that the strains were capable of producing biofilms, exopolysaccharide (EPS), and siderophores and exhibited arsenite oxidase and arsenate reductase activities in the presence of HM ions. In the case of biofilm quantification, it was observed that in the presence of As^{5+}, As^{3+} and Pb^{2+} HM ions, the

biofilm production was boosted in the AS3 strain, except for Cd^{2+} HM ions. Similar results were observed for the AS4 strain for $As^{5+}$and As^{3+} HM ions. However, in the AS4 strain, there was a lack of biofilm formation in the presence of Pb^{2+} and Cd^{2+} HM ions. However, unlike both strains, the AS11 strain showed biofilm formation only in the presence of Pb^{2+} and Cd^{2+} HM ions. In the case of siderophores, the values of quantified siderophores varied in the presence and absence of HMs in all the strains. A similar observation of reduced siderophore production in the presence of Cd^{2+} HM ions was recorded in all the strains. In the case of EPS, all the HM treatments indicated enhanced EPS production in all the strains. The presence of arsenite oxidase and arsenate reductase in all the strains was marked by the appearance of yellow and brown colouration during the addition of silver nitrate solution to 72-hour-old culture plates.

Further, scanning electron microscopy (SEM) and energy-dispersive X-ray spectroscopy (EDX) analyses revealed the presence of HM ions (As^{5+}, Pb^{2+} and Cd^{2+}) on the outer surface of the AS3, AS4, and AS11 strains. However, there was a lack of As^{3+} HM ions in all the strains, possibly due to the presence of efflux pathways or other mechanisms for detoxification of As^{3+} HM ions. Additionally, the transmission electron microscopy coupled with energy-dispersive X-ray spectroscopy (TEM-EDX) analyses of AS3 and AS4 strains indicated the accumulation of As^{5+}, Cd^{2+}, and Pb^{2+} HM ions. However, in the AS11 strain, only As^{5+} accumulation was observed, as evident from the EDX spectra. Further, the available functional groups on the cell surface of the selected strains were observed to be shifted in the Fourier transform infrared (FTIR) spectroscopy as compared to the control in the presence of the HM ions. Such alterations may be the result of their association with the metal-binding process, indicating their active involvement in the adsorption of the HM ions.

The adaptive behaviour of the selected bacterial strains in the presence of HM was further assessed by stress enzyme activity. The total protein content (TPC) in the presence of all the tested HM ions was enhanced in both the AS3 and AS4 strains, possibly due to the synthesis of proteins in response to HM stress. However, in the AS11 strain, the TPC was reduced in the presence of HM ions, possibly due to the adverse effects of the HMs on the protein synthesis process. Further, changes in the levels of superoxide dismutase (SOD), catalase (CAT), malondialdehyde (MDA), glutathione reductase (GR), and glutathione peroxidase (GPx) indicate the active

participation by the stress enzymes in all the strains to combat the oxidative stress imparted by the HM ions.

Assessment of the strains as potent bioremediating agents indicates the removal of substantial amounts of As^{5+}, As^{3+}, Pb^{2+} and Cd^{2+} HM ions by all the strains, which was determined through ICP-MS. The AS3 strain removed almost 99 to 67 % of HM ions, while AS4 removed 97 to 88 % of HM ions, and AS11 removed almost 99 to 79 % of HM ions. This indicates their effective bioremediation potential, possibly due to their ability to generate microbial metabolites and diverse inherent mechanisms that aid in the bioremediation process.

For each strain, the synthesis of ammonia and indole-acetic acid (IAA), which are essential plant growth promotion (PGP) traits, was also evaluated. The strain AS3 showed the highest production of ammonia and IAA, followed by the AS4 and AS11 strains. Though *Staphylococcus equorum* strain AS11 showed less production of both ammonia and IAA as compared to the other strains, it was found to be effective towards plant growth in the phytotoxicity assay. Thus, there is a possibility of bioprospecting the selected bacterial strain as plant growth promoters in HM-contaminated terrestrial environments.

Seed phytotoxicity assays are performed to assess the toxicity of the HMs on the germination and development of mung bean (*Vigna radiata*) seeds. The results indicated that the inclusion of bacterial strains had a stimulating effect on the growth of seedlings, whereas treatments with HMs alone had an inhibitory effect, which was observed through germination index (GI) and germination vigour index (GVI) values. Additionally, brine shrimp toxicity studies indicated the absence of mortality upon inclusion of the selected bacterial strains. When bacterial strains and HM-amended treatments were used, the mortality percentage was lower compared to HM-treated samples. The highest mortality percentages were recorded for As^{5+} HM ions, followed by As^{3+}, Pb^{2+}, and Cd^{2+}. Based on the findings, all the strains exhibit intriguing biotechnological potential for HM bioremediation, especially as plant growth supporters in environments contaminated with antibiotics and HMs.

Keywords: Heavy metal (HM), Nagaland, Bacteria, Exopolysaccharides (EPS), Stress Enzyme, Bioremediation, Phytotoxicity, Plant Growth Promotion (PGP)

Chapter 1: Introduction

1.1. *Metal*

Metal can be defined as a material that possess specific properties *viz*. mostly hard texture, shiny luster, opaque, ductile, fusible, solid, sonorous, good conductor of heat and electricity, produces cations on losing electrons, forms oxides and hydroxides, and high melting and boiling point (Ali et al., 2019). These properties are shown by all the known metals except for few *viz*., mercury (Hg) exist in liquid state at room temperature, Gallium (Ga) and Cesium (Cs) exhibit lower melting points, sodium and potassium have soft texture etc. (Greenwood and Earnshaw, 2012).

1.2. *Types of Metal*

There are different criteria for the classification of metals *viz*. based on the quantity of iron component present (ferrous-containing or without ferrous), based on atomic structure (alkaline, alkaline earth and transition metals), and based on behaviour towards magnet (ferromagnetic, paramagnetic, and diamagnetic) (Schweitzer, 2003).

1.3. *Natural Sources of Metal*

The chief natural sources for most of the metals are earth's crust and mantle (Garrett, 2000). Metals are mostly found in ore-bearing rocks. Apart from that certain metals *viz*. sodium and potassium are present in abundance in dissolved form in seawater, in the form of dust in atmosphere, and phases of rock cycle (Garrett, 2000). Further, volcanic activities and various other geological processes such as erosion, leaching, whethering etc. releases various metals including the heavy metals (HMs) into the environment matrices (Angon et al., 2024; Devy and Vasudevan, 2025).

1.4. *Role and Significance of Metals*

Metals are extensively used in electronics *viz*. gold (Au), silver (Ag), platinum (Pt), and palladium (Pd), energy storage, energy generation, construction [iron (Fe)], transportation, consumer goods [iron (Fe), copper (Cu)], and medical devices [titanium (Ti)] (Benvenuto, 2016; Cutler, 2018). Apart from their daily use in industry and household level, metals play a vital role in biological system and in therapeutics (Moustakas, 2021). Based on the requirements for body functioning, metals are classified as micronutrient metal also referred as microminerals *viz*. zinc (Zn),

manganese (Mn), copper (Cu), iron (Fe), chromium (Cr), molybdenum (Mo), cobalt (Co), selenium (Se) etc., which are required in trace quantity (< 100 mg per day) while macronutrients metals also called trace minerals *viz*. calcium (Ca), magnesium (Mg), sodium (Na), potassium (K) etc., are required in larger quantity (>100 mg per day) (Moustakas, 2021). Hypoconcentration (deficiency) and hyperconcentration (excessive) of micro- and macronutrient metals in the body of plants, animals and human are reported have major health issues (Graham, 2008; Ali and Ahirwar, 2025). Mainly metals are required by the organism for maintaining body functions *viz.*, iron (Fe^{2+}) - hemoglobin for oxygen transportation, sodium (Na^{+}) and potassium (K^{+}) gated ion channels in nerve cells, calcium (Ca^{2+}) binding with troponin C and calmodulin in muscles tissues, co-factor (Mg^{2+}) in most of the enzymatic reaction etc., and in therapeutics as medicines, supplements, manufacturing of surgical tools and prosthetic implants and several others (Peters et al., 2024). Metals in general, are vital for carrying out the important physiological processes in plants and animals, but at elevated levels, can have detrimental effects in the organisms (Ojuederie and Babalola, 2017).

1.5. *Heavy Metal*

Among the known elements, the term 'heavy metal (HM)' is generally referred as a group of naturally occurring metals whose density is relatively higher density ≥ 5 g/cm^3 compared to water, atomic number > 20, molecular weight ranges between 63.5–200.6 g/mol, exhibit the properties of metals, and exert toxicity in living beings even at ppb concentration (Cook, 1977; Tchounwou et al., 2012; Badr and El-Habit, 2018; Briffa et al., 2020). At lower concentration certain HM are vital for biological function *viz.* Fe, Cu, Zn, and Mn. However, at higher concentration they exert detrimental effect (Ohiagu et al., 2022). Other HMs including arsenic (As), cadmium (Cd), lead (Pb), mercury (Hg) and, thallium (Tl), are not associated with any biological function (Wróblewski et al., 2025). However, some of these toxic HMs have been reported to be associated with severe health implication in humans (Wróblewski et al., 2025).

1.6. *Sources of HMs*

The general sources of HMs are released mostly to industrial and diverse anthropogenic activities (Oladimeji et al., 2025). A number of industrial discharges originating from mining, natural gas, paper, coal, dyes and several others have been contaminating the environmental matrices with traces of HMs such as Hg, Cu, Cd, Pb and even As (Karn et al., 2021; Oladimeji et al., 2024). In general, the HM As mostly originates from pesticides, wood preservatives or volcanic eruptions (Gomez-Caminero et al., 2001; Garelick et al., 2008). Further, Pb occurs mostly due to firing ranges, battery industries and cosmetics (Laidlaw et al., 2017; Mathur and Chauhan, 2018; Alasmary, 2025). Another HM, Cd can originate even from cigarettes as well as plastics production and nickel-cadmium (Ni-Cd) battery manufacturing (Khan et al., 2022). Likewise, Hg occurs mostly as toxic methyl mercury coal-fired power plants, pulp and paper industries, mining and smelting activities as well weathering of Hg-containing rocks (Sundseth et al., 2017; Pavithra et al., 2023). Similarly, yet another toxic HM, Cr causing significant health hazard, is often found in steel industries, tanning of leather as well as dye industries (Zhitkovich, 2011; Hausladen et al., 2018; Liu et al., 2025). Overall, both anthropogenic and natural sources contribute to the release of HMs into the environment (Oladimeji et al., 2025).

1.7. *HM Pollution*

UNEP (United Nations Environment Programme) defines HM pollution as the release of HMs into environment at levels which become harmful to humans and ecosystems (UNEP, 2025). WHO (World Health Organization) also defines HMs as naturally occurring substances causing harm to environment and living beings at elevated concentrations (Rajkumar et al., 2023). In recent years, HM pollution has become a global environmental challenge affecting human health significantly (Rajendran et al., 2022). Thus, active research pertaining to HM pollution is crucial to reducing HM pollution at a global level (Bayraktar et al., 2022). Among the extensive array of HMs, five are identified as the most detrimental, commonly termed the 'five big evils': As, Cd, Pb, Hg, and Cr. Their chemistry is defined by fluctuating oxidation states, elevated reactivity, and a propensity to generate stable complexes with both organic and inorganic ligands (Alloway, 2012).

1.8. *Eco-toxicity of HMs*

HMs become toxic to living organisms as they enter the living body through air, water or food and bind specifically with the cellular components, displacing metal ions in proteins and enzymes, thereby damaging the structures and vital physiological functions (Wu et al., 2016). This induces an oxidative damage or stress, with generation of reactive oxygen species (ROS), damage to deoxy ribonucleic acid (DNA) or cellular membranes (Mansoor et al., 2023). HMs can also bind with sulphydryl (–SH) groups in enzymes and can also affect the antioxidant molecules like glutathione and damage the defense system of living organisms (Ajsuvakova et al., 2020; Abd Elnabi et al., 2023). Further, HMs being persistent in environment, also accumulate in different tissues and biomagnified in trophic levels increasing their toxicity (Almashhadany et al., 2024; Saidon et al., 2024).

Some of the negative impacts of HMs on plants include the decrease of seed germination and lipid content by Cd, decreased enzyme activity and plant growth by Cr, the inhibition of photosynthesis by Cu and Hg, the reduction of seed germination by Ni and the reduction of chlorophyll production and plant growth by Pb (Gardea-Torresdey et al., 2005).

Generally, damages to vital organs like liver, kidneys, heart, lungs are often associated with exposure to HMs (Yu et al., 2023; Azeh Engwa et al., 2019). The damages to the nervous system, resulting in cognitive, behavioural or motor functions are also observed with HMs (Abd Elnabi et al., 2023). They can weaken the immune system, or even cause chronic reproductive toxicity, result in developmental defects or even cancer through damages to DNA or cell functioning (Abd Elnabi et al., 2023).

1.9. *Types of HM Remediation*

Remediation of habitats contaminated by HMs is an important global issue due to the severity of their effects. With different degrees of achievement, substantial research has been done over several decades to find a simple, effective, and affordable way to remove HMs. The most commonly used conventional mechanisms for the removal of these HMs are physico-chemical approaches (including chemical precipitation, ion exchange, ion flotation, coagulation, flocculation, photocatalysis, electrodialysis, hydrogel, membrane separation etc.), adsorption (through activated

carbon, carbon nanotube, agricultural wastes etc.), and electrochemical approaches (including electroflotation, electrocoagulation, and electrodialysis) (Fig. 1).

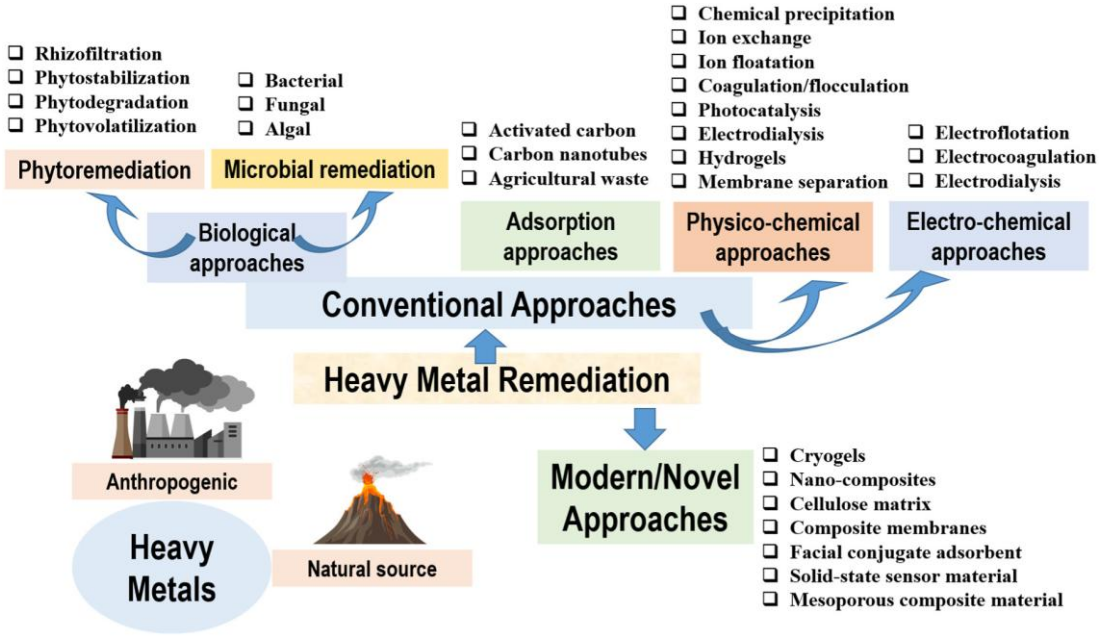

Figure 1. Different technological approaches to remediate HM pollution

Apart from the physico-chemical based remediation approaches, biological remediation, especially those that use microorganisms (bacteria, fungi, algae etc.) and plants (rhizofiltration, phytostabilization, phytodegradation, phytovolatization etc.), have drawn interest as sustainable, economical, and environmentally beneficial substitutes (Khalil and Hassan, 2024; Khalifa et al., 2025). Recently, several novel approaches *viz*. cryogel, nano-composites, cellulose matrix, composite membrane, facial conjugate adsorbent, solid-state sensor material, mesoporous composite material etc. have been devised and are in use to enhance the sequestration of HM pollutant from different environmental matrixes.

1.10. *Limitations with HM Remediation Technologies*

In recent years, the removal of toxic HMs from different environmental matrixes poses a great challenge. Because of the toxicity and persistence in nature, the levels of HMs in the environment need to be controlled by mandating waste treatment at the sources of pollution (Hidayati et al., 2014). Traditionally, HMs are treated by chemical precipitation methods, ion exchange method, electro-winning, electro-

coagulation, cementation process *via* electrochemical mechanism, reverse osmosis and electro-dialysis etc., which are not completely capable of reducing the HMs concentration to a level required by environmental legislation. Moreover, these technologies have several limitations, including labour intensive, high sludge generation, low removal efficiency, and high-energy consumption (Shrestha et al., 2021). The common problems associated with such approaches are their high operational costs and generation of bulk quantity of toxic sludge that makes secondary problems or secondary pollution risks (Vijayanand and Divyashree, 2015; Fu and Wang, 2011). Due to such major downsides, conventional approaches need to be replaced or searching more alternatives with practical, cost-effective, and environmentally benign features. Among the available treatment technologies, bioremediation-based techniques are getting more attention because they are economically viable, effective, and environmentally compatible (Wuana and Okieimen, 2011; Vijayanand and Divyashree, 2015). Bioremediation is the use of organisms or their bioactive molecules to break down or immobilized and thereby detoxify hazardous chemicals in the environment (Obayori et al., 2009). It plays a major role in making the environment clean from pollutants and contamination (Vullo et al., 2008; Karnwal and Bhardwaj, 2014). Bio-based approaches *viz*. rhizofiltration, phytostabilization, phytodegradation, phytovolatization etc. are even though ecologically benign but quite slower, sensitive to physical parameters such as pH, temperature and presence of toxicants (Gadd, 2010). Thus, the employment of integrated approaches often paves a way for tackling HM pollution. Moreover, strict guidelines for methods of remediation or rehabilitation have been set out by authorities to prevent the spread of pollutants to the surrounding environment.

1.11. *Efficacy of Microbial based Remediation Technologies (MBRT)*

The advent of MBRT which includes the practice of employing bacteria, fungi, and algae, has unmasked a sustainable approach for remediation of HM polluted environments. It utilizes the inherent ability of microorganisms to interact with metal ions through mechanisms like biosorption, a rapid passive binding of metals on microbial surfaces; bioaccumulation, an active transportation of metals intracellularly using metal binding proteins (MBPs); biotransformation, an enzymatic conversion of

metals into less toxic and mobile forms such as the reduction of Cr(VI) to Cr(III) by bacteria; biomineralization, a precipitation of metals as insoluble minerals thereby reducing bioavailability and several other biological system based physico-chemical processes (Jin et al., 2018; Tang et al., 2024). These technologies are quite ecologically benign, cost-effective and often used as an alternative to conventional remediation technologies (Jin et al., 2018). However, their applications are also influenced by environmental factors such as pH, temperature, nutrient availability, and metal toxicity, which can limit large-scale or rapid applications (Tang et al., 2024).

1.12. *Bacterial based Remediation Techniques of HMs*

Bacteria have persistently evolved in response to HM exposure, thereby acquiring resistance to various HMs through several mechanisms including metal resistance systems (Diba et al., 2021), extracellular metal sequestration (Voica et al., 2016), biosorption (Sevak et al., 2021), reduction of heavy metal ions (Ukkund et al., 2021), and morphological alterations (Mathivanan et al., 2021). Unlike organic pollutants, bacteria cannot degrade HMs. However, the complex structure of bacteria implies that there are many ways for the metal to be taken up by the bacterial cell. In bacteria-based bioremediation techniques, bacteria remove the HMs through mechanisms like- biodegradation, biosorption, bioaccumulation, biotransformation, biomineralization, and bioleaching. Bacteria have the ability to manage the metallic contaminants through extracellular secretions such as exopolysaccharides (EPS) on their cellular surfaces (Verma et al., 2025), active binding with HM pollutants through different functional groups such as –OH, –COOH and $–NH_2$ (Igiri et al., 2018), conversion of toxic forms to less toxic forms such as conversion of As (III) to As (V) (William and Magpantay, 2023), and immobilization as insoluble precipitates (George and Wan, 2023).

As biosorbent, bacteria are of particular interest because their surface: volume ratio is often relatively high, especially in the case of non-spherical forms (Pham et al., 2022). Bacterial cell surface-mediated process such as biosorption is thought to play a key role in the immobilization and detoxification of HMs in the environment. Such natural process could be enhanced through the alteration of bacterial cell surface and immobilization (Kanamarlapudi et al., 2018). Further, *in situ* bioaugmentation of the

efficient bacterial strain seems to be more reliable instead of introducing foreign bacterial or genetically modified (GM) strain because in several instances it has been found that introduction of exotic strains severely disturbs the original integrity of the microbial diversity at the site of its application. Moreover, due to high adaptability, eco-benign nature and metabolic diversity they are often employed in HM remediation of polluted environments including soil and water (Kang et al., 2016; Tang et al., 2024; Patil et al., 2025).

Furthermore, bacterial-based remediation of HMs (As, Cd and Pb) aligns well with the framework of bioeconomy, whereby the polluted environment matrices are restored, capable of supporting agriculture and aquaculture. This technology also aligns with the sustainable development goals (SDG) such as 'Zero Hunger (SDG 2)' with improved crop productivity in HM stress areas, 'Clean Water and Sanitation (SDG 6)' through eliminating toxic HMs from the environments, 'Responsible Consumption and Production (SDG 12)' incorporating greener bioremediation, 'Life Below Water (SDG 14)' through safeguarding aquatic biodiversity from HM stress, and 'Life on Land (SDG 15)' by restoring polluted soils and ecosystems (United Nations General Assembly, 2015).

1.13. *Limitations with Bacterial-based Remediation Technologies*

Bacterial remediation systems, being effective and eco-friendly has also certain barriers that restricts its growth and significant progress. Microbes are greatly influenced by high metal toxicity, pH, nutrient deficiencies and temperature fluctuations which can affect the removal efficiency (Nnaji et al., 2023). Moreover, technologies such as biosorption often have to tackle survival of the strains, competition of the introduced strains with the native microbes, genetic stability etc., making the field application challenging (Kurniawan et al., 2022). Further, due to limited research on multi-metal and co-contaminant systems, it can also impact the effectiveness of the remediation process (Upadhyay et al., 2023). Overall, the need for enhanced microbial amendments, proper optimization and integrated techniques is necessary for proper bacterial-based HM remediation (Das et al., 2025).

1.14. *Current Scenario of HM Remediation in India and Nagaland*

HM pollution in India is accomplished through monitoring frameworks and a range of physico-chemical and biological remediation strategies, including phytoremediation and microbial remediation techniques (Mandal et al., 2014; Sodhi et al., 2022; Pande et al., 2022). With reference to coal mining in Nagaland, an estimated 4.51 km^2 of active coalfields are there in the district of Mokokchung. Majority of these coal mines are operated by open pit method and are located mostly at the immediate proximity of major rivers including Tsurang, Dikhu, Milak, Bhogdoi, Doyang etc. (Semy and Singh, 2021a). The impact of coal mining at the proximity of the rivers are expected to adversely affect the physico-chemical quality of river water with its known environmental problems such as acid mine drainage and HM leaching. Prior records of Changki indicate the presence of HMs, such as Zn, Cu and Cd, beyond the permissible limit (Semy and Singh, 2021a; 2021b). Reports have revealed the presence of harmful HMs, such as As, in naturally occurring acid mine drainage (NOAMD) (Morgante et al., 2015).

The majority of existing scientific literature primarily focuses the physicochemical alterations in various water and soil properties following HM quantification, predominantly from coal mining effected regions (Baruah et al., 2003; Jamir et al., 2011; Hussain et al., 2021; Semy and Singh, 2021a, 2021b). However, detailed investigation on the existing HM resistant/tolerant bacterioflora in the HMs contaminated environment of Nagaland are very limited.

HM-specific remediation is still insufficient in Nagaland despite the operation of effluent treatment plants and the proposal of hybrid plant-algae-microbial technology (Morung Express News, 2024; India Today NE, 2025). Currently, available studies indicate that anthropogenic activities such as mining, quarrying, and land use may be the cause of As and Pb pollution (Baruah et al., 2003; Jamir et al., 2011; Hussain et al., 2021). Moreover, As is a major pollutant in the aquifers of Nagaland and surrounding states, according to regional surveys and groundwater assessments (Goswami et al., 2023; Central Ground Water Board, 2024). Nevertheless, there are few thorough baseline data on the distribution of HMs. Thus, systematic investigation using native microbial resources is crucial for establishing effective remediation and in formulation of environmental policy.

1.15. *Aims and Objectives of the present study*

Existing scientific data clearly demonstrate the importance and necessity of a comprehensive study of the indigenous bacterioflora of Nagaland in addressing the prevailing HMs contamination. Thus, the current research was aimed at finding indigenous bacterial species resistant to selected HMs and determining their potential traits which required for achieving effective bioremediation of HM contaminated environments of Nagaland. The main objectives of the present study are as follows:

1. Isolation and characterization of bacteria resistant to heavy metal.
2. Enzyme profiling of the selected bacterial strains under heavy metal stress.
3. Determination of heavy metal accumulation in the selected bacterial strains.
4. Bioactivity of the selected bacterial strains

2.1. *Introduction*

In general, HM occurring in the environment can be due to both natural causes, *viz*., natural rock weathering, microbial leaching, volcanic eruptions, etc., and anthropogenic causes that include mining, agriculture, microplastics, and many others, as described in Table 1. However, the term 'pollution' is attributed mostly to human beings, as most anthropogenic sources exerts negative impacts on the ecosystem and biodiversity, human well-being, disruption of the environment and its services (Masindi and Muedi, 2018; Brat and Pathak, 2020; Okorondu et al., 2022).

Table 1. Different sources of environmental contamination by major HMs- As, Cd, Pb, Cr and Hg

Sl. No.	Sources of contamination	Type of HMs	Reference
1.	Mining	Pb, Cd, As	Saha and Paul (2016); Bouida et al. (2022); Sun et al. (2022); Wen et al. (2022); Qi et al. (2023)
2.	Ore smelting	Pb, Cd	Ludolphy et al. (2022); Li et al. (2023)
3.	Coal industry	Pb	Yan et al. (2022)
4.	Storage Battery industry	Pb	Kumar et al. (2022)
5.	Automobile industry	Pb	Parsoya and Perwej (2022)
6.	Metal plating industry	Pb	Khan et al. (2022)
7.	Leather tanning industry	Pb	Bouida et al. (2022)
8.	Fertilizer industry	Pb, Cd, As	Suhani et al. (2021); Khosravi-Darani et al. (2022); Rosariastuti and Astuti (2022); Su et al. (2025)

9.	Pesticide industry	Pb, As	Rani et al. (2022); Tarfeen et al. (2022); Wan et al. (2024)
10.	Pigments additive	Pb	Masri et al. (2022)
11.	Gasoline	Pb	Rubio et al. (2022)
12.	Chlor-alkali	Cd	Wu et al. (2022)
13.	Paint	Cd	Goyal et al. (2021)
14.	Copper alloys	Cd	Gujre et al. (2021)
15.	Alkaline batteries	Cd	Suhani et al. (2021)
16.	Zinc refining	Cd	Zhou et al., 2021
17.	Natural geochemical processes *viz*., natural rock weathering, microbial leaching; volcanic eruption	As, Cd, Pb	Press and Sievers (1994); Bradl (2005); Szumińska et al. (2018); Li et al. (2022); Raju (2022); Mahmoud et al. (2022); Umana et al. (2022); Li et al. (2023)
18.	Wood preservatives	As	Hassan et al. (2022)
19.	Industrial waste, Mining and Urbanization	Cr, Hg, Cd, Pb	Ondrasek et al. (2025)
20.	Geochemical and Electrical industry	Cr	Dange et al. (2024)
21.	Mining, Industrial discharge	Cr, Hg	Angon et al. (2024)
22.	Landfill leaching, Industrial effluents	Hg	Laoye et al. (2025)
23.	Agricultural Practices	Pb, Cd, As, Cr, Hg	Yu and Tsunoda (2004); Cai et al. (2012)
24.	Microplastic	Pb, Cd, As, Cr, Hg	Namim and Mahalleh (2024)

Among the 'five big evils' HMs *i.e*. As, Cd, Pb, Hg, and Cr, the present study focuses on the association of As, Cd and Pb HM ions with different bacterial systems.

The HM arsenic (As)-metalloid occurs in minerals as arsenic trioxide (As_2O_3) and in several oxidation states such as −III, 0, +III, +V (Zhu et al., 2014). In aerobic conditions, As (V) is dominant as arsenate (AsO_4^{3-}) in various protonation states including arsenic acid (H_3AsO_4), dihydrogen arsenate ion ($H_2AsO_4^-$), hydrogen arsenate ion ($HAsO_4^{2-}$), and arsenate ion (AsO_4^{3-}). Moreover, in reducing conditions, As(III) is dominant in the form of AsO_3^{3-}, and has different protonated forms *i.e.* H_3AsO_3, $H_2AsO_3^-$, and $HAsO_3^{2-}$ (Wuana and Okieimen, 2011).While, Cd often occurs as divalent Cd(II) ion, substituting Zn and causing malfunctioning of metabolic processes (Campbell, 2006). Cd can also occur as complex oxides (CdO), sulphides (CdS), or as carbonates ($CdCO_3$) (UNEP, 2022). Further, Pb predominantly occurs as divalent cation Pb^{2+}, that dissolves into soil, sediments affecting bioavailability. Further, Pb can also occur as insoluble carbonates [cerussite ($PbCO_3$)], insoluble sulphides [galena (PbS)], and lead oxides (PbO) or hydroxides [$Pb(OH)_2$] (Mishra et al., 2025). The table 2 summarizes the permissible limits of selected HMs (As, Cd and Pb) in environmental matrices, as recommended by regulatory authorities such as World Health Organization (WHO), Central Pollution Control Board (CPCB) and Bureau of Indian Standards (BIS).

Table 2. Guidelines and permissible limits for As, Cd and Pb by WHO, CPCB and BIS

Heavy Metal	WHO Guideline Value in Drinking Water	Indian Standard / Permissible Limit (Water / Wastewater / Environment)	References
Pb	0.01 mg/L	Effluent discharge (inland surface waters): 0.1 mg/L	WHO (2022); CPCB (2010); BIS (2012)
Cd	0.003 mg/L	Effluent discharge (industrial wastewater): 0.02 mg/L	
As	0.01 mg/L	Groundwater / Drinking Water (India, BIS 10500:2012): 0.05 mg/L	

The three HMs *i.e.* As, Cd, and Pb are particularly of concern because they have emerged as global contaminants due to their persistence and extensive application

in industry and agriculture (Tchounwou et al., 2012; Alloway, 2012). The global issues of As, Cd and Pb pollution persist with long term ecosystem risk, which is also mirrored in India (Table 3).

Table 3. Global status and national status of As, Cd and Pb pollution

Heavy Metal	Global Status	National Status (India)	References
As	Widespread groundwater and soil contamination in South/Southeast Asia, Latin America, and parts of Africa	Groundwater contamination hotspots in West Bengal, Bihar, Assam, and other states; drinking water contamination; chronic health risk	Smith et al. (2000); Chakraborti et al. (2013); WHO (2022)
Cd	Released from industrial activities, mining, phosphate fertilizers; persistent, bioaccumulative; reported in soils, water, crops globally	Elevated in soils near industrial zones, mining belts, battery industries; enters crops and food chain; chronic exposure risk	Alloway (2012); Tchounwou et al. (2012); Kumar et al. (2019)
Pb	Global contamination from mining, smelting, past use of leaded gasoline, paints, batteries; persists in soil, water, and air; neurotoxic	Industrial zones, urban areas, mining belts, e-waste and battery recycling areas show high Pb levels; soil, water, and air contamination; high human and environmental risk	Järup (2003); Adimalla (2020); WHO (2022)

Exposure to As, mainly *via* contaminated groundwater, is associated with carcinogenesis, dermal lesions, and developmental abnormalities (Yu et al., 2006; Tolins et al., 2014; Karagas et al., 2015). Batteries, electroplating, and fertilisers produce Cd, which builds up in crops and animals and results in bone abnormalities, renal dysfunction, and infertility (Godt et al., 2006). Pb, which is frequently found in paints, pipes, and batteries, damages the immune system, cardiovascular system, and neurological development (Needleman, 2004).

At molecular level, As can lead to the deactivation of enzymes in microorganisms (Bissen and Frimmel, 2003). Castro et al. (2015) even reported that environmentally available concentrations of As adversely affect the periphyton, which plays a significant role in the functioning of aquatic ecosystems. The association between bacteria, fungi, protozoans, algae, cyanobacteria, and diatoms confined in an extracellular matrix forms these periphytons (Sabater and Admiraal, 2005). Other HMs like Cd can damage the nucleic acids and inhibit cell division and transcription processes. Moreover, the mineralization process of carbon and nitrogen is also inhibited by Cd exposure (Sankarammal et al., 2014; Ayangbenro and Babalola, 2017). The HM Pb can denature nucleic acids as well as proteins. It can also inhibit the transcription process and the activities of different enzymes (Ayangbenro and Babalola, 2017).

Plants are often seen to be susceptible to the presence or absence of HM ions, as these can be essential micronutrients to the plants. However, increased concentrations of metal ions like- Zn, Cu, etc., or some other ions like- Hg, As, or Cd can harm the plants' metabolic activities and various studies around the world have supported the toxic effects of HMs on plants (Fernandes and Henriques, 1991; Nagajyoti et al., 2010). These potent toxic metals are seen to contaminate agricultural fields and thus are regarded as soil pollutants with both acute and chronic effects on the plants when exposed to these metals (Nagajyoti et al., 2010). As can induce damage to the plant cell membranes and inhibit plant growth, root extension, and proliferation. It can also interfere with critical metabolic processes, causing fertility, yield, and food productivity loss. Moreover, it induces oxidative stress on exposure and physiological irregularities in the plant species (Ayangbenro and Babalola, 2017). While, several researchers have reported visible injuries with Cd exposure at high concentrations with

indications of growth retardations, chlorosis or browning with root tips, and even death (Wojcik and Tukiendorf, 2004; Mohanpuria et al., 2007; Guo et al., 2008; Nagajyoti et al., 2010). Fashola et al. (2016) and Ayangbenro and Babalola (2017) have also reported nutrient reduction, chlorosis, and reduction in the germination of seeds on Cd exposure. Moreover, Cd causes inhibition of several plant enzymes (Nagajyoti et al., 2010). Further, the abundant toxic metal Pb can affect plants' growth, morphology, and photosynthetic activity (Nagajyoti et al., 2010). Pb caused inhibition in the germination of seeds in plants such as *Pinus helipensis* (Nakos, 1979) and *Spartiana alterniflora* (Mrozek and Funicelli, 1982). Pb can also inhibit early seedling growth in various plant species such as soybeans, rice, tomato, maize, eggplant, legumes, and barley (Nagajyoti et al., 2010). Moreover, the elongation of stem and roots, as well as the expansion of leaves, can be inhibited by Pb exposures in the plant species of leek (*Allium porrum* L.), barley (*Hordeum vulgare*), and even in radish (*Raphanus sativus*) (Nagajyoti et al., 2010).

HMs such as As, Cd and Pb can also be very toxic to the invertebrates in different concentrations. Lee and Kim (2008) reported in a study that As adversely affects the growth of *Eisenia fetida*, along with affecting the survival and even the reproduction of the earthworm species. A study by Button et al. (2010) reported that damage to the DNA occurred in *Lumbricus terrestris* when exposed to As in mesocosm soil. Moreover, several studies are indicative of pathological damages from As exposures (Fischer and Koszorus, 1992; Langdon et al., 2001; Wang et al., 2019). In a study by Rodriguez et al. (2013) conducted on *Eisenia foetida*, the toxic effects of Cd exposure were observed. Cd caused disturbances in the normal physiology or behaviour, and other effects such as curling, release of excess amounts of mucus, sluggish movements, coiling, and even loss of movement were observed in the earthworm. Moreover, certain histological damages, such as destruction of the cuticle, lesions, and body wall, along with bleeding, were also observed. In an another study by Muangphra and Gooneratne (2011), Cd showed acute toxicity and genotoxic effects on the earthworm (*Pheretima peguana*). Further, according to Langdon et al. (2005), Pb causes toxic effects on food uptake, behaviour, and survival of the earthworms. In another study by Žaltauskaitė et al. (2020) on the *Eisenia fetida*, it was observed that chronic Pb exposures caused a reduction in the growth rate of the earthworm.

The discussed HMs can also exert toxic effects in fishes, birds and mammals. In a study by Wang et al. (2004), cytotoxicity was observed in fish cell lines on exposure to sodium arsenite ($NaAsO_2$). In another study by Seok et al. (2007), similar effects were observed. Cases of oxidative stress and decreasing antioxidant enzyme activity were also observed in two fish species *i.e. Laoenereis acuta* and *Clarias batrachus* on exposures to As_2O_3 (Bhattacharya and Bhattacharya, 2007; Ventura-Lima et al., 2007). In case of birds, several toxic effects were reported in a study on broiler chicks by Khan et al. (2013). The birds on As exposure showed symptoms of dullness or fatigue, increased thirst, depression, and even diarrhoea. In case of mammals, in laboratory conditions along with natural habitats, rodents showed evidence of As toxicity as humoral immunity response was suppressed on As exposure (Sikorski et al., 1991; Flora and Kumar, 1996; Nain and Smits, 2012). Moreover, As was reported to inhibit the delayed hypersensitivity reaction.

In case of Cd, reports indicate sublethal effects like reduction in the growth of fishes, inhibition of reproduction, and changes in population, which occur on chronic exposures to Cd (Levit, 2010). Moreover, Cd can also act as an endocrine disruptor, as Vetillard and Bailhache (2005) reported. Further, it is seen that Palmipeds and birds are generally highly contaminated by metals such as Cd (Lock et al., 1992; Elliott and Scheuhammer, 1997). In a study, high Cd concentrations were found in the kidneys of Spectacled eiders (*Somateria fischeri*), which could cause diseases such as renal interstitium inflammation and deteriorating effects in the testes (Lucia et al., 2009). Cd can also be toxic to mammals, as evidenced by the studies of Wätjen et al. (2002). It has been reported that Cd, in C6 rat glioma cells, can cause the breakdown of the membrane potential of the mitochondria, along with the activation of the caspase-9. Furthermore, in NIH3T3 murine fibroblasts cell line, Cd was seen to induce apoptosis while overexpressing the antiapoptotic protein Bcl-2 (Wätjen et al., 2002).

In case of Pb, a study by Kim and Kang (2015) reported that aquatic animals showed fatality after bioaccumulation when exposed to lower concentrations of Pb. In another case of *in vivo* studies conducted in fishes, Pb exposures were seen to induce a significant increase in antioxidant activity *via* the production of ROS (Maiti et al., 2010; Kim and Kang, 2017; Kim et al., 2017). Moreover, a study by Gurer and Ercal (2000) showed that Pb exposures brought toxic effects on the structure of the

membrane and increased susceptibility to oxidative stress. While, in birds, a study on American robins (*Turdus migratorius*), Northern cardinals (*Cardinalis cardinalis*), and waterfowl collected from a mining area indicates that birds with Zn concentrations in their tissues showed positive cases of disruption in the biological functions, along with evident cases of Pb poisoning (Beyer et al., 2004). Additionally, the death of many mallard species like- *Anas platyrhynchos*, pintail species like- *A. acuta* and Teal like- *A. crecca* have been attributed to Pb poisoning (Grinnell, 1931). Further, various reports on Pb indicate its toxicity to humans, causing abortions in females (Rom, 1976). In another study by Jacquet et al. (1975), it was found that dietary Pb in pregnant mice resulted in reduced fertility and growth in the uterus. Moreover, Pb can even have toxic effects on the embryo and even in the foetus of rats (McClain and Siekierka, 1975). When combined, these three HMs pose a serious threat to both human health and environmental safety.

2.2. *Biological remediation of HM contaminated environment*

There are several ways through which the HM contaminant can be separated or removed from the polluted environmental matrices. Most of the available technologies are based on physico-chemical, adsorption and electrochemical approaches accompanying with both promises and limitations. Moreover, most of known technologies are site specific. Among the remediation technology, the term "bioremediation" is broad and includes the implementation of biomass, plants, bacteria, fungi, algae and other biologically generated materials (Kumar et al., 2011). The bioremediation process can be of various types depending on the type of material used, such as phytoremediation that incorporates plants; microbial remediation utilizes microorganisms, and newly adopted technologies, combining microorganisms with green composites and several others (Jin et al., 2018).

Bioremediation technique incorporating microorganisms either as dead or living biomass to remove or convert harmful contaminants, such as HMs, into less harmful substances and degrade organic materials before mineralizing them into other substances, such as water, carbon dioxide, or nitrogen gas. Microorganisms generally perform redox reactions, which affect the remediation processes by either mobilizing or immobilizing the metal pollutant (Kapahi and Sachdeva, 2019). Employing a

multitude of (*ex-* or *in-situ*) strategies, such as biosorption, bioaccumulation, bioassimilation, biomineralization, bioleaching, and biotransformation, microbes can also immobilize metals and act as metal sinks (Mosa et al., 2016; Ahemad, 2019). The diverse strategies that the microorganisms have adopted to detoxify HMs contamination are schematically represented in figure 2.

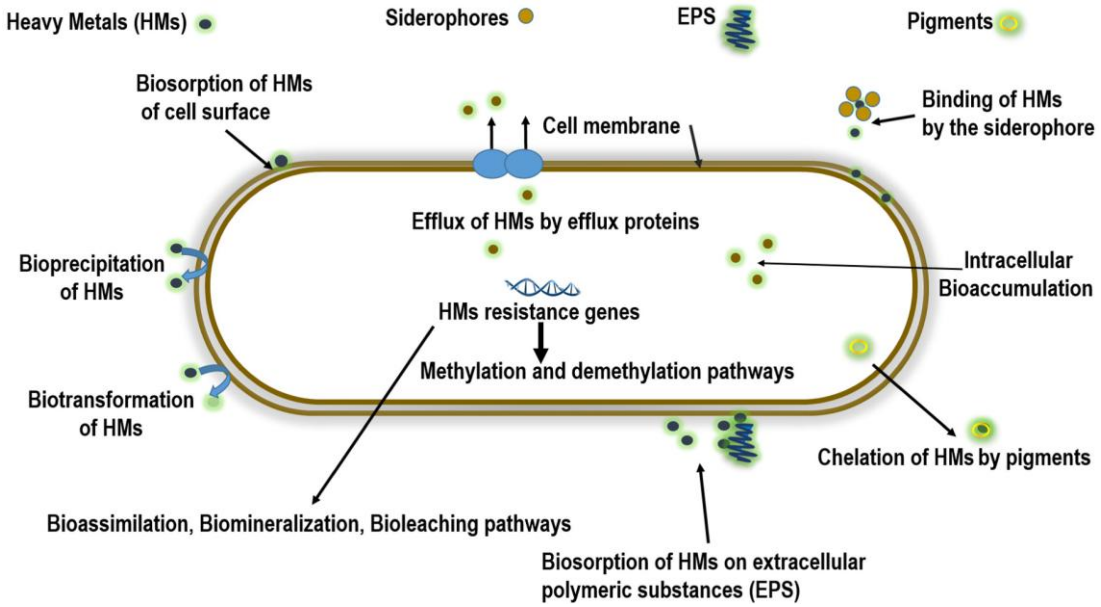

Figure 2. Mechanisms of microbial remediation of HMs

Bioremediation processes are economic and cost-effective for restoring the environment and are thus a feasible alternative solution to combat HM pollution. Further, adopting an appropriate microbial strain is crucial for both efficiency and economics. However, bioremediation-based technologies also have some limitations. These include the fact that HMs cannot be biodegraded and that in certain cases, bacteria might produce hazardous metabolites (Igiri et al., 2018). Therefore, the bioremediation strategy necessitates a comprehensive and all-encompassing methodology for systematic, achievable, and sustainable strategy that are easily adaptable to each scenario.

2.2.1. *Biological remediation utilizing bacteria*

Recent studies indicate that microbes such as bacteria have the potential to remediate environments polluted with toxic HMs such as As, Cd and Pb by different inherent mechanisms such as bacterial oxidation and reduction, secreting

exopolysaccharides (EPS), pigmentation, methylation, demethylation, presence of efflux proteins, volatilization, extrusion, formation of siderophores and several others (Gogoi et al., 2023). Thus, they have been extensively used in bioremediation systems.

Bacteria are considered as versatile and most adaptable organisms, which can readily survive in various environments including psychrophilic habitat (Gupta et al., 2023), volcanic environment surroundings (Gaidos et al., 2004), thermal vents (He and Zhang, 2016), deep oceans hydal habitat (Wu et al., 2024), space (Checinska et al., 2019), over the surface of household articles (Judah et al., 2024), edibles such as curd and cheese (Çetin et al., 2024; Chakraborty and Mandal, 2025) and even in those environment that are heavily loaded with toxic metals for instance HMs (Wang et al., 2025).

With multiple evolutions, bacterial species have inherited the capabilities to tolerate and resist toxicity to various environmental pollutants especially to hazardous HMs, which enable them to survive in hostile habitats. Such bacterial population that flourished in HM laden environments have thereby developed inherent mechanisms to resist and combat toxicity exerted by HMs (Nnaji et al., 2024).

Several bacterial genera encompassing *Pseudomonas*, *Bacillus*, *Enterobacter*, *Acinetobacter* and even *Staphylococcus* are reported to decontaminate environments polluted with HMs (Pande et al., 2022; Kelany et al., 2023; Kumar et al., 2024; Timková et al., 2024). The strains from these genera have been successful in removing As, Cd as well as Pb HMs through oxidation/reduction reactions, precipitation, immobilization using EPS (Extracellular Polymeric Substances), biofilms and even siderophores (Chien et al., 2013; Giovanella et al., 2017; Pande et al., 2022; Maity et al., 2023). Bacterial bioremediation systems have recently been discovered to be exceptionally successful in dealing with HM pollution including As, Cd, and Pb in most of the aquatic and terrestrial habitats (Yu et al., 2023; Yani et al., 2025). Bacteria such as *Lactobacillus acidophilus* (Singh and Sarma, 2010), *Acidithiobacillus ferrooxidans* (Yan et al., 2010), *Staphylococcus xylosus (*Aryal et al., 2010; 2011)*, Rhodococcus* spp. (Prasad et al., 2011), *Bacillus cereus* (Mohd Bahari et al., 2013; Titah et al., 2018) and *Arthrobacter globiformis* (Titah et al., 2018), are known to be very effective as biosorbents of As HM (Sahmoune, 2016). Also, bacterium namely

Delftia spp. BAs29 are reported to be effective in As HM polluted groundwater remediation by 'arsenite oxidation' (Biswas et al., 2019).

Bacterial species like *Enterobacter* spp. (Lu et al., 2006; Feria-Cáceres et al., 2022), *Pseudomonas aeruginosa* (Wang and Can, 2009), *Pseudomonas putida* (Shamim and Rehman, 2015; Deng et al., 2022), *Pseudomonas* spp. (Wang and Can, 2009), *Ochrobactrum anthropi* (Girawale et al., 2022), *Sphingomonas paucimobilis* (Tangaromsuk et al., 2002), *Aeromonas* spp. (Ibrahim et al., 2020), and *Staphylococcus xylosus* (Lata et al., 2019) are reported to be very proficient biosorbents in the remediation of Cd HM polluted environments. Also, bacteria such as *Clostridium thermoaceticum* can cause the bioprecipitation of toxic Cd ions (Dalei, 2014) while *Rhizobium metallidurans* can remediate Cd HM polluted environments by secreting EPS (Kowalkowski et al., 2019).

Several bacterial species such as *Bacillus firmus* (Shiomi, 2015), *Corynebacterium glutamicum* (Tiquia-Arashiro, 2018), *Enterobacter* spp. (Okpara-Elom, 2022), *Pseudomonas putida* (Gürgan et al., 2022), and *Streptomyces rimosus* (Timková et al., 2018) are found to be decent biosorbents in Pb HM polluted environments.

2.2.2. *Biological remediation utilizing fungi*

Fungi, being powerful and eco-friendly, have extensive utility in HM remediation. Their cell wall is supported by functional groups that help in binding with HM ions, enabling removal by biosorption, bioaccumulation (Refaey et al., 2021; Aslam et al., 2025). Several filamentous fungi such as *Aspergillus*, *Trichoderma*, *Penicillium* and others have shown tolerant against high concentrations of toxic HMs such as Cd, Pb, As, Hg and more (Shukla and Vankar, 2014; Govarthanan et al., 2017; Ghosh et al., 2023). Several studies have reported utility of fungi in combatting HM remediation and the same is presented in Table 4.

Table 4. HM remediation studies with fungi

No.	Fungus	Heavy Metal(s) Removed / Tested	Key Findings (Metal Removal / Tolerance)	Reference

1.	*Aspergillus niger*	Zn, Hg, Pb, Cd, Co, As, Cr etc.	100 % removal of Zn(II), 83.2 % Hg(II), 71.4 % Co(II), 59.0 %, Pb(II)	Acosta-Rodríguez et al. (2018)
2.	*Aspergillus niger, Aspergillus fumigatus, Penicillium rubens*	Cd, Cr	Bioaccumulation efficiency up to ~ 98% for Cd	Khan et al. (2019)
3.	*Trichoderma viride; Aspergillus terreus; Aspergillus flavus; Phanerochaete chrysosporium*	Pb, Cd, Cr, Ni	Some isolates removed Pb up to ~ 59.67 mg/g biomass; Cd uptake ~ 16.25 mg/g biomass	Joshi et al. (2011)
4.	*Fusarium verticillioides; Fusarium oxysporum; Aspergillus fischeri; Epicoccum mackenziei*	Zn, Pb, Cd, Cr, Cu, Ni, Co	Highest uptake recorded: 8.31 mg/g for Zn by F. *verticillioides*	Amin et al. (2024)
5.	*Serendipita indica*	As(V)	> 98 % removal of As	Shukla et al. (2025)
6.	*Talaromyces* spp. KM-31	As(V)	achieved up to ~ 96 % removal of As(V)	Nam et al. (2019)

2.2.3. *Biological remediation utilizing algae*

A wide array of micro- and macroalgae have showed strong potential for bioremediation of As, Cd and Pb, due to their ability to adsorb these HMs on the cellular surface and detoxify them through sequestration by phytochelatins and metallothioneins (Leong et al., 2020). A number of mechanisms like ion-exchange, surface binding, redox-based detoxification etc. are utilized by algae and makes them affordable and eco-friendly (Sarma et al., 2024). Various studies highlighted the utility of algae in HM remediation and the same is mentioned in Table 5.

Table 5. HM remediation studies with algae

No.	Alga (type)	Metal(s) studied	Key findings	Reference
1.	*Chlorella vulgaris* (Microalga)	As (III)	High As(III) uptake; optimized conditions gave up to ~93 % removal	Ghayedi et al. (2019)
2.	*Chlorella vulgaris* (bio-composite CV-nZVI)	As(III)	Chlorella-supported nanoscale zero-valent iron composite removed ~99 % As(III)	Yue et al. (2023)
3.	*Scenedesmus obliquus* (Microalga)	Cd^{2+}	Efficient Cd removal (≥ 95 % at ≤ 0.5 mg/L) *via* biosorption and bioaccumulation	Xu et al. (2024)
4.	*Scenedesmus incrassatulus* (Microalga)	Cd^{2+}, Cr(VI), Cu^{2+}	Continuous-culture removal; removal percentages 25–78 % depending on metal and conditions (older but relevant methodology).	Pena-Castro et al. (2004)
5.	*Chlorella vulgaris*	Co^{2+}	96.44 % removal in cell-free supernatant, when combined with amine-functionalized $MgFe_2O_4$ nanoparticles	Fóris et al. (2025)

6.	*Chlorella Sorokiniana*	As(III)	89 % removal with 0.5 g/L composite containing 60 % microalgae + 12 % kaolin + 28 % $FeCl_3$	Tabatabaei et al. (2025)

2.2.4. *Biological remediation utilizing plants*

Plants play a pivotal role in bioremediation of HMs through numerous mechanisms like- phytoextraction, which involves uptake of metal in shoots, phytostabilization involving immobilizing metals in roots, phytovolatilization and Rhizofiltration (Nedjimi, 2021; Kafle et al., 2022). Hyperaccumulator plants like *Pteris vittata* (Prabhu et al., 2019), *Brassica juncea (*Kaur et al., 2025), *Helianthus annuus* (Chauhan and Mathur, 2020), *Vetiveria zizanioides* (Mabaso et al., 2025) and others can efficiently remove HMs such as As, Cd, Pb, Zn, Ni and Cr from different environmental matrices. This type of remediation is economic as well, with suitability for larger areas, however slower than other techniques (Lavanya et al., 2024). Studies reporting HM remediation by plants are discussed in Table 6.

Table 6. HM remediation studies with plants

No.	Plant Species	HMs Targeted	Key Findings	Reference
1.	*Pteris vittata* (Chinese brake fern, arsenic hyperaccumulator)	As	Accumulates up to 22,630 mg/kg dry weight	Wang et al. (2002)
2.	*Pteris cretica*, *Spinacia oleracea* L.	As	88 % removal rate	Kama et al. (2025)
3.	*Avera javanica, Portulaca oleracea, Tephrosia nubica, Dipterygium glaucoma, Tetraena coccinea, Fagonia indica, Eleusine*	Cr, Zn, Mn, Co, Ba, Fe, Al, and Pb	The BCF(Bioconcentration Factor) values of the studied HMs reduced in the order of Cr > Zn > Mn > Co > Ba > Fe > Al > Pb	Alghamdi et al. (2024)

	indica, Cenchrus ciliaris, and Pennisetum divisum			
4.	*Rosa gallica*	Pb, Ni, Cd, and Zn	High levels of HMs in plant tissues rather than soil	Esringu et al. (2015)
5.	*Helianthus annuus* L.	Cd and Pb	Malic acid and tartaric acid assisted removal of Cd and Pb	Niu et al. (2025)

2.3. *Role of stress biomarkers in HM remediation in bacteria*

HMs impose on exposure to living organisms, lead to generation of reactive oxygen species (ROS) and the cells thereby respond to changing levels of superoxide dismutase (SOD), catalase (CAT), glutathione reductase (GR), glutathione peroxidase (GPx) and also by generating malondialdehyde (MDA) as lipid peroxidation product. SOD in general catalyzes the dismutation of superoxide ($O_2^{\bullet-}$) radical to hydrogen peroxide (H_2O_2). The changing upregulation or reduction in SOD levels act as a defensive barrier against HM stress (Mansoor et al., 2023). Catalase decomposes H_2O_2 into water and oxygen, thereby restricting the formation of hydroxyl radical (•OH). It also changes with HM exposure and CAT and SOD together indicate the effective removal of H_2O_2 produced by SOD (Kumari et al., 2014). However, the CAT responses vary with species, cells, and metal types (Mansoor et al., 2023). Moreover, MDA, which is an end product of membrane lipid peroxidation, is often widely used to indicate damages to the living tissues or cells. Thus, the increase in levels of MDA indicates cellular damages by ROS on HMs exposure (Ayala et al., 2014). Furthermore, GR is responsible for maintaining optimum cellular redox buffering and supply of reduced glutathione (GSH) to GPx for metal chelation pathways (Caregnato et al., 2008). However, continued exposures of HMs can impair the GSH levels and thereby GR function (Hossen et al., 2023). Likewise, GPx plays a vital role in reducing H_2O_2 and organic hydroperoxides (ROOH) utilizing GSH as donor for electrons (Jomova et al., 2025).

2.4. *Utility of microbial metabolites in HM remediation*

When important microbial metabolites such as sidero-phore, a molecule that binds Fe and helps organisms tackle iron deficiency, along with biofilm, EPS, and IAA (Indole-3-Acetic Acid), together, they are capable of enhancing the bioremediation efficiency (Roskova et al., 2022; Sharma, 2022; Wei et al., 2024). In general, siderophore production stimulates microbial inhabitability in HM-contaminated soils and assisting in pausing the metals from seeping into groundwater (Rajkumar et al., 2010). In addition, the formation of chlorophyll and the healthy functioning of enzymes depend on the amount of iron that siderophores make available to plants (Bera et al., 2022, Radzki et al., 2013).

As microbial communities progress on an exopolymeric matrix biofilm guards them from environmental stresses, including HMs (Yin et al., 2019). The formation of a microenvironment that safeguards cells from toxic metal augments microbial resistance, a phenomenon known as biofilm formation, which is common in soils that are polluted with metals (Prinzi and Rohde, 2023). The EPS, through ionic and complexation interactions, enhances HM binding significantly by reducing its mobility and bioavailability in wastewater (Flemming and Wingender, 2010). To efficiently bioremediate such complex substrates, biofilms are indispensable for sustaining commensalisms among bacteria (Sharma et al., 2023) and broadening the metabolic diversity of the bioremediators (Mangwani et al., 2016; Mishra et al., 2022).

Moreover, EPS are high molecular weight biopolymers secreted by microorganisms that help in the immobilization of hazardous metals and the accumulation of soil particles (Zhang et al., 2024). The functional groups of EPS such as –OH, –COOH, and $–NH_2$ can interact with HM ions (Li et al., 2021). These groups are responsible for reducing the toxicity imposed by the HMs which takes place with reduction in the metal's bioavailability (Gupta and Diwan, 2017). Further, EPS can change soil structure as well as enhance the microbial diversity in soil through biofilm formation, cell-to-cell cohesion or induced adaptive capability (Flemming et al., 2016; Costa et al., 2018). Moreover, it can upsurge the water retention capacity of soil, which is vital for soil health (Morcillo and Manzanera, 2021).

Current research shows the beneficial role played by plant growth-promoting strains, or PGPs, which reside near plant roots and actively participate in upliftment of

the plant health in innumerable ways *viz*. breaking nitrogen, phosphate or secreting hormones which enhance plant growth such as IAA, or fight plant pathogens (Lugtenberg and Kamilova, 2009; de Andrade et al., 2023). Further, they are also capable in reducing HM stress in plants by secreting organic acids or compounds which hold the metals (Khanna et al., 2019; Mushtaq et al., 2022; Qin et al., 2024). They are also seen in generating antioxidants which combat with the oxidative stress induced by the HMs in plants (Iqbal et al., 2024).

Such intrinsic capabilities have been previously reported in a number of bacterial strains such as *Burkholderia* spp. EIKU24 (Basak et al., 2024), *Pseudomonas fluorescens* (Upadhyay et al., 2018), *Variovorax* spp. S12S4 (Zouagui et al., 2024), and IAA producing *Sphingobium* spp. strain AEW4 were reported to be a potent PGPs that demonstrated effective bioremediation (Minari et al., 2020; Ganesh et al., 2024,). Thus, inherent capabilities of PGPs *viz*. resistant to HMs contaminated soil, reduced bioavailability of HMs, promote interactions among microorganisms and assist in building a symbiotic relationship with plants and microorganisms, thereby demonstrating the positive impacts of mixed microbial communities in soil which is crucial for effective remediation (Kramer et al., 2020; Timofeeva et al., 2022).

2.5. *Challenges of HM remediation in antibiotic polluted soils*

There is a clear association between bacteria that resist HMs and those that resist antibiotics. This happens because when bacteria are exposed to HMs, the same genetic traits that help them survive in high metal laden environment can also make them resistant to antibiotics—a process known as co-selection (Vats et al., 2022). Many HM-resistance genes and antibiotic-resistance genes are found together on the same mobile genetic elements. This leads to co-selection, even when antibiotics are not present (Baker-Austin et al., 2006). Shared mechanisms, such as multidrug efflux pumps, also provide resistance to both metals and antibiotics (Seiler and Berendonk, 2012). The co-resistance of microbes against HMs and antibiotics can be driven by intertwined evolutionary history whereby genes regulating this resistance are transferred by horizontal gene transfer (HGT) with plasmids, transposons and integrons (Gillieatt and Coleman, 2024). HMs remain in the environment, creating long-term pressure that supports antibiotic-resistant microbial populations thereby

encourages the growth and spread of antibiotic resistance. Thus, HM exposure plays a significant role in the rise and spread of multidrug-resistant bacteria.

2.6. *Existing Environmental challenges and Research gaps*

HM pollution has been problematic in India following industrialization, mining, and release of effluents from different industries. Various scientific evidences highlight the pollution by the major evils- As, Cd, Pb, Cr, and Hg contaminating soils and water bodies of India (Adimalla et al., 2019; Kumar et al., 2020; Botle et al., 2025; Patra and Ghosh, 2025; Prasath, 2025). Among adverse scenarios of HM toxicity, the rise in the number of cancer cases has been tremendous in recent years, with cases such as colon cancer (Kiani et al., 2021), breast cancer (Romaniuk et al., 2017), thyroid cancer (Gianì et al., 2021) and several others. Moreover, HMs have been targeted as potential biomarkers for cancer development in the lungs, prostate, and liver (Men et al., 2020). India, among all other nations, has seen quite a remarkable rise in cancer cases, with new cases spanning over 1.6 million each year (Krishnatreya and Kataki, 2020).

In order to tackle HM pollution, several government regulations, combined with technological advances and biological based remediation methods are often employed in India (Sodhi et al., 2022). A multitude of technologies involving physico-chemical, adsorption and biological processes are often employed. Most of the reported explorative and pilot scale studies cover phytoremediation which employs plants and microbial remediation through biosorption and bioaugmentation (Mandal et al., 2014; Pande et al., 2022). Moreover, adsorption-based approaches reported the usage of low-cost sorbents, biochar, activated carbon, chemical immobilization, or physical processes involving soil washing and excavation (Singh et al., 2022; DRIIV, 2025).

Presently, in Nagaland, the Nagaland Pollution Control Board (NPCB) has reported that all the water polluting industries in the state mandatory to install effluent treatment plants (ETPs) (Morung Express News, 2024) in order to reduce the pollutant level in the effluent. Nagaland University has recently announced a research project on the development of a hybrid treatment technology incorporating the use of plants, algae and microbes aiming to convert wastewater into clean water, nutrients, biofuel

and biogas (India Today NE, 2025). Still, remediation technologies to tackle HM pollution is very limited. Most of the studies are scheme specific, short-term or done at pilot scale with lack of comprehensive data on HMs such as As, Cd and Pb, Hg present in soil or river water.

Further, in Nagaland, data pertaining to HM pollution research is limited. Recent works in Lumami, Zunheboto screened for various pollutants and trace metals. The authors noted the potential for HM contamination in the region because of prevailing anthropogenic stressors like rock-quarrying, sand mining, shifting cultivation, soil erosion, deforestation and disruption of fresh water ecosystem which are plausible factors for enhancing HM mobilization (Hussain et al., 2021). Further, geochemical investigations on carbonaceous materials from North-Eastern India, inclusive of Nagaland have revealed measurable As load (~ 56.0–68.0 μg/kg) from lignite carbon deposits (Baruah et al., 2003). Such As rich minerals can undergo leaching under the influence of weathering or during mining operations, finally entering the soil and water systems, causing long term effects on the living organisms. Regional reviews and surveys also highlighted As occurrences in parts of several states of Assam, Tripura, Arunachal Pradesh, Manipur and Nagaland, with groundwater risk from As pollution (Goswami et al., 2023). Investigations of surface water from springs, ponds and wells indicate the presence of Pb above threshold limits in certain water sources of Nagaland, indicating high possibility of Pb pollution in water bodies (Jamir et al., 2011). Further, Central Ground Water Board's recent state bulletin for Nagaland has listed As among key pollutants monitored in aquifers, during local ground water quality assessment (Central Ground Water Board, 2024). Likewise, isolated HM-resistant rhizobacterial species from riverbanks adjacent to coal mining sites in Nagaland provides enough biological evidence consistent with HM exposure in the environment (Tatung and Deb, 2024).

The current research was undertaken to address the gaps of research in terms of HM pollution with respect to Nagaland. Currently, Nagaland has data scarcity in terms of regional scientific literature on bioremediation. Thus, a through systematic study will aid to establish baseline data for Nagaland, which could direct future environmental monitoring and in policy making for remediation processes. Utilizing indigenous strains of microbial diversity could help to discover native microbe suited

locally to ecosystem, with better efficacy and adaptive behaviour. Moreover, this could contribute to policy relevance for local and regional authorities to take proper decisions on disposal of waste, regulation of industries and effective remediation efforts.

In bacteria-based remediation technology, certain limitations exist while introducing genetically modified microorganisms (GMOs) such as unpredictability of ecological interactions. Since the engineered strains can compete with the native microorganisms and create disturbance in the microbial networks, thereby affecting the nutrient cycling and the fertility of the soil (Sharma et al., 2024). Due to HGT, whereby the engineered genes, conferring metal or xenobiotic degrading abilities might travel to native microorganisms, creating ecological disturbances (Muhammad and Jega, 2024). Further, the behaviour of GMOs in natural environments may vary with the laboratory conditions such as reduced growth, efficiency or stability due to competition, stress or lack of selective pressure (Janssen and Stucki, 2020). Additionally, issues may arise with public acceptance, biosafety regulations or monitoring for large scale applications (Calatrava et al., 2024).

The indigenous strains however, are more preferred as they are ecologically compatible, safe and provide more efficacy, economic and more adapted to their local habitat (Singh et al., 2011; Omoregie et al., 2025). This facilitates better remediation, agriculture and restoration of the ecosystem as compared to exotic and non-indigenous strains (Omoregie et al., 2025). Further, incorporating bacterial consortium is very effective as compared to single strains, as different microbes contribute complementary metabolic pathways to neutralize the toxic pollutants, tolerate stress or utilize substrates very efficiently (Chen et al., 2020). They show synergistic interactions leading to faster and complete biodegradation, with enhanced nutrient cycling and maintaining a proper ecosystem stability as compared to single strains (Alidoosti et al., 2024). Thus, addressing these gaps is crucial in accomplishing the ultimate goal for HMs detoxification in the environmental matrices, and thereby strengthening the bacterial remediation systems.

3.1. *Chemicals and Reagents*

Chemicals, reagents and salts including Na_3AsO_4, $NaAsO_2$, $CdCl_2$, $Pb(NO_3)_2$, NaCl, Na_2HPO_4, NaH_2PO_4, KCl, Hexadecyltrimethylammonium bromide [HDTMA, $CH_3(CH_2)15N(Br)(CH_3)_3$], $FeCl_3.6H_2O$, KBr, $CuSO_4.5H_2O$, Na_2CO_3, $NaHCO_3$, Sodium tartrate ($C_4H_4Na_2O_6$), NaOH, Ethylenediaminetetraacetic acid (EDTA, $C_{10}H_{16}N_2O_8$), Sodium azide (NaN_3), Silver nitrate ($AgNO_3$), Glutaraldehyde (2%, $C_5H_8O_2$), Phenol (C_6H_5OH), ethanol, Acetone, glacial acetic acid (33%), H_2SO_4 and HCl were of analytical grade (AR) purchased from Qualigens fine chemicals, Thermo Fisher Scientific India Private Limited, Mumbai, India and Merck Specialities Private Limited, Mumbai, India. MTT [3-(4,5-dimethylthiazol-2-yl)-2,5-diphenyltetrazolium bromide], Muller Hinton broth, Tryptic Soy broth, Luria Bertani broth, Agar, Crystal Violet dye, Safranin, Bicinchoninic Acid (BCA, $C_{20}H_{10}N_2Na_2O_4$), Nicotinamide adenine dinucleotide phosphate (NADPH, $C_{21}H_{30}N_7O_{17}P_3$), Cumene hydroperoxide ($C_9H_{12}O_2$), Glutathione disulphide (GSSG, $C_{20}H_{32}N_6O_{12}S_2$), Bovine serum albumin (BSA), Nitro blue tetrazolium (NBT, $C_{40}H_{30}C_{l2}N_{10}O_6$), Potassium peroxymonosulphate (PMS, $KHSO_5$), Potassium pyrophosphate ($K_4P_2O_7$), Glutathione (GSH, $C_{10}H_{17}N_3O_6S$), Riboflavin, $(NH_4)_6Mo_7O_{24}$, Malondialdehyde, Trichloroacetic acid (TCA, $C_2HC_{l3}O_2$), Thiobarbituric acid (TBA, $C_4H_4N_2O_2S$), and H_2O_2, were purchased from HiMedia Laboratories Private Limited, Mumbai, India. Whatman Filter paper (Grade 1) was purchased from Cytiva, Global Life Science Solutions Operations UK Limited.

3.2. *Study area and sample collection*

The present study was focused on a stream line region that was situated in the close proximity to several operational coal mines of Changki area, an Ao village located in Mangkolemba Circle of Mokokchung district, Nagaland. Six distinct sampling sites along the chosen stream were selected to gather the soil samples. Three of these sample collection sites were situated upstream, while the remaining three were located downstream. Using sterile spatulas, sub-surface soil (approximately of 5 cm below the surface) was collected from each sample collection site. After the collection, soil samples were transferred to sterile plastic containers separately, brought right to the laboratory, and stored at 4 °C until used for further characterization and analysis.

Google Earth application (Google Earth Pro Version 7.3) developed by Google, was used for the mapping process of the investigated sampling sites.

3.3. *Physico-chemical characterization of the collected soil samples*

3.3.1. *pH, electrical conductivity and temperature*

The pH and electrical conductivity of the collected soil samples were measured with the help of a Multiparameter Waterproof Meter (Systronics Water Analyser 371), which consist of various probes for measuring different water quality parameters. Calibration of the instrument was done as instructed by the manufacturer before taking the measurements. The soil sample (10 g) was mixed in a beaker containing 25 mL of distilled water. Afterward, the calibrated probe was dipped in the resultant soil suspension solution and the measurements were recorded accordingly.

3.3.2. *Available potassium*

The available potassium (K) in the soil sample was estimated according to the method of Tandon (2009) with the help of a Flame Photometer (Systronics Flame Photometer 128). Initially, 2.5 g of oven dried soil was taken. Afterward, 25 mL of 1 N ammonium acetate (pH 7) was taken and stirred for 10 minutes in an orbital shaker (Kolosh KI WB12). The content was then filtered through Whatman No. 1 filter paper. The filtrate was collected and subsequently analyzed for the quantification of K in the soil sample. K was calculated using a liquid petroleum gas (LPG)-air flame (Indane) with a fuel pressure of approximately 0.5–1.0 kg/cm², a warm-up period of 10–15 minutes, and a calibration range of 5–25 ppm at 766.5 nm. The available K in the soil sample was calculated using the equation 3.1.

$$\text{Available K (kg/ha)} = 10x \times 2.24 \qquad \text{Equation 3.1}$$

Where, 2.24 is conversion factor of mg/kg to kg/ha and x= available K (ppm or mg/kg). Since, 2.5 g soil and 25 ml ammonium acetate were added for K extraction, so the dilution is 25/2.5 = 10.

3.3.3. *Soil moisture*

The moisture content in the collected soil was estimated by standard gravimetric method as described by Chukbe in 1936 and outlined in Tandon (2009). Initially, an empty crucible was weighed (W_1). Afterward, 20 g of collected moist soil

sample was transferred to the pre-weighed crucible and then weighed (W_2). Next, the crucible with moist soil was placed in a hot air oven at 105 ºC for about 24 hours. Subsequently, it was allowed to cool at room temperature in a desiccator and weighed again (W_3). Finally, the soil moisture content was calculated gravimetrically using the equation 3.2.

$$\text{Moisture } \% = \frac{W_2 - W_3}{W_3 - W_1} \times 100 \qquad \text{Equation 3.2}$$

Where, W_1 is weight of empty crucible, W_2= weight of crucible + moist soil sample and W_3= weight of crucible + dry soil sample.

3.3.4. *Nitrogen estimation*

Nitrogen (N) content in the collected soil samples were estimated using a Kjeldahl system (KEL PLUS Nitrogen Analyzer-Classic DX), following the standard of Association of Official Analytical Collaboration International (AOAC, 1990). Initially, 5 g of the soil sample was taken in the digestion tube along with a small amount (10 mL) of water and subsequently 25 mL of 0.32 % (w/v) $KMnO_4$ solution was added. The sample loaded digestion tube was then fitted in the distillation unit. This was followed by an addition of 25 mL of 2.5 % NaOH (w/v) solution through the distillation system-dosing pump. Next, 20 mL of 2 % (w/v) of boric acid was transferred to a conical flask (250 mL) with the help of a measuring cylinder. The resultant distilled ammonia gas thus produced from the digestion tube was collected in the receiver end and introduced into the conical flask containing 20 mL boric acid solution. Afterward, 5 drops of methyl red indicator was added to the boric acid solution and titrated with 0.02 N H_2SO_4. The available nitrogen in the soil sample was calculated using the following equation 3.3.

Available Nitrogen (AVN): $\frac{14\times(T.V.)\times 0.02N\times 2.24\times 10^6}{5\times 1000}$ $\left(\frac{kg}{ha}\right)$

or AVN (kg/ha) = 125.44 × T.V.

Where, T.V is titration volume, N refers normality of titrant H_2SO_4, and ha stands for hectare. In order to calculate kg/acre, conversion factor (1 hectare= 2.47105 acre) was multiplied to the result

$$\text{So, AVN (kg/acre)} = \frac{Available\ Nitrogen\ in\ kg/ha}{2.47105} \qquad \text{Equation 3.3}$$

3.3.5. *Total organic carbon*

The total organic carbon was estimated using wet digestion method as described by Walkley and Black (1934). First, 0.5 g of collected soil was weighed after sieved to 0.2 mm size and was placed in a 250 mL Erlenmeyer flask. To this, 10 mL of 1 N $K_2Cr_2O_7$ was added using a glass pipette. After that, 20 mL of concentrated H_2SO_4 was slowly added and the mixture was kept undisturbed for about 30 minutes to complete the oxidation process. Next, the solution was allowed to cooled at room temperature followed by addition of 200 mL of distilled water. Afterwards, 10 mL of orthophosphoric acid and 1-2 drops of diphenylamine indicator was added to the solution. Then, the solution was titrated with 0.5 N ferrous ammonium sulphate till the colour of the solution changes from bluish-violet to bright green. A blank was also run using the same reagents. The organic carbon content (%) in the collected soil sample was determined using the equation 3.4.

$$\text{Organic carbon (\%)} = \left(\frac{10\,(B-T)}{B}\right) \times \frac{0.003\times 100}{wt\ of\ soil\ (g)} \qquad \text{Equation 3.4}$$

Where, B is volume (mL) of ferrous ammonium sulphate solution required for blank titration, T is volume of ferrous ammonium sulphate solution needed for titration of soil sample.

3.3.6. *Available phosphorous*

The available phosphorous was estimated according to the methodology as described previously by Bray and Kurtz (1945) and Malgwi et al. (2019). Briefly, 1 g of dried soil sample was shaken with extracting solution (0.03N NH_4F + 0.025 N HCl) and filtered. Further, the filtrate was mixed with molybdate reagent (Appendix I) forming a blue colour complex. The intensity of the blue colour was measured spectrophotometrically at 882 nm using UV-Vis spectrophotometer (Thermo Fisher Scientific A51119700C) using standard concentrations (0.080, 0.160, 0.240, 0.320 and 0.400 µg/mL). The available phosphorous was finally estimated using the equation 3.5

$$\text{Available P } \left(\frac{\text{kg}}{\text{hectare}}\right) = \text{R} \times 4.48 \qquad \text{Equation 3.5}$$

Where, R is absorbance value expressed as µg P in the aliquot

3.3.7. *HM analysis of soil samples*

The soil samples were collected from the sampling sites S1, S2, S3, S4, S5 and S6 and outsourced for heavy metal (HM) analysis that include As, Cd, and Pb at

National Institute of Pharmaceutical Education and Research Guwahati (NIPER-G) Guwahati, Assam. The samples were collected in replicates from the six sampling sites and collected after sieved through 0.22 mm size in falcon tubes. The samples were microwave digested following the standard method 3015A (US EPA, 2007). Briefly, about 0.5 g of sieved soil was placed in Teflon digestion vessels, followed by adding about 10 mL of HNO_3 and 2 mL of HCl. Further, the vessels were heated to 170-180 ºC under stable pressure for about 20 minutes for proper oxidation. Then, the digest was diluted to a known volume (120 dilution) with deionized water and filtered before metal analysis. The HM content in the samples (As, Cd and Pb) were estimated with the help of inductively coupled plasma mass spectrometry (ICP-MS) (ICP–MS, Agilent 7900 Series). The instrument was operated in standard mode under optimized conditions. Radio frequency (RF) power 1550-watt, plasma gas (Argon) flow rate of 15 L/minutes, auxiliary gas flow at 0.9 L/minutes, nebulizer gas flow at 1.05 L/ minutes, sampling depth 8 mm, and a peristaltic pump speed of 0.10 revolutions per second (rps) were maintained. A MicroMist concentric nebulizer and quartz spray chamber were used. The isotopes monitored were ^{75}As, ^{111}Cd and ^{208}Pb. Calibration was done using external standards at 0, 5, 10, 25, 50, 75 and 100 ppb. Further, using an autosampler, the digested samples were introduced to ICP-MS and the metals were quantified based on calibration curve and expressed as ppb (U.S. EPA, 2014; Aniş et al., 2024).

3.4. *Isolation of As-resistant bacteria*

The culturable arsenic (As) resistant bacteria were isolated from the collected soil samples following the enrichment culture technique with slight modifications as described by Bowman et al. (2018). Briefly, 100 mL of Luria Bertani (LB) broth (25 g/L) (Appendix I) along with Na_3AsO_4 (300 µg/L) and $NaAsO_2$ (300 µg/L) were prepared in a 250 mL screwcap Erlenmeyer flask, sterilized by autoclaving and allowed to cool down to room temperature. The collected soil samples were adequately mixed with the help of a sterile spatula and sieved to separate the debris. 10 g of the sieved soil sample was weighed and carefully introduced to a previously sterilized As-loaded LB broth medium inside a laminar airflow chamber and was subsequently transferred to an orbital incubator shaker, which was set at 37 ºC with 160 rpm. The

culture medium was incubated for three days. After the competition of the first three days of enrichment cycle, 1.0 mL of the saturated culture broth was transferred to a fresh Erlenmeyer flask culture containing As-loaded LB broth medium precisely prepared with the same composition as described previously for the second cycle of enrichment and incubated in a similar fashion as that of the first cycle. The process was repeated up to three cycles. After the completion of the third cycle, an aliquot of 1.0 mL of culture inoculum was taken and then serially diluted through serial dilution approach. Using spread plate method technique, 0.1 mL of diluent from each dilution stock of 10^{-2}, 10^{-3}, 10^{-4} and 10^{-5} were transferred and uniformly spread over the surface of Petri dishes containing sterile solidified Luria Bertani agar (LBA) medium (Appendix I) supplemented with, Na_3AsO_4 (300 µg/L) and $NaAsO_2$ (300 µg/L) (Sanders, 2012) followed by incubation of culture plates at 37 ºC for 48 hours. After 48 hours, appeared As-resistant bacterial colonies were adequately documented based on their distinct morphological characteristics.

3.5. *Screening of potential As-resistant bacteria*

The 96-well microtiter plate was initially loaded with sequentially diluted As^{3+}, As^{5+}, Cd^{2+}, and Pb^{2+} solution in separate rows individually at concentrations ranging from 50,000 to 0 ppm and eventually increased with increased tolerance to metals by the bacterial strains. Then, fresh LB broth cultures of overnight grown bacterial isolates obtained from enrichment culture (100 µL) were added to each well of the microtiter plate. Sterile LB broth was used as negative control. Afterwards the microtiter plate was incubated for 24 h at 37 ºC, followed by addition of MTT (Appendix I). The MTT stock was prepared at 5 mg/mL in sterile PBS, which was filter sterilized and stored protected from direct exposure of light at 4 ºC. Further, 20 µL of the stock was added to each well and kept in dark for about 20-30 minutes to allow reduction of MTT to formazan crystals and the absorbance was measured at 600 nm using a Multiskan SkyHigh Microplate Spectrophotometer (Thermo Fisher Scientific A51119700C). The measured optical density (OD) values of the wells based on the colour change from bluish to pale yellowish upon the administration of MTT, the response of the bacterial isolates towards As^{3+}, As^{5+}, Cd^{2+}, and Pb^{2+} metal ion exposure was recorded, and the values of MIC (minimum inhibitory concentration),

MBC (minimum bactericidal concentration), and MTC (maximum tolerable concentration) were computed (Agarwal et al., 2020). The MTC is defined as the highest concentration of the tested HMs at which the bacteria can survive and grow, while MIC is the lowest concentration of the selected HMs at which, there is visible inhibition of the bacterial growth and finally MBC is the lowest concentration of HMs that kills almost 100 percentage of the organism (Agarwal et al., 2020).

3.6. *Morphological and biochemical characterization*

Colony characteristics of the selected bacterial isolates were examined for their morphological identification using Bergey's Manual of Determinative Bacteriology, 9th Edition (Bergey, 1994). In addition, the morphological features of bacterial cells were examined using Gram staining, spore staining, and motility tests, following the methodology as described by Hassan et al. (2013). The biochemical characterization of the selected bacterial isolates was carried out using standard procedures that include enzyme activity (indole, catalase, and oxidase), methyl red test, Voges–Proskauer test, nitrate reduction test, citrate, hydrogen sulphide production and usage of various carbon sources (Banerjee et al., 2011).

3.7. *Molecular characterization of bacterial isolate AS3 and AS4*

3.7.1. *Isolation of bacterial DNA*

In accordance with the standard methodology provided by Cardinal et al. (1997), the genomic DNA of bacteria was isolated. Initially, fresh nutrient broth (Appendix I) was inoculated with a sterilized inoculation loop containing the bacterial culture and incubated in an orbital incubator shaker at 37 °C with 160 rpm for overnight period. Next, an aliquot of 1.0 mL of bacterial culture was removed from the fresh overnight grown culture broth and centrifuged at 12,000 rpm for 2-5 minutes. The supernatant was discarded, and the pellet was recovered. 200 µL of lysis buffer (Appendix I) was then added to the bacterial cell pellet and vortexed vigorously to produce a cell suspension. The mixture was heated in a water bath at 65 ºC for 20 minutes and shaken well at 5 minutes interval. Subsequently, 100 µL of 5 M NaCl was added and vortexed vigorously. The mixture was then stored at –20 ºC for 20 minutes before centrifugation at 12,000 rpm for 10 minutes at room temperature. After

centrifugation, the supernatant was removed and 500 µL of phenol: chloroform (25:24 v/v) was added. It was mixed until a milky emulsion form. After centrifuging the emulsion mixture at 12,000 rpm for 10 minutes at room temperature, the aqueous phase was removed and 500 µL of chloroform: isoamyl alcohol (24:1 v/v) solution was added. This was followed by another centrifugation at 12,000 rpm for 10 minutes at 4 ºC. After centrifugation, the uppermost layer was removed once more, and 2.5 volumes of 100 % (500 µL) chilled ethanol (Merck, Germany) was added to precipitate the genomic DNA (g-DNA). The temperature of the resultant ethanolic g-DNA solution was maintained at –20ºC for the overnight period. On the following day, the eppendorf tubes containing the ethanolic g-DNA solution were centrifuged at 12,000 rpm for 10 minutes at 4 ºC. Afterward, a thin pellet of g-DNA was obtained, which was later rinsed with 100 µL of 70 % (v/v) ethanol and allowed to air dry for 30 minutes at room temperature. In order to dissolve the obtained g-DNA pellet, 30 µL of TE (1mM Tris-HCl and 1 mM EDTA) (Appendix I) was added and allowed to stabilize at –20 ºC for 60 minutes.

3.7.2. *Agarose gel electrophoresis of the isolated g-DNA*

For running the g-DNA, 0.8 % (w/v) of agarose gel was prepared in 1X TBE (Tris-Borate-EDTA) buffer (Appendix I). Initially, 0.8 g of agarose was taken. Then, it was well dissolved in 100 mL of 1X TBE buffer by boiling it in a microwave. The solution was further allowed to cool down at a temperature about 50 ± 5 ºC. To the solution, 4 µL of EtBr (Ethidium Bromide) was added. The mixture was further poured into a gel caster, equipped with gel combs. The gel was then allowed to solidify at room temperature, after which the combs were removed and the gel was transferred to a gel tank, filled with 1X TBE gel running buffer.

Before loading into the gel, 4 µL of distilled water and 2 µL loading dye (Appendix I) was loaded in a small piece of parafilm sheet. Next, 6 µL of sample g-DNA was added and mixed with the help of a micropipette. Then, with the same micropipette, the sample was loaded into the appropriate well. A commercial 1 kb DNA ladder (size range about 250 bp to 10,000 bp) was used as molecular marker fragments (bands) and 1 µL of DNA ladder was loaded twice *i.e.* in the first and the last well while the remaining wells were loaded with g-DNA samples. After loading the DNA sample including the DNA ladder, the gel was run at about 10 V/cm of gel

length using a DC power supply until the xylene cyanol of loading dye reached the bottom of the gel. The gel was then removed from the electrophoresis system and observed in the Gel Doc system (Bio-Rad Gel Doc™ EZ Imager).

3.7.3. *Spectral analysis of isolated g-DNA*

Nanodrop 1000 Spectrophotometer (Thermo Fisher Scientific, USA) was used to quantify the isolated g-DNA and verify its purity. To determine the amount of DNA in the specific solution, the absorbance of g-DNA was measured at 260 nm. In order to determine the degree of protein contamination in the isolated DNA, the absorbance at 280 nm was also measured. The spectral characteristics listed below were chosen as standards for identifying high-quality DNA.

$$A_{260} / A_{280} \geq 1.8$$

$$A_{280} / A_{280} \leq 0.55$$

For the quantification, 1 µL of DNA sample was mixed with 3 mL of TE buffer in the cuvette. Absorbance of the sample was then recorded at 260 nm and 280 nm in a Nanodrop system. The concentration of DNA was calculated using the given equation 3.6.

$$\text{Concentration of DNA} = (A_{260} \times 50 \times \text{dilution factor}) \ \mu g/mL \qquad \text{Equation 3.6}$$

3.7.4. *Polymerase chain reaction (PCR) amplification of isolated g-DNA*

For the PCR, master mixture was prepared for bacterial g-DNA samples. The detail composition of master mixture is included in Appendix I. For PCR amplification the primers used were U16SF (Forward) and U16SR (Reverse) with the sequences of 5'-AGAGTTTGATCCTGGCTCAG-3' and 5'-GGTTACCTTGTTACGACTT-3', respectively. First, an aliquot of 48 µL of master mixture solution was added to each of the reaction tube containing 2 µL of g-DNA samples. Thus, the total reaction volume was 50 µL and the components of reaction mixture were then mixed well by spinning in R-8C table-top mini-centrifuge (REMI, India). Finally, the tubes were then subjected to PCR in a thermo cycler system (Eppendorf Mastercycler Series, Germany). The standard conditions that were established for amplification are included in Appendix I. 35 cycles of the PCR were allowed to run. After the completion of the reaction, the resultant PCR products were then stored at –20 ºC in a laboratory grade upright deep freezer (RQVD-400 Plus Remi, India).

3.7.5. *Agarose gel electrophoresis of PCR product*

The amplification of the 16S rRNA conserve gene sequence was observed by running the PCR product in 1.5 % (w/v) Agarose gel. PCR product was loaded in the similar manner to that of g-DNA and run at 10–15 V/cm. Afterward, the agarose gel was observed in a Gel Doc system (Bio-Rad Gel Doc™ EZ Imager).

3.7.6. *Molecular characterization of bacterial isolates*

For molecular identification, the amplified sequences of 16S rRNA gene of the selected bacterial isolates were sent to Xcelris Labs. Limited, Ahmedabad, Gujrat, India, for partial sequencing. Sanger dideoxy sequencing method was used to sequence the obtained 16S rRNA gene sequences. Subsequently, NCBI Gene Bank database was used for BLAST (Basic Local Alignment Search Tool) analysis, which allowed for genus and species-level identification based on maximal identity score. Later, multiple sequence alignments were made using muscle alignment, and a consensus maximum likelihood tree was constructed using the Molecular Evolutionary Genetics Analysis (MEGA) software (version 11.0) (Tamura et al., 2021).

3.8. *Molecular characterization of bacterial isolate AS11*

For the molecular characterization, the AS11 isolate was outsourced to Novelgene Technologies Pvt Ltd, Hyderabad for CGAS (Comprehensive Genome Analysis service). The whole genome sequencing was done using Illumina NovaSeq 6000 (PE 150) sequencing platform. FASTP, which is a program for searching protein sequence, was used for pre-processing of the reads/bases to get high quality reads on the parameter of <Q20 (Quality Score <20). SPAdes (St. Petersburg genome assembler) genome assembler was used for this study. Assembly quality was assessed using Quast software (Quast v5.1).

The closest reference and representative genomes were identified by Mash/MinHash (MinHash Alignment-based Sequence Hashing) (Ondov et al., 2016). Global protein families (PGFams) available in PATRIC (Pathosystems Resource Integration Centre) were selected from the reference genomes to accurately determine the phylogenetic position of the genome under study (Davis et al., 2016). The protein sequences from these PGFams were aligned using MUSCLE (MUltiple Sequence Comparison by Log-Expectation programme) software program (Edgar, 2004), and

the corresponding nucleotide sequences for each protein were then back-mapped onto the protein alignment to generate codon-based nucleotide alignments. The combined amino acid and nucleotide alignments were joined into a single data matrix, which was then analyzed using RAxML software program (Stamatakis, 2014). Fast bootstrapping was performed to generate the branch-support values for the resulting phylogenetic tree (Stamatakis et al., 2008).

3.9. *Growth kinetics of the selected bacterial strains*

The approach of Ka-ot and Joshi (2022) with modifications was used to examine the growth behaviour of the chosen bacterial strain. A set of five 250 mL volume conical flasks holding 100 mL of LB broth were used to study the growth kinetics of the chosen bacterial strain. Together with the bacterial inoculum, four conical flasks were supplied with the appropriate HM salts, namely Na_3AsO_4, $NaAsO_2$, $Pb(NO_3)_2$, and $CdCl_2$, according to the MTC value of the chosen strain. The remaining conical flask was used as a control which contains culture broth without any HM salt. The cultures were kept in an orbital incubator shaker at 37 °C with 160 rpm. For the first 12 hours, 3 mL of culture broth was collected at an interval of every two hours. After that, 12-hour interval readings were considered for the next seven days. The optical density (OD) was measured in a UV-VIS spectrophotometer (Lambda 35, PerkinElmer) at 600 nm. The growth curves of every treatment and the control were plotted together, and their growth patterns were compared. In a similar manner, the growth behaviour of other two selected bacterial strains were determined in the presence of tested HM.

3.10. *Antibiotic susceptibility test and multiple antibiotic resistance (MAR) index*

To study the antibiotic sensitivity of the selected bacterial strains, different standard antibiotics in microgram concentration (mcg) were used such as tetracycline (30 mcg), ampicillin (10 mcg), penicillin (1 unit = 0.6 mcg), cefaloridine (30 mcg), kanamycin (5 mcg), chloramphenicol (30 mcg), streptomycin (10 mcg), cephalexin (30 mcg), ciprofloxacin (5 mcg), azithromycin (15 mcg), norfloxacin (10 mcg), clarithromycin (15 mcg), erythromycin (15 mcg) and amoxicillin (10 mcg) (Dey et al., 2016). Isolated HM-resistant strains were tested for antibiotic sensitivity and resistance

according to the Kirby Bauer disc diffusion method (Bauer et al., 1996) as well as agar well diffusion method (Balouiri et al., 2016). For the experiment, Mueller Hinton (MH) agar (Appendix I) plates were used and the selected bacterial strains were cultured along with the test antibiotic in the plates. After incubation, the appearance of inhibition zones facilitates to classify the organisms as sensitive or resistant to an antibiotic according to the diameter of inhibition zone which was measured using an Antibiotic Zonescale – C (HiMedia Laboratories Pvt Ltd., Mumbai, India) ruler.

The MAR indices of the selected bacterial strains against the antibiotics tested were determined using the equation 3.7 (Sarter et al., 2007).

$$\text{MAR index} = \frac{X}{Y \times Z} \qquad \text{Equation 3.7}$$

Where, X = total of resistance antibiotic, Y = total of antibiotic used in the study, and Z = total of test bacterial strains.

3.11. *Evaluation of biofilm forming capacity*

The biofilm forming ability of the selected bacterial strain was ascertained using the tube technique method, a qualitative biofilm detection test (Christensen et al., 1985; Kırmusaoğlu, 2019). The bacterial strain after forming linings on the walls of the polystyrene test tubes, containing tryptic soy broth (TSB) (Appendix I), was rinsed with phosphate buffer saline (PBS) (Appendix I) and further stained with crystal violet (0.1 % w/v) stain (Appendix I) for about an hour. During post staining steps, bacterial cells were washed with PBS, air dried and observed for visible film lining on the walls of test tube.

To enumerate the generation of biofilm quantitatively, the procedure as described by Kırmusaoğlu (2019) was used with slight modification. Initially, bacterial cell suspension with a density equivalent to 0.5 McFarland constant (1×10^8 cfu/mL) was inoculated in MH broth medium supplemented with 1% (w/v) glucose and incubated at 37 °C in an incubator shaker with 160 rpm for overnight period. Next, bacterial cell suspension density of 5×10^6 cfu/mL was achieved by diluting the freshly grown bacterial culture in sterile MH broth for 20 times. Subsequently, a 96-well flat-bottomed sterile polystyrene microplate was then filled with 20 µL of the aforementioned bacterial suspension and 180 µL of MH broth supplemented with 1% (w/v) glucose. The final density of the bacterial cell suspension was adjusted to a value

of 5×10^5 cfu/mL. The microplate plate was later incubated at 37 ºC for 24 hours. Following a 24-hour incubation, culture medium in the wells were discarded and the wells were washed twice with PBS (pH 7.2). The samples were then dried approximately for 60 minutes at 60 °C to fix the biofilm (Christensen et al., 1985). Next, 100 µL of 0.1 % (w/v) crystal violet solution was added to each well that contained dried biofilm (Lade et al., 2019). The wells took around five minutes to dry after being dyed. To remove the unbounded crystal violet stain, the stained wells were further rinsed twice using PBS. After 30 minutes, 150 µL of 33 % (v/v) glacial acetic acid was added to each well in order to dissolve the stained adhering biofilm. Finally, a 96-well microplate reader was used to measure the absorbance at 595 nm in order to quantify the developed biofilm (Lade et al., 2019). Wells with only MH broth medium supplemented with 1% (w/v) glucose were kept as negative control. The purpose of the blank absorbance readings was to ascertain whether the bacterial strain had developed a biofilm or not. A cut-off OD value (OD_c) was used to categorize bacterial strain as either biofilm producer of or not (Kırmusaoğlu, 2019). Using equation 3.8 and equation 3.9, OD_c and OD_{strain} values of the strain were determined. A zero denotes the presence of biofilm development, whereas a negative number indicates the absence of biofilm growth. The data may be analyzed and categorized using the OD_c values (equation 3.10 to equation 3.13) as follows: (i) no biofilm; (ii) weak biofilm (+ or 1); (iii) moderate biofilm (++ or 2); and (iv) strong biofilm (+++ or 3) (Kırmusaoğlu, 2019).

OD_c = Average OD of negative control + (3 × standard deviation of negative control) Equation 3.8

OD_{strain} = Average OD of strain – OD_c Equation 3.9

$OD_{strain} \leq OD_c$: lack of biofilm production Equation 3.10

$ODc < OD_{strain} \leq 2 \times OD_c$: weak biofilm production Equation 3.11

$2 \times OD_c < OD_{strain} \leq 4 \times OD_c$: moderate biofilm production Equation 3.12

$4 \times OD_c < OD_{strain}$: strong biofilm production Equation 3.13

3.12. *Evaluation of siderophore producing capacity*

The universal CAS (Chrome Azurol Sulfonate) test was used to screen the siderophore production in the selected bacterial strains (Schwyn and Neilands, 1987).

With slight modification, the procedure outlined by Arora and Verma (2017) was used for the qualitative estimation. Initially, 90 mL of autoclaved LB agar medium was combined with 10 mL of CAS reagent (Appendix I) to prepare CAS agar plates. The CAS plate was spot-inoculated with the selected bacterial strain, while a control plate was kept uninoculated. The inoculation plates were then incubated at 30 ºC for about six days. According to Louden et al. (2011), the formation of an orange zone around the bacterial colony suggested the existence of a siderophore.

Using a 96-well microtiter plate, quantitative estimation was carried out with minor adjustments in accordance with the technique as described by Arora and Verma (2017). Initially, selected bacterial strain was grown in LB broth in an incubator shaker for overnight period at 37 °C with 160 rpm. Next, the freshly grown culture was centrifuged at 6000 rpm for six minutes and the resultant cell free culture supernatant (CFCS) was collected. Then, pre-assigned wells of a 96-well microtiter plate were filled with 100 µL of the collected CFCS and 100 µL of CAS reagent and the plate with the resultant mixture were kept for around next 30 minutes at room temperature. Using a microplate reader, the OD of the mixture solution was measured at 630 nm. The siderophore production was quantified using the equation 3.14 and expressed as percent siderophore units (psu) (Payne, 1993).

$$\text{Percent Siderophore Units (psu)} = \frac{\{(A_r - A_s) \times 100\}}{A_r} \qquad \text{Equation 3.14}$$

Where, A_s represents sample absorbance (CAS solution and CFCS) and A_r represents absorbance of reference (CAS solution and uninoculated broth)

3.13. *Evaluation of EPS producing capacity*

For the screening of EPS production, the dry weight of EPS generated by the selected bacterial strains were measured using a gravimetric method as described by Nwosu et al. (2019) with slight modification. Initially, 50 mL of nutrient broth (Appendix I) supplemented with 2 % (w/v) glucose was infused with fresh cell suspension of an overnight grown culture containing 1.5×10^8 cfu/mL of bacterial cells. The resulting mixture was then incubated at 37 ºC for three days at 160 rpm and eventually centrifuged at 12000 rpm. EPSs were precipitated after being further extracted from the CFCS using equal amounts of cold ethanol and kept in a refrigerator for an overnight period at 4 °C. Centrifugation was done for 20 minutes at 12000 rpm

for collecting the precipitates. To get a consistent weight, the pellets underwent further drying at 60 ºC, and their total dry weight was determined. As part of the quantification process, the total carbohydrate in the dried EPS was calculated using the standard anthrone technique (Ludwig and Goldberg, 1956). The total carbohydrate content in the isolated EPS was determined by measuring its OD at 630 nm, with glucose serving as a reference.

3.14. *Oxidation and reduction potential of As by the selected bacterial strains*

With slight modification, the methodology as outlined by Dey et al. (2016) was used to determine the oxidation and reduction potential of arsenic by the selected bacterial strains. By using $AgNO_3$ solution, the capacity of the selected bacterial strain to oxidize (As^{3+}) or reduce (As^{5+}) arsenic was examined (Banerjee et al., 2011). The bacterial strain was initially inoculated in the LB agar plates that contained As^{5+} or As^{3+}. The LB agar culture plates were then incubated at 37 ºC for a duration of 72 hours. After 72 hours of incubation, the culture plates were inundated with a modest volume of $AgNO_3$ solution (1 mM) (Appendix I). On exposure to $AgNO_3$ if the plates became brown, indicates the presence of silver arsenate; on the other hand, development of yellow colour indicates the presence of silver arsenite (Dey et al., 2016).

3.15. *Cellular study of the selected strain*

3.15.1. *Scanning electron microscopy-energy dispersive X-ray spectroscopy (SEM-EDX)*

The influence of As exposure on the surface properties of the bacterial cell and changes in cell morphology under stress were examined using SEM-EDX (Carl Zeiss NTS GMBH, Germany; JSM 6390LV, Japan). With a slight modification, the bacterial samples were prepared as stated by Pandey and Bhatt (2015). The bacterial strains were grown in 50 mL LB broth supplemented with 100 ppm Na_3AsO_4 and 100 ppm $NaAsO_2$ individually, and were incubated at 37 ºC with 160 rpm for 48 hours. Subsequently, the cultures were centrifuged at 6000 rpm, and the bacterial pellets were collected and rinsed three times with PBS (pH 7) (Appendix I). The bacterial pellets were then stored at 4 °C for overnight period in a fixative solution containing 2 % (v/v) glutaraldehyde in Na-phosphate with a pH of 7.2. Subsequently, bacterial pellets were

washed thrice and finally suspended in the Na-phosphate buffer. Afterwards, the cells underwent a succession of ethanol dehydration that comprises exposure to 30 % (v/v), 50 % (v/v), and 70 % (v/v) ethanol for 5 minutes and 1 minute with 100 % ethanol. In order to study the morphology and microstructure of the bacterial strain, the samples were then coated with gold and observed under electron microscope using a 3-kV accelerating voltage (Fischer et al., 2024). The SEM Microscope (Carl Zeiss NTS GMBH, Germany; JSM 6390LV, Japan) was utilized for mapping and point ID on the samples for EDX analysis of elemental composition.

3.15.2. *Fourier transform infrared (FTIR) spectroscopy of bacterial biomass*

With minor adjustments, the approach described by Singh et al. (2016) was used for FTIR analysis. The bacterial strains were cultured both with and without the test HM salts individually at 37 ºC with 160 rpm for 48 hours. Subsequently, bacterial biomass pellets were obtained after centrifuging the mature cultures for 10 minutes at 6000 rpm. The pellets underwent two rounds of washing in sterile distilled water before being dried for 48 hours at 40 °C. A Perkin Elmer FTIR spectrophotometer (Spectrum Two, Perkin Elmer) was used to analyse the dehydrated samples further. After mixing potassium bromide (KBr) with the powdered bacterial sample, a manual hydraulic press was used to press the mixture into a translucent pellet disc and was used for the analysis. The 4000-400 cm^{-1} scan range was used to produce the FTIR spectrum.

3.15.3 *Transmission electron microscopy-energy dispersive X-ray spectroscopy (TEM-EDX) analysis*

Bacterial cells that had been exposed to selected HMs (As^{5+}, Pb^{2+} and Cd^{2+}) as well as control bacterial cells without HMs exposure were examined under a TEM to verify the intracellular accumulation of HMs. Initially, the bacterial cell samples were prepared in the similar manner as described for SEM analysis and the same is mentioned in the section 3.15.1. Afterwards, embedding of bacterial sample was carried out in epoxy resin, while the same buffers and dehydration procedure were used as performed in SEM analysis (Pandey and Bhatt, 2015). Microscopic imaging of thin sections of cells was performed in a TEM (FEI Philips Morgagni 268D) at 100 kV accelerating voltage. TEM–EDX analysis was carried out using a liquid-nitrogen-

free EDX/EDS system equipped with a 129 eV, 100 mm² crystal detector at all India institute of medical science (AIIMS), New Delhi.

3.16. *Stress enzyme activity*

3.16.1. *Protein estimation*

The total protein content (TPC) was estimated in the bacterial cell lysate of the selected bacterial strains using a standard Bradford assay, which was used to estimate stress indicator enzyme units per mg protein (Rahman et al., 2006). The experiment was performed with appropriate HM salts, namely Na_3AsO_4, $NaAsO_2$, $Pb(NO_3)_2$, and $CdCl_2$, according to the MTC value of the chosen strain. The bacterial strains were cultured in 250 mL volume conical flasks, containing 100 mL of LB broth and were incubated in an orbital incubator shaker for three days at 37 ºC with an rpm of 160. Bacterial cultures devoid of HM treatment were grown as control, while the remaining four HM treatments for each strain were selected based on their MTC values against respective HMs. For the preparation of standard curve, initially Bradford reagent was added to wells of a 96 well microtiter plates and followed by 5 µL of bovine serum albumin (BSA) of different concentrations (200-1000 µg/mL). The plate was then incubated for 15 minutes at room temperature. Afterwards, absorbance was taken at 595 nm using an ELISA Microplate Reader (iMark Bio-Rad) and a standard curve was plotted based on the recorded OD values. The bacterial cell lysates were prepared by harvesting cultures at the desired growth stages *via* centrifugation at 4,000 × g for 10 minutes at 4 °C. Further, the cell pellets were washed with cold PBS and resuspended in a lysis buffer (Appendix I) containing protease inhibitors. The cells were disrupted using lysozyme of 0.5 mg/mL for 30 minutes, followed by sonication in the presence ice. The lysates were further centrifuged at 12,000 × g for 15 minutes at 4 ºC and the resulting supernatant was used for protein estimation.

For the estimation of TPC in the selected bacterial strain, 200 µL of Bradford reagent was added to the 20 µL of bacterial cell lysate sample in each well and were mixed thoroughly. The microtiter plate containing the mixtures was then incubated for 15 minutes at room temperature. Afterwards, absorbance of reaction mixture at 595 nm was recorded and using the standard curve, the protein contents were estimated. The experiments were performed thrice to determine the standard deviation.

3.16.2. *Determination of superoxide dismutase (SOD) activity*

500 mg of bacterial biomass of the selected bacterial strain was obtained after exposure to the selected HMs at their MTC values and homogenized in 500 µL of phosphate buffer. Homogenate was centrifuged to get a clear supernatant, which was further used for the bioassay. All reagents and homogenate were brought to 37 °C. The test samples, blank, standard, and control tubes, were prepared and then pipetted into 96 well plates. SOD enzyme was diluted at different concentrations (6.25 to 100 U/mL) to prepare the standard curve. For the reaction mixture, initially 1.2 mL potassium pyrophosphate buffer (0.025 M; pH 8.3) (Appendix I) was taken. To it, 1.0 mL of PMS (phenazine methosulfate, 186 µM) and 0.3 mL of NBT (Nitro Blue Tetrazolium, 300 µM) were added and mixed thoroughly. Then, 0.5 mL of PBS (1X) and 0.05 mL crude enzyme extract (10 times diluted) were added to the blank and the sample cuvette respectively, and mixed appropriately.

Finally, 1.15 mL distilled water was added to the reaction mixture followed by the addition of 0.2 mL GSH (glutathione, 780 µM) to initiate the reaction. The change in absorbance was recorded at 560 nm from 0 to 30 minutes. SOD activity was calculated according to Equation 3.15 of Weydert and Cullen (2010) and expressed as units per mg protein (U/mg protein).

$$\text{SOD Activity (U/mg protein)} = = \frac{\Delta A560\ \text{Blank} - \Delta A560\ \text{Sample}}{\Delta A560\ \text{Blank}} \times 2 \times \frac{V}{v} \times D$$

Equation 3.15

Where, V= Volume of the reaction mixture, v = Volume of samples, D= Sample dilution factor, ΔA_{560}= Change in absorbance at 560 nm

3.16.3. *Determination of catalase (CAT) activity*

500 mg of bacterial biomass of the selected bacterial strain was obtained after exposure to the selected HMs at their MTC values and homogenized in 1000 µL phosphate buffer. Homogenate was centrifuged to get a clear supernatant, which was further used for the bioassay. All reagents and homogenate were brought to 37 °C. To the 10 µL of the test sample, 1000 µL of hydrogen peroxide (20 mM H_2O_2 in Phosphate buffer pH 7.4) was mixed thoroughly through vortexing and incubated at 37 °C for 3 minutes; after that, ammonium molybdate (32.4 mM in 25 mM H_2SO_4) was added to

the mixture solution. Blank (without cell homogenate and H_2O_2), standard (without cell homogenate), and control tubes (without H_2O_2) were prepared, and absorbance of the reaction mixtures at 320 nm were determined through a UV-VIS spectrophotometer (Lambda 35, PerkinElmer). The absorption was recorded at 374 nm. The catalase activity was further calculated with the help of the following equation 3.16 (Weydert and Cullen, 2010)

$$\text{CAT activity (U/mg protein)} = \frac{2.303}{t} * \left[\log \frac{S^O}{S-M}\right] * \frac{Vt}{Vs} \quad \text{Equation 3.16}$$

where, t = time, S° = absorbance of standard tube, S = absorbance of test tube, M = absorbance of control test (correction factor), V_t = total volume of reagents in test tube, and V_s= Volume of bacterial cell lysate.

3.16.4. *Estimation of malondialdehyde (MDA) content*

Bacterial cells were exposed to the selected HMs at their MTC values for 24 hours, and the lysate was prepared in PBS (50,000-80,000 cells lysate in 200 µL). Further, 100 µL of cell lysate was mixed thoroughly with 500 µL TCA (Trichloroacetic acid; 8 % w/v). Samples were centrifuged at 2500 rpm for 5 minutes to remove the protein precipitate, and the supernatant was used for further assay. 200 µL of supernatant was mixed with 1.8 mL of TBA (Thiobarbituric acid) reagent and the solution was heated for 15 minutes in a boiling water bath. A dilution factor of 20 was used and the absorbance was measured at 532 nm against a blank that contained all the reagents except the cell lysate samples. Using the equation 3.17, malondialdehyde concentration was calculated considering an extinction coefficient of 1.56×10^5 $M^{-1}cm^{-1}$ (Olszewska-Słonina et al. 2011).

$$\text{MDA concentration (U/mg protein)} = \frac{\text{Absorbance}_{532nm}}{1.56\times10^5} \times D \quad \text{Equation 3.17}$$

where, D = Sample dilution factor and 1.56×10^5 $M^{-1}cm^{-1}$ = extinction coefficient

3.16.5. *Estimation of glutathione peroxidase (GPx) activity*

For glutathione peroxidase estimation, initially bacterial cell lysates were prepared as per the protocol for protein estimation. Then, the reaction mixture was prepared where 1740 µL of potassium phosphate buffer/ EDTA/NaN_3 solution (50 mM/1 mM/1 mM), 100 µL of NADPH (4 mM), 100 µL of GSH (20 mM), 50 µL of cumene hydroperoxide (40 mM), and 10 µL of cell lysate were added and mixed. A

control set carried all the reagents except 10 µL of cell lysate. The reaction mixture was taken in a quartz cuvette, and readings were recorded at 340 nm at an interval of 60 second for 6 minutes (Flohé and Günzler 1984). GPx activity was calculated using the equation 3.18

$$\text{GPx Activity (U/mg Protein)} = \frac{(\Delta A340\ Sample - \Delta A340\ Blank \times V)}{v \times \varepsilon \times D} \qquad \text{Equation 3.18}$$

where, V= Volume of the reaction mixture, v = Volume of samples, D = Sample dilution factor, ε = Molar extinction coefficient of NADPH at 340 nm (0.00622 $\mu M^{-1} cm^{-1}$) and ΔA_{340}= Change in Absorbance at 340 nm

3.16.6. *Estimation of Glutathione reductase activity*

For glutathione reductase estimation, after preparing the cell lysates, 100 µL GSSG (20 mM, oxidized glutathione), 100 µL NADPH (2 mM, nicotinamide adenine dinucleotide phosphate), 1800 µL potassium phosphate buffer (prepared with 2mM EDTA) (Appendix I) and 10 µL of bacterial cell lysate were taken in a quartz cuvette. Readings were recorded at 340 nm at 1minute intervals for 15 minutes. Glutatione reductase activity was calculated using the equation 3.19 (Rahman et al. 2006)

$$\text{Glutatione Reductase (U/mg Protein)} = \frac{\Delta A340\ \text{Blank} - \Delta A340\ \text{Sample} \times V}{\epsilon \times v} \times D \qquad \text{Equation 3.19}$$

where, ΔOD= Change in absorbance per minute at 340 nm, V= Volume of the reaction mixture, v = Volume of sample, ε = Micromolar extinction coefficient 0.00622 μM^{-1} cm^{-1}, and D= Sample dilution factor

3.17. *Bioremediation potential of the selected strains*

In order to assess the bioremediation potential of the selected As-resistant strain, the method described by Pandey and Bhatt (2015) was followed with slight modifications (Figure 3). Initially, the bacterial strains were cultured in Erlenmeyer flasks with 100 mL of LB both medium supplemented with selected HMs at their MTC values individually. The cultures were incubated for 72 hours with an agitation of 160 rpm at 37 ºC. After 72 hours, the cultures were centrifuged at 6000 rpm and pelleted. The obtained supernatant was passed through membrane filter (0.22 µm) for each HM treatment and further undergone microwave digestion method (Xing, 2022) for the quantification of available HM in the test sample using an ICP-MS (Inductively

Coupled Plasma Mass Spectrometry) system (Agilent 7850 ICP-MS). The HM removal percentage was then calculated using the equation 3.20.

$$\text{Removal } \% = \frac{C_i - C_f}{Ci} \times 100 \qquad \text{Equation 3.20}$$

where, C_i is initial concentration and C_f is final concentration/concentration of sample.

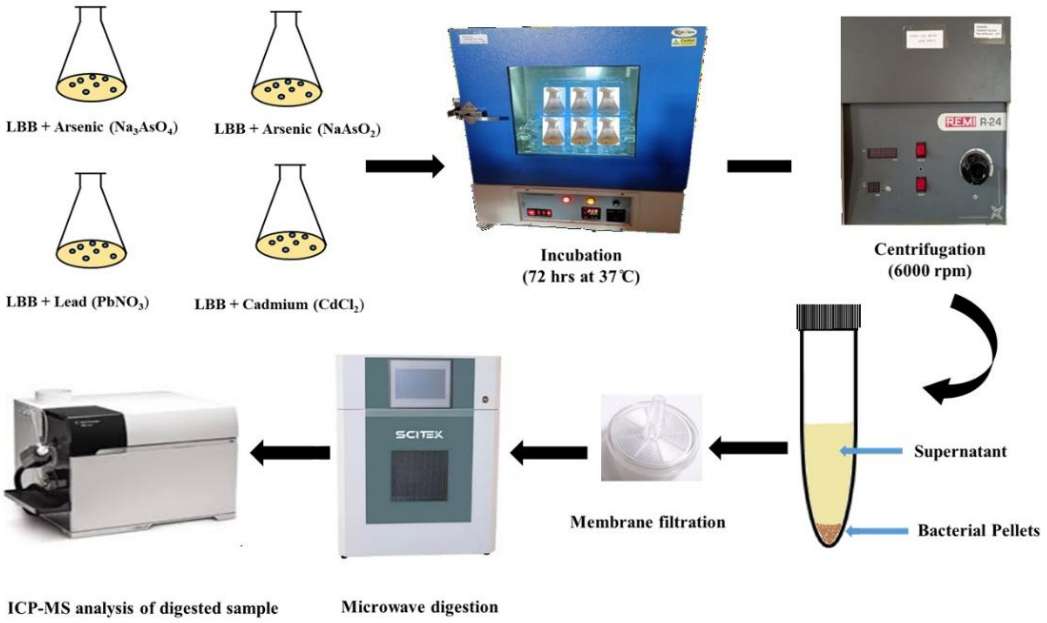

Figure 3. Bioremediation study of bacterial strain AS3, AS4 and AS11 in presence of selected HMs

3.18. *Estimation of ammonia production*

Qualitative estimation of ammonia was done by following the methodology of Sharma et al. (2021), with slight modification. Peptone broth (Appendix I) was utilized for the experiment. Initially, the bacterial strains were cultured in test tubes containing 10 mL peptone broth and incubated in an orbital incubator shaker with an agitation of 160 rpm at 37 ºC for 3 days. After the incubation, the test tubes containing the bacterial broth cultures were checked for ammonia production by adding of 1mL of Nessler's reagent (Appendix I). Indications of light yellow to dark yellow and finally to orange colour of the bacterial broth cultures indicated low to medium to high production of ammonia, respectively.

Further, quantification of ammonia was done, following the methodology as described by Raud et al. (2013). Briefly, 1.0 mL of bacterial culture broth was taken

after incubation as per qualitative estimation, and further centrifuged at 4000 × g. To the supernatant, 2 mL of Nessler's reagent was added and mixed by vortexing. Further, the reaction mixture was kept at room temperature for 15 minutes, till appearance of a yellow to brown colour and finally the produced ammonia was spectrophotometrically measured at 425 nm. A standard curve was prepared using ammonia at a range of 20-100 µg/mL. During the analysis precipitate are produced and interfere with the spectrophotometric analysis. Thus, the samples were centrifuged at 4000 × g for 5 minutes and the resultant clear supernatant was used for the study.

3.19. *Evaluation of indole acetic acid (IAA) production*

The production of IAA was measured following the methodology of Widawati (2020) with slight modifications. Tryptic soy broth (TSB) medium (100 mL) supplemented with L-Tryptophan (100 mg/mL) (Appendix I) served as the culture medium for culturing the selected bacterial strains. After the inoculation, the cultures were incubated in an orbital incubator shaker at 37 ºC with 160 rpm for 48 hours until turbidity was observed in the culture medium. After 48 hours, broth cultures were centrifuged at 8000 rpm for 10 minutes to recover the cell free culture supernatant (CFCS). Afterwards, 1 mL of CFCS was mixed slowly with 2 mL of Salkowski reagent (Appendix I), and incubated at room temperature in dark for about 20 minutes. The qualitative indication of IAA presence was indicated by the appearance of pinkish colouration of the reaction mixture solution. The quantification of IAA was done with the help of UV-Vis Spectrophotometer at a wavelength of 530 nm for all the bacterial strains. IAA in the sample was estimated with the help of IAA standard curve (20 µg/mL–100 µg/mL). Uninoculated TSB medium (1mL) with Salkowski reagent (2mL) served as control.

3.20. *Phytotoxicity study*

The phytotoxicity of tested HMs in the presence of selected bacterial strains was evaluated using the standard protocol of Gidudu and Chirwa (2022) with some modifications. Healthy and good quality seeds of Mung bean (*Vigna radiata*) were used for the assay. Initially, the bacterial strains were cultured in Erlenmeyer flasks with 100 mL of LB broth medium individually supplemented with selected HMs at their respective MTC. The cultures were incubated for 72 hours with an agitation of

160 rpm at 37 ºC. Selected HMs at MTC without the bacterial strains were maintained as blank. After the incubation period, the broth cultures were centrifuged at 6000 rpm. The cell free culture supernatant (CFCS) was collected, passed through a membrane filter (0.22 µm) (Whatman) and the resultant filtrate was used for the phytotoxicity assay.

Toxicity was determined in cleaned glass Petri dishes (90 × 15 mm) containing one Whatman Filter Paper (Grade No.1 Size 110 mm) each. Initially, twelve healthy seeds were pre-treated with surface sterilizer 70 % (v/v) ethanol for 1 minute and were washed twice with sterile distilled water to remove the excess leftover ethanol fraction from the seeds. Afterwards, surface sterilized seeds were transferred in each Petri dish along with 1 mL of the filtered CFCS at room temperature. In a similar manner, sets with only selected bacterial strains individually, with only HMs individually, and with only distilled water together with 12 seeds for each treatment were served as control. The different treatments used in the experiment are mentioned in Table 7. After five days of incubation in dark at room temperature; seed germination and root elongation (≥5 mm) were evaluated. The germination index (GI), relative root length (RRL), and relative seed germination (RSG) and germination vigour index (GVI) were then calculated (Gidudu and Chirwa, 2022; Sencan et al., 2024) using the following equations (Equation 3.21 – 3.24).

$$\text{RSG \%} = \frac{\text{number of seeds germinated in the CFCS}}{\text{number of seeds germinated in the control}} \times 100\% \qquad \text{Equation 3.21}$$

$$\text{RRL \%} = \frac{\text{mean root length in the CFCS}}{\text{mean root length in the control}} \times 100\% \qquad \text{Equation 3.22}$$

$$\text{GI} = \frac{\text{\% of root growth} \times \text{\% of seed germination}}{100\ \%} \qquad \text{Equation 3.23}$$

$$\text{GVI} = \frac{\text{Seedlings length (mm)} \times \text{Germination Percentage (\%)}}{100} \qquad \text{Equation 3.24}$$

Table 7. Treatments for phytotoxicity assay

Sl No.	HM treatment	Treatment with selected bacterial strain	Type of treated HM salt in treatments	Concentration of HMs per 100 mL medium

1.	As^{5+}	*Lysinibacillus* sp. AS3	Na_3AsO_4	62500 ppm
2.	As^{3+}	*Lysinibacillus* sp. AS3	$NaAsO_2$	781.25 ppm
3.	Pb^{2+}	*Lysinibacillus* sp. AS3	$Pb(NO_3)_2$	6250 ppm
4.	Cd^{2+}	*Lysinibacillus* sp. AS3	$CdCl_2$	1562.50 ppm
5.	-	*Lysinibacillus* sp. AS3	_	0 ppm
6.	As^{5+}	*Lysinibacillus* sp. AS4	Na_3AsO_4	15625 ppm
7.	As^{3+}	*Lysinibacillus* sp. AS4	$NaAsO_2$	1562.50 ppm
8.	Pb^{2+}	*Lysinibacillus* sp. AS4	$Pb(NO_3)_2$	6250 ppm
9.	Cd^{2+}	*Lysinibacillus* sp. AS4	$CdCl_2$	1562.50 ppm
10.	-	*Lysinibacillus* sp. AS4	_	0 ppm
11.	As^{5+}	*Staphylococcus equorum* AS11	Na_3AsO_4	125000 ppm
12.	As^{3+}	*Staphylococcus equorum* AS11	$NaAsO_2$	781.25 ppm
13.	Pb^{2+}	*Staphylococcus equorum* AS11	$Pb(NO_3)_2$	6250 ppm
14.	Cd^{2+}	*Staphylococcus equorum* AS11	$CdCl_2$	48.82 ppm
15.	-	*Staphylococcus equorum* AS11	_	0 ppm
16.	-	Distilled water	_	0 ppm
17.	As^{5+}	Distilled water	Na_3AsO_4	62500
18.	As^{5+}	Distilled water	Na_3AsO_4	15625
19.	As^{5+}	Distilled water	Na_3AsO_4	125000
20.	As^{3+}	Distilled water	$NaAsO_2$	781.25
21.	As^{3+}	Distilled water	$NaAsO_2$	1562.50
22.	Pb^{2+}	Distilled water	$Pb(NO_3)_2$	6250
23.	Cd^{2+}	Distilled water	$CdCl_2$	1562.50
24.	Cd^{2+}	Distilled water	$CdCl_2$	48.82

3.21. *Brine shrimp toxicity study*

Artemia cysts brine shrimp eggs purchased from Megha Aqua Farms (MAF) Kochi, Kerala, India under the trade name MAF Peqon Artemia, were used for the study and cultured as per the instruction provided by the supplier. The methodology as described by Amutha et al. (2023) with slight modifications was used for the larvicidal assay. For the experiment, 2.5 g of NaCl was dissolved in 100 mL of distilled water. Afterwards, 0.5 g of brine shrimp eggs were added to the NaCl solution and

kept for 48 under a continuous white light exposed aerated condition. After 48 hours, the hatched larvae were separated with the help of a small dropper and 20 larvae were transferred to each test tube containing selected HM solutions which was prepared based on MTC values of the strains AS3, AS4 and AS11 together with the individual bacterial strain. In a similar fashion, sets with only selected bacterial strains individually, with only HMs individually, and with only distilled water together with 20 larvae for each treatment were served as control. The list of treatment is presented in Table 8. Triplicates were used for each treatment. The mortality of the shrimp larvae was recorded after 24 hours. Abbot's formula was used to calculate the percentage of mortality (Amutha et al., 2023) and it represented as equation 3.25,

$$\text{Mortality } (\%) = \left(\frac{Y}{X}\right) \times 100 \qquad \text{Equation 3.25}$$

Where, X is the number of larvae in control (distilled water) and Y is number of larvae died after treatment.

Table 8. Treatments for brine shrimp toxicity study

Sl No.	HM treatment	Treatment with selected bacterial strain	Type of treated HM salt used	Concentration of HMs
1.	As^{5+}	*Lysinibacillus* sp. AS3	Na_3AsO_4	62500 ppm
2.	As^{3+}	*Lysinibacillus* sp. AS3	$NaAsO_2$	781.25 ppm
3.	Pb^{2+}	*Lysinibacillus* sp. AS3	$Pb(NO_3)_2$	6250 ppm
4.	Cd^{2+}	*Lysinibacillus* sp. AS3	$CdCl_2$	1562.50 ppm
5.	-	*Lysinibacillus* sp. AS3	_	0 ppm
6.	As^{5+}	*Lysinibacillus* sp. AS4	Na_3AsO_4	15625 ppm
7.	As^{3+}	*Lysinibacillus* sp. AS4	$NaAsO_2$	1562.50 ppm
8.	Pb^{2+}	*Lysinibacillus* sp. AS4	$Pb(NO_3)_2$	6250 ppm
9.	Cd^{2+}	*Lysinibacillus* sp. AS4	$CdCl_2$	1562.50 ppm
10.	-	*Lysinibacillus* sp. AS4	_	0 ppm
11.	As^{5+}	*Staphylococcus equorum* AS11	Na_3AsO_4	125000 ppm
12.	As^{3+}	*Staphylococcus equorum* AS11	$NaAsO_2$	781.25 ppm

13.	Pb^{2+}	*Staphylococcus equorum* AS11	$Pb(NO_3)_2$	6250 ppm
14.	Cd^{2+}	*Staphylococcus equorum* AS11	$CdCl_2$	48.82 ppm
15.	-	*Staphylococcus equorum* AS11	_	0 ppm
16.	-	Distilled water	_	0 ppm
17.	As^{5+}	Distilled water	Na_3AsO_4	62500 ppm
18.	As^{5+}	Distilled water	Na_3AsO_4	15625 ppm
19.	As^{5+}	Distilled water	Na_3AsO_4	125000 ppm
20.	As^{3+}	Distilled water	$NaAsO_2$	781.25 ppm
21.	As^{3+}	Distilled water	$NaAsO_2$	1562.50 ppm
22.	Pb^{2+}	Distilled water	$Pb(NO_3)_2$	6250 ppm
23.	Cd^{2+}	Distilled water	$CdCl_2$	1562.50 ppm
24.	Cd^{2+}	Distilled water	$CdCl_2$	48.82 ppm

3.22. *Statistical analysis*

All the experiments were conducted in triplicate and analysed statistically using SPSS (Statistical Package for Social Sciences) software. The obtained values were expressed as mean ± standard deviation (SD). The experimental data were checked for one-way analysis (ANOVA) at $P \leq 0.05$ confidence level.

4.1. *Study area and sample collection*

The collected soil samples were wet and had yellowish precipitation of acid mine drainage (AMD). The six sampling sites (i) 26º 26’ 4.10’’ N; 94º 25’ 18.23’’ E, (ii) 26º 26’ 3.28’’ N; 94º 25’ 16.09’’ E, (iii) 26º 25’ 59.38’’ N; 94º 25’ 18.04’’ E, (iv) 26º 24’ 57.87’’ N; 94º 22’ 52.17’’ E, (v) 26º 24’ 55.95’’ N; 94º 22’ 51.80’’ E, and (vi) 26º 24’ 53.03’’ N; 94º 22’ 47.61’’ E were mapped with the help of Google Earth Pro (Version 7.3) and the same is shown in figure 4a and 4b.

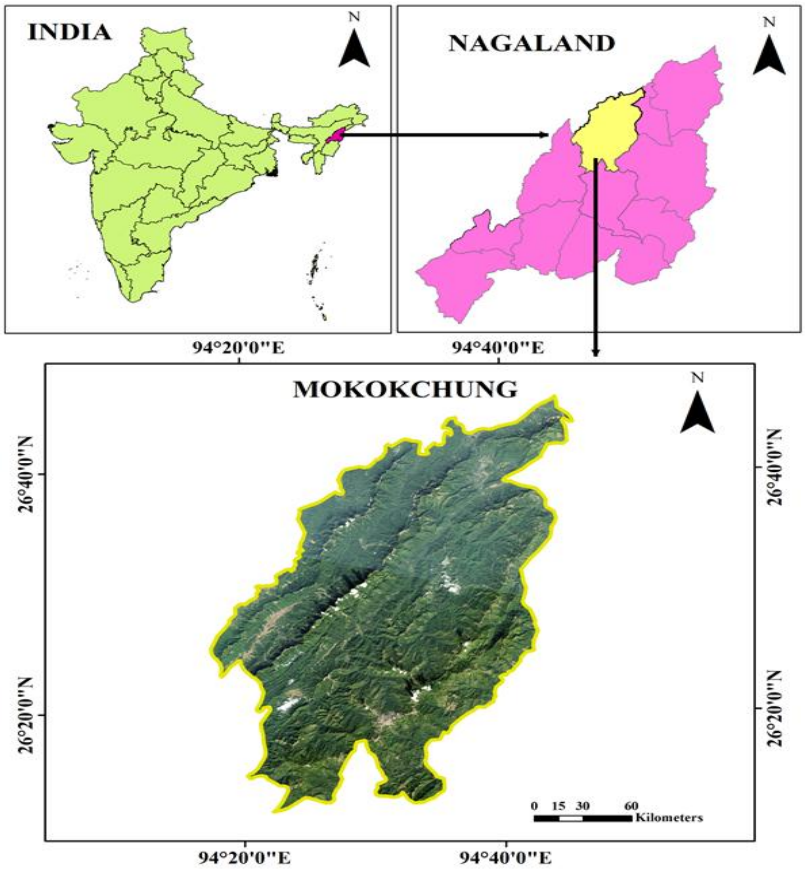

Figure 4a. Map of Mokokchung district

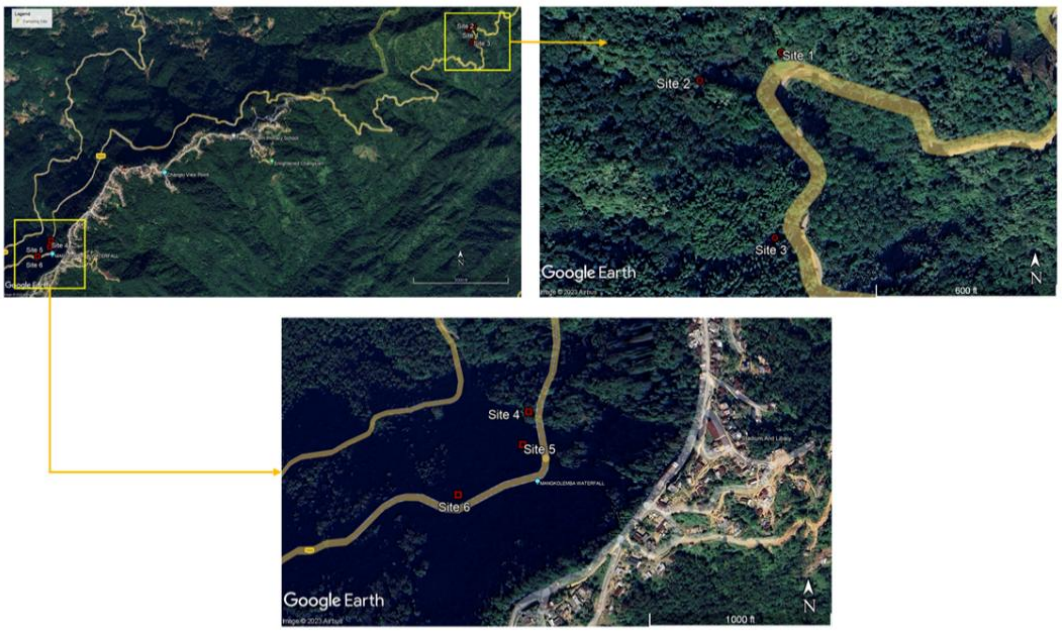

Figure 4b. Sampling sites of the study area

4.2. *Physico-chemical characteristics of the soil*

4.2.1. *Electrical conductivity*, *pH*, *and temperature*

The observed electrical conductivity (EC) values indicated that soil samples from Site 1 had the highest EC value (5.71 ± 0.113 mS), while the samples from Site 5 had the lowest value (2.38 ± 0.006 mS) as indicated in Table 9.

Table 9. EC value of soil samples collected from the sampling sites

Sampling site	EC (mS)
Site 1	5.71 ± 0.113
Site 2	5.307 ± 0.015
Site 3	5.317 ± 0.067
Site 4	3.247 ± 0.032
Site 5	2.383 ± 0.006
Site 6	2.753 ± 0.015

The pH values of all the collected soil samples were around acidic pH (5.1-5.6) as shown in Table 10. Soil sample from site 4 had the highest pH (5.576 ± 0.015), while Site 3 had the lowest pH (5.177 ± 0.015).

Table 10. pH value of collected soil samples

Sampling site	pH
Site 1	5.347 ± 0.181
Site 2	5.307 ± 0.015
Site 3	5.177 ± 0.015
Site 4	5.576 ± 0.015
Site 5	5.18 ± 0.01
Site 6	5.553 ± 0.032

The readings of the soil temperature indicated that Site 4 had highest temperature (23.7 ºC), followed by Site 5 (22.8 ºC), Site 6 (22.4 ºC), Site 3 (21.2 ºC), Site 2 (20.1 ºC) and Site 1 (19.8 ºC) with the lowest temperature.

4.2.2. Available K

The available K (kg/ha) was found to be highest in the soil samples of Site 4 (107.744 ± 0.224), while the lowest in soil samples of Site 1 (89.002 ± 0.466) as shown in Table 11.

Table 11. Available K in collected soil samples

Sampling site	Available K (kg/ha)
Site 1	89.002 ± 0.466
Site 2	95.872 ± 1.568
Site 3	107.147 ± 0.563
Site 4	107.744 ± 0.224
Site 5	92.810 ± 0.129
Site 6	101.770 ± 0.466

4.2.3. *Soil moisture*

The soil moisture was found to be highest in the soil samples from Site 3 (23.831 ± 1.756), while it was found to be lowest in the soil samples from Site 2 (18.703 ± 1.011) as shown in Table 12.

Table 12. Soil moisture content in the collected soil samples

Sampling site	Moisture %
S1	23.092 ± 3.099
S2	18.703 ± 1.011
S3	23.831 ± 1.756
S4	18.918 ± 2.744
S5	21.022 ± 4.189
S6	21.011 ± 0.899

4.2.4. *N estimation*

The available N (kg/acre) was found to be highest in the soil samples from Site 3 (184.442 ± 2.931), while it was found to be lowest in soil samples collected from Site 2 (52.456 ± 11.723) as shown in Table 13.

Table 13. Available N for collected soil samples

Sampling site	Total N (kg/acre)
S1	67.685 ± 10.567
S2	52.456 ± 11.723
S3	184.442 ± 2.931
S4	77.838 ± 14.654
S5	93.067 ± 19.219
S6	65.993 ± 8.793

4.2.5. *Total organic carbon (TOC)*

The estimated values of TOC in percentage are given in Table 14. Soil samples collected from Site 5 had the highest percentage of TOC (2.252 ± 0.903 %), while soil samples from Site 4 had the lowest percentage of TOC (1.107 ± 0.058 %).

Table 14. TOC of collected soil samples

Sampling site	TOC (%)

S1	1.262 ± 0.089
S2	1.281 ± 0.117
S3	1.476 ± 0.187
S4	1.107 ± 0.058
S5	2.252 ±0.903
S6	1.417 ±0.178

4.2.6. *Available P*

The available phosphorous (kg/ha) was found to be highest in the soil samples collected from Site 6 (1.839 ± 0.042), while it was found to be lowest for the soil samples collected from Site 1 (1.228 ± 0.018) as presented in Table 15.

Table 15. Available P in the collected soil samples

Sampling site	**P (kg/ha)**
S1	1.228 ± 0.018
S2	1.769 ± 0.004
S3	1.700 ± 0.043
S4	1.546 ± 0.020
S5	1.478 ± 0.045
S6	1.839 ± 0.042

4.2.7. *HM analysis of collected soil samples*

The HM analysis of the soil samples collected from the six sampling sites revealed presence of the HMs *i.e.* As, Cd and Pb and the same is presented in Table 16. Site 1 had highest concentration of As per gram of soil (1.63 ± 0.15 ppm) while site 3 had lowest concentration for As (0.75 ± 0.07 ppm). For Cd, highest concentration was observed in Site 6 (0.095 ± 0.01 ppm), and lowest in Site 3 (0.06 ± 0.008 ppm). In case of Pb, highest concentration was observed in Site 6 (13.09 ± 1.80 ppm), while Site 3 (8.46 ± 1.14 ppm) had the lowest concentration.

Table 16. Concentration of As, Cd and Pb in the collected soil samples

Sampling site	As (ppm)	Cd (ppm)	Pb (ppm)
Site 1	1.63 ± 0.15	0.092 ± 0.014	11.85 ± 1.66
Site 2	1.40 ± 0.05	0.091 ± 0.005	12.05 ± 0.79
Site 3	0.75 ± 0.07	0.06 ± 0.008	8.46 ± 1.14
Site 4	0.91 ± 0.05	0.07 ± 0.006	9.51 ± 0.74
Site 5	1.25 ± 0.12	0.08 ± 0.01	10.41 ± 1.36
Site 6	1.53 ± 0.16	0.095 ± 0.01	13.09 ± 1.80

4.3. *Isolation of As-resistant bacteria*

After completing the third cycle of enrichment culture, followed by serial dilution (Figure 5a and 5b) and spread plate technique, ten bacterial isolates appeared from Site 1, 2 and 3 that could grow in an As-loaded medium, while no arsenic resistant isolates were observed from Site 4, 5 and 6 (Table 17). These ten isolates were further assessed for their tolerance for As, based on the obtained MTC values. Eventually, three bacterial isolates, namely AS3, AS4 and AS11, were selected.

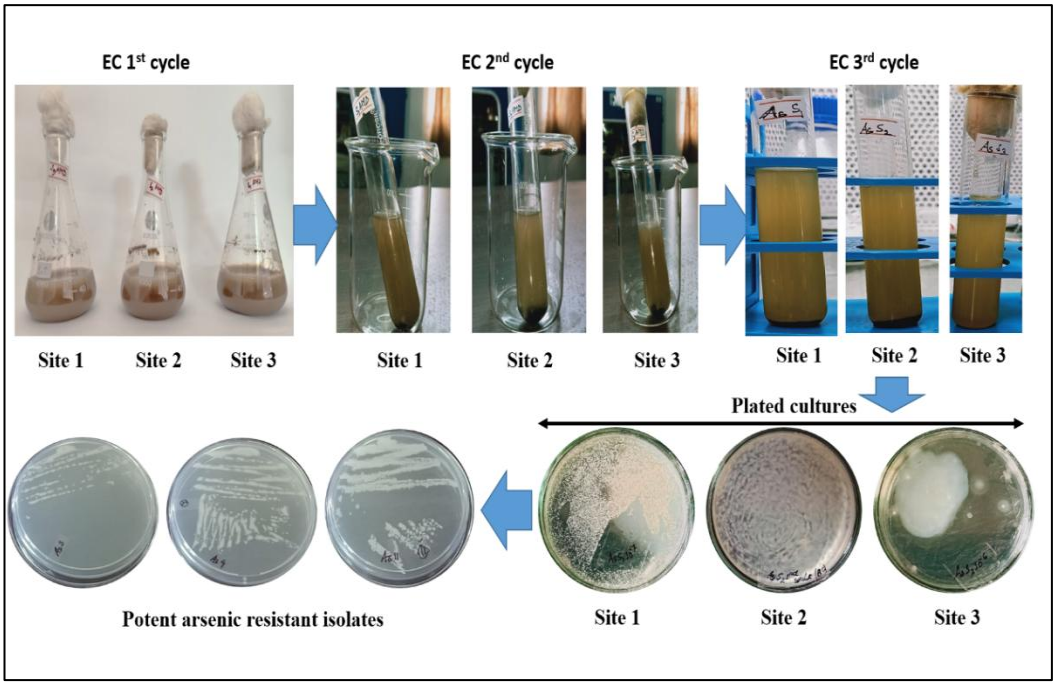

Figure 5a. Enrichment culture method for isolation of As resistant isolates from site 1, 2 and 3

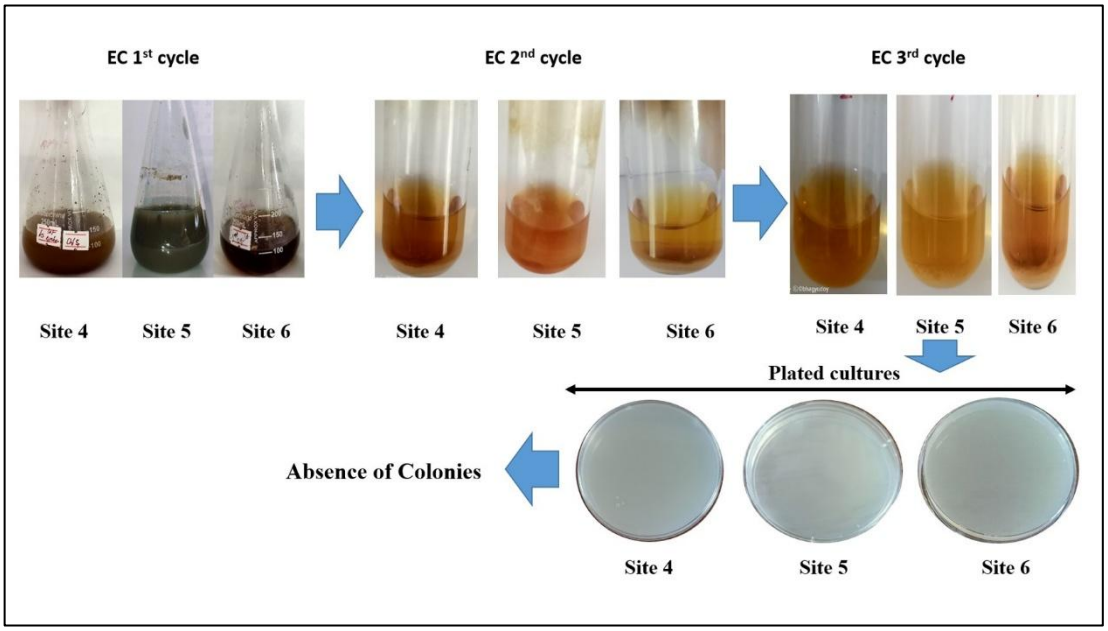

Figure 5b. Enrichment culture method for isolation of As resistant isolates from site 4, 5 and 6

Table 17. Morphological characterization of the As-resistant isolates

Sl No	Isolate	Shape	Margin	Elevation	Texture	Colour	Opacity
				Site 1			
1.	As 11	Round	Entire	Raised	Shiny	Whitish	Opaque
2.	Cd6	Irregular	Filiform	Flat	Dull	Pale white	Opaque
3.	Cd10	Punctiform	Entire	Raised	Shiny	Creamy	Opaque
				Site 2			
4.	AS1	Irregular	Undulated	Flat	Shiny	Creamy	Opaque
5.	As 3	Irregular	Undulated	Raised	Shiny	Creamy	Opaque
6.	As 4	Round	Entire	Raised	Shiny	Creamy	Opaque
				Site 3			
7.	AS8	Punctiform	Entire	Raised	Shiny	Creamy	Opaque
8.	AS10	Irregular	Undulated	Raised	Dull	Pale yellow	Opaque

9.	Pb1	Punctiform	Entire	Flat	Shiny	Creamy	Opaque
10.	Pb6	Irregular	Undulated	Raised	Dull	Pale white	Opaque

4.4. Screening of potential As-resistant bacteria

The MIC, MBC, and MTC values of the chosen bacterial isolates against the selected HMs are shown in Table 18. According to the results of MIC, MBC and MTC, the bacterial isolate AS3 was shown to be least tolerant of As^{3+} HM ions up to a concentration of 781.25 ppm followed by Cd^{2+} up to 1562.50 ppm, and Pb^{2+} up to 6250 ppm, and extremely tolerant of As^{5+} HM ions up to a concentration of 62500 ppm. On the other hand, strain AS4 was found to be least tolerant to both As^{3+} (1562.50 ppm) and Cd^{2+} (1562.50 ppm) HM ions, followed by Pb^{2+} (6250 ppm), with highest tolerance to As^{5+} (15625 ppm) HM ions. Similarly, AS11 was found to be least tolerant to Cd^{2+} (48.22 ppm), followed by As^{3+} (781.25 ppm), Pb^{2+} (6250 ppm) and As^{5+} (125000 ppm).

Table 18. MIC, MTC and MBC of selected isolates against selected HMs

Bacterial isolate	Type of HMs tested	MIC (ppm)	MBC (ppm)	MTC (ppm)
AS3	Na_3AsO_4	125000	125000	62500
	$NaAsO_2$	1562.50	1562.50	781.25
	$Pb(NO_3)_2$	12500	12500	6250
	$CdCl_2$	3125	3125	1562.50
AS4	Na_3AsO_4	31250	31250	15625
	$NaAsO_2$	3125	3125	1562.50
	$Pb(NO_3)_2$	12500	12500	6250
	$CdCl_2$	3125	3125	1562.50
AS11	Na_3AsO_4	250000	250000	125000
	$NaAsO_2$	1562.50	1562.50	781.25
	$Pb(NO_3)_2$	12500	12500	6250
	$CdCl_2$	97.64	97.64	48.82

4.5. Characterization of selected potential As-resistant bacterial isolates

4.5.1. *Biochemical characterization of selected bacterial isolates*

The biochemical characteristics of the isolates are presented in Table 19.

Table 19. Biochemical properties of the selected bacterial isolate

Sl No.	Parameters	AS3	AS4	AS11
1.	Catalase	+ve	+ve	+ve
2.	Oxidase	+ve	+ve	+ve
3.	Motility	+ve	+ve	-ve
4.	Indole	-ve	-ve	-ve
5.	Citrate utilization	-ve	-ve	-ve
6.	Methyl Red	-ve	-ve	+ve
7.	Voges–Proskauer	-ve	-ve	-ve
8.	Glucose fermentation	-ve	-ve	-ve
9.	Lactose fermentation.	-ve	-ve	-ve
10.	Sucrose fermentation	-ve	-ve	-ve
11.	Gram Staining	+ve	+ve	+ve
12.	Urea	+ve	+ve	+ve
13.	Spore formation	+ve	+ve	-ve

4.5.2. *Molecular characterization of selected bacterial isolates*

The spectral analysis of the extracted g-DNA from the selected bacterial isolate AS3 and AS4 confirmed the quality of DNA and found to be suitable for PCR amplification. Data are presented in Table 20.

Table 20. Spectral analysis of genomic DNA of AS3 and AS4 isolates

Bacterial isolate	A_{260}/A_{280}	A_{260}/A_{230}	DNA concentration (ng/µL)
AS3	2.02	2.74	279.31
AS4	1.96	2.92	208.75

Through 16s ribosomal RNA gene sequencing approach, the chosen bacterial isolates were identified as *Lysinibacillus* sp. strain AS3 and *Lysinibacillus* sp. strain

AS4 (Figure 6 and 7). The obtained sequences were later submitted to the NCBI database with the accession numbers OQ202230 and OQ202231. The strain AS3 was found to be nearly 94 % similar to *Lysinibacillus* sp. strain R2-3-2 (MN696519), while strain AS4 was found to be closely 90 % similar to *Lysinibacillus* sp. strain AS3.

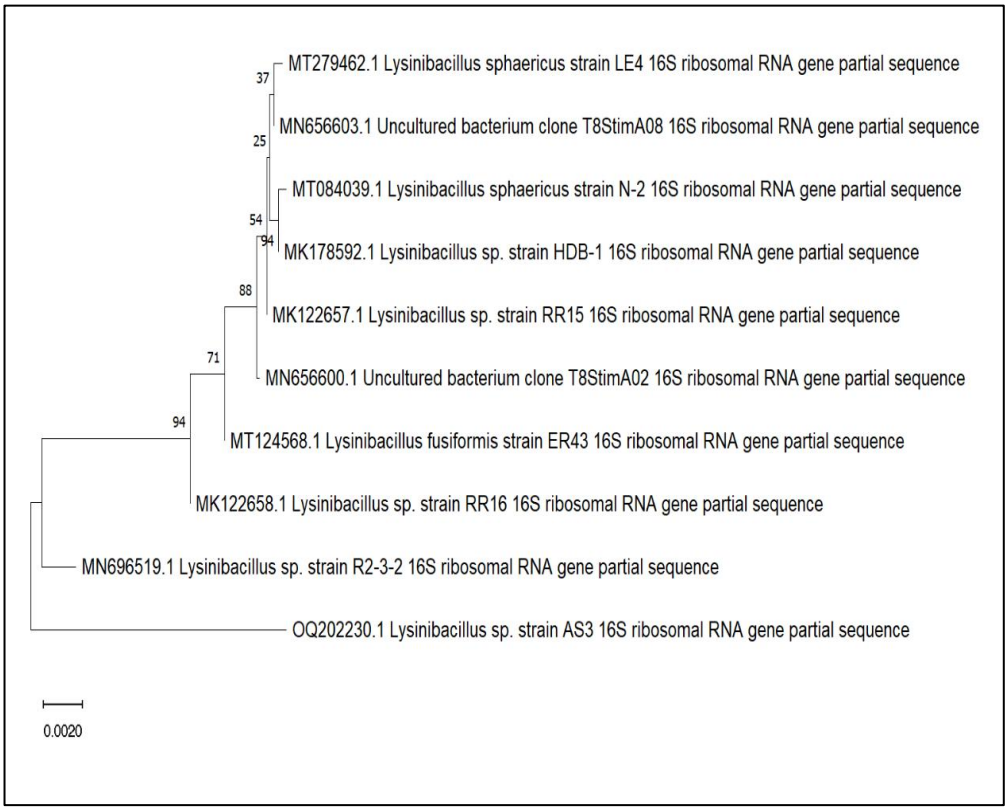

Figure 6. Phylogenetic tree of bacterial strain AS3

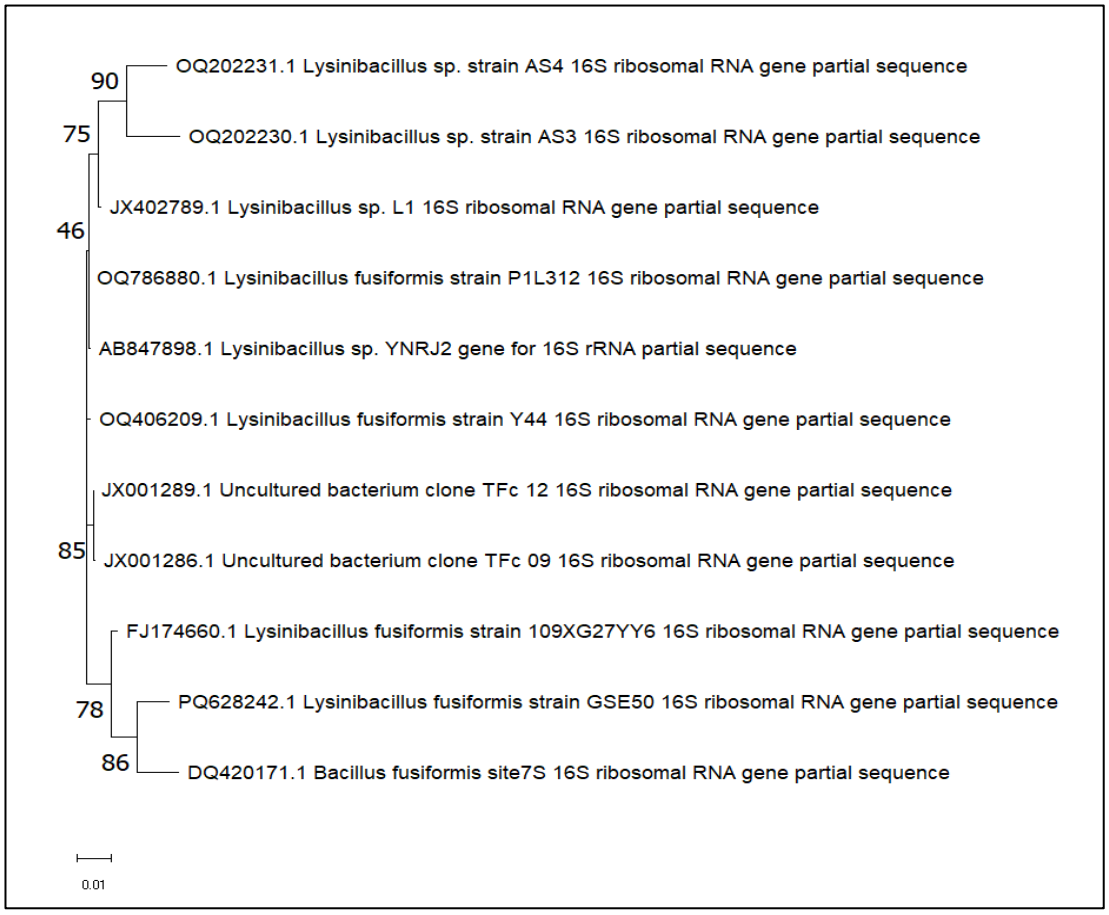

Figure 7. Phylogenetic tree of bacterial strain AS4

The assembled genome of AS11 isolate had 1,611 contigs, with the total length of 5,274,124 bp and an average G+C content of 51.58 % (Table 21).

Table 21. Genome assembly details of bacterial strain AS11

De Novo Assembly Software	**SPAdes (St. Petersburg) genome assembler v3.15.3**
Total No. Contigs	1611
GC Content	51.58
Contig	55
Genome Length	5274124
Contig N50	6970
Largest	225653

The closest reference and representative genomes with respect to AS11 isolate was found to be *Staphylococcus equorum* subsp. *equorum* Mu2 (Figure 8). The whole

genome of AS11 strain was submitted at NCBI database with the Accession ID of SAMN47297582.

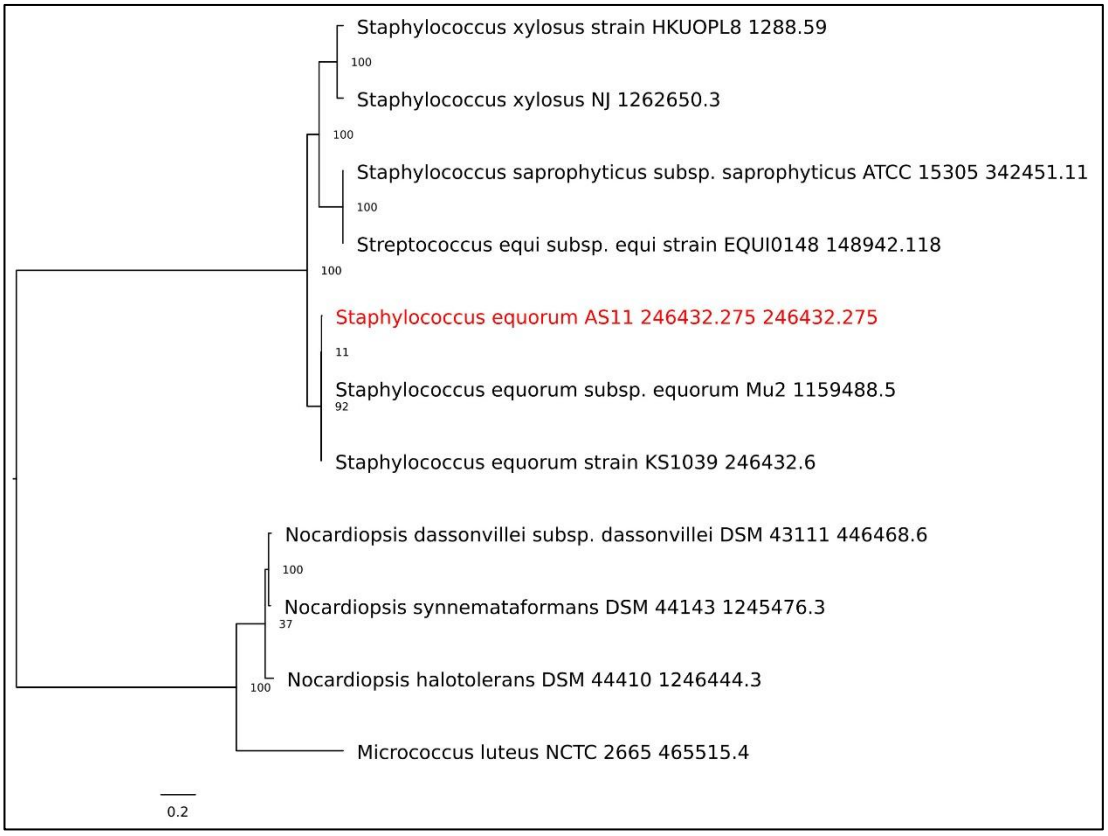

Figure 8. Phylogenetic tree of bacterial strain AS11

4.6. *Growth kinetics*

In the case of AS3 strain, prolonged lag phase and late exponential phase was observed in presence of As^{3+}, As^{5+} as well as Cd^{2+} HM ions (Figure 9, 10, 11, 12, and 13). In the presence of As^{5+} and Cd^{2+} HM ions, the lag phase was more prolonged which extended up to 12 hours compared to As^{3+} HM ions that lasts for 6 hours. Further, the stationary phase in the presence of both As^{5+} and As^{3+} HM ions was achieved after 72 hours with gradual decline of growth after 120 hours, while in the case of Cd^{2+} HM ions, exponential phase was achieved after 24 hours with a brief stationary phase followed by a sharp retardation in the growth after 48 hours. However, in the control (without any HM) and in the presence of Pb^{2+} an early initiation of exponential phase *i.e.* within 2 hours of incubation was observed and continued till 96 hours. Lastly, death/decline phase with sharp weakening of growth after 96 hours was

observed in the presence of Pb^{2+}. However, in control the growth was reduced gradually.

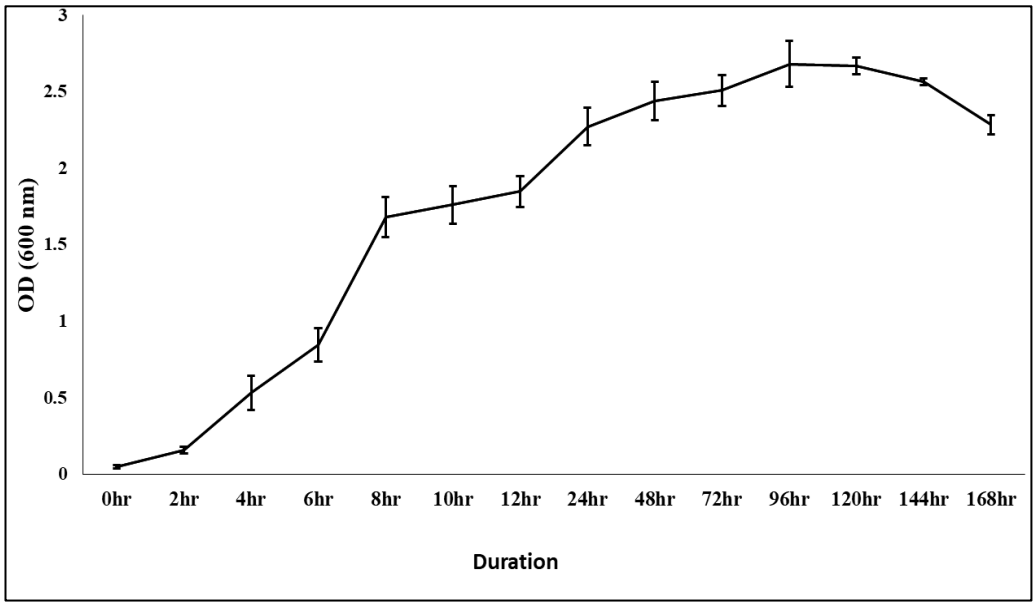

Figure 9. Growth curve of AS3 in control

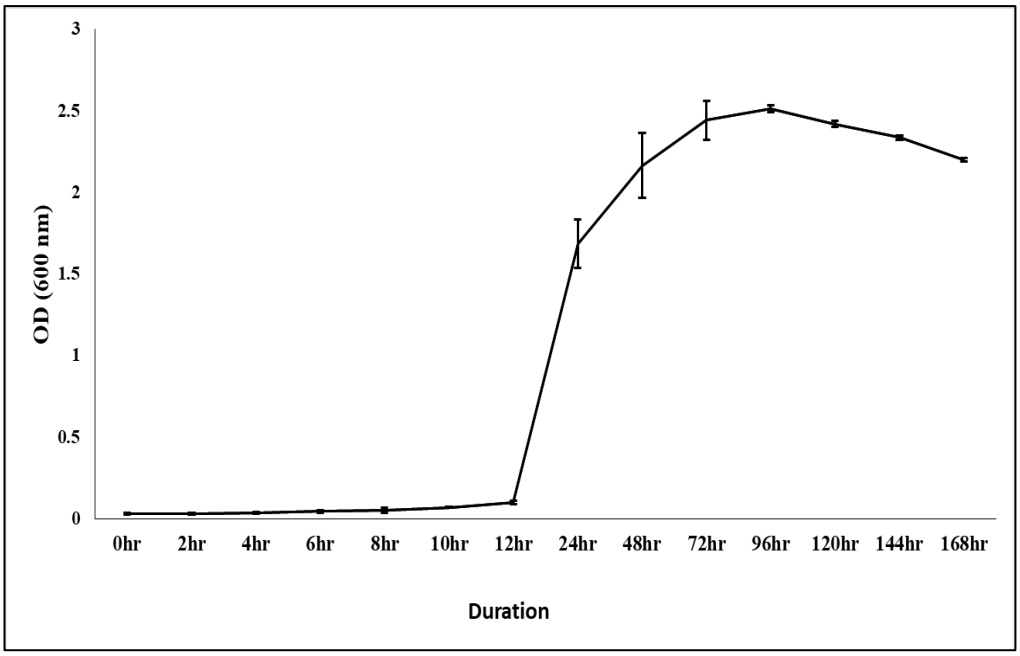

Figure 10. Growth curve of AS3 treated with As^{5+}

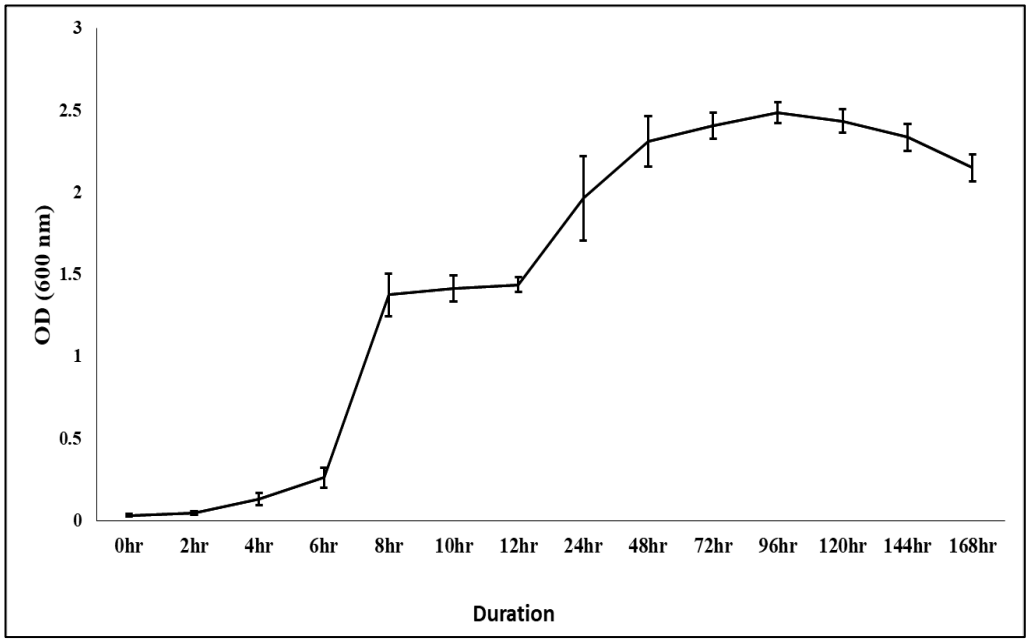

Figure 11. Growth curve of AS3 treated with As^{3+}

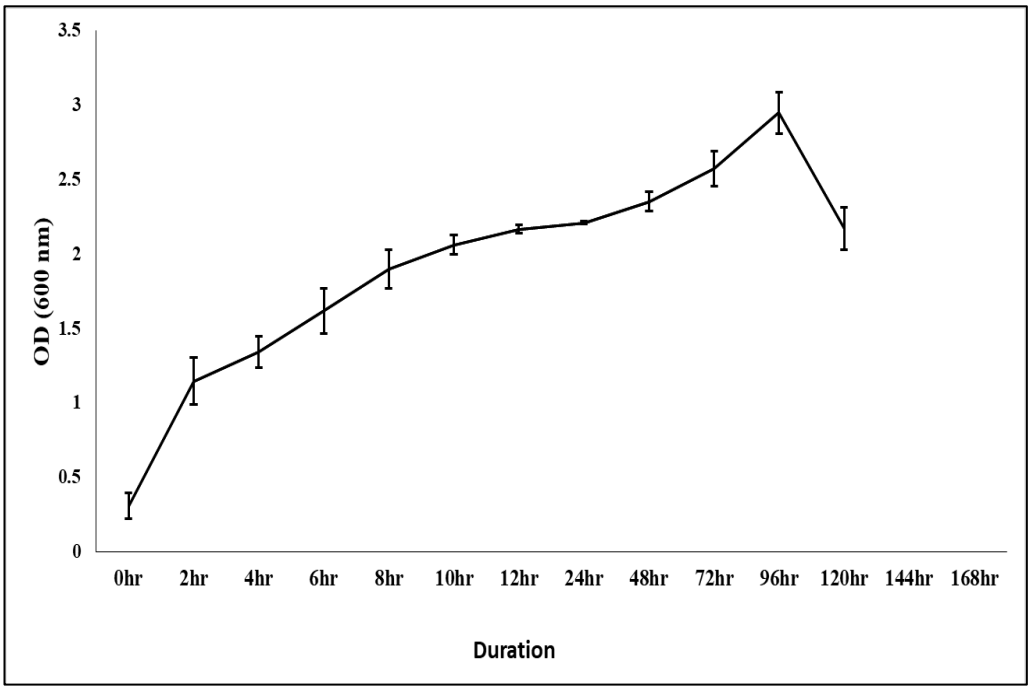

Figure 12. Growth curve of AS3 treated with Pb^{2+}

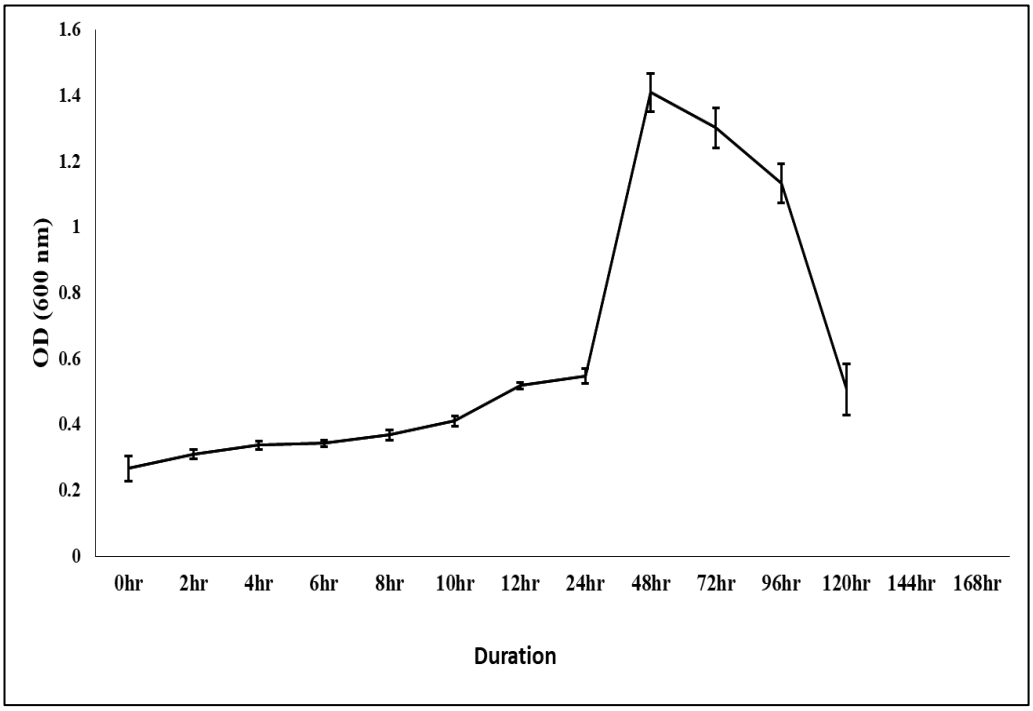

Figure 13. Growth curve of AS3 treated with Cd^{2+}

In the growth curves of AS4 strain in the presence of $As^{3+}$and Cd^{2+} HM ions showed a prolonged lag phase (Figure 14, 15, 16, 17, and 18). The lag phase in the presence of As^{5+} HM ions was found to be similar with that of the control. Further, an early exponential phase was seen after 2 hours of incubation in the presence of As^{5+}, Pb^{2+} and control and continued till approximately around 48 hours. On the other hand, in the presence of As^{3+} and Cd^{2+} exponential phase was initiated after 4 hour and 6 hours, respectively. The exponential phase was continued till 72 hours in the presence of As^{3+} and was not well defined in the presence of Cd^{2+}. Further, the stationary phase in the presence of As^{5+} and control was achieved after 48 hours with gradual decline of growth after 96 hours. In the presence of As^{3+} and Pb^{2+} HM ions, the stationary phase was attained after 72-96 hours and weakening of growth was observed thereafter. However, in the presence of Cd^{2+} the stationary phase was not well defined and attained within 24 hours of incubation followed by a sharp decline in the growth.

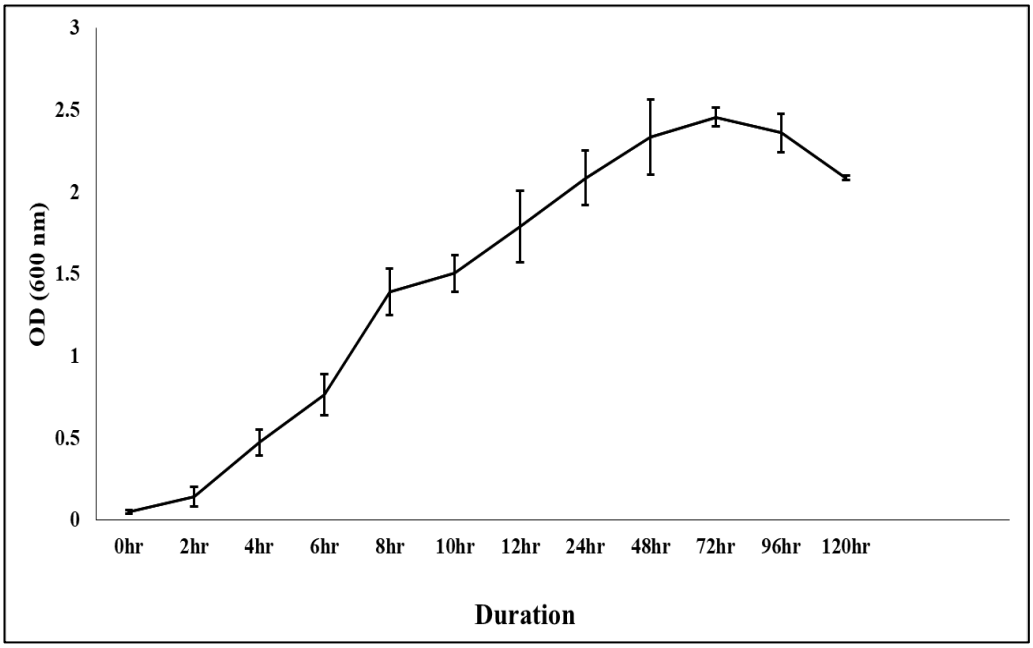

Figure 14. Growth curve of AS4 treated with control

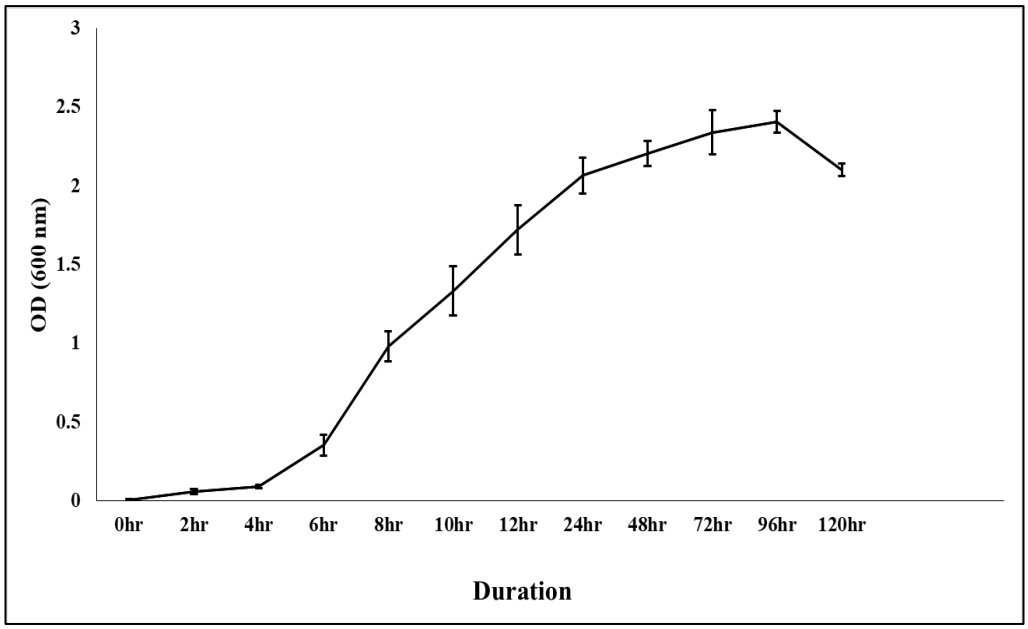

Figure 15. Growth curve of AS4 treated with As^{5+}

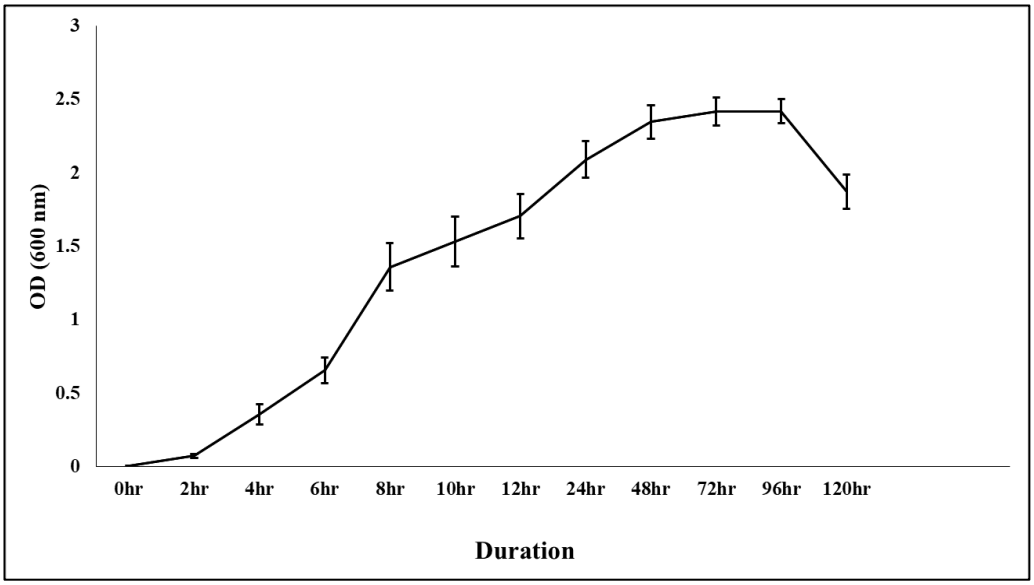

Figure 16. Growth curve of AS4 treated with As^{3+}

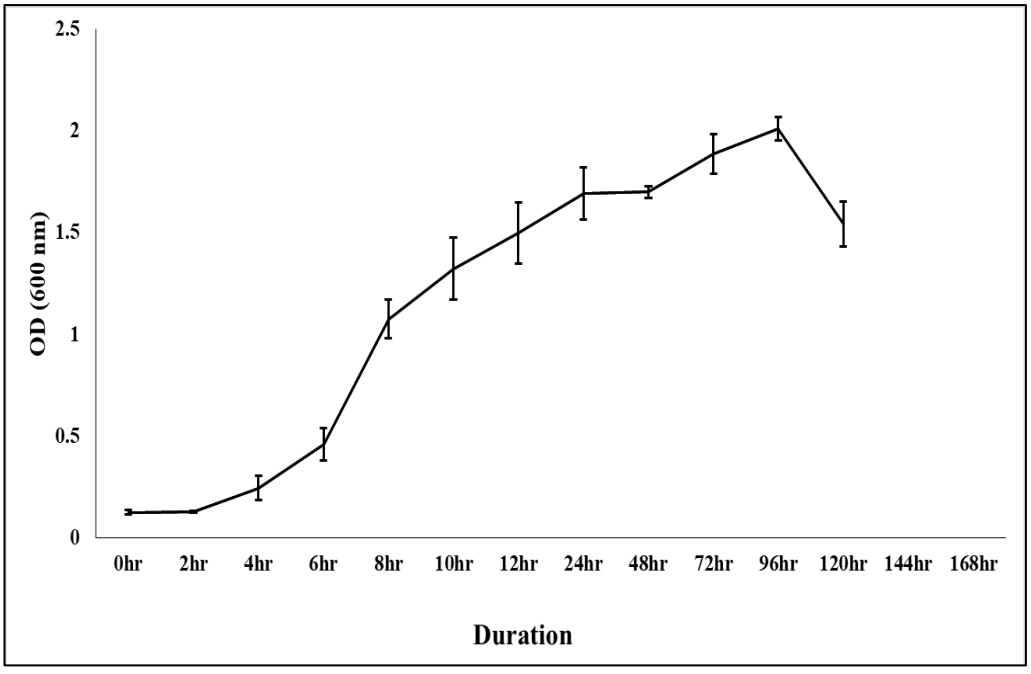

Figure 17. Growth curve of AS4 treated with Pb^{2+}

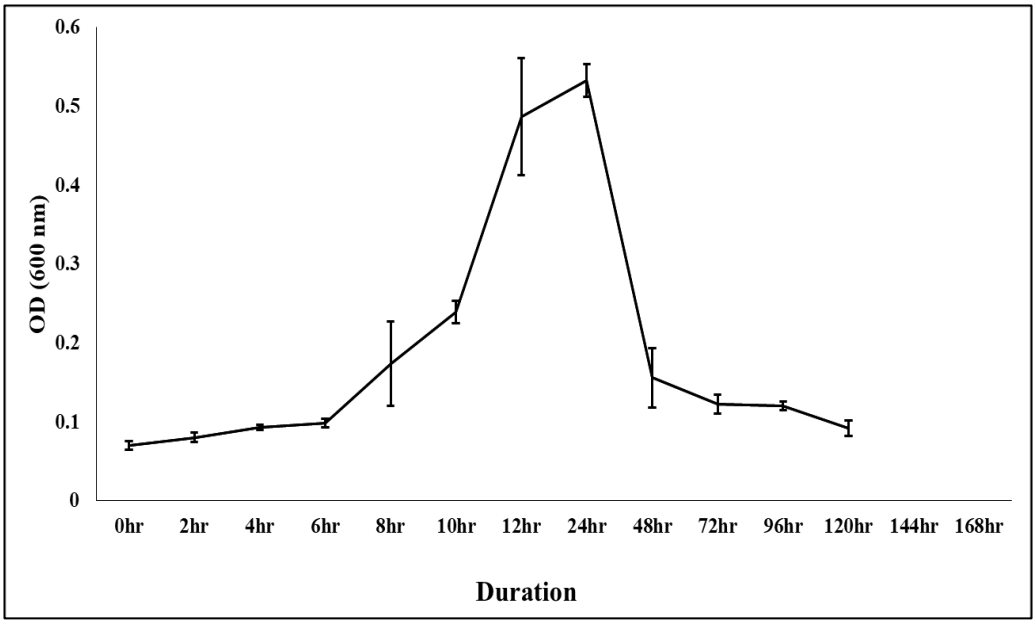

Figure 18. Growth curve of AS4 treated with Cd^{2+}

The growth curves of AS11 strain indicated that, in presence of As^{5+} and Cd^{2+} HM ions the lag phase was prolonged up to 12 hours (Figure 19, 20, 21, 22, and 23). However, the lag phase in As^{3+} treatment was up to 4 hours, similar to that of control. In control and As^{3+} treatment, the exponential phase was initiated almost after 4th hour, while As^{5+} and Cd^{2+} showed exponential phase after 12th hour. Unlike other HMs, early exponential phase was observed before 2nd hour in Pb^{2+} treatment. In control and As^{3+} stationary phase was attained after 48 hours while in the presence of As^{5+} and Pb^{2+} stationary phase achieved after 24 hours and was not well distinct in the presence of Cd^{2+}. Among the HMs, early death phase was observed in the presence of Pb^{2+} and As^{5+} after 48 hours, while in the presence of As^{3+} and Cd^{2+} death phase appeared after 96 hours. In control without HMs showed a prolonged stationary phase was observed and the death phase initiated only after 144 hours of incubation.

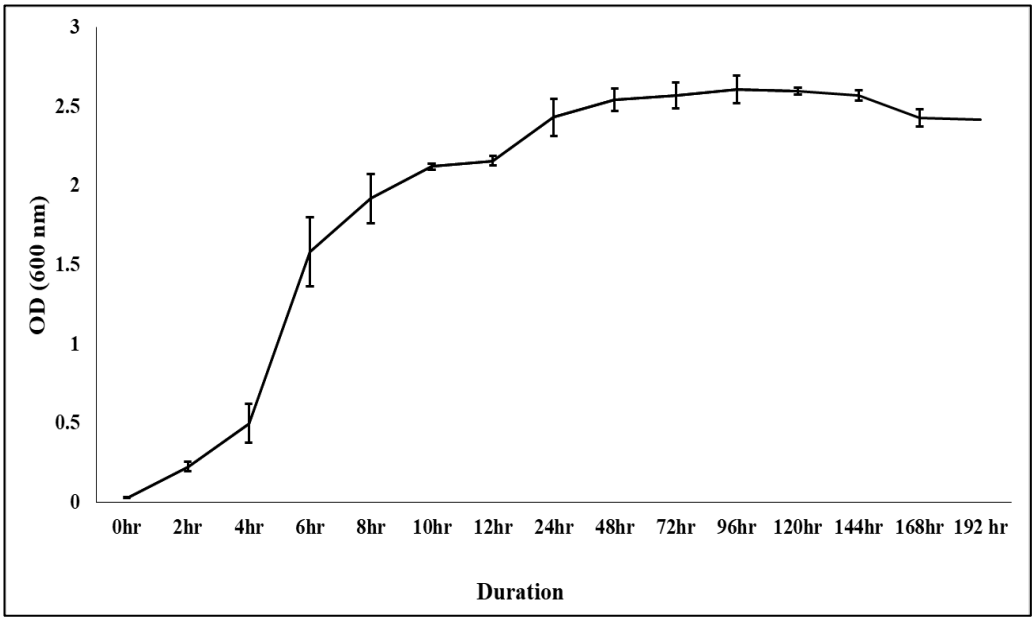

Figure 19. Growth curve of AS11 treated with control

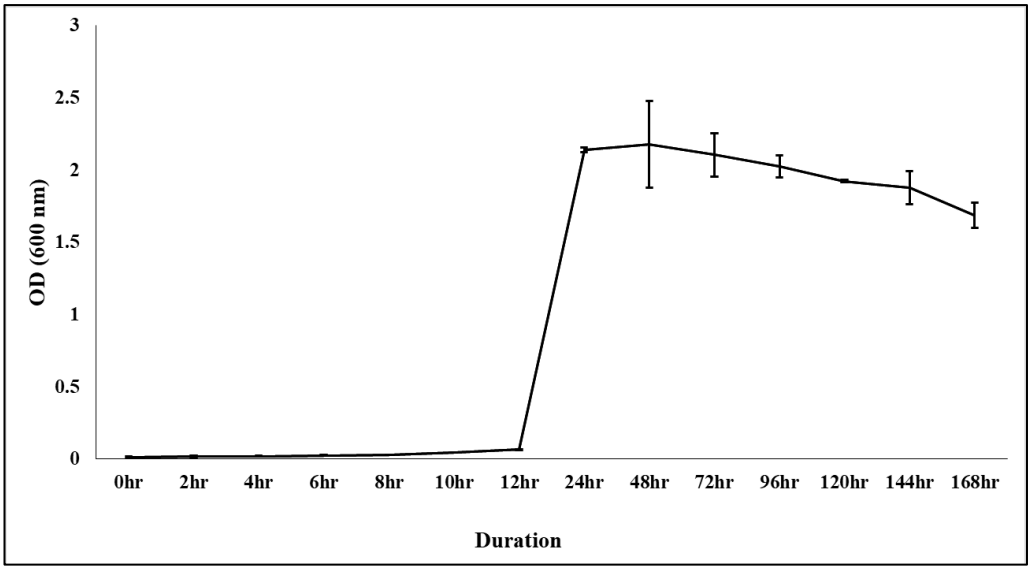

Figure 20. Growth curve of AS11 treated with As^{5+}

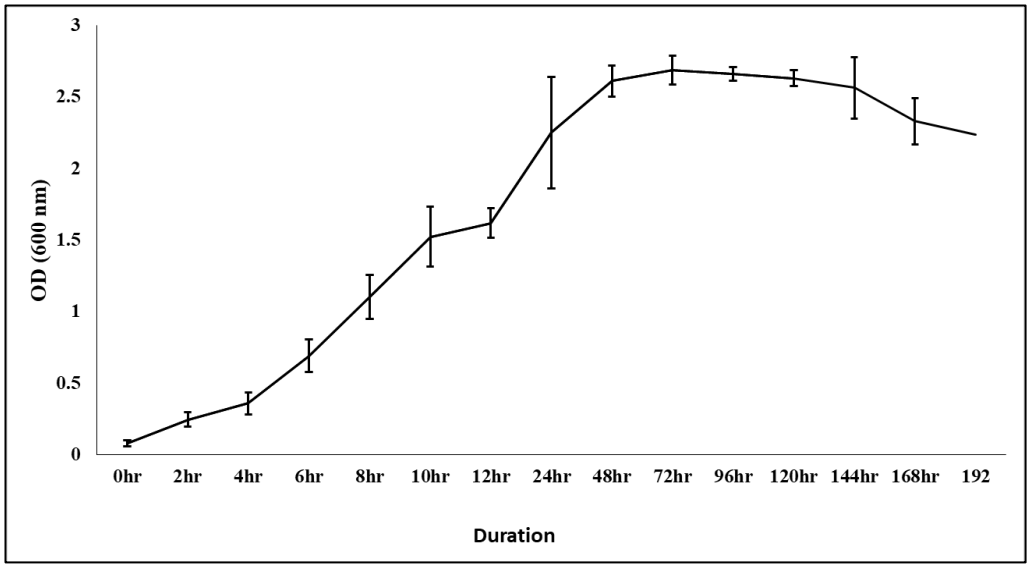

Figure 21. Growth curve of AS11 treated with As^{3+}

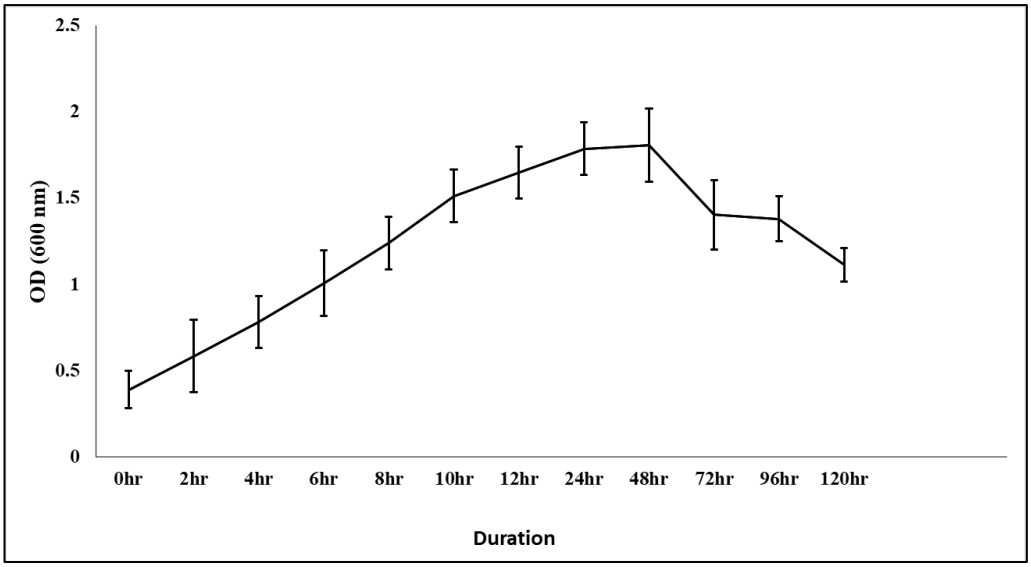

Figure 22. Growth curve of AS11 treated with Pb^{2+}

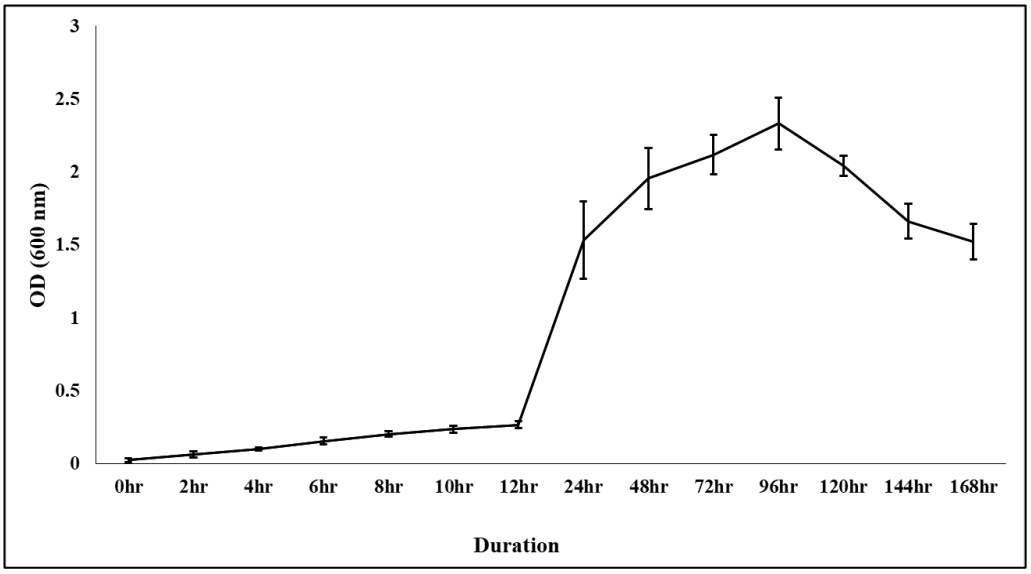

Figure 23. Growth curve of AS11 treated with Cd^{2+}

4.7. *Antibiotic susceptibility test and index*

Based on the antibiotic susceptibility assay, strain AS3 was found to be resistant to 8 major antibiotics, however, it was found to be susceptible to 6 other major antibiotics. Strain AS4 was found to be resistant to 6 major antibiotics and susceptible to the other 8 major antibiotics. Similarly, strain AS 11 was also found to be resistant to 6 major antibiotics and susceptible to the rest 8 major antibiotics. The diameter of growth inhibition zones (mm) showed by the selected strain in the presence of test antibiotics are presented in Table 22.

Table 22. Antibiotic susceptibility of strains AS3, AS4 and AS11

Antibiotics	Class of antibiotics	Range of activity	Zone of inhibition		
			AS 3	AS 4	AS 11
Tetracycline (30 mcg)	Tetracycline	Broad	0	28.67±1.16	29.67±0.58
Ampicillin (10 mcg)	β-lactam	Broad	0	0	0
Penicillin (0.6 mcg)	β-lactam	Narrow	0	0	0
Cefaloridine	β-lactam	Broad	0	0	0

(30 mcg)					
Kanamycin (5 mcg)	Amino-glycoside	Broad	0	0	18±1.73
Chloramphenicol (30 mcg)	Chloramphenicol	Broad	20	16.33±0.57	23
Streptomycin (10 mcg)	Aminoglycoside	Broad	0	14	21
Cephalexin (30 mcg)	Cephalosporin	Broad	0	23	0
Ciprofloxacin (5 mcg)	Quinolone	Broad	25.67±0.57	27	32
Azithromycin (15 mcg)	Macrolide	Broad	0	16	0
Norfloxacin (10 mcg)	Quinolone	Broad	14.67±0.58	0	23
Clarithromycin (15 mcg)	Macrolides	Broad	30.67±0.57	30	17
Erythromycin (15 mcg)	Macrolides	Broad	19	0	0
Amoxicillin (10 mcg)	Penicillin-type	Broad	34.33±0.58	40±0.58	31

The multiple antibiotic resistance (MAR) values of the present study indicated that the isolated As-resistant strains have high risk exposure to the tested antibiotics in which the MAR value recorded was 0.476, higher than the normal value of 0.2.

4.8. ***Evaluation of biofilm producing capacity***

4.8.1. *Biofilm producing capacity of the AS3 strain*

The qualitative assay for biofilm production in the presence of different HM treatments indicate the occurrence of lining on the tubes which confirm the biofilm producing capacity of AS3 strain. However, AS3 strain displayed comparatively frail lining development on the inner surface of the polypropylene tube and the same is displayed in figure 24. According to Table 23, the findings of quantitative assay based

on microtiter plate test showed that the AS3 strain unable to produce biofilm (0.49 ± 0.12) without the presence of HMs. However, biofilm development was boosted in the presence of HMs, with As^{5+} (1.09 ± 0.16) surpassing Pb^{2+} (1.02 ± 0.19) and As^{3+} (0.87 ± 0.28). Moreover, findings also showed that biofilm formation was absent when HM Cd^{2+} ions were present.

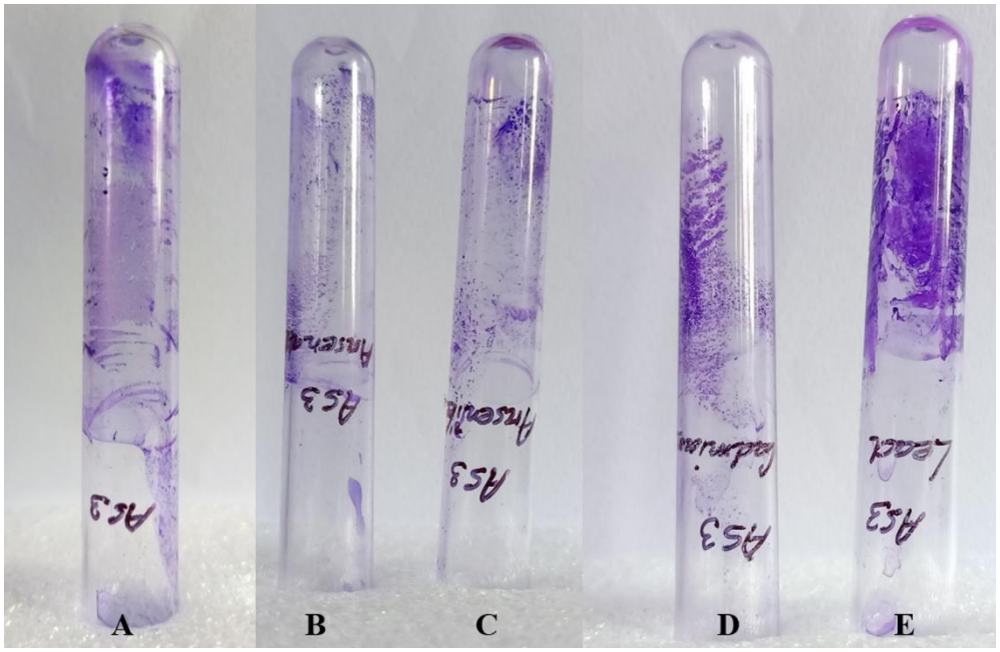

Figure 24. Tube method for the screening of biofilm production of AS3 strain in (A) control and in the presence (B) As^{5+}, (C) As^{3+}, (D) Cd^{2+}, and (E) Pb^{2+}

Table 23. Biofilm production capacity of the AS3 strain under different treatments

Test samples	Observed OD value	Biofilm forming potential
Bacterial strain AS3 without HM	0.49 ± 0.12	lack of biofilm since, OD < ODc
Bacterial strain AS3 with AS^{5+} ions	1.09 ± 0.16	weak biofilm (+ or 1) production since, ODc < OD < 2 × ODc
Bacterial strain AS3 with AS^{3+} ions	0.87 ± 0.28	weak biofilm (+ or 1) production since, ODc < OD < 2 × ODc
Bacterial strain AS3 with Pb^{2+} ions	1.02 ± 0.19	weak biofilm (+ or 1) production since, ODc < OD < 2 × ODc

Bacterial strain AS3 with Cd^{2+} ions	0.03 ± 0.01	lack of biofilm since, OD < ODc

4.8.2. *Biofilm producing capacity of the AS4 strain*

AS4 strain also showed weak lining formation on the inner surface of the polypropylene tube and the same is displayed in figure 25. According to table 24, the microtiter plate test findings showed that the AS4 strain was unable to produce biofilm (0.369 ± 0.2137) without the presence of HMs. On the other hand, biofilm development was boosted in the presence of HMs, with As^{5+} (1.144 ± 0.09) surpassing As^{3+} (0.727 ± 0.017). The findings also showed that biofilm formation was absent when Cd^{2+} and Pb^{2+} ions were present.

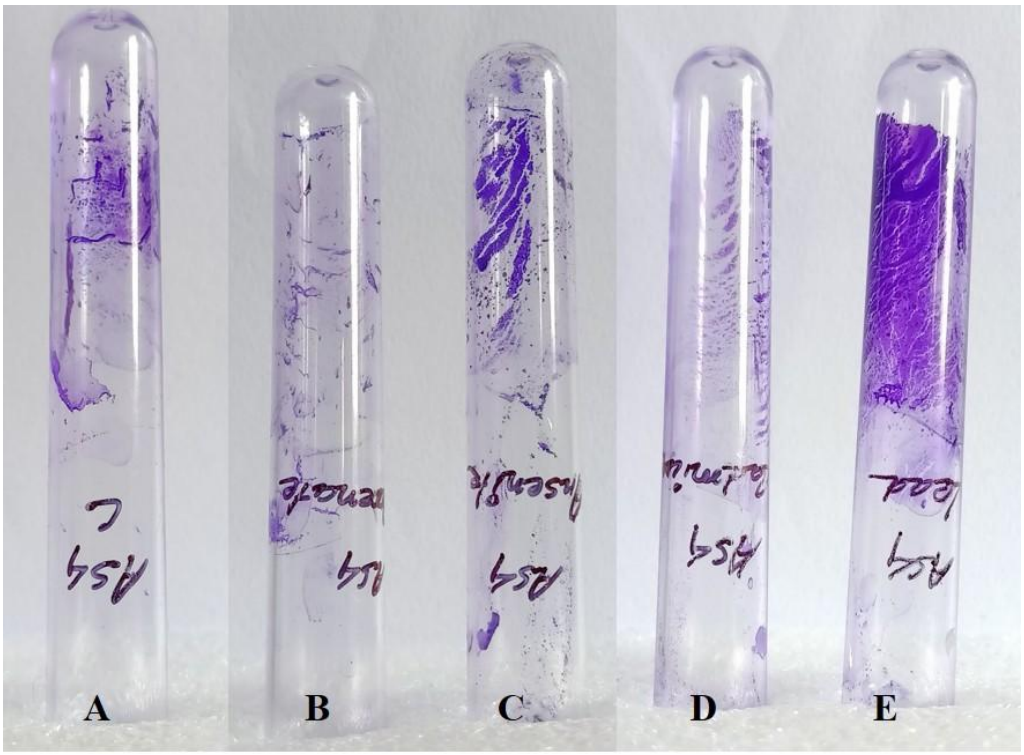

Figure 25. Tube method for the screening of biofilm production of AS4 strain in (A) control and in the presence (B) As^{5+}, (C) As^{3+}, (D) Cd^{2+}, and (E) Pb^{2+}

Table 24. Biofilm production capacity of the AS4 strain under different treatments

Test samples	Observed OD value	Biofilm forming potential

Bacterial strain AS4 without HM	0.369 ± 0.2137	Lack of biofilm since, OD < ODc
Bacterial strain AS4 with AS^{5+} ions	1.144 ± 0.09	Weak biofilm (+ or 1) production since, ODc < OD < 2 × ODc
Bacterial strain AS4 with AS^{3+} ions	0.727 ± 0.017	Weak biofilm (+ or 1) production since, ODc < OD < 2 × ODc
Bacterial strain AS4 with Pb^{2+} ions	0.234 ± 0.023	Lack of biofilm since, OD < ODc
Bacterial strain AS4 with Cd^{2+} ions	0.062 ± 0.048	lack of biofilm since, OD < ODc

4.8.3. *Biofilm producing capacity of the AS11 strain*

AS11 strain showed weak lining formation on the inner surface of the polypropylene tube and the same is displayed in figure 26. According to Table 25, the microtiter plate test findings showed that the AS11 strain was unable to produce biofilm without the presence of HMs as well as in presence of arsenic HMs. On the other hand, biofilm development was moderate to weak in the presence of Pb^{2+} and Cd^{2+} HMs, with Pb^{2+} (1.294 ± 0.076) surpassing Cd^{2+} (1.004 ± 0.015).

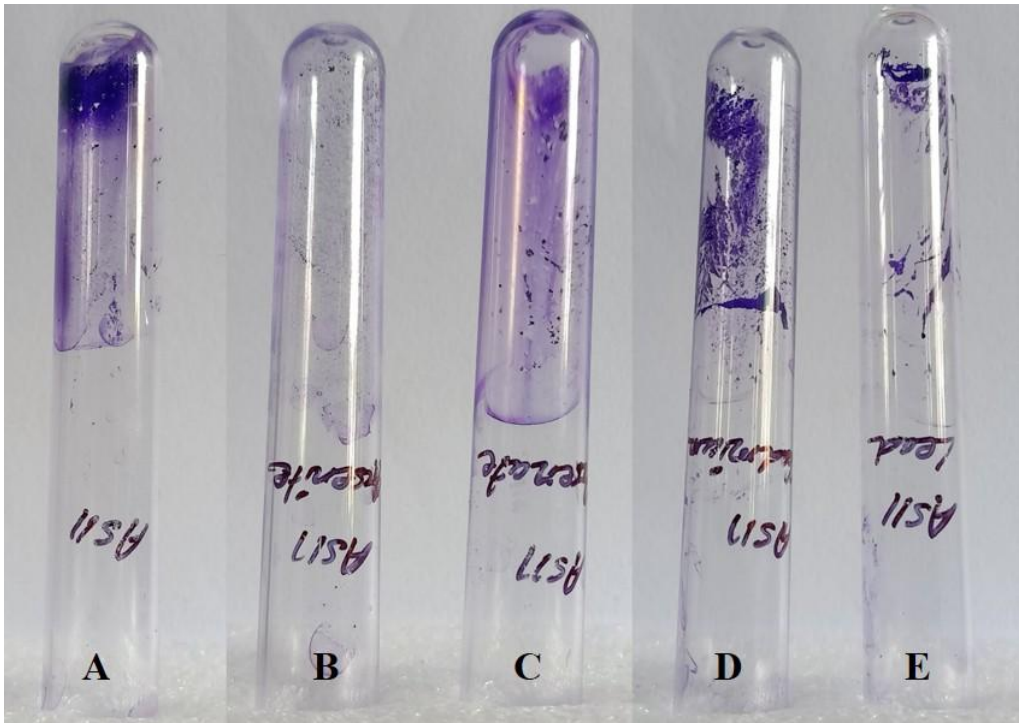

Figure 26. Tube method for the screening of biofilm production of AS11 strain in (A) control and in the presence (B) As^{3+}, (C) As^{5+}, (D) Cd^{2+}, and (E) Pb^{2+}

Table 25. Biofilm production capacity of the AS11 strain under different treatments

Test samples	Observed OD value	Biofilm forming potential
Bacterial strain AS11 without HM	0.607 ± 0.031	lack of biofilm since, OD < ODc
Bacterial strain AS11 with AS^{5+} ions	0.092 ± 0.057	lack of biofilm since, OD < ODc
Bacterial strain AS11 with $AS3^{+}$ ions	0.482 ± 0.067	lack of biofilm since, OD < ODc
Bacterial strain AS11 with Pb^{2+} ions	1.294 ± 0.076	moderate biofilm (++ or 2) production since, 2 × ODc < OD < 4 × ODc
Bacterial strain AS11 with Cd^{2+} ions	1.004 ± 0.015	weak biofilm since, ODc < OD < 2 × ODc

4.9. *Evaluation of siderophore producing capacity*

4.9.1. *Siderophore production by the AS3 strain*

AS3 strain clearly showed production of siderophore in presence of HMs such as As^{3+}, As^{5+}, Cd^{2+} and Pb^{2+} ions. The production of siderophore was qualitatively estimated by the formation of an orange-coloured halo around the bacterial colonies on CAS agar in the presence and absence of selected HMs at their MTC values and the same is presented in figure 27. Further, quantification of siderophore production was done using culture broth in presence of CAS reagent. The concentration of siderophore production varied from 20.22 ± 1.64 psu to 84.33 ± 1.09 psu and are listed in table 26.

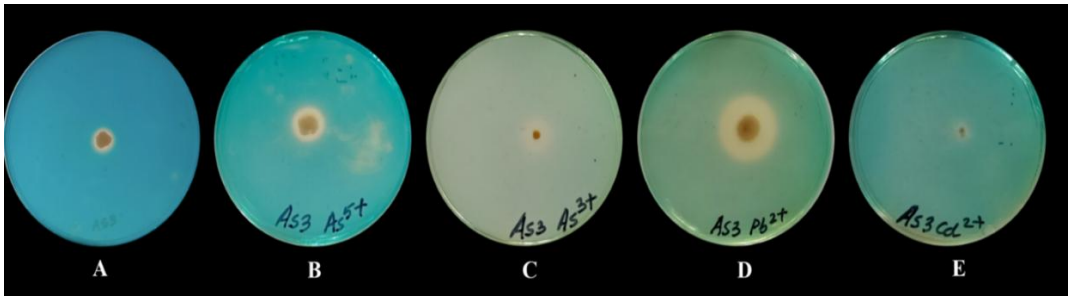

Figure 27. Halo formation by AS3 strain in CAS agar assay in (A) control and in the presence (B) As^{5+}, (C) As^{3+}, (D) Pb^{2+}, and (E) Cd^{2+}

Table 26. Siderophore production capacity of AS3 strain under different treatments

Tested HMs	Qualitative analysis	Quantitative analysis (psu)
Control	++	35.71 ± 0.96
As^{5+}	+++	84.33 ± 1.09
As^{3+}	+	29.78 ± 0.76
Pb^{2+}	+++	21.43 ± 1.64
Cd^{2+}	+	20.22 ± 1.64

NB: (+++) High production, (++) medium production, and (+) low production

4.9.2. *Siderophore production by the AS4 strain*

AS4 strain clearly showed production of siderophore in presence of HMs such as As^{3+}, As^{5+}, Cd^{2+} and Pb^{2+} ions by the formation of an orange-coloured halo around the bacterial colonies on CAS agar in the presence and absence of selected HMs at their MTC values and the same is presented in figure 28. The concentration of siderophore production varied from 19.31 ± 1.39 psu to 46.85 ± 2.47 psu and are listed in table 27.

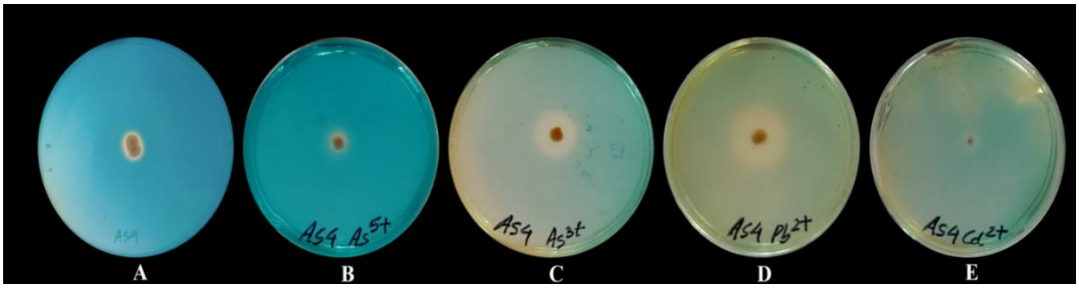

Figure 28. Halo formation by AS4 strain in CAS agar assay in (A) control and in the presence (B) As^{5+}, (C) As^{3+}, (D) Pb^{2+}, and (E) Cd^{2+}

Table 27. Siderophore production capacity of AS4 strain under different treatments

Tested HMs	Qualitative analysis	Quantitative analysis (psu)

Control	+++	40.79 ± 1.31
As^{5+}	++	46.85 ± 2.47
As^{3+}	+++	29.18 ± 1.31
Pb^{2+}	+++	36.80 ± 3.1
Cd^{2+}	+	19.31 ± 1.39

NB: (+++) High production, (++) medium production, and (+) low production

4.9.3. *Siderophore production by the AS11 strain*

AS11 strain clearly showed production of siderophore in presence of HMs such as As^{3+}, As^{5+}, Cd^{2+} and Pb^{2+} ions by the formation of an orange-coloured halo around the bacterial colonies on CAS agar in the presence and absence of selected HMs at their MTC values and the same is presented in figure 29. The concentration of siderophore production varied from 28.93 ± 0.84 psu to 86.99 ± 1.41 psu and are listed in table 28.

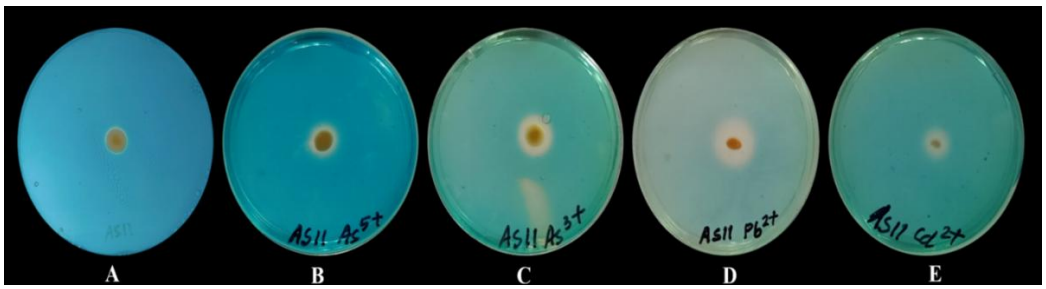

Figure 29. Halo formation by AS11 strain in CAS agar assay in (A) control and in the presence (B) As^{5+}, (C) As^{3+}, (D) Pb^{2+}, and (E) Cd^{2+}

Table 28. Siderophore production capacity of AS11 strain under different treatments

Tested HMs	Qualitative analysis	Quantitative analysis (psu)
Control	+++	44.92 ± 1.11
As^{5+}	+++	86.99 ± 1.41
As^{3+}	+++	49.39 ± 2.19
Pb^{2+}	+++	53.87 ± 2.84

Cd^{2+}	++	28.93 ± 0.84

NB: (+++) High production, (++) medium production, and (+) low production

4.10. *Evaluation of EPS producing capacity*

4.10.1. *EPS production by the AS3 strain*

EPS produced by the AS3 strain was initially quantified by weighing the extracted EPS sample, which were formed under identical conditions to those used in the siderophore production experiment. Table 29 illustrates the results, which indicated that the AS3 strain without HM treatment had an EPS yield (dry weight) of 96 mg/100 mL which was higher than in the presence of Cd^{2+} (32 mg/100 mL) followed by Pb^{2+} (20 mg/100 mL), AS^{3+} (16 mg/100 mL), and As^{5+} (8 mg/100 mL).

Table 29. Dry weight of EPS produced by AS3 strain

Bacterial Strain	Dry weight (mg) per 100 mL of treatment
AS3 Control	95.7 ± 0.58
AS3 As^{5+}	8.3 ± 0.58
AS3 As^{3+}	16.3 ± 2.5
AS3 Pb^{2+}	20.3 ± 0.58
AS3 Cd^{2+}	32.3 ± 1.15

Further, results demonstrated that the dried EPS had a considerably higher carbohydrate content when HMs were present (Figure 30). The bacterial sample that was exposed to Pb^{2+} had the highest carbohydrate content (53.01 ± 1.69 mg/100 mg of EPS), followed by As^{5+} (49.34 ± 1.22 mg/100 mg of EPS), AS^{3+} (39.23 ± 0.99 mg/100 mg of EPS), and Cd^{2+} (34.70 ± 1.11 mg/100 mg of EPS). Without any HM treatment, the carbohydrate content in the isolated EPS sample was found to be the lowest (5.69 ± 1.07 mg/100 mg of EPS).

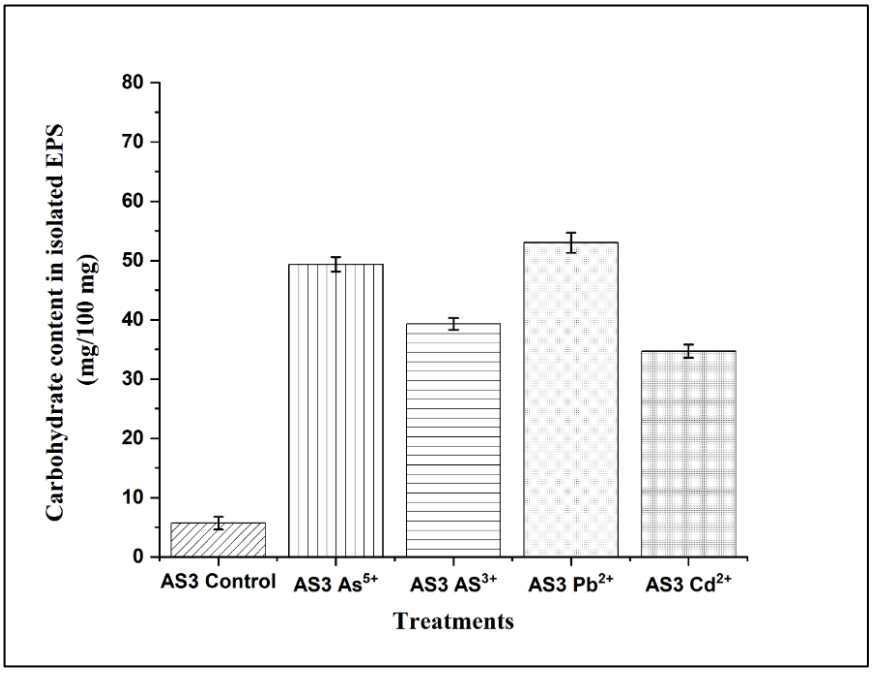

Figure 30. Carbohydrate content in the isolated EPS produced by the AS3 strain under different HM treatments

4.10.2. *EPS production by the AS4 strain*

EPS produced by the AS4 strain was firstly quantified by weighing the extracted EPS, which were formed under identical conditions to those used in the siderophore production experiment. Table 30 shows the results, which indicated that the AS4 strain without HM treatment had an EPS yield (dry weight) of 146 mg/100 mL followed by Cd^{2+} (34 mg/100 mL), As^{5+} (22 mg/100 mL), Pb^{2+} (18 mg/100 mL), and AS^{3+} (6 mg/100 mL).

Table 30. Dry weight of EPS produced by AS4 strain

Bacterial Strain	Dry weight (mg) per 100 mL of treatment
AS4 Control	145.67 ± 2.08
AS4 As^{5+}	22 ± 1.0
AS4 AS^{3+}	6.33 ± 1.53
AS4 Pb^{2+}	18.33 ± 2.08
AS4 Cd^{2+}	34 ± 1.0

The results further indicated that the dried EPS had a considerably higher carbohydrate content when HMs were present (Figure 31). The bacterial samples that were exposed to Pb^{2+} (59.58 ± 1.95 mg/100 mg of EPS) had highest carbohydrate content, followed by As^{3+} (50.93 ± 1.82 mg/100 mg of EPS), Cd^{2+} (32.41 ± 2.14 mg/100 mg of EPS), and As^{5+} (14.02 ± 0.65 mg/100 mg of EPS). Without any HM treatment, the carbohydrate content in the isolated sample was found to be the lowest (8.22 ± 0.23 mg/100 mg of EPS).

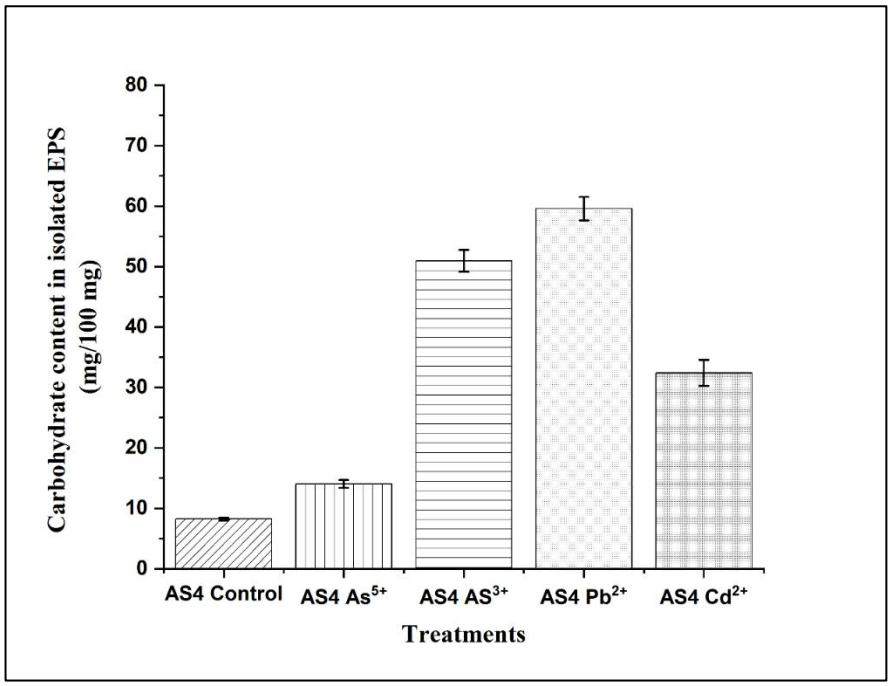

Figure 31. Carbohydrate content in the isolated EPS produced by the AS4 strain under different HM treatments

4.10.3. *EPS production by the AS11 strain*

EPS produced by the AS11 strain was primarily quantified by weighing the extracted EPS, which were formed under identical conditions to those used in the siderophore production experiment. Table 31 demonstrates the results, which indicated that the AS11 strain without HM treatment had an EPS yield (dry weight) of 72 mg/100 mL followed by As^{5+} (14 mg/100 mL), Pb^{2+} (12 mg/100 mL), Cd^{2+} (10 mg/100 mL) and As^{3+} (4 mg/100 mL).

Table 31. Dry weight of EPS produced by AS11 strain

Bacterial Strain	Dry weight (mg) per 100 mL of treatment
AS11 Control	71.67 ± 2.08
AS11 As^{5+}	14.33 ± 1.53
AS11 AS^{3+}	4.33 ± 0.58
AS11 Pb^{2+}	12 ± 1.0
AS11 Cd^{2+}	10.33 ± 0.58

The results further indicated that the dried EPS had a considerably higher carbohydrate content when HMs were present (Figure 32). The bacterial samples that were exposed to As^{3+} (74.48 ± 1.12 mg/100 mg of EPS) had highest carbohydrate content, followed by Cd^{2+} (64.58 ± 1.56 mg/100 mg of EPS), Pb^{2+} (44.68 ± 1.88 mg/100 mg of EPS), and As^{5+} (44.49 ± 0.90 mg/100 mg of EPS). Without any HM treatment, the carbohydrate content in the isolated sample was found to be the lowest, which was 16.17 ± 0.47 mg/100 mg of EPS.

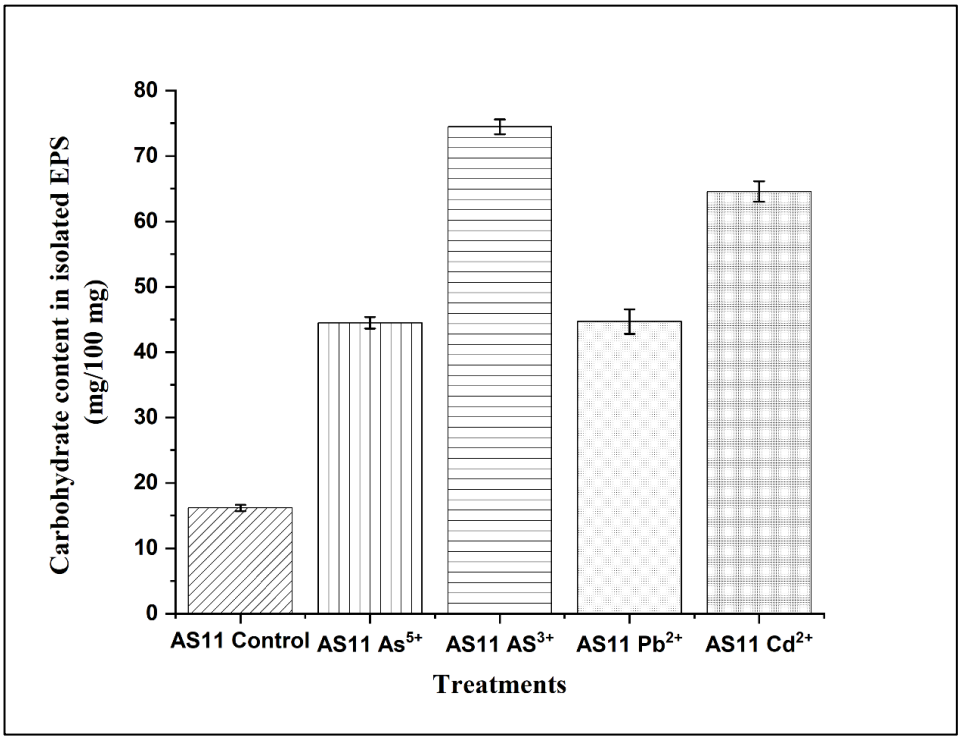

Figure 32. Carbohydrate content in the isolated EPS produced by the AS11 strain under different HM treatments

4.11. *Oxidation and reduction potential of As by the selected bacterial strain*

Results clearly confirms the potentiality of the AS3, AS4 and AS11 strain to reduce As^{5+} to As^{3+} as well as oxidize As^{3+} to As^{5+} and the same are displayed in figure 33 and figure 34. When silver nitrate was added to the As^{5+} containing culture, it became yellow, demonstrating the existence of As^{3+}. Furthermore, when silver nitrate was added to a 72-hour-old culture plate containing As^{3+}, the media steadily became brown, confirming the existence of As^{5+} in the media. Therefore, all the three bacterial strains have the potential to reduce arsenate to arsenite as well as oxidize arsenite to arsenate.

Figure 33. Plate exhibiting arsenate reduction ability of AS3, AS4 and AS11 strains

Figure 34. Plate exhibiting arsenite oxidation ability of AS3, AS4 and AS11 strains

4.12. *Cellular study of the selected bacterial strain*

4.12.1. *SEM-EDX analysis of selected bacterial strains under different treatments*

The SEM-EDX results confirm the presence of As^{5+} ions over the surface of the selected bacterial strains, which were previously grown in Na_3AsO_4 supplemented

medium. However, the strains did not show adsorption of As^{3+} metal ions on their surfaces (Figure 36, 39, and 42). Furthermore, distinct changes in morphological features were observed in both As^{5+} and As^{3+} treated samples as compared to controls (Figure 35, 38, and 41) such as decrease in population size and increase in cell volume. In As^{3+} treated samples, the bacterial surface was rough as compared to the control. Moreover, SEM-EDX analysis of Pb and Cd HM treated samples indicates the presence of Cd^{2+} and Pb^{2+} metal ions on the surface of the bacterial strains (Figure 37, 40, and 43). In Pb and Cd treated samples, bacterial cells appeared quite rough and in aggregation indicating possible high adsorption of Pb^{2+} and Cd^{2+} ions which was also evident from the occurrence of multiple peaks in EDX spectra especially in Pb treated samples.

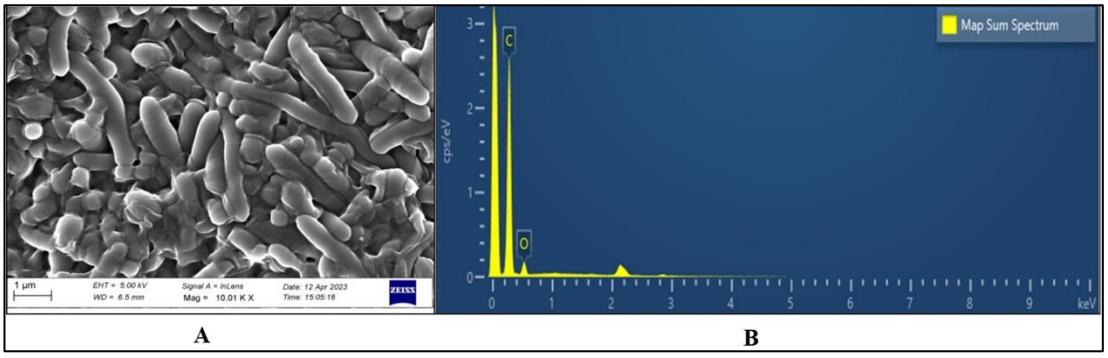

Figure 35. (A) SEM micrograph of AS3 control and (B) EDX graph of AS3 Control

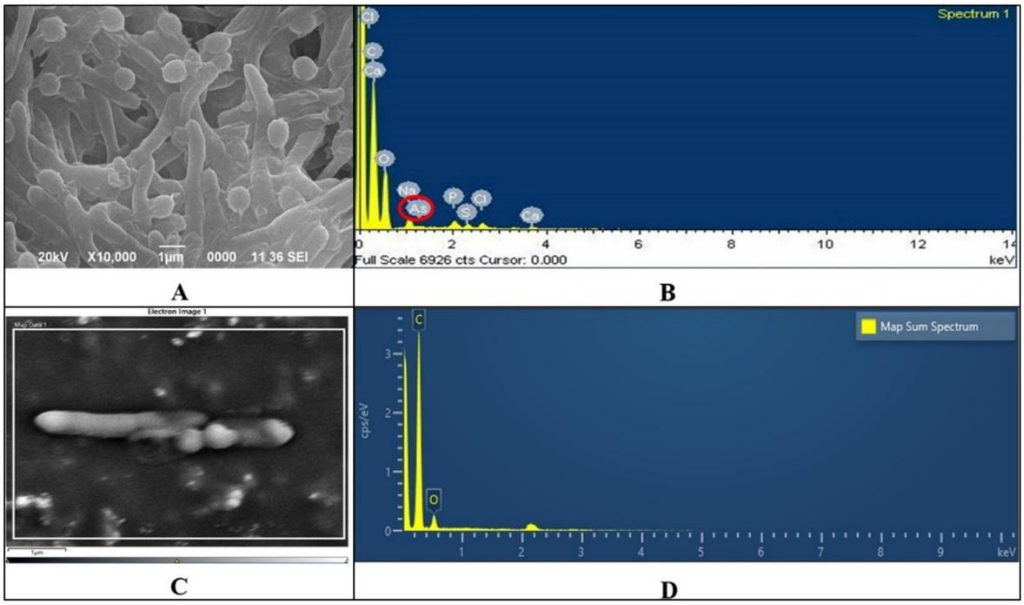

Figure 36. (A) SEM micrograph of AS3 treated with As^{5+}, (B) EDX spectrum of AS3 treated with As^{5+}, (C) SEM micrograph of AS3 treated with As^{3+}, and (D) EDX spectrum of AS3 treated with As^{3+}

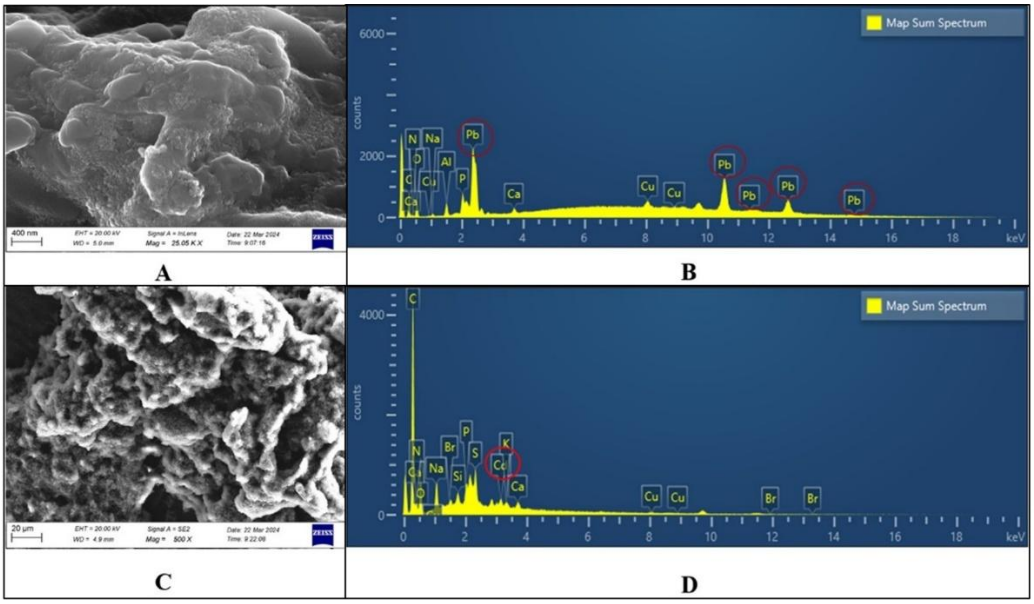

Figure 37. (A) SEM micrograph of AS3 strain treated with Pb^{2+}, (B) EDX spectrum of AS3 strain treated with Pb^{2+}, (C) SEM micrograph of AS3 strain treated with Cd^{2+}, and (D) EDX spectrum of AS3 strain treated with Cd^{2+}

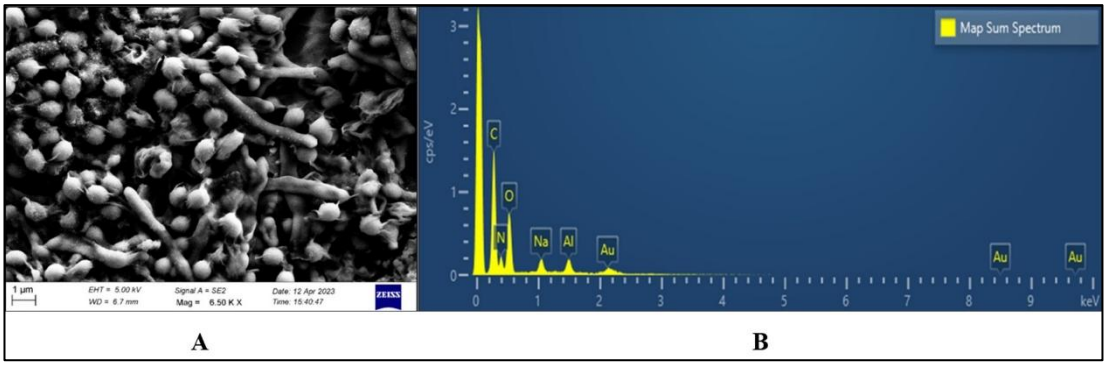

Figure 38. (A) SEM micrograph of AS4 control and (B) EDX spectrum of AS4 Control

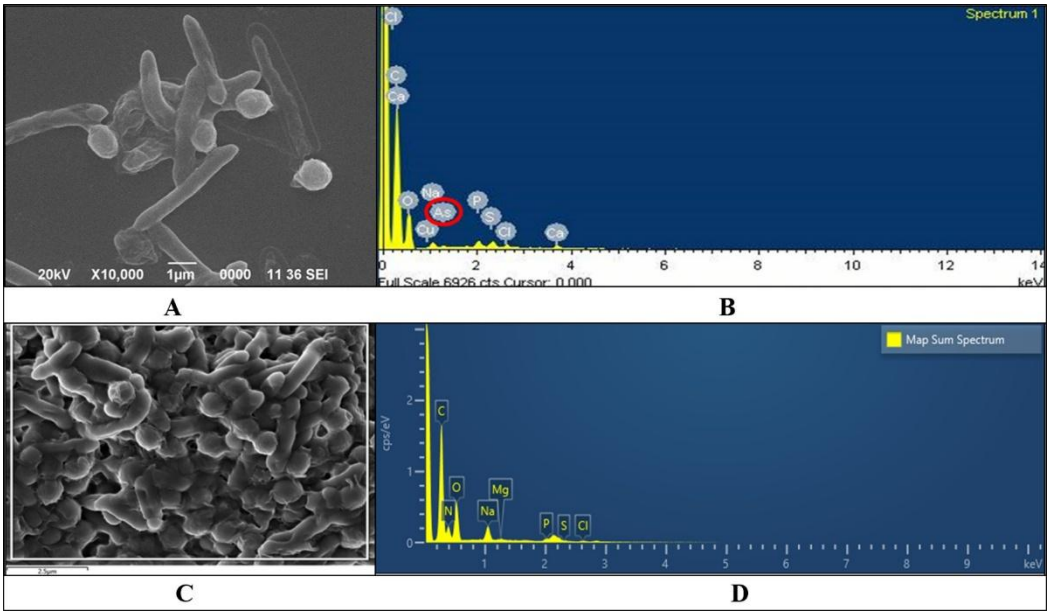

Figure 39. (A) SEM micrograph of AS4 treated with As^{5+}, (B) EDX spectrum of AS4 treated with As^{5+}, (C) SEM micrograph of AS4 treated with As^{3+}, and (D) EDX spectrum of AS4 treated with As^{3+}

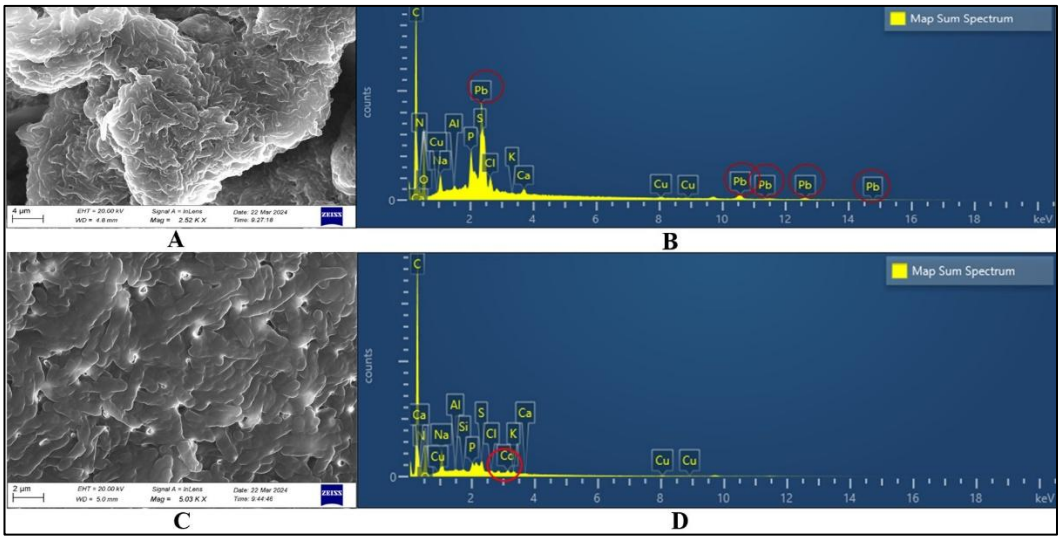

Figure 40. (A) SEM micrograph of AS4 strain treated with Pb^{2+}, (B) EDX spectrum of AS4 strain treated with Pb^{2+}, (C) SEM micrograph of AS4 strain treated with Cd^{2+}, and (D) EDX spectrum of AS4 strain treated with Cd^{2+}

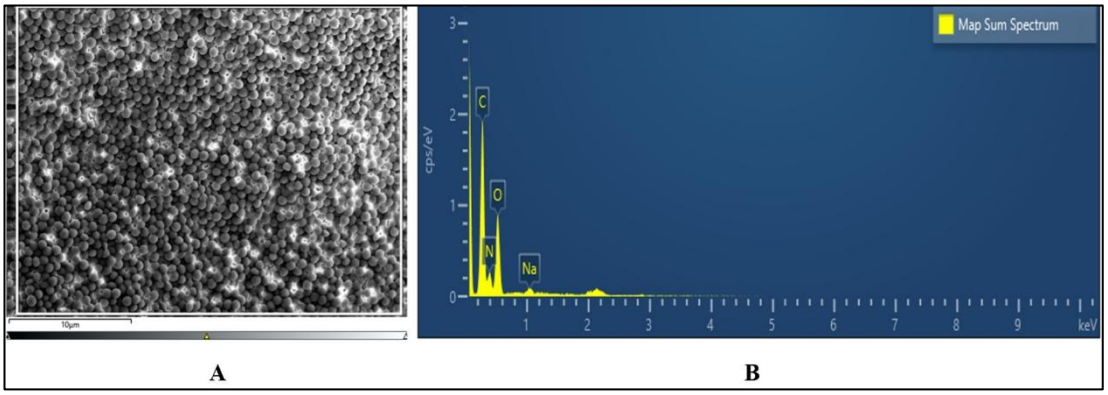

Figure 41. (A) SEM micrograph of AS11 control and (B) EDX spectrum of AS11 Control

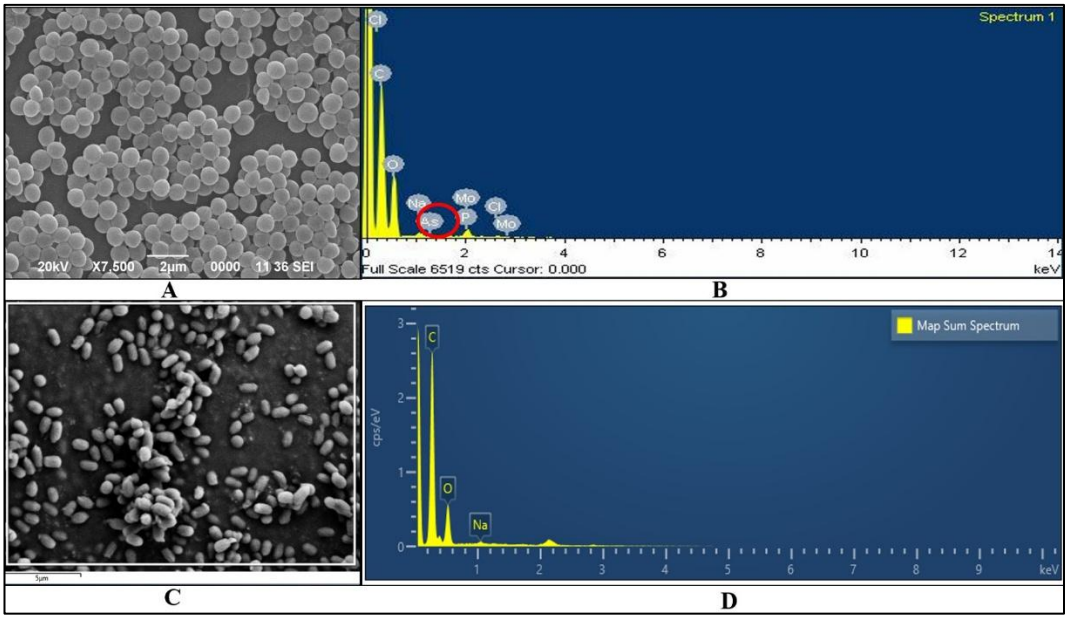

Figure 42. (A) SEM micrograph of AS11 treated with As^{5+}, (B) EDX spectrum of AS11 treated with As^{5+}, (C) SEM micrograph of AS11 treated with As^{3+}, and (D) EDX spectrum of AS11 treated with As^{3+}

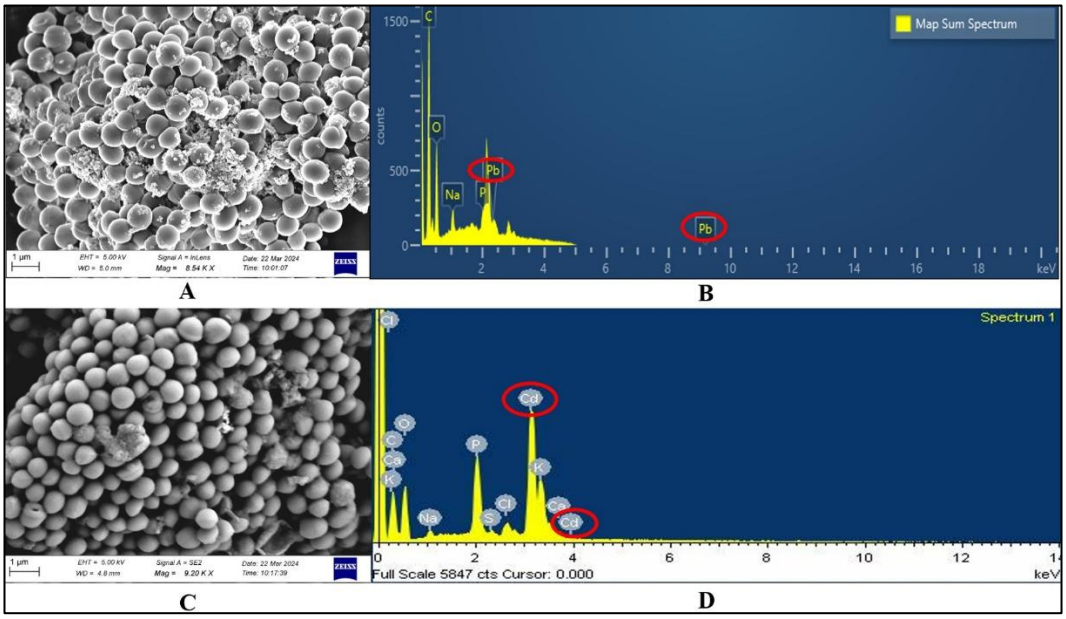

Figure 43. (A) SEM micrograph of AS11 strain treated with Pb^{2+}, (B) EDX spectrum of AS11 strain treated with Pb^{2+}, (C) SEM micrograph of AS11 strain treated with Cd^{2+}, and (D) EDX spectrum of AS11 strain treated with Cd^{2+}

4.12.2. *FTIR analysis of the biomass of bacterial strains under different treatments*

4.12.2.1. *IR spectroscopic analysis of AS3 strain biomass*

The IR spectra of the dry bacterial biomass of strain AS3 in the presence of various HMs at their MTC in comparison to a control without HM are presented in figure 44. The resulting spectra varied noticeably depending on the HMs present compared to the control. The IR absorption frequencies of each peak and the corresponding functional groups of control are presented in table 32.

Table 32. FTIR peaks and their assignments of AS3 strain under different treatments

Sl No.	Peaks (cm^{-1})	Assignments	Range (cm^{-1})	References
1.	3462, 3477, 3478	Alcohols and phenols (O-H stretching vibrations)	3,200-3,600	Krishnan (1961)
2.	2969, 2972, 2968, 2964	CH_3, $–CH_2$, and –CH stretching vibrations	3000-2800	Xu et al. (2021); Shi et al. (2020)

3.	1647	Amides (N-H bending vibrations)	1,550-1,670	Xu et al. (2021)
4.	1691	Amide (C=O stretching vibrations)	1600-1700	Usoltsev et al. (2019)
5.	1659	Amides (N-H bending vibration)	1,550-1,670	Kassem et al. (2023)
6.	1530, 1536, 1543, 1546	Amides (N-H in-plane bending or the CN stretching vibration)	1546	Gupta et al. (2022)
7.	1400, 1403, 1411	COO− stretching vibrations	1400	Saraeva et al. (2023)
8.	1236, 1238, 1240	Phosphate (P=O asymmetric vibrations)	1236-1240	Parikh and Chorover (2006); Quilès et al. (2010)
9.	1092, 1096, 1097, 1070, 1076	C–O–C and C–O stretching vibrations	1000-1200	Makarem et al. (2019); Atykyan et al. (2020)
10.	987, 989, 993	Fingerprint regions	993	Quilès et al. (2010)
11.	872	As-O bending vibrations	872	Fan and Zhang (2019)
12.	545, 581	Halo compound (C-Br stretching)	515-690	Theivandran et al. (2015)

In this study, it was observed that, the peak values shifted from 3462 cm^{-1} (control) to higher wavenumbers in all the HM treatments in the range of 3,200–3,600 cm^{-1}, corresponding to O-H stretching vibrations, except Cd whereby no such prominent peak was observed in this range. The range between 3000-2800 cm^{-1}, corresponding to methyl, methylene and methine stretching vibrations, the peaks were observed around 2969 cm^{-1} in control along with all other HM treatments. In the range

of 1,550–1,700 cm^{-1}, 1647 cm^{-1} peak was recorded in the control, corresponding to N-H bending vibrations. However, the peak shifted to 1659 and 1691 cm^{-1} corresponding to N-H bending and C=O stretching vibrations. A significant peak was observed at 1546 cm^{-1} in control was attributed to N-H in-plane bending or the CN stretching vibration. The peak value was found to shift to a lower wavenumber in HM treatments, except Cd^{2+} treatment where it was absent. Another significant peak at 1400 cm^{-1} was observed which was attributed to COO− stretching vibrations. The peak was not found in As amended treatments but was found to intensify in Pb^{2+} (1403 cm^{-1}) and Cd^{2+} (1411 cm^{-1}) amended treatments. Moreover, the peaks around 1236-1240 cm^{-1}, which were attributed to P=O asymmetric vibrations, was observed in control and Pb and Cd treatments, and was not observed in AS^{5+} and AS^{3+} treatments. In the range 1000–1200 cm^{-1}, the peak value in control treatment was observed at 1092 cm^{-1}. This peak was shifted to higher wavenumber in As^{5+} (1096 cm^{-1}), As^{3+} (1097 cm^{-1}), and Cd^{2+} (1096 cm^{-1}) HM treatments, whereas it was unchanged in Pb treatment. Moreover, peaks around 993 cm^{-1} which attributed for fingerprint regions were observed in control, Pb^{2+} and Cd^{2+} treatments, but was not found in AS^{5+} and AS^{3+} treatments. Another significant peak at 872 cm^{-1} was found in both As^{5+} and As^{3+} treatments. Lastly, peaks around 515-690 cm^{-1} were observed in both Pb^{2+} and Cd^{2+} treatments.

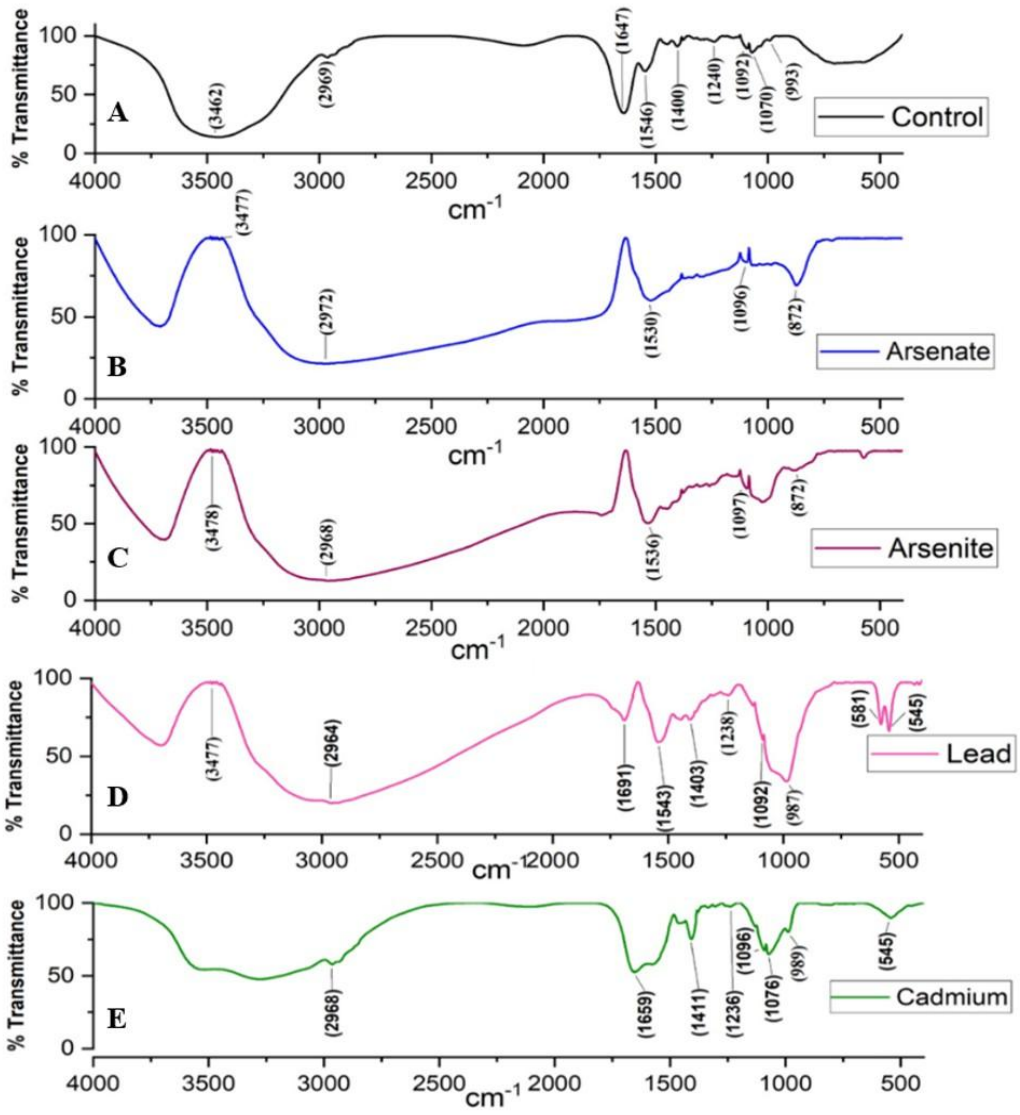

Figure 44. FTIR study of AS3 strain biomass in the presence of (A) Control, (B) As^{5+}, (C) As^{3+}, (D) Pb^{2+}, and (E) Cd^{2+}

4.12.2.2. *IR spectroscopic analysis of AS4 strain biomass*

The IR spectra of the dry bacterial biomass of strain AS4 in the presence of various HMs at their MTC in comparison to a control without HM are presented in figure 45. The resulting spectra varied noticeably depending on the HMs present compared to the control. The IR absorption frequencies of each peak and the corresponding functional groups of control are presented in table 33.

Table 33. FTIR peaks and their assignments of AS4 strain biomass under different treatments

Sl No.	Peaks (cm^{-1})	Assignments	Range (cm^{-1})	References
1.	3403, 3381, 3477	Alcohols and phenols (O-H stretching vibrations)	3,200–3,600	Krishnan (1961)
2.	1647, 1637, 1648, 1643,	Amides (N-H bending vibrations)	1,550–1,670	Xu et al. (2021)
3.	1659	Amides (N-H bending vibration)	1,550–1,670	Kassem et al. (2023)
4.	1546, 1559	Amides (N-H in-plane bending or the CN stretching vibration)	1546	Gupta et al. (2022)
5.	1403, 1412, 1413, 1411, 1388	COO− stretching vibrations	1400	Saraeva et al. (2023)
6.	1305,1245	Amide III, combination of C-N stretching and N-H bending	1305–1200	Maity et al. (2013)
7.	1240	Phosphate (P=O asymmetric vibrations)	1236-1240	Parikh and Chorover (2006); Quilès et al. (2010)
8.	1090,1092, 1096, 1076, 1077	C–O–C and C–O stretching vibrations	1000–1200	Makarem et al. (2019); Atykyan et al. (2020)
9.	987, 989, 993, 991	Fingerprint regions	993	Quilès et al. (2010)
10.	872, 855	As-O bending vibrations	730-930	Fan and Zhang (2019)

11.	545, 581, 539	Halo compound (C-Br stretching)	515-690	Theivandran et al. (2015)

In this study, peaks around 3,200–3,600 cm^{-1} were observed in both As^{5+} and As^{3+} treatments, corresponding to O-H stretching vibrations, except for Pb^{2+} where high wavenumbers (3477 cm^{-1}) was observed accompanied by absence of peak in Cd^{2+} treatment. In the range of 1,550–1,700 cm^{-1} and 1647 cm^{-1} peak was recorded in the control, corresponding to N-H bending vibrations. However, the peak shifted to higher wavenumbers 1648 cm^{-1} and 1659 cm^{-1} in As^{3+} and Cd^{2+} treatments respectively, which corresponding to N-H bending vibrations. Though, it shifted to lower wavenumbers *i.e.* 1637 cm^{-1} and 1673 cm^{-1} in As^{5+} and Cd^{2+} treatments respectively, with N-H bending vibrations. A significant peak was observed at 1546 cm^{-1} in control was attributed to N-H in-plane bending or the CN stretching vibration. The peak value was found to shift to a higher wavenumber *i.e.* 1559 cm^{-1} in Pb^{2+} treatment, while it was not observed in other HMs treatments. Another significant peak at 1403 cm^{-1} was observed which was attributed to COO− stretching vibrations. The peak was found to intensify in As^{5+} (1412 cm^{-1}), As^{3+} (1413 cm^{-1}) and Cd^{2+} (1411 cm^{-1}) amended treatments while it was found to lessen in Pb^{2+} treatment. The peaks around 1305-1200 cm^{-1}, corresponding to C-N stretching and N-H bending vibrations was observed only in As^{5+} (1305 cm^{-1}) and As^{3+} (1245 cm^{-1}) treatments, while it was absent in control and other treatments. Moreover, the peak at 1240 cm^{-1}, attributed to P=O asymmetric vibrations, was observed in control while absent in all HMs treatments. In the range 1000–1200 cm^{-1}, the peak value in control treatment was observed at 1090 cm^{-1} and 1070 cm^{-1}. This peak was observed in As^{5+} (1096 cm^{-1} and 1071 cm^{-1}), As^{3+} (1076 cm^{-1}), Pb^{2+} (1092 cm^{-1}) and Cd^{2+} (1076 cm^{-1}) HM treatments. Moreover, peaks around 993 cm^{-1}, attributed for fingerprint regions were observed in all HMs treatments. Another significant peak around 730-930 cm^{-1} was found in both As^{5+} and As^{3+} treatments, corresponding to As-O bending vibrations. Lastly, peaks around 515-690 cm^{-1} were observed in both Pb^{2+} and Cd^{2+} treatments, which is basically due to C-Br stretching vibrations.

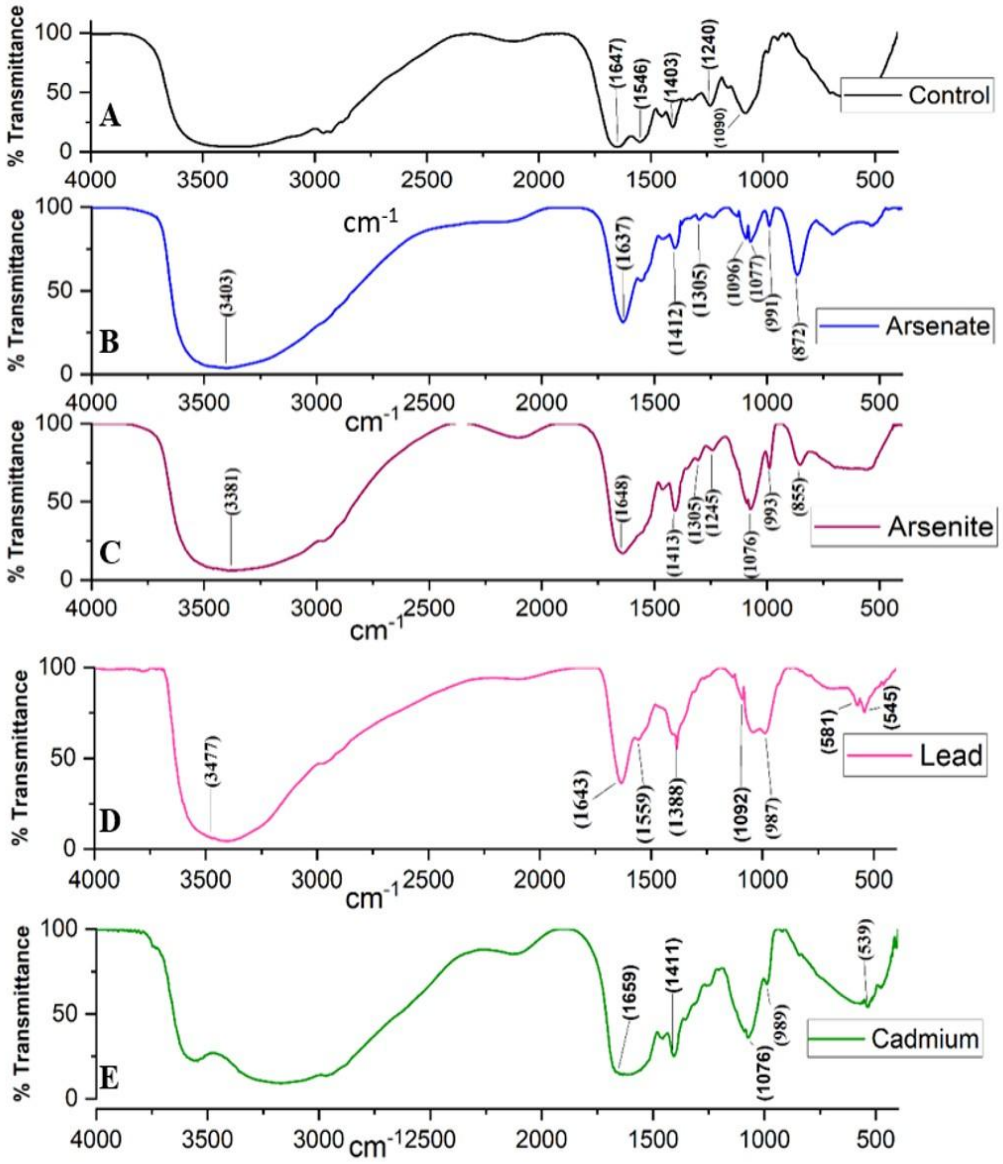

Figure 45. FTIR study of AS4 strain biomass in the presence of (A) Control, (B) As^{5+}, (C) As^{3+}, (D) Pb^{2+}, and (E) Cd^{2+}

4.12.2.3. *IR spectroscopic analysis of AS11 strain*

The IR spectra of the dry bacterial biomass of strain AS3 in the presence of various HMs at their respective MTC in comparison to a control without HM are presented in figure 46. The resulting spectra varied noticeably depending on the HMs present compared to the control. The IR absorption frequencies of each peak and the corresponding functional groups of control are presented in table 34.

Table 34. FTIR peaks and their assignments of AS11 strain under different treatments

Sl No.	Peaks (cm^{-1})	Assignments	Range (cm^{-1})	References
1.	1646, 1658, 1657	Amides (N-H bending vibrations)	1,550–1,670	Xu et al. (2021)
2.	1530, 1541, 1546, 1549, 1557	Amides (N-H in-plane bending or the CN stretching vibration)	1546	Gupta et al. (2022)
3.	1408, 1413, 1416, 1420	COO− stretching vibrations	1400	Saraeva et al. (2023).
4.	1235, 1236, 1238, 1240, 1241, 1244	Amide III, combination of C-N stretching and N-H bending; Phosphate (P=O asymmetric vibrations)	1305–1200; 1236-1240	Maity et al. (2013)
6.	1018, 1074, 1096, 1097, 1100	C–O–C and C–O stretching vibrations	1000–1200	Makarem et al. (2019); Atykyan et al. (2020)
7.	866	Carbonate (CO_3^{2-}) out of plane bending vibration	850-890	Fleet (2009)

In AS11 strain, in the range of 1,550–1,700 cm^{-1}, 1646 cm^{-1} peak was recorded in the control, corresponding to N-H bending vibrations. However, the peak shifted to higher wavenumbers in As^{5+}(1658 cm^{-1}) and Pb^{2+} (1657 cm^{-1}) treatments corresponding to N-H bending vibrations. While, it was absent in presence of As^{3+} and Cd^{2+} HM treatments. Moreover, significant peaks around 1546 cm^{-1} were observed in all treatments, attributed to N-H in-plane bending or the CN stretching vibration. These peaks were shifted to lower wavenumbers in As^{5+} (1530 cm^{-1}) and As^{3+} (1541 cm^{-1}) treated samples, while, it was shifted to higher wavenumbers in Pb^{2+} (1557 cm^{-1}) and Cd^{2+} (1549 cm^{-1}) treatments. Another significant peak at around 1400 cm^{-1} was observed in control (1413 cm^{-1}), which was attributed to COO− stretching vibrations.

The peak was found to intensify in As^{3+} (1420 cm^{-1}) and Pb^{2+} (1416 cm^{-1}) while it was not observed in As^{5+} treated samples. Moreover, it was seen to decrease in Cd^{2+} (1408 cm^{-1}) treatment. Further, the peaks around 1305-1200 cm^{-1}, corresponding to C-N stretching and N-H bending vibrations was observed in control (1241 cm^{-1}), with slight decreased in As^{3+} (1238) and slight elevated in Pb^{2+} (1244 cm^{-1}) treatments, while it was absent in As^{5+} and Cd^{2+} treatments. In the range 1000–1200 cm^{-1}, the peak value in control treatment was observed at 1018 cm^{-1}. This peak was observed to elevate in presence of all the HM treatments such as As^{5+} (1096 cm^{-1}), As^{3+} (1097 cm^{-1}), Pb^{2+} (1074 cm^{-1}) and Cd^{2+} (1100 cm^{-1}) HM treatments. Lastly peak around 850-890 cm^{-1} was attributed to carbonate bending vibrations, which was present only in Pb^{2+} HM treatment.

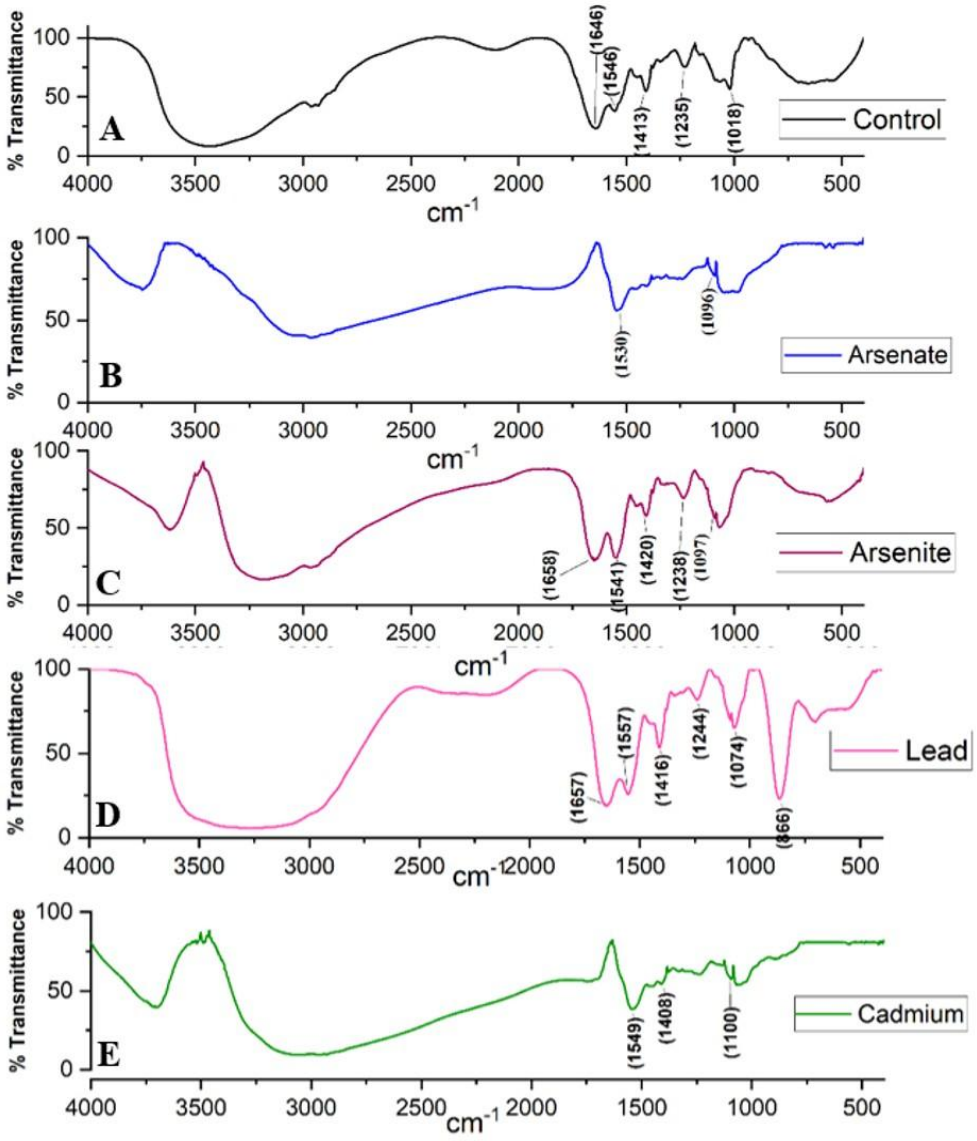

Figure 46. FTIR study of AS11 strain in the presence of (A) Control, (B) As^{5+}, (C) As^{3+}, (D) Pb^{2+}, and (F) Cd^{2+}

4.12.3. *TEM-EDX analysis*

The findings of TEM-EDX analyses of AS3 and AS4 strains indicate the presence of As HM in control samples (Figure 47 B and 48 B). The TEM-EDX analysis of AS3 further indicated the presence of As^{5+} accumulation along with Pb^{2+} and Cd^{2+} as evident form EDX spectra (Figure 47 D, 47 E and 47 F). Due to absence of As^{3+} HM ions as confirmed from SEM-EDX analysis in the samples, the TEM analysis for As^{3+} HM ions was not performed. In AS4 strain, TEM-EDX analysis

confirmed the accumulation of As^{5+}, Pb^{2+} and $Cd^{2+}$with the appearance of respective HM characteristic peaks in the EDX spectra (Figure 48 D, 48 E and 48 F). In the case of AS11 strain, TEM-EDX analysis confirms only the presence of As^{5+} accumulation while Pb^{2+} and Cd^{2+} HM ions were absent in the tested samples as evident form EDX spectra (Figure 49 D, 49 E and 49 F)

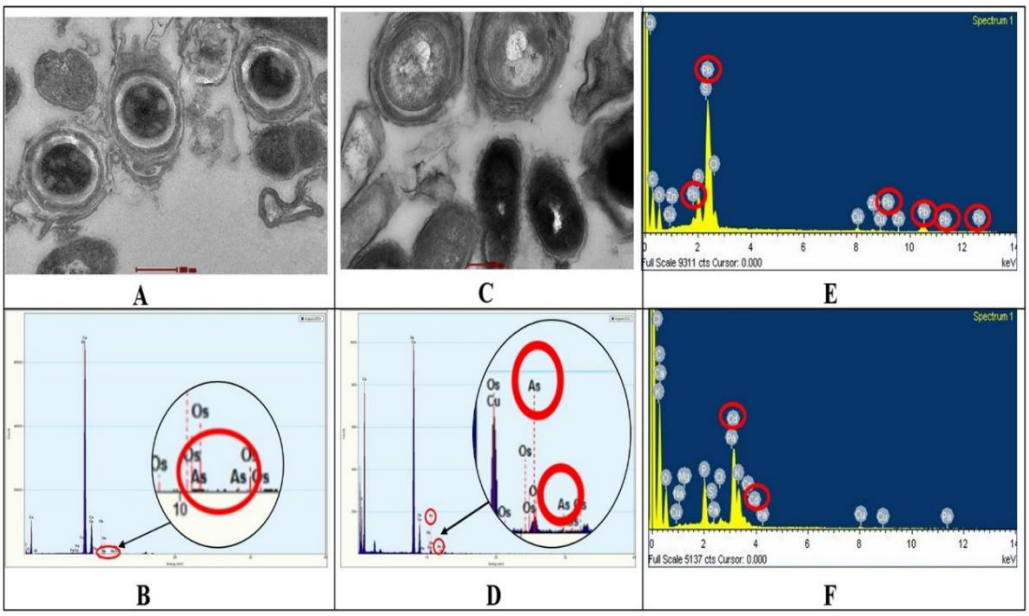

Figure 47. (A) TEM image of AS3 strain (control), (B) EDX graph of AS3 strain (control), (C) TEM image of AS3 strain (HM treated), (D) EDX graph of AS3 strain (As^{5+}), (E) EDX graph of AS3 (Pb^{2+}), and (F) EDX graph of AS3 (Cd^{2+})

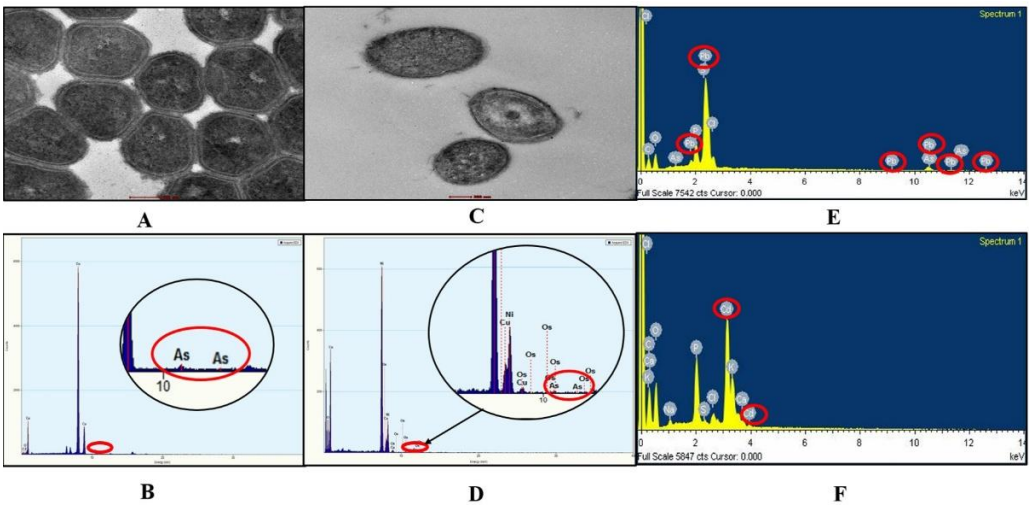

Figure 48. (A) TEM image of AS4 strain (control), (B) EDX graph of AS4 strain (control), (C) TEM image of AS4 strain (HM treated) and (D) EDX graph of AS4 strain (As^{5+}), (E) EDX graph of AS4 (Pb^{2+}), and (F) EDX graph of AS4 (Cd^{2+})

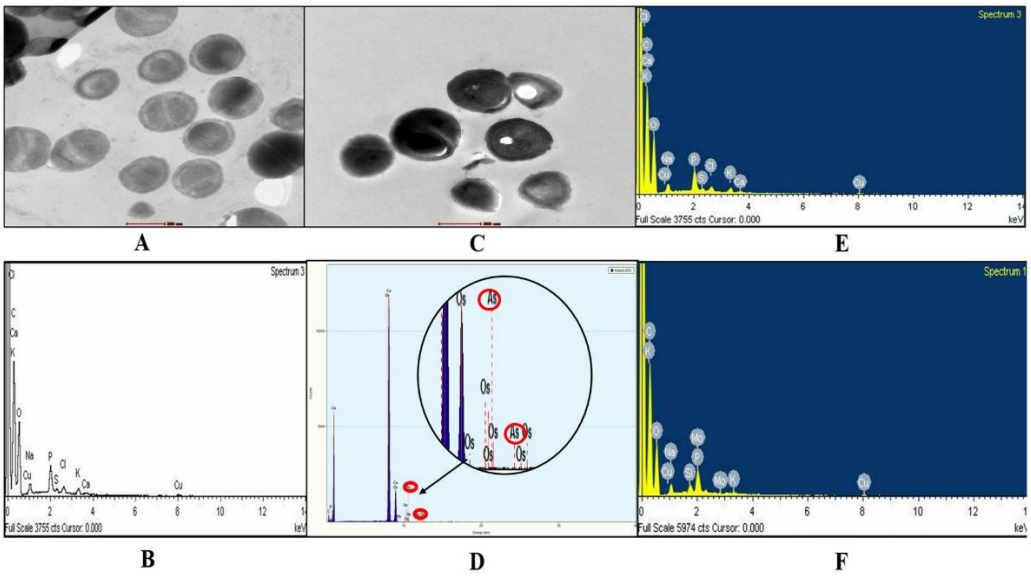

Figure 49. (A) TEM image of AS11 strain (control), (B) EDX graph of AS11 strain (control), (C) TEM image of AS11 strain (HM treated), (D) EDX graph of AS11 strain (As^{5+}), (E) EDX graph of AS11 (Pb^{2+}), and (F) EDX graph of AS11 (Cd^{2+})

4.13. *Stress enzyme activity*

4.13.1. *Total Protein Content (TPC)*

The TPC (µg/mL) in the selected bacterial strain *i.e.* AS3, AS4 and AS11 in the presence and absence of tested HMs at their respective MTC values was estimated with the help of the obtained standard curve. Data of the same are presented in table 35 and figure 50, 51, and 52. In the strain AS3, TPC was found to be higher against all the HM treatments. It was highest in the presence of $NaAsO_2$ (24.324 ± 1.261 mg/mL) followed by Na_3AsO_4 (22.462 ± 0.275 mg/mL), $CdCl_2$ (19.70 ± 0.812 mg/mL), and $Pb(NO_3)_2$ (18.559 ± 1.571 mg/mL) compared to the control (16.755 ± 0.619 mg/mL). In the case of strain AS4, TPC was found to be highest in the presence of $Pb(NO_3)_2$ (25.05 ± 0.95 mg/mL) followed by $CdCl_2$ (21.98 ± 0.79 mg/mL), Na_3AsO_4 (19.28 ± 1.36 mg/mL), and $NaAsO_2$ (19.16 ± 0.38 mg/mL) compared to the control (18.26 ± 0.52 mg/mL). Furthermore, in the strain AS11, TPC was significantly lesser in the presence of tested HMs *i.e.* $Pb(NO_3)_2$ (22.16 ± 1.88 mg/mL), Na_3AsO_4

(19.88 ± 0.58 mg/mL), $CdCl_2$ (18.80 ± 2.32 mg/mL), and $NaAsO_2$ (18.32 ± 1.47 mg/mL) as compared to the control (24.744 ± 0.812 mg/mL).

Table 35. Estimated values of TPC under different HM treatments

Bacterial Strain with HM treatment	Protein Concentration (mg/mL)
AS3 (Without HM) Control	16.76 ± 0.62
AS3 (Na_3AsO_4)	22.46 ± 0.28
AS3 ($NaAsO_2$)	24.32 ± 1.26
AS3 ($CdCl_2$)	19.70 ± 0.81
AS3 ($Pb(NO_3)_2$)	18.56 ± 1.57
AS4 (Without HM) Control	18.26 ± 0.52
AS4 (Na_3AsO_4)	19.28 ± 1.36
AS4 ($NaAsO_2$)	19.16 ± 0.38
AS4 ($CdCl_2$)	21.98 ± 0.79
AS4 ($Pb(NO_3)_2$)	25.05 ± 0.95
AS11 (Without HM) Control	24.74 ± 0.81
AS11 (Na_3AsO_4)	19.88 ± 0.58
AS11 ($NaAsO_2$)	18.32 ± 1.47
AS11 ($CdCl_2$)	18.80 ± 2.32
AS11 ($Pb(NO_3)_2$)	22.16 ± 1.88

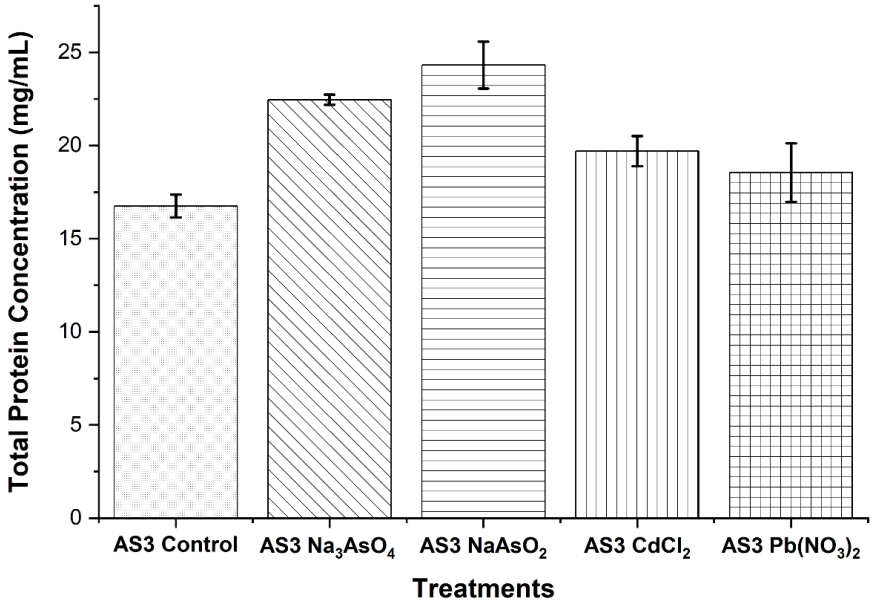

Figure 50. TPC of AS3 strain under HM treatments

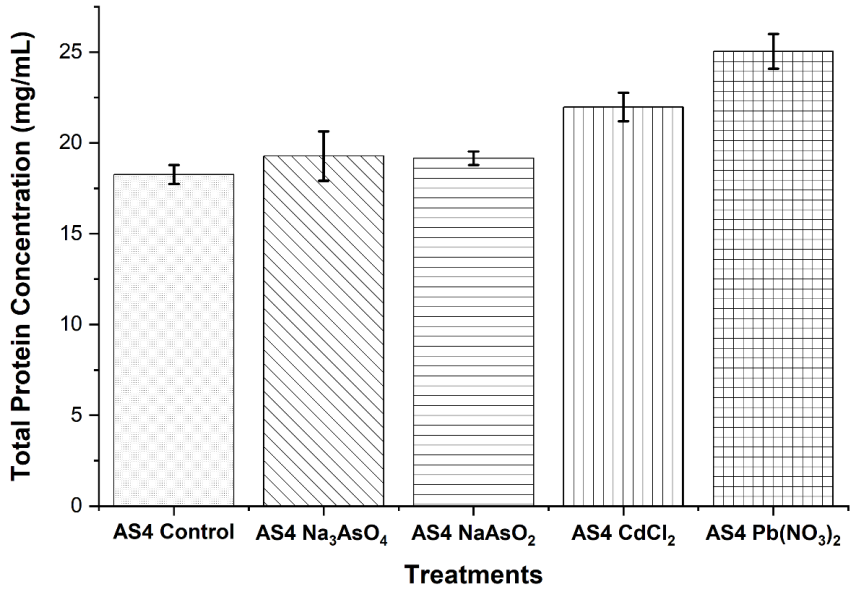

Figure 51. TPC of AS4 strain under HM treatments

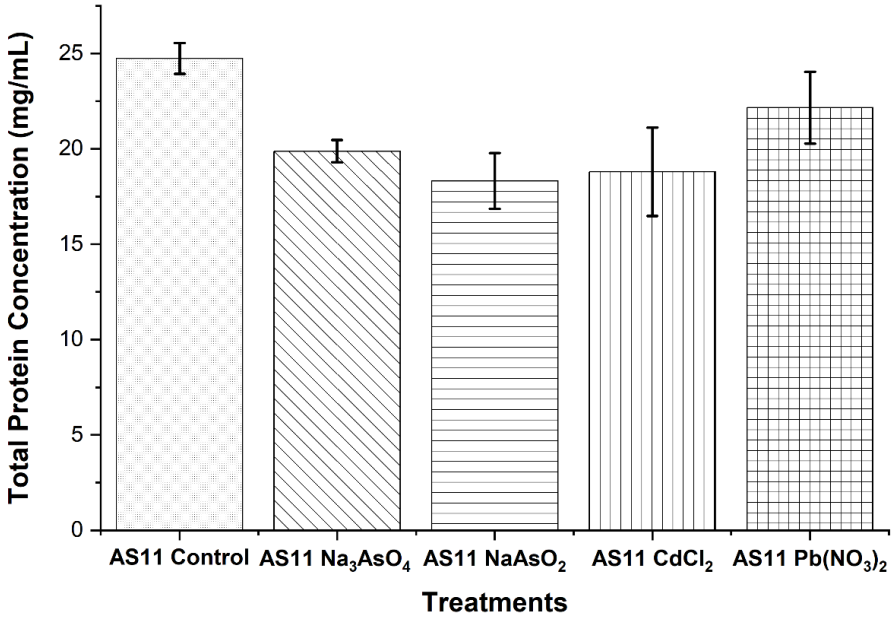

Figure 52. TPC of AS11 strain under HM treatments

4.13.2. *Activity of SOD, CAT, GR, GPx and MDA of AS3 strain*

SOD activity was found to be comparatively lower than the control (0.185 ± 0.006 U/mg protein) against all the tested HMs at their respective MTC values. Moreover, CAT activity of AS3 strain against Na_3AsO_4 (0.18 ± 0.01) and $Pb(NO_3)_2$ (0.16 ± 0.003) was slightly lesser than the control (0.728 ± 0.003 U/mg protein) while significantly higher in the presence of $NaAsO_2$ (0.902 ± 0.004 U/mg protein) and $CdCl_2$ (0.768 ± 0.021 U/mg protein).

GR activity in AS3 strain was found to be significantly higher compared to control (0.880 ± 0.019 U/mg protein) against all the tested HMs at their respective MTC values specifically against $Pb(NO_3)_2$ of 4.801 ± 0.035 U/mg protein followed by Na_3AsO_4 (4.43 ± 0.01), $CdCl_2$ (4.38 ± 0.04), and $NaAsO_2$ (4.12 ± 0.09).

AS3 strain showed significantly higher activity of GPx in presence of $CdCl_2$ (12.873 ± 0.125 U/mg protein) followed by $NaAsO_2$ (4.190 ± 0.102 U/mg protein), and $Pb(NO_3)_2$ (2.533 ± 0.000 U/mg protein) at their respective MTC values compared to control (3.14 ± 0.00 U/mg protein). Moreover, GPx activity was found to be lower only in presence of Na_3AsO_4 (1.428 ± 0.000 U/mg protein).

Bacterial strain AS3 showed significantly ($p < 0.05$) higher MDA level in the presence of $Pb(NO_3)_2$ (0.672 ± 0.019 U/mg protein) followed by Na_3AsO_4 (0.038 ± 0.008 U/mg protein), and $CdCl_2$ (0.036 ± 0.004 U/mg protein) at their respective MTC values compared to the control (0.05 ± 0.00). Moreover, lowermost MDA level (0.021 ± 0.004 U/mg protein) was observed in $NaAsO_2$ treated samples at its MTC value compared to the control. The figures of stress enzyme activity of AS3 strain are presented in figure 53, 54, 55, 56, and 57.

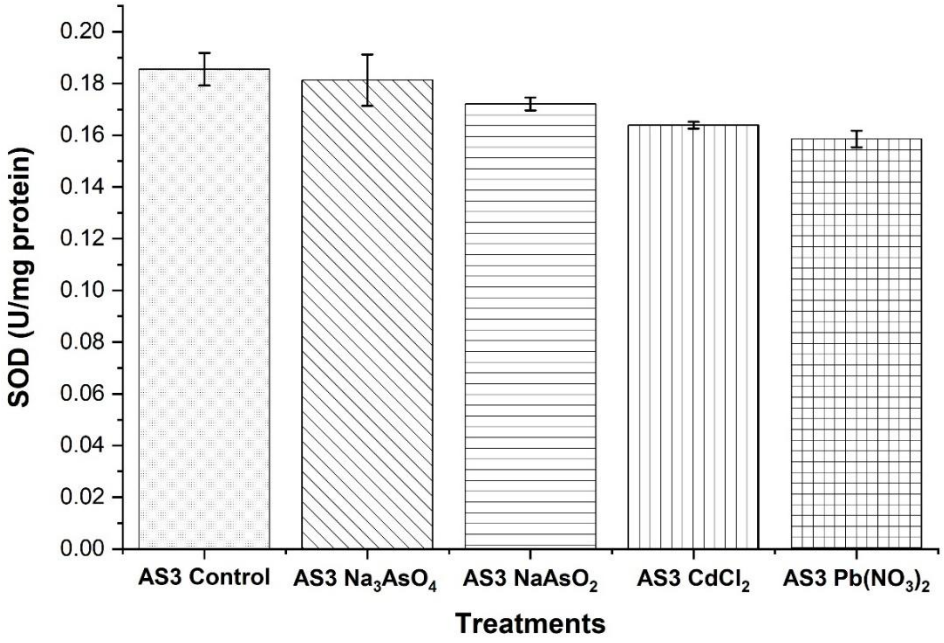

Figure 53. SOD activity of AS3 strain under HM treatments

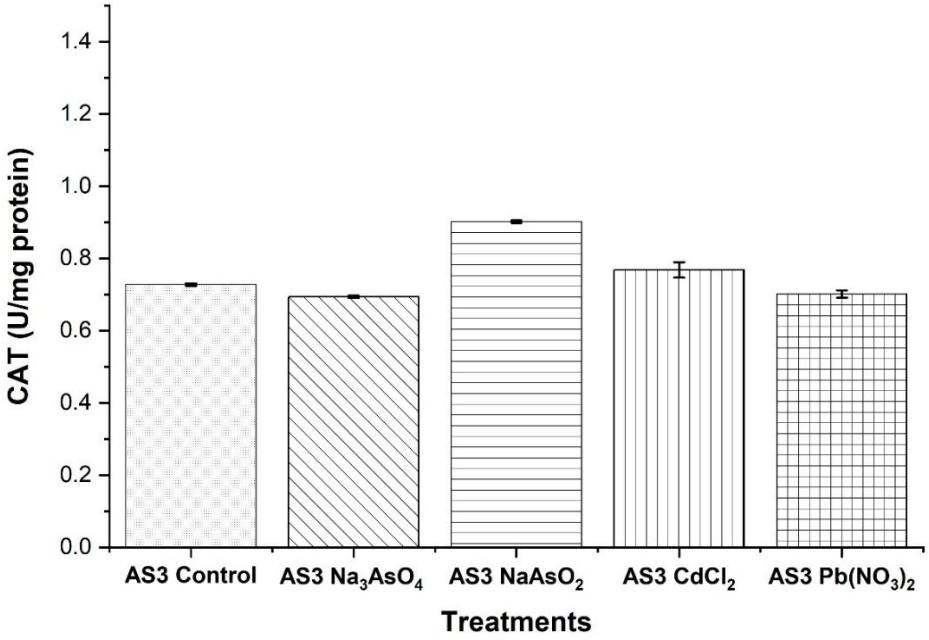

Figure 54. CAT activity of AS3 strain under HM treatments

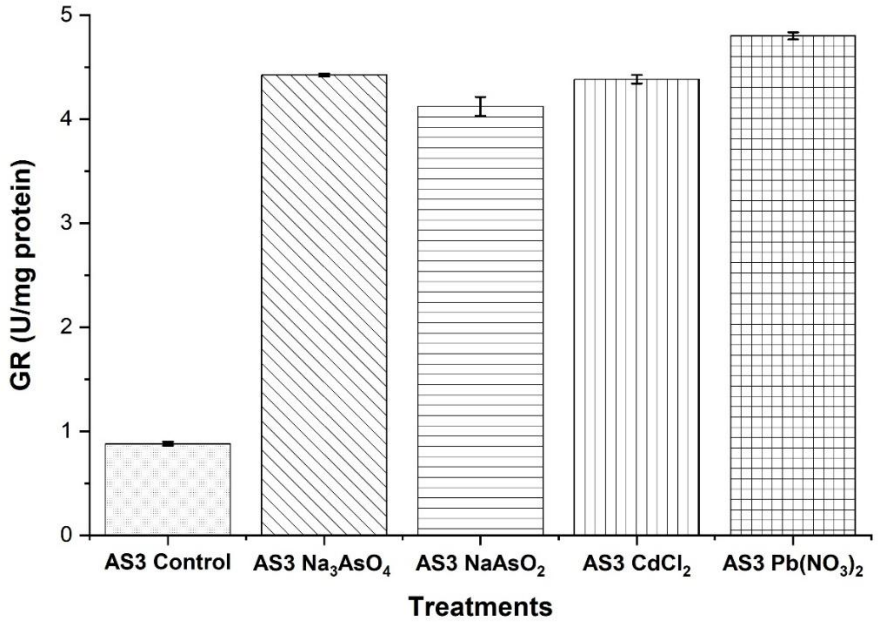

Figure 55. GR activity of AS3 strain under HM treatments

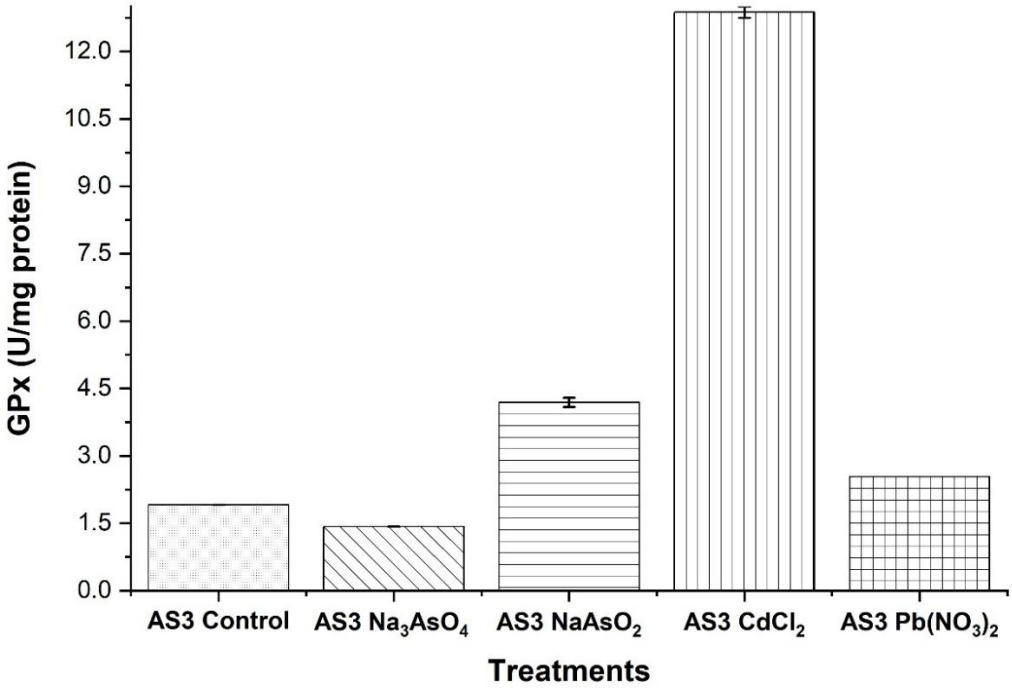

Figure 56. GPx activity of AS3 strain under HM treatments

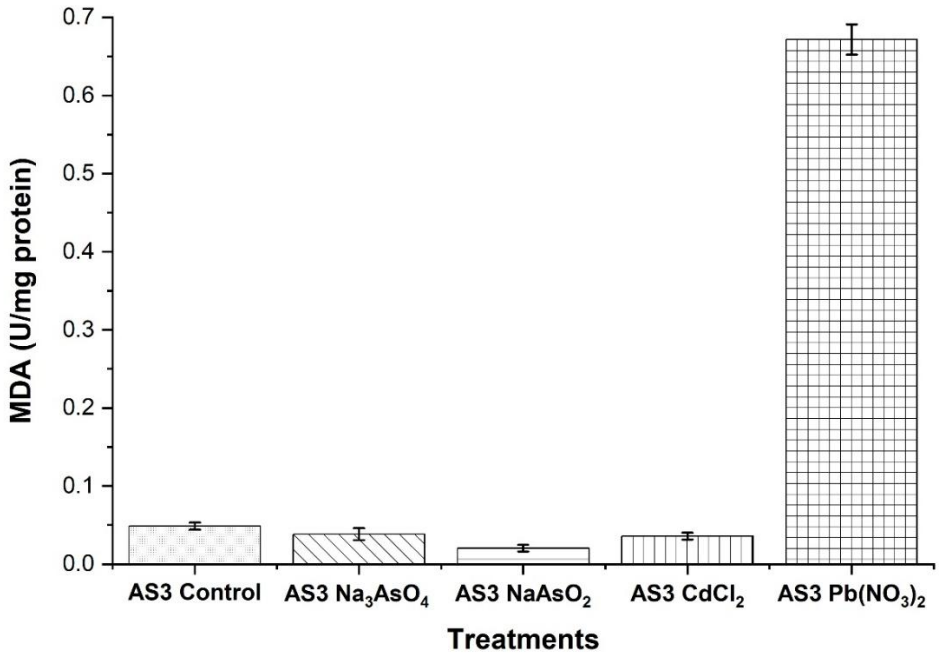

Figure 57. MDA activity of AS3 strain under HM treatments

4.13.3. *Activity of SOD, CAT, GR, GPx and MDA of AS4 strain*

SOD activity of AS4 strain was found to be comparatively lower than the control (0.1571 ± 0.0029 U/mg protein) in Na_3AsO_4 (0.15 ± 0.00 U/mg protein) and $NaAsO_2$ (0.16 ± 0.01 U/mg protein) treatments at their respective MTC values. Whereas, it was found to be elevated in presence of $CdCl_2$ (0.1621 ± 0.0073U/mg) and $Pb(NO_3)_2$ (0.1647 ± 0.0036 U/mg). CAT activity of AS4 bacterium against Na_3AsO_4 (0.74 ± 0.00 U/mg protein) and $Pb(NO_3)_2$ (0.76 ± 0.00 U/mg protein) was slightly lesser than the control (0.776 ± 0.00 U/mg protein) while it was higher in the presence of $CdCl_2$ (0.784 ± 0.01 U/mg protein) and alike with that of $NaAsO_2$ (0.776 ± 0.00 U/mg protein) treatment at their respective MTC values. GR activity in AS4 bacterium was found to be very high compared to control (1.8866 ± 0.0062 U/mg protein) against all the HMs specifically against $Pb(NO_3)_2$ (12.7638 ± 0 U/mg protein) followed by Na_3AsO_4 (4.09 ± 0.01 U/mg protein), $CdCl_2$ (0.62 ± 0.03 U/mg protein), and $NaAsO_2$ (0.70 ± 0.02 U/mg protein) treatment at their respective MTC values. AS4 strain also showed significantly higher activity of GPx in presence of $Pb(NO_3)_2$ (4.5889 ± 0.14 U/mg protein), followed by $NaAsO_2$ (4.2322 ± 0.14 U/mg protein), and Na_3AsO_4 (3.8955 ± 0.26U/mg protein) while it was lower in presence of $CdCl_2$ (1.6311 ± 0.16 U/mg protein), as compared to control (2.9045 ± 0.14 U/mg protein) at their respective MTC values. Moreover, MDA concentrations for AS4 strain against all the HMs were found to be comparatively higher especially for $Pb(NO_3)_2$ (0.02 ± 0.00 U/mg protein) treatment at their respective MTC values than that of the control (0.00128 ± 0.000256 U/mg protein) except for $NaAsO_2$ (0.00068 ± 0.000148 U/mg protein). The figures of stress enzyme activity of AS3 strain are presented in figure 58, 59, 60, 61, and 62.

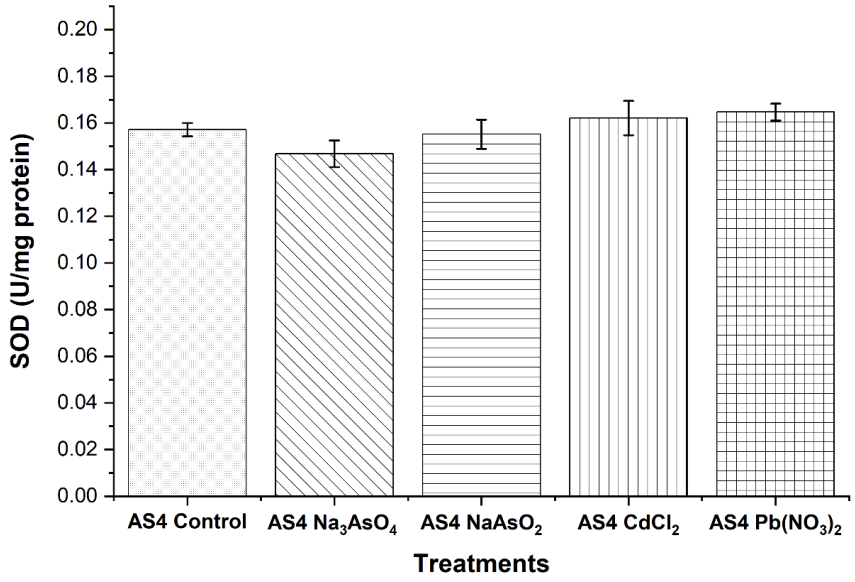

Figure 58. SOD activity of AS4 strain under HM treatments

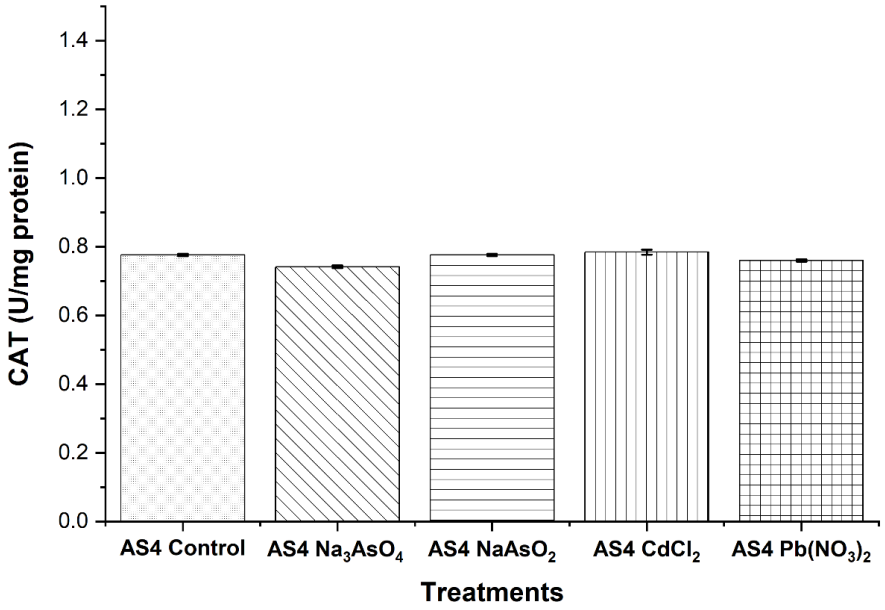

Figure 59. CAT activity of AS4 strain under HM treatments

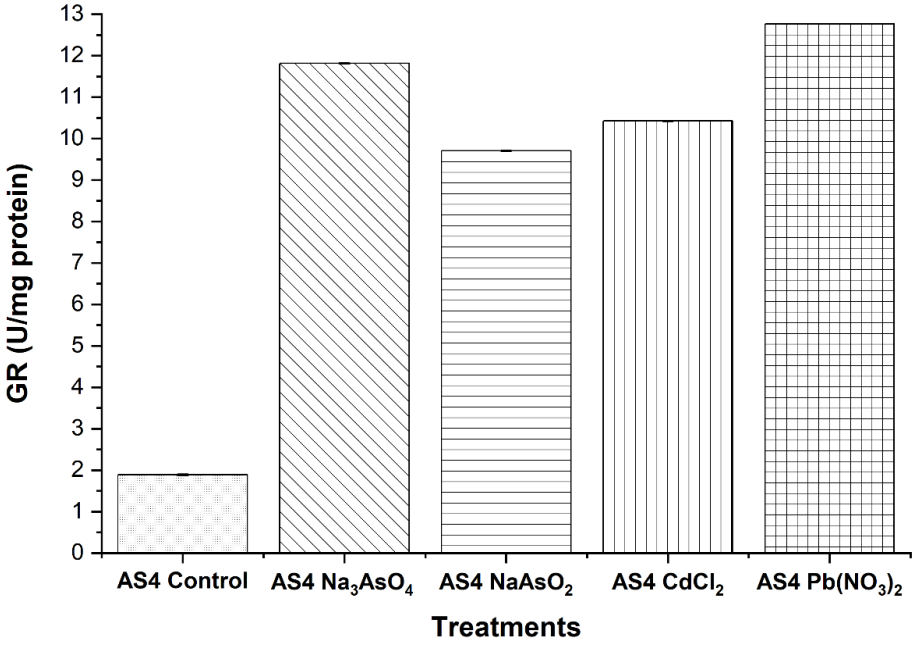

Figure 60. GR activity of AS4 strain under HM treatments

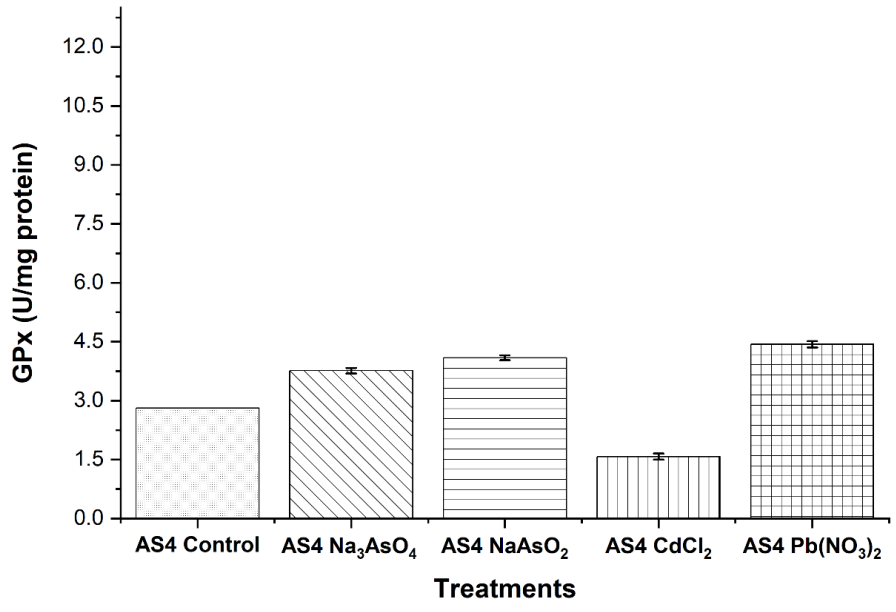

Figure 61. GPx activity of AS4 strain under HM treatments

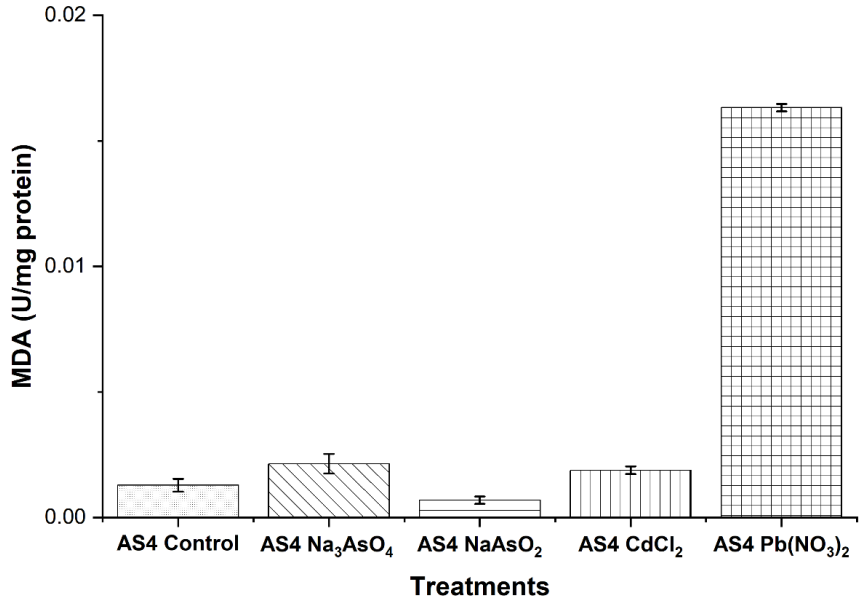

Figure 62. MDA activity of AS4 strain under HM treatments

4.13.4. *Activity of SOD, CAT, GR, GPx and MDA of AS11 strain*

In AS11 strain, SOD activity was found to be comparatively lower than the control (0.1637 ± 0.0027 U/mg protein) in $CdCl_2$ (0.1521 ± 0.0102 U/mg protein) and Na_3AsO_4 (0.1594 ± 0.0019 U/mg protein) while higher in $Pb(NO_3)_2$ (0.1702 ± 0.0078 U/mg protein) and $NaAsO_2$ (0.1661 ± 0.0103 U/mg protein) treatment at their respective MTC values. CAT activity of AS11 strain against Na_3AsO_4 (0.417 ± 0.00 U/mg protein) and $NaAsO_2$ (0.422 ± 0.00 U/mg protein) was similar to that of the control (0.42 ± 0.00 U/mg protein) while higher in the presence of $Pb(NO_3)_2$ (3.50 ± 0.05 U/mg protein) and $CdCl_2$ (0.45 ± 0.00 U/mg protein) at their respective MTC values. Moreover, comparatively GR activity in AS11 strain was found to be higher than control (0.0069 ± 0.0000 U/mg protein) against all the tested HMs in the order of $CdCl_2$ (5.45 ± 0.01 U/mg protein), $Pb(NO_3)_2$ (4.21 ± 0.04 U/mg protein), $NaAsO_2$ (3.51 ± 0.01 U/mg protein), and Na_3AsO_4 (3.26 ± 0.03 U/mg protein) at their respective MTC values. Further, AS11 strain showed comparatively lower GPx activity in the presence of all HMs at their respective MTC values as compared to the control (4.21558 ± 0.1674 U/mg protein) in the order of $CdCl_2$ (3.04 ± 0.00 U/mg protein), $Pb(NO_3)_2$ (1.96 ± 0.49 U/mg protein), Na_3AsO_4 (1.71 ± 0.13 U/mg protein), and

$NaAsO_2$ (1.58 ± 0.12 U/mg protein). MDA concentrations in the presence all the heavy were found to be comparatively lesser than that of the control (0.142 ± 0.016 U/mg protein) in the order of Na_3AsO_4 (0.11 ± 0.01 U/mg protein), $NaAsO_2$ (0.109 ± 0.00 U/mg protein) and $CdCl_2$ (0.102 ± 0.00 U/mg protein) at their respective MTC values. However, MDA concentrations was remarkably higher compared to the control in the presence of $Pb(NO_3)_2$ (0.704 ± 0.016 U/mg protein). The figures of stress enzyme activity of AS11 strain are presented in figure 63, 64, 65, 66, and 67.

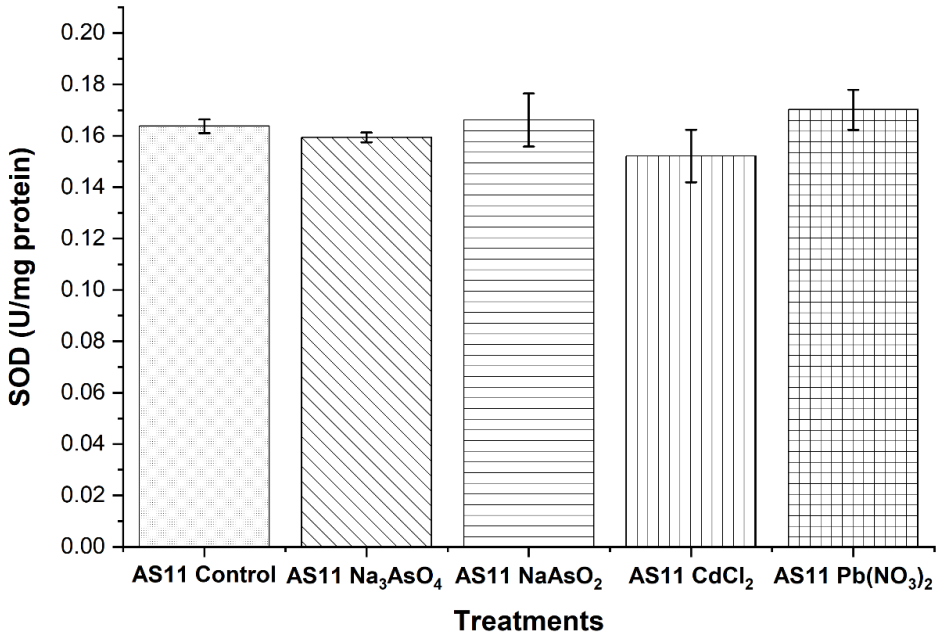

Figure 63. SOD activity of AS11 strain under HM treatments

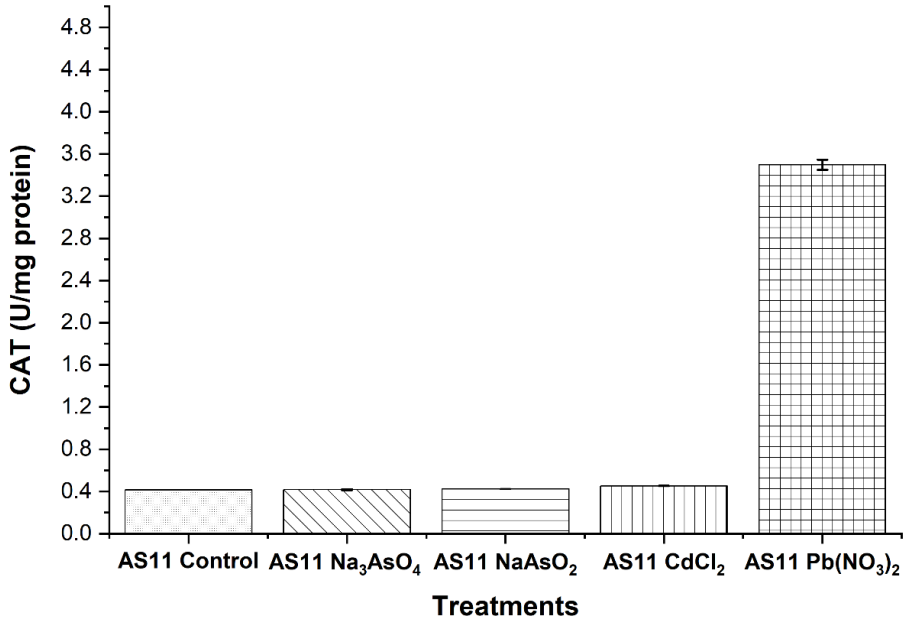

Figure 64. CAT activity of AS11 strain under HM treatments

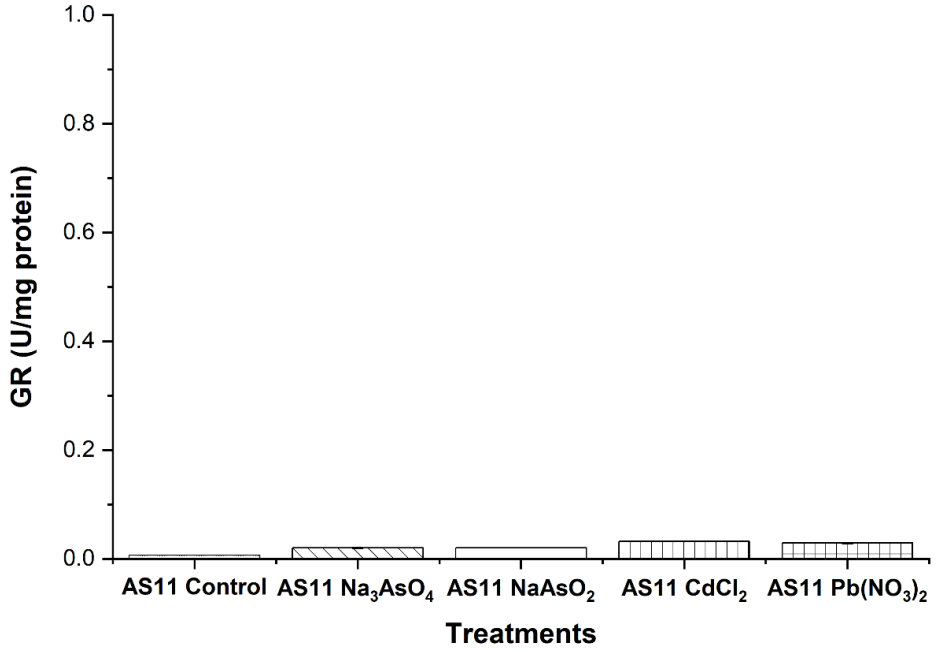

Figure 65. GR activity of AS11 strain under HM treatments

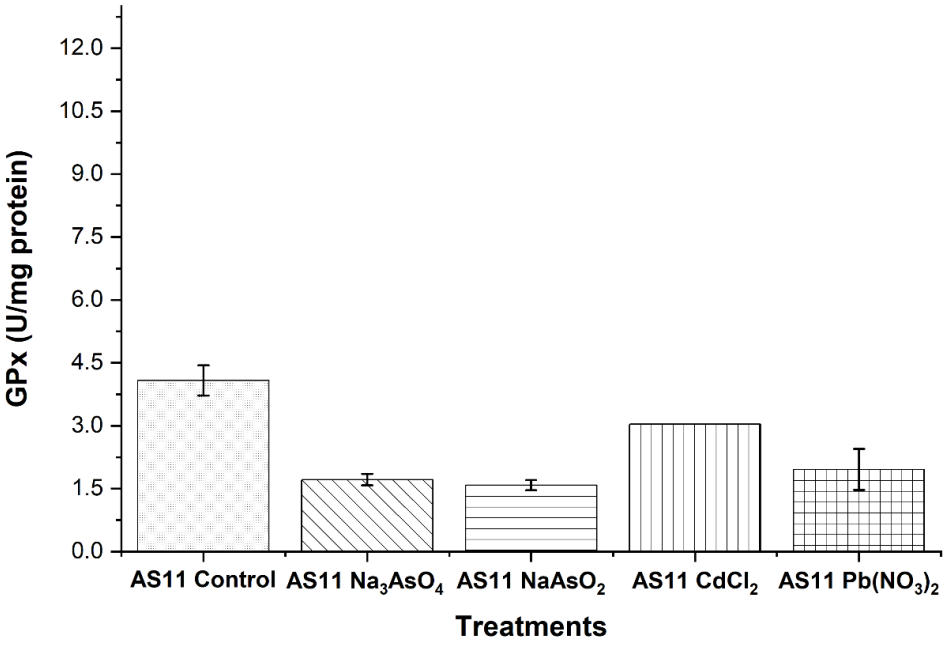

Figure 66. GPx activity of AS11 strain under HM treatments

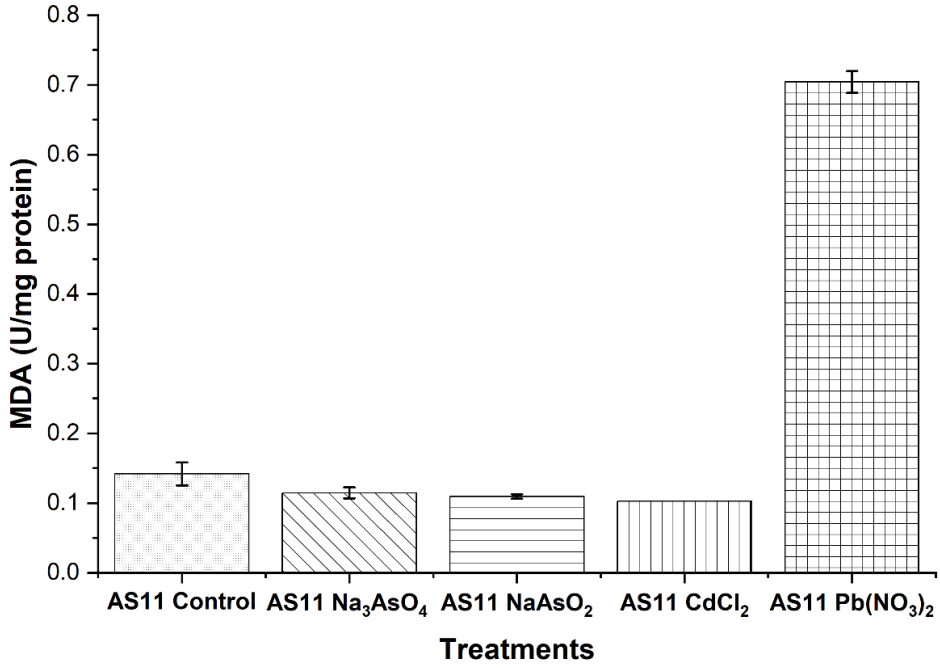

Figure 67. MDA activity of AS11 strain under HM treatments

4.14. *Bioremediation potential of the selected strains*

The bioremediation efficiencies of the tested HM ions by the selected bacterial strains was determined through ICP-MS. Findings revealed that strain AS3 has higher removal capacity for both As^{3+} (99.94 % ± 0.005) and As^{5+} (99.49 % ± 0.59) whereas for Cd^{2+} and Pb^{2+} removal efficiency was found to be 87.53 % ± 1.50 and 67.33 % ± 0.79, respectively.

In a similar manner, AS4 strain exhibited higher removal capacity for As^{3+} (95.67 ± 3.43 %) and As^{5+} (97.23 ± 2.69 %). Additionally, AS4 strain could able to remove 97.31 ± 2.02 % and 88.18 ± 2.69 % of Pb^{2+} and Cd^{2+} HM ions, respectively.

In the case of AS11 strain, removal of As^{5+} (99.93 ± 0.02 %) was comparatively higher than As^{3+} (97.34 ± 2.12 %) HM ions. Moreover, removal of Pb^{2+} was notably higher (93.27 ± 2.34 %) than that of Cd^{2+} (79.98 ± 2.53 %) HM ions.

4.15. *Estimation of Ammonia production by the selected bacterial strains*

The qualitative estimation of ammonia based on the development of orange coloration of the reaction mixture solution indicates the higher production of ammonia by AS3 strain followed by AS4 and AS11 (Figure 68). Moreover, quantitative estimation revealed that strain AS3, AS4, and AS11 could able to produced 73.06 ± 4.61 µg/mL, 48.09 ± 3.24 µg/mL, and 44.12 ± 3.17 µg/mL of ammonia (Table 36).

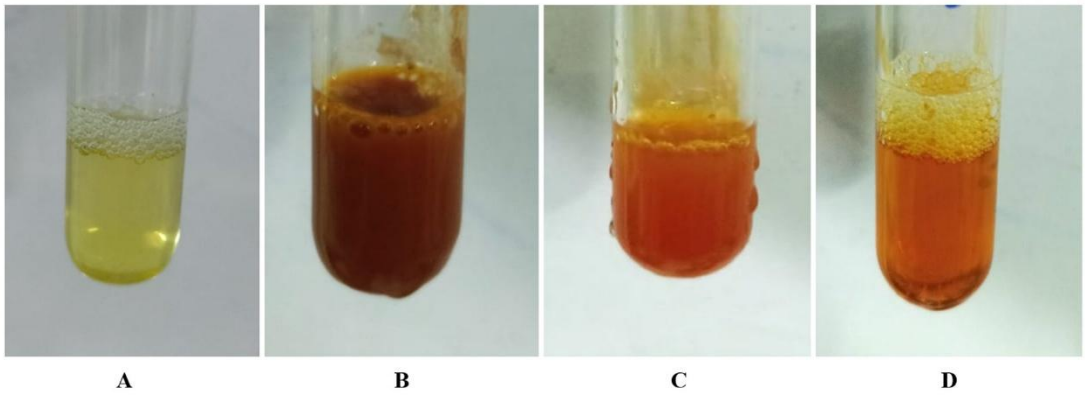

Figure 68. Ammonia production by (A) Control, (B) AS3, (C) AS4, and (D) AS11 strains

Table 36. Estimated ammonia and IAA production by the selected bacterial strains

Bacterial Strain	Ammonia production (µg/mL)	IAA production (µg/mL)
AS3	73.06±4.61	69.32 ± 7.04
AS4	48.09 ±3.24	61.77 ± 3.60
AS11	44.12 ±3.17	13.75 ± 3.83

4.16. *Evaluation of IAA producing capability*

Qualitative analysis indicated that AS3, AS4 and AS11 strain had IAA producing ability (Figure 69). The dark colouration of the reaction mixture indicates high production of IAA by the AS3 strain followed by pinkish colour of AS4 strain; indicating medium production and finally dim pinkish colour of AS11 strain; indicating least production of IAA. Further, on quantification, IAA produced by AS3 was determined to be 69.32 ± 7.04 µg/mL while for AS4 and AS11 strain, it was 61.77 ± 3.60 µg/mL and 13.75 ± 3.83 µg/mL, respectively (Table 29).

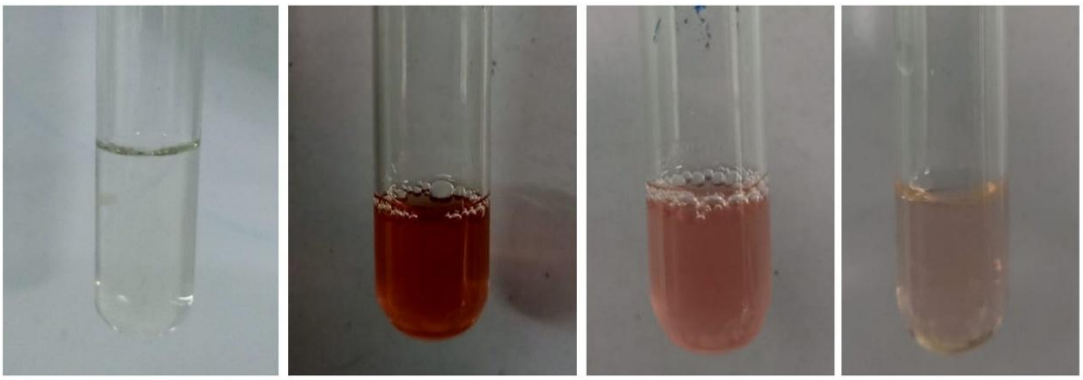

Figure 69. IAA production by (A) Control, (B) AS3, (C) AS4 and (D) AS11 strains

4.17. *Phytotoxicity assay of treated bacterial supernatant*

In the phytotoxicity experiment, seed germination was observed in almost all the treatments except in HMs consisting of As^{5+} (62500 ppm), As^{5+} (125000 ppm), As^{3+} (1562.50 ppm) and Cd^{2+} (1562.50 ppm), where none of the seeds could able to germinate. The phytotoxicity assay was thus performed based on the remaining treatments. The impact of different treatments *i.e.* only HMs, HMs along with

individual bacterial strain, and with bacterial strain only, on the germination of *Vigna radiata* seeds was investigated (Figure 70 and 71). This was done by analysing the germination indices (GI) data, which involved assessing the results of RSG (%) and RRL (%) at a significance level of P value < 0.05.

4.17.1. *Determination of RSG %*

The RSG (%) for seed samples treated with only AS3 strain, AS3 strain with As^{5+}, AS3 strain with As^{3+}, and AS3 strain with Pb^{2+} was determined to be 100 % (Table 30). However, the RSG (%) decreased in AS3 strain with Cd^{2+} seed treated samples (93.33%). In case of AS4 strain, the RSG (%) for seed samples treated with only AS4 strain, AS4 strain with As^{5+}, AS4 strain with As^{3+}, AS4 strain with Pb^{2+} and AS4 strain with Cd^{2+} was observed to be 100 % (Table 31). Likewise, AS11 strain also had 100 % RSG (%) for all the treatments, *i.e.* with only AS11 strain, AS11 strain with As^{5+}, AS11 strain with As^{3+}, AS11 strain with Pb^{2+} and AS11 strain with Cd^{2+} (Table 32).

However, in case of simply HM treatments, Pb^{2+} treated seed samples (91.67 ± 14.43 %) had the highest RSG (%), followed by Cd^{2+} (58.33 ± 14.43 %), and was lowest for both As^{5+} and As^{3+} (50 %) treated seed samples (Table 33).

4.17.2. *Determination of RRL %*

In case of AS3 strain, the highest RRL (%) was observed in seeds treated with only AS3 strain (349.16 ± 137.12 %), followed by seeds treated with AS3 strain + Pb^{2+} (169.82 ± 71.73 %), AS3 strain + As^{3+} (99.20 ± 40.02 %), AS3 strain + As^{5+} (96.44 ± 7.34 %) and AS3 strain + Cd^{2+} (86.05 ± 44.06 %) (Table 30). Likewise, in case of AS4 strain, the RRL (%) was found to be highest with only AS4 strain (353.32 ± 145.50 %), followed by seeds treated with AS4 strain + As^{5+} (224.38 ± 67.99 %), AS4 strain + As^{3+} (170.20 ± 36.13 %), AS4 strain + Cd^{2+} (107.72 ±23.69 %) and AS4 strain + Pb^{2+} (154.30 ± 12.89 %) (Table 31). Further, in case of AS11 strain, the RRL (%) was found to be highest with only AS11 strain (199.60 ± 41.07 %), followed by seeds treated with AS11 strain + Pb^{2+} (197.35 ± 59.18 %), AS11 strain + As^{3+} (157.57 ± 54.14 %), AS11 strain + Cd^{2+} (133.96 ± 36.71%) and AS11 strain + As^{5+} (124.74 ± 69.85 %) (Table 32). Further in the case of only HM treatments, Pb^{2+} (98.50 ± 33.04

%) had the highest RRL (%), followed by Cd^{2+} (43.98 ± 17.79 %), As^{5+} (41.32 ± 14.27 %), and As^{3+} (30.22 ± 6.97 %) (Table 33).

4.17.3. *Determination of GI % and GVI*

Seeds treated with only AS3 strain without any metallic treatments exhibited the highest GI and GVI of 349.16 ± 137.12 % and 13.84 ± 1.97, respectively (Table 37). Further, seeds treated with AS3 strain + Pb^{2+} had the second highest values of GI and GVI with 169.82 ± 71.73 % and 5.81 ± 1.21, respectively. This was followed by seeds treated with AS3 strain + As^{3+}, with a GI of 99.20 ± 32.68 % and a GVI of 2.43 ± 0.75. Seeds treated with AS3 strain + As^{5+} had a GI of 96.44 ± 7.34 % and a GVI of 2.38 ± 0.08. Lastly, seeds treated with AS3 strain + Cd^{2+} had a GI of 83.43 ± 48.26 % and a GVI of 1.811 ± 0.74.

Table 37. RSG, RRL, GI and GVI of AS3 strain in different treatments

Treatment	AS3	AS3 + As^{5+}	AS3 + As^{3+}	AS3 + Pb^{2+}	AS3+ Cd^{2+}
RSG%	100.00	100.00	100.00	100.00	93.33 ± 11.55
RRL%	349.16 ± 137.12	96.44 ± 7.34	99.20 ± 40.02	169.82 ± 71.73	86.05 ± 44.06
GI	349.16 ± 137.12	96.44 ± 7.34	99.20 ± 32.68	169.82 ± 71.73	83.43 ± 48.26
GVI	13.84 ± 1.97	2.38 ± 0.08	2.43 ± 0.75	5.81 ± 1.21	1.81 ± 0.74

In case of AS4 strain, the GI and GVI were found to be highest in seeds treated with AS4 strain alone with a GI of 353.32 ± 145.50 % and a GVI of 10.92 ± 1.94 (Table 38). Seeds treated with AS4 strain + As^{5+} had the next highest values, with a GI of 224.38 ± 67.99 % and a GVI of 6.94 ± 1.32. This was followed by seeds treated with AS4 strain + As^{3+}, with a GI of 170.21 ± 36.13 % and a GVI of 5.31 ± 0.44. Further, seeds treated with AS4 strain + Cd^{2+} had a GI of 144.39 ± 25.06 % and a GVI of 4.81 ± 0.51. Finally, seeds treated with AS4 strain + Pb^{2+} had the least GI and GVI of 107.72 ± 36.13 % and 4.05 ± 0.35, respectively.

Table 38. RSG, RRL, GI and GVI of AS4 strain in different treatments

Treatment	AS4	AS4 + As^{5+}	AS4 + As^{3+}	AS4 + Pb^{2+}	AS4 + Cd^{2+}
RSG%	100.00	100.00	100.00	100.00	100.00
RRL%	353.32 ± 145.50	224.38 ± 67.99	170.21 ± 36.13	107.72 ± 23.69	154.30 ± 12.89
GI	353.32 ± 145.50	224.38 ± 67.99	170.21 ± 36.13	107.72 ± 23.69	144.39 ± 25.06
GVI	10.92 ± 1.94	6.94 ± 1.32	5.31 ± 0.44	4.05 ± 0.35	4.81 ± 0.51

In case of AS11 strain, GI and GVI were highest in seeds treated with AS11 strain alone with 199.60 ± 41.07 % and 8.19 ± 1.64, respectively (Table 39). Seeds treated with AS11 strain + Pb^{2+} had the second highest values for GI and GVI with 197.35 ± 59.18 % and 5.6 ± 0.56, respectively. This was followed by seeds treated with AS11 strain + As^{3+}, with a GI and GVI of 157.57 ± 54.14 % and 5.6 ± 0.56, respectively. Further, seeds treated with AS11 strain + Cd^{2+} had a GI of 133.96 ± 36.71 % and a GVI of 4.58 ± 0.59. Finally, seeds treated with AS11 strain + As^{5+} showed a GI and GVI of 124.74 ± 69.85 % and 4.68 ± 1.82, respectively.

Table 39. RSG, RRL, GI and GVI of AS11 strain in different treatments

Treatment	AS11	AS11 + As^{5+}	AS11 + As^{3+}	AS11 + Pb^{2+}	AS11 + Cd^{2+}
RSG%	100.00	100.00	100.00	100.00	100.00
RRL%	199.60 ± 41.07	124.74 ± 69.85	157.57 ± 54.14	197.35 ± 59.18	133.96 ± 36.71
GI	199.60 ± 41.07	124.74 ± 69.85	157.57 ± 54.14	197.35 ± 59.18	133.96 ± 36.71
GVI	8.19 ± 1.64	4.68 ± 1.82	5.91 ± 1.50	5.60 ± 0.56	4.58 ± 0.59

When the seeds were treated with only HMs, the GI value was found to be highest for Pb^{2+} (93.05 ± 41.49 %), followed by Cd^{2+} (25.91 ± 11.99 %), As^{5+} (20.66

± 7.14 %), and lastly As^{3+} (15.11 ± 3.48 %). The GVI was shown to be greatest for Pb^{2+} (2.26 ± 0.84), followed by Cd^{2+} (1.18 ± 0.65), As^{3+} (0.76 ± 0.04), and lastly As^{5+} (0.72 ± 0.19) (Table 40).

Table 40. RSG, RRL, GI and GVI under different HM treatments

Treatment	As^{5+}	As^{3+}	Pb^{2+}	Cd^{2+}
RSG%	50.00 ± 0.00	50.00 ± 0.00	91.67 ± 14.43	58.33 ± 14.43
RRL%	41.32 ± 14.27	30.22 ± 6.97	98.50 ± 33.04	43.98 ± 17.79
GI	20.66 ± 7.14	15.11 ± 3.48	93.05 ± 41.49	25.91 ± 11.99
GVI	0.72 ± 0.19	0.76 ± 0.04	2.26 ± 0.84	1.18 ± 0.65

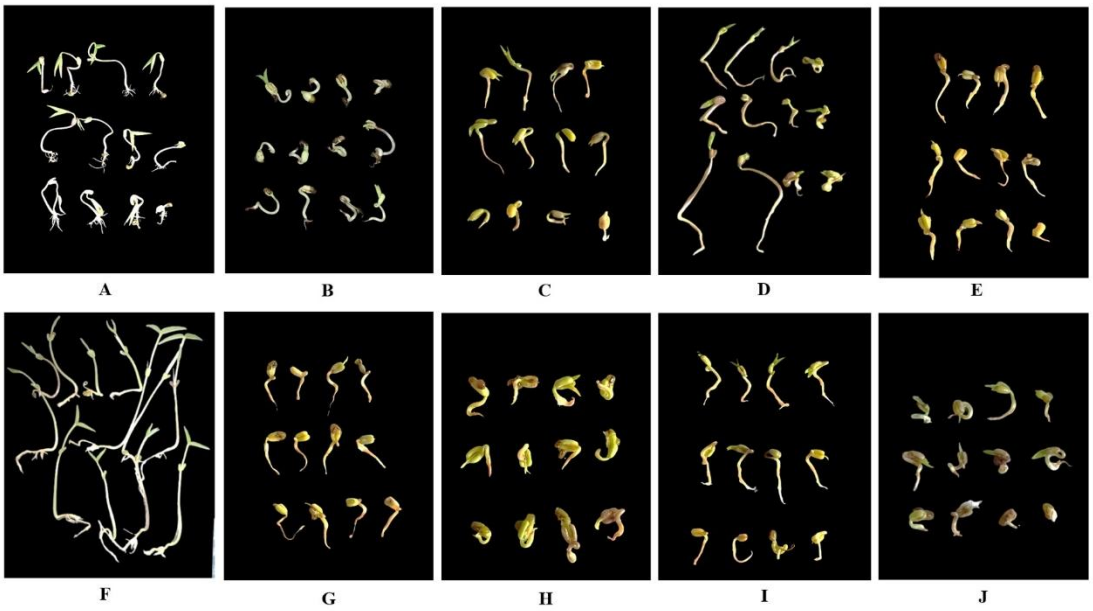

Figure 70. Phytotoxicity assay of *Vigna radiata* seeds in the presence of (A) distilled water only, (B) AS3 strain and As^{5+}, (C) AS3 strain and As^{3+}, (D) AS3 strain and Pb^{2+}, (E) AS3 strain and Cd^{2+}, (F) only AS3 strain, (G), only As^{5+}, (H) only As^{3+}, (I) only Pb^{2+}, and (J) only Cd^{2+}

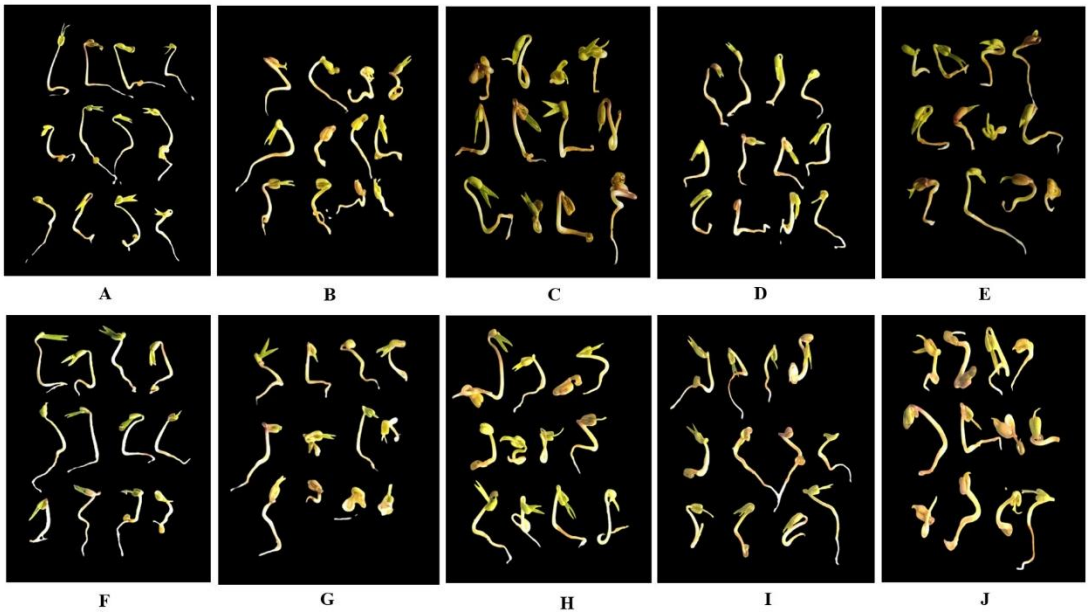

Figure 71. Phytotoxicity assay of *Vigna radiata* seeds in the presence of (A) only AS4 strain, (B) AS4 strain and As^{5+}, (C) AS4 strain and As^{3+}, (D) AS4 strain and Pb^{2+}, (E) AS4 strain and Cd^{2+}, (F) only AS11 strain, (G) AS11 strain and As^{5+}, (H) AS11 strain and As^{3+}, (I) AS11 strain and Pb^{2+}, and (J) AS11 strain and Cd^{2+}

4.18. *Brine shrimp toxicity study*

Findings of brine shrimp toxicity studies with HMs treatment revealing higher mortality (%) of 90 ± 10 %, 66.67 ± 5.77 %, 60 ± 10 %, 46.67 ± 15.28, 43.33 ± 5.77 %, 40 ± 10 %, and 33.33 ± 5.77 % on exposure to As^{5+} (125000 ppm), As^{5+} (62500 ppm), As^{3+} (1562.50 ppm), As^{5+} (15625 ppm), Pb^{2+} (6250 ppm), As^{3+} (781.25 ppm), and Cd^{2+} (1562.50 ppm) respectively. However, Cd^{2+} (48.82 ppm) treatment exhibited significantly reduced larvicidal activity (13.33 ± 11.55) (Table 41). Presence of bacterial strain *viz*. both AS3 + As^{3+} and AS4 + As^{5+} treatments exhibited similar larvicidal activity of 23.33 ± 5.77 %, while it was 20 ± 10 % for AS3 + Cd^{2+}. Further, larvicidal activity was found to be lower in AS3 + As^{5+} (16.67 ± 15.28 %), AS4 + As^{3+} (13.33 ± 5.77 %), AS4 + Pb^{2+} (13.33 ± 5.77 %), AS11 + As^{5+} (13.33 ± 11.55 %), and AS11 + Pb^{2+} (13.33 ± 5.77 %), AS4 + Cd^{2+} (10 %), and AS11 + As^{3+} (10 %). Moreover, larvicidal activity decreased further to 3.33 ± 5.77 % in the presence of AS3 + Pb^{2+}which was even lesser than that of the control (6.67 ± 5.77 %). Additionally, an

exceptional no mortality was observed in the presence of only AS3, AS4 and AS11 strains.

Table 41. Larvicidal activity of brine shrimp larvae under different HMs treatments

Sl. No.	Treatment	Concentration of HM (ppm)	Average Mortality (%)
1.	AS3 + As^{5+}	62500	16.67 ± 15.28
2.	AS3 + As^{3+}	781.25	23.33 ± 5.77
3.	AS3 + Pb^{2+}	6250	3.33 ± 5.77
4.	AS3 + Cd^{2+}	1562.50	20.00 ± 10.00
5.	AS3	0	0
6.	AS4 + As^{5+}	15625	23.33 ± 5.77
7.	AS4 + As^{3+}	1562.50	13.33 ± 5.77
8.	AS4 + Pb^{2+}	6250	13.33 ± 5.77
9.	AS4 + Cd^{2+}	1562.50	10.00 ± 0.00
10.	AS4	0	0
11.	AS11 + As^{5+}	125000	13.33 ± 11.55
12.	AS11+ As^{3+}	781.25	10.00 ± 0.00
13.	AS11 + Pb^{2+}	6250	13.33 ± 5.77
14.	AS11 + Cd^{2+}	48.82	23.33 ± 5.77
15.	AS11	0	0
16.	Saline water	0	6.67 ± 5.77
17.	As^{5+}	62500	66.67 ± 5.77
18.	As^{5+}	15625	46.67 ± 15.28
19.	As^{5+}	125000	90.00 ± 10.00
20.	As^{3+}	781.25	40.00 ± 10.00
21.	As^{3+}	1562.50	60.00 ± 10.00
22.	Pb^{2+}	6250	43.33 ± 5.77

23.	Cd^{2+}	1562.50	33.33 ± 5.77
24.	Cd^{2+}	48.82	13.33 ± 11.55

4.19. ***Statistical analysis***

All the experiments were checked for one-way ANOVA wherever applicable and found as F greater than the critical value and thus found to be significant at $p<0.05$. One-way ANOVA was performed to compare soil physico-chemical parameters (pH, EC, Temperature, organic carbon, available N, P, and K, soil moisture, and HM analyses) across the 6 sites of sample collection. Since, the site 1, 2, 3 were from similar area, the analysis revealed no significant differences ($p > 0.05$) in soil pH, EC, temperature, organic carbon, available N, P, and K, Soil Moisture. Likewise, it was similar for Site 4, 5, 6. However, for HM analysis of soil, ($p < 0.05$) was observed for all the sites.

The analyses showed a significant variation in MICs among the AS3, AS4 and AS11 bacterial strains at $p < 0.05$. These results confirm that As-resistance levels differ among the tested bacteria, with certain isolates exhibiting strong tolerance. Further, growth kinetics and antibiotic susceptibility studies showed significant differences among the three strains at $p < 0.05$.

One-way ANOVA was carried out to compare the production levels of biofilm, siderophores, and EPS among the selected bacterial strains at $p < 0.05$. The analysis revealed a significant variation in biofilm formation and siderophore production across the selected bacterial strains.

Significant differences ($p < 0.05$) were observed in TPC, CAT, SOD, and GR, GPx and MDA activities among the selected bacterial strains. However, there was huge variation among AS3, AS4 and AS11 with respect to the enzyme activity highlighting their different way of dealing with HM stress.

To compare the bioremediation potential of selected bacterial strains one-way ANOVA was performed. At $p < 0.05$, the analysis showed significant variation among the bacterial strains for different HMs. Likewise, ammonia and IAA production also showed significant differences in terms of production ability at $p < 0.05$.

For assessing the phytotoxicity effects among the selected bacterial strains one-way ANOVA was performed. The analysis at $p < 0.05$ revealed a significant variation

in the degree of phytotoxic effects among the bacterial strains, suggesting differential influence on plant growth parameters. Moreover, one-way ANOVA was also applied to evaluate the larvicidal activity of selected bacterial strains. Results indicated a significant difference ($p < 0.05$) among the groups tested, demonstrating that larvicidal potential varied significantly across bacterial strains.

5.1. *Study area and sample collection*

Nagaland, characterized by its hills and forests, is a state in Northeast India that possesses immense mineral potential found within the Naga Hills. The natural resources encompass forests, river systems, and coal deposits found in the Mokokchung-Wokha belt and adjacent ranges. The Directorate of Geology and Mining, Nagaland has listed numerous coal blocks with resources and described the coal as non-coking, sub-bituminous, with high moisture along with different gross calorific values (Directorate of Geology and Mining, Nagaland).

The Mokokchung district, located in central-northeast Nagaland, predominantly features a plateau and hilly terrain, with coal deposits found along the Changkikong/Tsurangkong ranges and adjacent ranges. The rivers in Mokokchung district flow through the coal-bearing hills, with recent investigations indicating unorganized small-scale mining activities in the Changkikong/Changkikong–Tsurangkong ranges. The findings indicated a low pH alongside elevated metal concentrations in areas downstream of mining activities (Vadeo et al., 2023).

Changki or Changkikong refers to certain village areas or blocks in Mangkolemba sub-division of Mokokchung district. Changki Coal Blocks A and B are designated as specific exploration blocks in the Government exploration reports and Nagaland Directorate of Geology and Mining [Changki Block A: exploration 2014–2017 and Changki Block B: exploration reported 2017–2021 (Directorate of Geology and Mining, Nagaland)]. Furthermore, as indicated by the topographic sheets from the Survey of India cited in the official reports, the blocks are situated within the Mokokchung sector (Directorate of Geology and Mining, Nagaland, n.d.).

Changki has experienced prolonged small-scale or rat-hole extraction by local operators since 2000s, with an increase in intensity around the 2010s. The exploration by government took place in phases from 2010-2014, 2014-2017 (Changki A) and 2017-2021 (Changki B) (Morung Express, 2016). Various primary field evidence for HM contamination in Changki area has been reported by Semy and colleagues (Semy and Singh, 2021). Prior records of Changki indicate the presence of HMs like Zn, Cd, Ni and Cu in forest soil and river water around coal mines beyond permissible limit (Semy and Singh, 2021a; Semy and Singh, 2021b). Due to its proximity to several natural springs and fresh water streams, and heavy precipitation during the rainy

season, the coal mine around the Changki are highly vulnerable to naturally occurring acid mine drainage (NOAMD). There is a close relationship between acid mine drainage (AMD) and HM pollution, which might be occurring in Changki. According to the previous scientific investigations, NOAMD frequently contains hazardous HMs like As, which increases the likelihood of arsenic pollution in the Changki area (Morgante et al., 2015). The oxidation of sulfur-rich minerals due to mining generally releases sulfuric acid, which lowers the pH of drainage water and increases the mobility of metalloids or trace metals from rocks into dissolved form. One possible geochemical mechanism connecting Changki coal mining to HM contamination in AMD areas is the enhanced downstream transfer of dissolved metal ions caused by this low pH (Kumar et al., 2024). Numerous regional and local studies have recorded AMD in rivers originating from the Changki, Tsurangkong, and Changkikong ranges (Semy and Singh, 2021b). Vadeo et al. (2023) observed that the spread of AMD from mine tailings and the absence of adequate mitigating measures led in downstream contamination of the Tzuong/Tsurang river system. Acidification, mining-related landslides, and subsequent waterway contamination have been published by Morung Express, a popular daily newspaper, at Changki (Morung Express, 2016). Hence, occurrence or deposition of those HMs which are frequently associated with coal mining will be maximum in the NOAMD effected areas. Further, HMs get dispersed and contaminated the surrounding environment around point source to a greater extent by means of runoff after heavy rain (Moghadam and Azadmehr, 2025) together with NOMAD (Anekwe and Isa, 2023).

Severely HM contaminated environments are known to habitat of several unique species of bacteria where they not only thrive and multiply but play a significant ecological role in their biotic community (Filali et al., 2000; Tatung and Deb, 2024; Abbas et al., 2025; Iimaa et al., 2025). Such bacterial species have persistently evolved in response to HM exposure, thereby attaining resistance through various mechanisms *viz*. through the regulation of metal resistance systems (Diba et al., 2021), extracellular metal sequestration (Voica et al., 2016), biosorption (Sevak et al., 2021), reduction of HM ions (Ukkund et al., 2021), morphological alterations (Mathivanan et al., 2021b), etc. With reference to the background information, in the present study soil samples were collected from both upside and downside of the coal

mines that covers the NOMAD areas, with the goal to screen and isolate indigenous HM metal resistance bacterial species inhabiting around mines of Changki hill. Further, limited research investigation on the soil microflora has been carried out so far in this region. Most of the available information are confined to the assessment of soil (Semy and Singh, 2021a) or water (Semy and Singh, 2021b; Vadeo et al., 2023) quality, however availability of previously published data on the microbiota are scarce. Recently, HM resistant rhizobacteria that may demonstrate resistance against Cu, Cr, Zn, Cd, Ni, Sb, and As were reported from coal mining area of Changki in a study conducted by Tatung and Deb (2024). A study conducted by Semy and Singh (2021a) reported the presence of Zn and Cd HMs beyond the standard limits in forest soil around coal mines of Changki.

5.2. *Physico-chemical characteristics of the collected soil samples*

The pH values of the collected soil samples were in the range of 5.2–5.6 indicating slightly acidic soil. The reason behind this could be attributed to the dead decaying biomass specially leaf litter which produces organic acids through decomposition process along with leaching of base cations by rain water or percolating water or due to long term pedogenesis of acidic bedrock (Motavalli et al., 1995; Jobbágy and Jackson, 2003; Zhang et al., 2025).

Moreover, EC of the collected soil samples was present in the range of 2.4-5.7 mS, indicating moderate (Site 4-6) to high salinity (Site 1-3). The high salinity in Site 1-3 could be attributed to the inflow of groundwater or evaporation (Li et al., 2021).

The available total N was found to be in the range of 52.5-184.4 kg/acre, indicating moderate to high N levels. P and K was found to be in low concentrations possibly due to active leaching or turnover by fresh water streams (Mendes et al., 2016; Gillespie et al., 2018; Krieg et al., 2021).

Furthermore, the soil moisture was found in the range of 19.4-22.1%, indicating moderate soil moisture levels as present in forest areas, suitable for microbial growth and decomposition of organic matter (Adams et al., 2019). The TOC was also present in the range of 1.1-2.3% indicating low to moderate levels for soil and microbial growth (Parvez et al., 2025).

The presence of As, Cd and Pb in the soil samples may be attributed to the human agricultural practices involving fertilizers, mine tailings (Vadeo et al., 2023) or

due to the whethering of parent rocks from where they have originated (Wuana and Okieimen, 2011; Łukaszek-Chmielewska et al., 2025). Furthermore, the organic acids by leaf litter can result in decreased soil pH, in turn increasing exchangeable cations and increased HMs in the soil with due time (Zhang et al., 2024). Previous studies have reported the contamination of soil and water with As and Cd HM by coal mine activities in Changki Hills of Mokokchung district (Semy and Singh, 2021a; Tatung and Deb, 2024).

5.3. *Isolation, identification and screening of potential As-resistant bacteria*

5.3.1. *Isolation and identification of As-resistant bacteria*

Finding bacterial species that are resistant to toxic HM ions specifically to As was the key objective of the present study. A total of ten bacterial isolates were obtained from the different soil samples using the enrichment culture technique where culture medium was supplemented with $NaAsO_2$ and Na_3AsO_4 salts. During the process of isolation and screening, the enrichment culture method facilitates the growth and multiplication of targeted microorganisms that possess the desired traits, hence increasing the population of target species. Identifying organisms based on the distinct metabolic abilities or adaptive features against certain toxic substance is a straightforward approach to discovering new species (Gupta, 2023). In addition, the enrichment culture method was performed not only to generate a population of bacteria resistant to HMs, but also to eliminate the auxotroph (Roncero, 1984).

Through the combination of ribotyping techniques and routine biochemical testing, the selected potential bacterial isolate AS3 and AS4 was identified as different strains of *Lysinibacillus* species. Further, isolate AS11 was identified through whole genome sequencing technique and found to be of *Staphylococcus equorum* species. The bacterial strain AS3 was found to be 94% identical to *Lysinibacillus* sp. strain R2-3-2 (Accession ID: MN696519) that had previously reported by Qianwen in 2019 (NCBI, 2019). The strain AS4 was found to be 90% identical to *Lysinibacillus* sp. strain AS3 (Accession ID: OQ202230), which was previously reported by Gogoi et al. (2025) and 75% similar to *Lysinibacillus* sp. L1 (Accession ID: JX402789.1) which was isolated by Vinod Shinde in 2012 (NCBI, 2012). The strain AS11 was found to be having almost 92% phylogenetic similarity with *Staphylococcus equorum* subsp. equorum Mu2 (Accession ID: CAJL00000000.1) which was previously reported by

Irlinger and colleagues, isolated from a French smear-ripened cheese (Irlinger et al., 2012).

As per our knowledge the present study reports on the first instance of *Lysinibacillus* species from North-Eastern India and Nagaland that exhibit great tolerance against HMs including As, Cd, and Pb ions. Several bacteria from the *Lysinibacillus* genus have been documented to exhibit resistance to HMs, including As, such as *Lysinibacillus* strain B1-CDA (Rahman et al., 2014), *Lysinibacillus* spp. DMAB5 (Mandal et al., 2022), and *L. boronitolerans* P2IIIb (Aguilar et al., 2020). Moreover, *Lysinibacillus* species including *L. fusiformis* L13 (Ma et al., 2023) and *L. varians* strain KUBM17 reported to exhibit resistance towards Cd^{2+} ions (Pal and Sengupta, 2019). In addition, *L. varians* strain KUBM17 also reported to exhibit resistance to Pb^{2+} HM ions (Pal and Sengupta, 2019).

Genus *Staphylococcus* also reported to exhibit the capacity to tolerate a number of HMs. Pradel et al. (2013) reported a Cr resistant *S. equorum* with a MIC 750 mM for Cr(VI) isolated from contaminated marine sediment. Rahman et al. (2019) reported a Pb^{2+} HM resistant strain of *S. hominis* AMB-2 from Mandoli industrial area, Delhi, India exhibiting the biosorption potential of Cd^{2+} and Pb^{2+} HM ions. *S. equorum* and *S. warneri* isolated from saffron soils of Kashmir have been reported to exhibit tolerance against Pb^{2+} and could sequestrate Pb^{2+} HM ions at varying MIC (Uqab et al., 2020). *S. equorum* PU1 isolated from Pu-erh rhizosphere soil reported to be exhibit high Cd^{2+} tolerance with a MIC of 500 mg/L (Chen et al., 2023).

5.3.2. *Screening of potential As-resistant bacterial strain*

The capacity to the bacterium to proliferate at elevated concentrations of HM was utilized to ascertain its tolerance threshold to a particular HM in the medium and was also confirmed by measuring the bacterium's growth on the resulting higher concentration. The capacity of strains to proliferate in severely HM-contaminated liquid media indicates that they could flourish in substantially HM-polluted aquatic settings, such as sewage channels or industrial effluents (Nnaji et al., 2024). Piotrowska-Seget et al. (2005) mentioned that as the concentration of HMs in the natural habitats grows, the prevalence of tolerant bacteria in metal-contaminated environments escalates.

The MIC values of AS3, AS4 and AS11 bacterial strains against the tested HMs were determined using LB broth. LB broth has been recommended by several researcher due to its instantaneous preparation, convenience of repeatability, affordability, and suitability for several HM assays (Hasselmann, 2003; Wiegand et al., 2008; Agarwal et al., 2020). The MIC values recorded in the present study, as presented in Tables 18, exceeded than those reported by previous researchers. Typically, elevated levels of HMs correlate with diminished bacterial proliferation, mostly due to compromised membrane functions and binding of metal ions to surfaces. Nevertheless, HM-resistant strains typically endure harsh HM-rich environment by means of various intrinsic mechanisms *viz*. synthesis of EPS, presence of efflux and transporter proteins, metal adsorption on cellular envelopes, methylation, reduction to less toxic forms, existence of multiple HM resistance genes and operons, and by several other additional pathways (Haferburg and Kothe, 2010; Gogoi et al., 2023).

Furthermore, all the three strains exhibited higher MIC values for arsenate ions compared to arsenite which suggests its lesser toxicity. These findings are quite consistent with those other reports which are presented in the Table 42. According to Abbas et al. (2014), such observation could be explained based on the greater solubility of metal arsenite relative to metal arsenate. Moreover, the selected bacterial strains also exhibited their efficiency to tolerate Pb^{2+} and Cd^{2+} ions with high MTC values compared to previous reports (Table 43) which confirms their multi-metal resistance capacity. Thus, signifying the prospect of employing the selected bacterial strains for the bioremediation.

Table 42. Previously reported MICs of bacteria against As^{5+} and As^{3+} HM ions

Sl No.	Bacterial strains	MIC against arsenate ions	MIC against arsenite ions	Type of media	Reference
1.	*Serratia marcescens* KG1D	2500 µg/mL	500 µg/mL	Minimal salts medium (MSM)	Roy et al. (2024)
2.	*Alcaligenes faecalis* PF14	1.8 mg/mL	0.6 mg/mL		

3.	*Alcaligenes faecalis* MNZ1	–	300 mg/mL	Acetate minimal medium broth	Abbas et al. (2014)
4.	*Klebsiella pneumoniae* MNZ4	_	300 mg/L		
5.	*Klebsiella pneumoniae* MNZ6	_	370 mg/L		
6.	*Sporosarcina luteola* M10	70 mg/mL	1.3 mg/mL	Minimal medium broth	Salam et al. (2020)
7.	*Serratia marcescens* TSU1	_	120 mg/mL	Nutrient agar	Tatung and Deb (2024)
8.	*Bacillus cereus* TSU3	_	840 mg/mL		
9.	*Microbacterium paraoxydans* DSM 15019	52.15 mg/mL	4.80 mg/mL	Luria Bertani agar	Mandal et al. (2024)
10.	*Lysinibacillus* sp.	31.20-156.00 mg/mL	1.95-3.90 mg/mL	Basal Salt Medium (BSM)	Pandey and Keshavkant (2019)

Table 43. Previously reported MICs of bacteria against Pb^{2+} and Cd^{2+} ions

Sl No.	Bacterial strains	MIC against Pb (II) ions	MIC against Cd (II) ions	Type of media	Reference
1.	*Lysinibacillus fusiformis* L13	_	100 mg/L	Luria Bertani broth	Ma et al. (2023)

2.	*Lysinibacillus varians* strain KUBM17	0.45 mg/mL	0.15 mg/mL	Nutrient agar	Pal and Sengupta (2019)
3.	*Lysinibacillus* sp. GY3	0.625 mg/mL	_	Luria Bertani broth	Li et al. (2021)
4.	*Lysinibacillus fusiformis* strain P6	0.7 mg/mL	_	Nutrient broth	Agarwala et al. (2024)
5.	*Staphylococcus equorum* PU1	_	0.5 mg/mL	_	Chen et al. (2023)
6.	*Staphylococcus equorum*	0.7 mg/mL	_	Mueller Hinton Broth	Nazir et al. (2020)
7.	*Staphylococcus hominis strain* AMB-2	3.5 mg/L	0.04 mg/L	Luria Bertani agar	Rahman et al. (2019)

5.4. *Growth kinetics*

Based on the findings, it was clear that metallic stress developed on the selected bacterial strain when grown along the tested HMs and the same could be simply seen in their growth curves patterns. However, growth behaviour of each bacterial strain on different HMs *i.e.* As, As, Cd, and Pb are quite distinct from one another. Even notable variations in the growth pattern among the bacterial strains with HM were also observed. In the presence of HMs, bacterial strains showed prolonged lag phase. For instance, AS3 and AS11 strain took over twelve hours to adjust to the stress in the presence of As^{5+} HM ions. According to Cristani et al. (2012), extended lag phase is mostly due to physico-chemical interaction that occurs between the bacterial cells and the metals, a lengthy process that occurred when bacteria multiplies in the presence of metals. Unambiguously, the extended lag phase and late exponential phase of the growth curve shows that the strains were under metallic stress or deliberately starts to oxidize As^{3+} as a defensive mechanism (Bachate et al., 2012; Bertrand, 2019).

Additionally, studies also reveal that As damages the bacterial cell wall, causing the bacteria to respond towards As stress with an extended lag phase during which cells strive to adjust to their new surroundings (Abbas et al., 2014). However, growth pattern in the presence of As^{3+} ions in certain strains was comparable with that of the control, suggesting that the bacteria were not under much stress.

Moreover, prior research indicates that bacteria exposed to Cd can also exhibit a longer lag phase. The rapid growth that occurs after 10–12 h may be explained by the acclimatization process, which activates detoxification mechanisms that include efflux pumps, sequestration, or the process of repairing damaged biomolecules that used to occur before the initiation of normal division (Roberts, 1983; Nnaji et al., 2024). It has been reported that HM causes cell damage when a bacterium is introduced into a fresh culture that contains them. Under such condition, bacterium utilize more of its energy to repair the cellular damage and adjust its enzymatic route to the altered environment (Gikas et al., 2009). Furthermore, in the presence of Pb^{2+} HM ions, the early exponential phase may indicate the initiation of lead-binding protein synthesis (Pal and Sengupta 2019), or the activation of the metal efflux pump (Shaw and Dussan, 2018), that allows the bacteria to initially resist the deleterious effects of Pb ions. In addition, the recurrence of exponential phase demonstrated that the strains had fully recovered from the stress and was able to proliferate, which was a clear sign of its great tolerance to the exposed metallic treatments (Neidhardt et al., 1990; Koch, 1997).

5.5. *Antibiotic susceptibility and MAR index*

Among the tested 14 different antibiotics, all the strains were sensitive to chloramphenicol (30 mcg), ciprofloxacin (5 mcg), clarithromycin (15 mcg) and amoxicillin (10 mcg), which are belonged to broad spectrum antibiotics. However, the strains were found to be resistant against two broad spectrums *i.e.* tetracycline (30 mcg) and ampicillin (10 mcg) and one narrow spectrum antibiotics *i.e.* penicillin (0.6 mcg). In addition, strain AS3 showed further resistance against few other broad-spectrum antibiotics *viz.* streptomycin (10 mcg), cephalexin (30 mcg) and azithromycin (15 mcg) while sensitive to two broad spectrum antibiotics *viz.* norfloxacin (10 mcg) and erythromycin (15 mcg). Likewise, strain AS4 was further found to be resistant against three broad spectrum antibiotics *viz.* kanamycin (5 mcg),

norfloxacin (10 mcg) and erythromycin (15 mcg) and sensitive to three other broad-spectrum antibiotics *i.e.* streptomycin (10 mcg), cephalexin (30 mcg) and azithromycin (15 mcg). Additionally, strain AS11 showed further resistance against three major broad-spectrum antibiotics *i.e.* cephalexin (30 mcg), azithromycin (15 mcg) and erythromycin (15 mcg). In general the resistance exhibited by a bacterium against an antibiotic indicates its adaptive capability (Motta et al., 2015) to survive and grow in the presence of that antibiotic and is attained by inheriting certain mechanisms such as producing enzymes (Coculescu, 2009), presence of certain efflux pumps (Schindler and Kaatz, 2016), altered targets (Walsh, 2000) and certain changes in the membrane permeability (Nikaido, 2001).

The present study employed environmental samples taken from the immediate vicinity of an open coal mine located in the rugged landscape of Changki. This location is inhabited by a substantial number of human populations near the top of the hill. Hence, it is apparent that the pharmaceutical antimicrobial medications can be spread from human-populated places to lower sections of hills by the washing of sewage water *via* rainwater runoff or natural waterways (Pan et al., 2023). According to Spain and Alm (2003), microorganisms that are both tolerant of metals and resistant to antibiotics seem to have been selected for resistance traits at the same time when they were exposed to metal-contaminated environments. Sabry et al. (1997), Ramteke (1997), Hassen et al. (1998), and Soltan (2001) have documented that isolates from environmental sources that can tolerate metals also exhibit resistance to a broad range of antibiotics, indicating a possible connection between HM tolerance and antibiotic resistance. A recent study conducted by Chen et al. (2019) demonstrated that bacteria in ecosystems polluted with HMs can develop resistance to both HMs and antibiotics concurrently. This phenomenon has also been observed in habitats affected with other types of pollutants (Cen et al., 2020). These studies clearly rationalize the necessity of avoiding the build-up of toxic metals in the soil and water bodies.

Metal-tolerant bacteria have developed several methods to resist and eliminate metals (Ledrich et al., 2005). The pathways associated with HM resistance are encoded in the chromosomal DNA or, more commonly, in plasmids of varying sizes that have the ability to be transferred to other bacteria by conjugation. These plasmids carry genes that confer resistance to metals (Piotrowska-Seget et al., 2005). At molecular

level, previous studies have proven a connection between exposure to HMs and the development of antibiotic resistance. This occurs through various mechanisms, including co-resistance (where different resistance factors are present on the same gene elements), cross-resistance (where genes encode resistance to both HMs and antibiotics), and shared regulatory responses to trace elements of environmental concern and antibiotic exposure. One example of a shared response is the induction of biofilm formation (Baker-Austin et al., 2006). The simultaneous occurrence of HMs and antibiotic resistance is a potentially significant health issue that affects both human and animal well-being. This might also impose economic hardships on the livestock industry (Spain and Alm, 2003; Al Salah et al., 2022). Furthermore, HM pollution is a persistent, pervasive, and resistant selection pressure that has therapeutic and environmental significance and may aid in continuing to spread and maintain of antibiotic resistance elements. Hence, a further detailed study is necessary to better understand the precise mechanisms that regulate antibiotic resistance.

5.6. *Biofilm production by the bacterial strains*

The analysis revealed a significant variation in biofilm formation across the strains. Further, findings indicate substantial strain-to-strain variation in biofilm forming ability, highlighting their differential potential in stress adaptation and bioremediation. Within active bacterial biofilms, it has been reported that both biosorption and bioaccumulation processes occur concurrently (Kumar et al., 2007). By employing the biofilm as a protective coating, bacterial cells may proliferate effectively in a variety of HM-stressed environments. EPS provides the protective layer of the biofilm and improves the immobilization and subsequent sequestration of the HMs (Ianeva, 2009; Priyadarshanee and Das, 2021). By means of electrostatic attraction, the positively charged cations readily adsorb on the negatively charged functional groups of the biofilm from the surrounding environment. Gupta and Diwan (2017) studied and verified such electrostatic interactions and identified a variety of biofilm producing bacterial strains that could be use as adsorbents for various HMs. Apart from the removal of HMs from the environment, biofilm have also been valued for a number of other bacterial-dominated processes (Balan et al., 2021; Haque et al., 2021).When exposed to As, Pavez et al. (2023) observed that *Exiguobacterium* strains, a Gram-positive HM resistant bacterium isolated from a highly As-contaminated

environment in Chile, formed biofilms more readily. This study suggests that biofilm plays a role in the bacterium's resistance to As. Teitzel and Parsek (2003) and Koechler et al. (2015) reported that bacteria in biofilms are 2-600 times more resistant to HMs than individual cells. According to Chien et al. (2013), *Pseudomonas* spp. forms biofilms and could thrive in medium polluted with Cd at concentrations of 2 nM. Teitzel and Parsek (2003) noted that biofilm generated by *P. aeruginosa* offered resistance against Pb, Zn, and Cu ions. According to Nocelli et al. (2016) strain *Sinorhizobium meliloti* was capable of generating biofilm to withstand a variety of substantially elevated levels of As and Hg elements. Grujić et al. (2017) found that the biofilm of *Rhodotorula mucilaginosa* increased the effectiveness of metal removal from 91.71 to 95.35 %. According to Van Houdt and Michiels (2010), interactions among bacterial cells, substrates, and the environment are generally necessary for the development of bacterial biofilms. Active biofilms have been shown to be successful in removing HMs from both actual industrial and municipal effluents (Gadd, 2009; Kotrba et al., 2011). Moreover, under the stress of HMs, plants grew more when biofilm-forming microorganisms were present (Sharma, 2022).

5.7. *Siderophore production by the bacterial strains*

Siderophore often facilitate the transform iron that is attached to proteins or water-soluble substances into a form that bacteria may access (Timofeeva et al., 2022). Primarily, siderophore acts as a chelating agent for metals, producing soluble metallophores that can solubilize and mobilize metals from the soil (Gaonkar and Bhosle, 2013; Gomes et al., 2024). The finding reveals a significant heterogeneity in siderophore production among the selected strains, underscoring their distinct capabilities in stress tolerance and bioremediation. In the present study, the increase in siderophore production in the presence of As^{5+} and As^{3+} ions can be attributed to the high resistance of the bacterial strain to As. These findings are consistent with previous investigations that have shown a correlation between siderophore production and increased arsenic resistance (Drewniak et al., 2008; Ghosh et al., 2015). The reduced production of siderophore in the presence of Pb and Cd HM ions may be attributed to the abiotic stress caused by these ions. This observation is in accordance with a study conducted by Gaonkar and Bhosle (2013), that similarly observed a decrease in siderophore production in the presence of Pb and Cd HM ions. Bacteria have been

seen to synthesize siderophores, which aid in the remediation of HM contaminated environments through many mechanisms, including enhancing the bioavailability of HMs and metalloids (Gaonkar and Bhosle, 2013; Roskova et al., 2022). The presence of microorganisms that produce siderophores has often been associated with the bioremediation of HM ions and was established by AAS analysis in a study conducted by Sarvepalli et al. (2023). Previous studies point out that HM ions can attach to siderophores, such as those found in *Pseudomonas azotoformans*, which are capable of binding As (Retamal et al., 2018). Naik and Dubey (2011) demonstrated the effectiveness of the siderophore generating strain *P. aeruginosa* 4EA in the remediation of Pb, Cd, and Zn. Sheng et al. (2008) conducted a study that identified two strains, *Microbacterium* spp. G16 and *P. fluorescens* G10, which have the ability to produce siderophores and may be used to remediate Pb. The work conducted by Dimkpa et al. (2008; 2009) and Retamal et al. (2018) demonstrated that siderophores from *Streptomyces acidiscabies* and *S. tendae* has the capacity to bind Cd and Ni, making them suitable for bioremediation purposes.

Additionally, siderophore can reduce the toxicity of HMs, serve as protective agents for plants against microbial pathogens, and stimulate the synthesis of indole-3-acetic acid (IAA) in the presence of HMs to promote plant growth (Rajkumar et al., 2010). A meta-analysis study done by Zhang et al. (2023) found that siderophore-producing bacteria had a stimulating impact on both plant growth and germination rate in a mixed-effect model.

5.8. *EPS production by the selected bacterial strains*

The study evaluated the effect of HMs on EPS generated by the AS3, AS4 and AS11 strains, taking into account their biological and agronomic importance. Results demonstrate considerable variability in EPS production among strains, underscoring their distinct capabilities in stress tolerance and bioremediation abilities. Selected bacterial strains demonstrate a notable production of EPS (dry weight of EPS) in absence of HMs, however the concentration of carbohydrate in the EPS was enhanced when exposed to HM ions such as Pb^{2+}, As^{5+}, As^{3+}, and Cd^{2+}. Pb^{2+} HM ions showed an enrichment of carbohydrate concentration of 47.32 % and 51.36 % in the EPS produced by AS3 and AS4 strains, respectively relative to untreated controls. Likewise, As^{3+} HM ions exhibited an enhancement of 58.3 % in carbohydrate content

in the EPS of AS11 strain compared to the untreated control. The other HMs also showed similar enhancements in carbohydrate content in all the strains.

The observed stimulating effect on EPS production by As is coincidence with the previous reports of Tournay et al. (2023), where they reported an enhancement in EPS production by *Rahnella laticis* PD12R, an endophytic bacterium, in response to As^{5+} and As^{3+} exposure. Additionally, it was observed that Cd^{2+} had the lesser stimulating effect on carbohydrate generation activity in the strains. EPS function as the initial barrier across the microbial cell and its surrounding environment; it is believed that metal stress circumstances would stimulate bacterial EPS synthesis to inhibit metals from interacting with essential cellular components (Sheng et al., 2005). Poli et al. (2011) reported that bacterial EPS synthesis serves as a shield for survival in harsh environments, notably during HM poisoning. Zeng et al. (2020) showed that toxic Cd^{2+}, Cr^{4+}, and Cu^{2+} ions induced the release of EPS in *Bacillus* spp. S3, markedly improving the adsorption and detoxifying efficacy of HMs. When present in excessive quantity, the metal ions penetrate the cells where their toxicity can be prevented by intracellular complexing or reduction to a less hazardous oxidation state (Nies, 1999). Mathivanan et al. (2021a) found that the production of EPS by *B. cereus* KMS3-1 strain augmented under metallic stress that confers increased thickness and rigidity to the bacterial cell enabling it to withstand the damage caused by metals. The strain transforming the absorbed toxic metal ions, specifically Cd^{2+}, Cu^{2+}, and Pb^{2+}, into less soluble and less toxic sulfides or oxides, such as CdS, CuS, and PbO, respectively, suggesting a role of EPS in the detoxification process.

The primary components of EPSs released by bacteria include polysaccharides, proteins, and nucleic acids. The EPS matrix contains negatively charged functional groups like carboxyl, hydroxyl, sulphate, phosphate, and amine groups. Therefore, chelating metal cations and avoiding direct cell-to-toxic metal contact are made possible by the total negative charge of bacterial EPS (Sheng et al., 2010; Wu et al., 2019). The role of EPS, which has negatively charged functional groups in addition to the proton-active sulfhydryl groups, was emphasized by Kenney and Fein (2011) in relation to the development of Cd binding and metal absorption onto bacterial cell walls. According to Bravo and Braissant (2022) the electrostatic interaction between Cd^{2+}ions and negatively charged reaction sites on the bacterial cell wall or the

generated EPS facilitate the bioadsorption of Cd^{2+}ions by bacterial biomass. Xu et al. (2017) documented the secretion of EPS by the *Enterobacter cloacae* TU strain in Cd-supplemented culture media, noting that the generated EPS binds to Cd in both the supernatant and on the cell surface, in addition to its intracellular accumulation. Moreover, bacterial cell's EPS, that comprises of polysaccharides, lipids, lipopeptides, glycolipids, and neutral lipids, may facilitate in bioleaching since they have significant surface activity to interact with HMs (Yang et al., 2018). Due to its binding capability, EPS has been proposed as a viable adsorbent for metal pollutants. The binding capacity and the specificity of metal adsorption on EPS, however, can vary depending on the its composition (variations in side chain length, functional group arrangement, and polymeric chain length), bacterial growth phase, as well as some external variables including pH, temperature, adsorbent and adsorbate concentrations (Wei et al., 2016; Bravo and Braissant, 2022). Determining the role of EPS in bacteria when exposed to toxic metal amended condition and finding the interaction occurs between EPS and metal ions is need to be explored. Understanding the optimal conditions for enhance metal adsorption by EPS would assist in bringing the adsorption process into application in a way that is more practical and profitable.

5.9. *Oxidation and reduction potential of selected bacterial strains*

Silver arsenate, which is primarily expressed in the presence of As^{3+}, indicates that bacterial strains are able to secrete the "arsenite oxidase" enzyme in the periplasm. Due to its oxidizing capabilities, bacteria are able to detoxify As^{3+} from its highly lethal state into a less hazardous As^{5+} state. When bacteria have the innate capacity to oxidize, they often use it to extract energy for growth, defence, or both. Although individuals of several bacterial species have arsenite oxidase enzyme, it was initially identified from the oxidant *Alcaligenes faecalis* (Roy et al., 2024). $AgNO_3$ also indicates that the bacterial strains have the innate capacity to synthesize "arsenate reductase," an enzyme in the periplasm that catalyses the reduction of As^{5+} to As^{3+} in the presence of As^{5+} (Poddar et al., 2021). Following the transformation of As^{5+} to As^{3+}, arsenate reductase enzyme aids in the extrusion of As^{3+} from the cell. According to earlier reports of Gladysheva et al. (1994) and Del Giudice et al. (2013), arsenate reductase has been found to be identified in *Saccharomyces cerevisiae*, *Escherichia coli*, *E. coli* R7773, and *Thermus thermophilus* HB27.

5.10. *SEM-EDX analysis of bacterial strains*

An attribute common to HM-resistant bacteria is the ability to adsorb metal ions on their surfaces, which can be established by the findings of SEM-EDX. SEM-EDX investigation clearly establish the ability of the selected bacterial strains to adsorb metal ions that includes As^{5+}, Pb^{2+}, and Cd^{2+} on their surfaces and confirming their multi-metal resistant capability. In a study conducted by Pandey and Bhatt (2015) obtained similar outcomes with As^{5+} ions adsorption on bacterial surfaces. However, in the present study As^{3+} HM ion was not detected in all the tested samples of bacterial strains. Lack of As^{3+} ions adsorption in the present study suggest that bacterial strains may have evolved with other adaptation mechanism, such as the extrusion of As^{3+} metal ions or the presence of efflux channels that allow the clearance of As^{3+} metal ions (Gogoi et al., 2023). The alterations in surface structure clearly show an adaptive characteristic either to adsorb more HMs ions or as a consequence of response against hazardous metallic environment. These observations are consistent with the previous results reported by Rani et al. (2009), Zolgharnein et al. (2010), Banerjee et al. (2011), Shakya et al. (2012), and Pandey and Bhatt (2015).

5.11. *FTIR analysis of bacterial biomass*

FTIR spectroscopy is an important analytical tool in the field of biological research that offers a detailed information about the molecular composition of biological samples (Al-Kelani and Buthelezi, 2024). The variations in IR spectra seen in comparison to the control are most likely caused by metal chelation, the process by which metals bind to ligands present on the surface of bacteria. Interactions with metal ions establish the involvement of functional groups in metal binding (Bueno et al., 2008; Singh et al., 2016). The shifts in peak regions suggest the presence of biosorption activity when metal ions interact with negatively charged groups on the cell wall through a variety of mechanisms, such as electrostatic interactions, van der Waals forces, and covalent bonds.

With the exception of the Cd^{2+} treatment, peak shifting to higher wavenumbers in the IR spectrum was seen in AS3 strain, possibly due to the conjugation effect. (Dai et al., 2023). Such changes were seen in samples treated with As, which suggest that the AS3 strain metabolized As (Watanabe and Hirano, 2013). Peak shifting to a higher

wavenumber in the Pb-treated samples of the AS4 strain was the same as that of the AS3 strain, which may be because of a similar conjugation effect. However, for As^{5+} and As^{3+} peak values were shifted to lower wavenumbers and for Cd^{2+} treated samples no such prominent peak was observed in the mentioned range. No discernible variation in the wavenumber has been noted in AS11 strain.

When comparing AS3 treatments to the control, there was no apparent change in the stretching variation within the 3000–2800 cm^{-1} range. However, in AS4 strain stretching vibrations corresponding to $–CH_3$, $–CH_2$, and –CH in membrane amphiphiles along with amphiphilic lipids was absent in HMs treatment, indicating its disintegration in presence of HMs (Shi et al., 2020; Sohlenkamp and Geiger, 2016). No comparable change in stretching vibration was observed in the AS11 strain.

A change to higher wavenumbers in the AS3 strain peak at 1647 cm^{-1} (control) corresponded to N-H bending and C=O stretching vibrations (Xu et al., 2021; Usoltsev et al., 2019; Kassem et al., 2023). Further, peak value 1546 cm^{-1} in control that corresponds to N-H bending or CN stretching vibration was found to shift to a lower wavenumber in HM treatments samples except for Cd^{2+} treatment where it was absent. In comparison to control, the peak corresponding to N-H bending in AS4 strain changed to higher wavenumbers in As^{3+} and Cd^{2+} treatments and to lower wavenumbers in As^{5+} and Pb^{2+} treatments. Further, N-H in-plane bending or the CN stretching vibration in AS4 strain at 1546 cm^{-1} (control) was shifted in presence of HMs (Usoltsev et al., 2019; Xu et al., 2021; Gupta et al., 2022; Kassem et al., 2023). Peaks at 1550–1670 cm^{-1} in AS11 are absent in As^{3+} and Cd^{2+} HM treatments but moved to higher wavenumbers in As^{5+} and Pb^{2+} HM treatments. Further, peaks at 1546 cm^{-1} in control were shifted to lower wavenumbers in As^{5+} and As^{3+} treated samples, whereas it was shifted to higher wavenumbers in Pb^{2+} and Cd^{2+} treatments. Such variations in N-H bending, C=O stretching and CN stretching vibration possibly suggest the influence of HMs on the degree of protein synthesis process.

In AS3 strain peak around 1400 cm^{-1} are indicative of capsular peptidoglycans (Saraeva et al., 2023). Moreover, the intensification of peak to higher wavenumbers Pb^{2+} and Cd^{2+} treatments compared to control and could indicate the increased production of peptidoglycan in the presence of HMs. However, such observation was not notable in As^{5+} and As^{3+} treatments. Similarly, in AS4 strain peak around 1400

indicates increased production in presence of all HMs but was lower in Pb^{2+} HM ions, which indicate possible disintegration of capsules in bacterial cells (Saraeva et al., 2023). Further, similar increase in the capsular peptidoglycans, in presence of all HMs was observed in AS11 strains.

As compared to control, Pb, and Cd treatments, AS3 strain showed many peaks about 1236–1240 cm^{-1}, which correspond to P=O asymmetric vibrations. However, AS^{5+} and AS^{3+} treatments did not show these vibrations. Only the control showed P=O asymmetric vibrations in AS4 strain, whereas none of the HMs treatments showed them. These peaks are often related with phosphodiester, phospholipids, lipopolysaccharide, nucleic acids, and ribose molecules and are associated with the production of bacterial membranes, nucleoid, and ribosomes (Parikh and Chorover, 2006; Quilès et al., 2010). Additionally, both control and HMs treated AS4 strain showed peaks around 1305 cm^{-1} which corresponds to phospholipids and RNA in the bacterial cell (Maity et al., 2013). The presence of As^{3+} HM ions in the AS11 strain peaks around 1200–1305 cm^{-1} decreased slightly, while As^{5+} and Cd^{2+} treatments did not appear, probably as a result of stress. However, peaks got enhanced in presence of Pb^{2+} HM ions, possibly indicating less stress imposed on the bacterial cells.

Glycosidic bond vibrations of cellulose are represented by the peaks in AS3 about 1000–1200 cm^{-1}, which were seen in both the control and HMs-treated AS3 and AS4 strains (Makarem et al., 2019; Atykyan et al., 2020). Moreover, it was unchanged in Pb treatment in AS3 strain. These peaks were found to be higher in all of the HMs that were tested for AS11, indicating active interactions with HM.

The ribose skelet (ARN), which is linked to the synthesis of ribosomes (Quilès et al., 2010), was identified in peaks around 993 cm^{-1} in AS3 strains under control, $Pb^{2+,}$ and Cd^{2+} treatments, but not in AS^{+5} and AS^{+3} treatments. In AS4 strain peaks around 993 cm^{-1} were observed in all HMs treatments but not notable in AS11 strain.

Further, peaks around 730-930 cm^{-1} in AS3 and AS4 strains indicate the presence of active As-O bending vibrations (Fan and Zhang, 2019) in presence of As^{5+} and As^{3+} HM ions. However, such peaks were not notable in the treated AS11 strains. Peaks around 515–690 cm^{-1} in the treated AS3 and AS4 strains may be the result of C–Br stretching, which mostly originates from KBr utilized in FTIR analysis.

5.12. *TEM-EDX analysis of bacterial strains*

The appearance of As in the EDX spectra of the control samples for both AS3 and AS4 strains might be because of delayed efflux mechanisms, residual stored As, or inherent As that both bacterial strains had previously absorbed from the environment (Muller et al., 2007). Moreover, the appearance of As in all HM treated strains indicate bioaccumulation of intracellular As^{5+} HM ions. The intracellular uptake of As has been observed in a number of bacteria such as *Bacillus subtilis* (Vishnoi et al., 2015), *Paenibacillus macerans* (Vishnoi et al., 2015) and *Exiguobacterium* spp. (Pandey and Bhatt, 2015). Moreover, Pb^{2+} and Cd^{2+} accumulation have also been reported in bacterial strains such as *Staphylococcus epidermidis* AS-1 (Kumar et al., 2024), *Cupriavidus metallidurans* CH34 (Hajdu and Slaveykova, 2012) and *Pseudomonas aeruginosa* strain DR7 (Zhang et al., 2024). This accumulation of HMs by bacterial strains is a part of their detoxification mechanisms which commonly takes place during the conversion of highly toxic forms to a less toxic form *via* inherent mechanisms possessed by the As-resistant bacterial strains (Gogoi et al., 2023).

The presence of Pb and Cd HM ions in the TEM-EDX study of both AS3 and AS4 signifies their intracellular bioaccumulation. Numerous studies have documented intracellular bioaccumulation by bacterial strains, including *Lactobacillus plantarum* MF042018, which demonstrates bioaccumulation of Cd and Pb for bioremediation (Ameen et al., 2020); *Exiguobacterium sp*., *Klebsiella variicola sp*., and *Enterobacter sp*., which exhibit biosorption of Cd HM ions (Feria-Cáceres et al., 2022). Furthermore, findings from *Lysinibacillus* and *Staphylococcus* species demonstrate the bioaccumulation of Cd, specifically *Lysinibacillus boronitolerans* QD4 (Gu et al., 2025); Cd and Pb HM ions by *Staphylococcus epidermidis* AS-1 (Kumar et al., 2024); and Cd HM ions by *Staphylococcus devriesei* MS (Shabaan et al., 2025). Thus, the accumulation of HMs in the selected bacterial strains indicate their potentiality as effective bioremediators of HMs contaminated environments.

5.13. *Stress enzyme activities in the bacterial strains in the presence of HMs*

In general, an increase in the metal concentration is accompanied with an inhibition of the protein synthesis (Mounaouer et al., 2014). However, in the present study the TPC in presence of tested HMs was found to be higher in the selected bacterial strains which might be due to the synthesis of certain proteins in response to

HM stress *viz*. heat shock proteins (HSPs) (Nover, 2022) and metal-binding proteins (MBPs) (Sharma et al., 2021). Nonetheless, the TPC observed in the presence of the tested HMs was relatively lower for the AS11 strain, potentially due to the adverse effects of HMs on the protein synthesis process (Mounaouer et al. 2014). The primary antioxidant enzymes that counteract superoxide and H_2O_2 are SOD and CAT, respectively (Halliwell and Gutteridge, 2015). Increased levels of oxidative damage, such as membrane lipid peroxidation, protein carbonylation, and DNA breakage, are frequently linked to decreased SOD activity (Yang et al., 2007; Wang et al., 2018).

In AS3 strain, SOD activity in the presence of $Pb(NO_3)_2$ (0.159 ± 0.003 U/mg protein) was lowest indicating high chances of oxidative damage which was also evident from MDA levels in $Pb(NO_3)_2$ (0.672 ± 0.019 U/mg protein), which showed highest activity as compared to control. MDA content is regarded as a reliable marker of cellular stress and damage. Elevated generation of MDA in bacterial cells in presence of HM reflects the degree of membrane damage (Zhang et al., 2022). Further lower SOD activity was also seen in the presence of $CdCl_2$ and $NaAsO_2$ confirming the development of oxidative stress in AS3 strain

The production of CAT was relatively lesser in the presence of Na_3AsO_4 and $Pb(NO_3)_2$ compare to control, suggesting development of inconsequential stress in AS3 strain. However, in the presence of $NaAsO_2$ and $CdCl_2$ content of CAT in AS3 strain was significantly higher compared to control which suggests that the enzyme was well protected and preserves its functional activity in the presence of these metals (Lima e Silva et al., 2012). This protection is important because in the absence of this enzyme H_2O_2 accumulates and may become lethal to bacteria. Higher activity of CAT in the presence of $NaAsO_2$ and $CdCl_2$ indicates their defence mechanism against the reactive oxygen species. An adaptive antioxidant response to counteract the higher H_2O_2 level could possibly be the cause of such elevated CAT activity (Behera et al., 2014). The results are in accordance with Crapart et al. (2007) and Gupta et al. (2012) where almost all the *Exiguobacterium* spp., *Bacillus weihenstephanensis* strain IA1 and *Exiguobacterium aestuarii* strain CE1, exhibit positive catalase activity on exposure to HMs. Wu et al. (2021) observed positive correlations between catalase activity and HMs (Cd, Cu, Hg, Pb, and Zn) in soil bacteria, indicative of a response to the oxidative stress induced by metals.

GPx and GR are important Reduced glutathione (GSH)-related enzymes and have an important role in Reduced glutathione (GSH)/ Oxidised glutathione (GSSG) maintenance which is crucial for cellular redox status (Bianucci et al., 2012). The increase in the activity of GPx and GR in response to metals (As, Cd and Pb) might be probably due to the alterations in the cellular thiol redox balance as a result of decrease in the GSH levels in the bacterial strain (Saikia, 2015). However, reduced GPx activity in presence of Na_3AsO_4 indicates that there was optimum GSH levels in the bacterial strain which prevented the changes in the cellular thiol redox balance, thus indicating the bacteria was able to tolerate the high concentration of Na_3AsO_4 (62,500 ppm).

The results from MDA content indicates that HMs might have affected the lipid peroxidation and plasma membrane permeabilization, leading to an increase in MDA (Hassan et al., 2008). The fact that the susceptibility of fatty acids to lipid peroxidation increases with the degree of fatty acyl chain unsaturation (Stohs and Bagchi, 1995) indicates a possible link with our results. Furthermore, metals, such as $Pb(NO_3)_2$, are known to be capable of inducing free radical production and promoting oxidative stress through their redox-cycling activity (Hassen et al., 1998). However, decrease in MDA levels in $NaAsO_2$, $CdCl_2$, and Na_3AsO_4 could indicate that AS3 strain was able to protect itself from the oxidative damage by HM ions, resulting from activation of the antioxidant enzyme system (Ajmal et al., 2022).

In the strain AS4, the increase in TPC production indicates that the strain might have produced certain vital proteins to tackle HM stress as discussed for AS3 strain. Moreover, the small decrease in SOD activity in the presence of Na_3AsO_4 and $NaAsO_2$ compared to the control could be attributed to the oxidative damage leading to various damages as discussed for AS3 strain. However, $Pb(NO_3)_2$ and $CdCl_2$ exposure stress caused higher SOD activity which in turn encourages a rise in the amount of defence enzymes linked to oxidative stress (Steunou et al., 2020). Besides, the slight decrease or similar values for CAT activity in AS4 strain suggests that the bacterium was able to sustain the treatments and keep the integrity of the CAT enzyme in presence of the metals. However, the decrease in CAT activity as well as increase could also be attributed to the similar reasons as discussed for AS3 strain. Furthermore, the elevated activity of GR and GPx enzymes could be attributed to the decline in GSH levels as discussed for AS3 strain. However, reduced GPx activity in presence of $CdCl_2$

(1,562.50 ppm) might indicate that the strain was able to maintain the necessary GSH levels to tolerate the concentration of Cd^{2+} ions. Results indicate that, except for $NaAsO_2$, all the other treatments imposed oxidative stress particularly by $Pb(NO_3)_2$ on the AS4 strain which led to elevated activity of MDA.

In the strain AS11, the reduction of TPC in the presence of all the HMs might be due to the retardation in protein synthesis process under stressful conditions as discussed in AS3 strain. Due to the relatively increased oxidative damage caused by Na_3AsO_4 and $CdCl_2$, might result in the decreased SOD activity. Further, increased SOD activity in the presence of $NaAsO_2$ and $Pb(NO_3)_2$ might be due to the rise in antioxidant enzymes activity under metal stress condition as a means to combat HM ions. Likewise, in order to combat higher H_2O_2 level, there was rise in CAT activity particurly in $Pb(NO_3)_2$ while similar CAT activity with control suggests that the functional activity of the enzyme was intact in presence of $NaAsO_2$, $CdCl_2$, and Na_3AsO_4. This indicates that strain was resistant to the respective HM ions which was evident from lower MDA levels compare to control. In strain AS11, the increased GR activity against all the HMs indicates the decrease in the GSH levels as discussed for AS3 and AS4 strain. Further, reduced GPx activity in presence of all HMs indicated optimum GSH levels for cellular thiol redox balance, indicating the bacteria was able to tolerate the treatments without significant damages. The decrease in MDA levels compared to the control could be attributed to the lesser damages to the cellular membrane except for $Pb(NO_3)_2$, where MDA content was found to be the maximum.

5.14. *Bioremediation potential of the selected strains*

The high removal efficiencies of all the three selected strains indicate their potential role as bioremediating agents. Till date, several species of *Lysinibacillus* have been reported to exhibit resistance to HMs. For example, *Lysinibacillus* strain B1-CDA, isolated from cultivated land in Chuadanga district, Bangladesh, demonstrated 50 % remediation of As^{5+} HM ions (Rahman et al., 2014); *Lysinibacillus* spp. DMAB5 isolated from Asanpara village (Bhagobangola I block) of Murshidabad district, demonstrated 32.33 %, 31.29 %, and 31.20 % bioremediation in the presence of 2 ppm, 10 ppm, and 50 ppm, respectively of As^{3+} HM ions (Mandal et al., 2022); and *Lysinibacillus boronitolerans* P2IIIb, isolated from soil of a gold mining area in Paracatu, Brazil, demonstrated 69.38 % and 85.72 % bioremediation of As^{3+} and As^{5+}

HM ions, respectively (Aguilar et al., 2020). Additionally, *Lysinibacillus* species have been used for Cd bioremediation. For example, *Lysinibacillus fusiformis* L13 isolated from farmland soil in the mining areas of Pingdu and Qingdao City, China, was able to remediate 38 % of Cd^{2+} HM ions (Ma et al., 2023), and *Lysinibacillus varians* strain KUBM17 demonstrated a removal of >33 % of Cd^{2+} HM ions (Pal and Sengupta, 2019). A number of *Lysinibacillus* species also have been reported to be able to remove Pb^{2+} HM ions. For example, *L. varians* strain KUBM17 was found to be able to remove 26 % of Pb^{2+} HM ions (Pal and Sengupta, 2019).

Furthermore, various strains from *Staphylococcus* species have demonstrated effective removal of HM ions, including *Staphylococcus epidermidis* AS-1, which achieved a sequestration rate of 90.89 % for Cd and 94.8 7% for Pb (Kumar et al., 2024). Another investigation conducted by Rahman and colleagues and demonstrated that the *Staphylococcus hominis* strain AMB-2 achieved nearly 88 % removal of Pb and 66 % removal of Cd (Rahman et al., 2019). A recent investigation revealed that *Staphylococcus equorum* PU1, sourced from Pu-erh tea rhizosphere soil, can remove nearly 58.7% of Cd (Chen et al., 2023). Results of the present investigation hence further suggest that the selected strains are effective bioremediating agents against As^{3+}, As^{5+}, Cd^{2+}, and Pb^{2+} HM ions. Additionally, because the strains contain siderophores, EPSs, and biofilm capacity, thereby aid in the effective bioremediation of the mentioned toxic HMs.

5.15. Ammonia production by the bacterial strains

The ability of bacterial cells to produce ammonia is a crucial plant growth promotion (PGP) characteristic because it offers plants the required quantity of nitrogen, a crucial macronutrient for biomass and plant growth (Fanai et al., 2024). Additionally, more ammonia in the rhizosphere can elevate the pH of the soil, suppressing certain phytopathogens and eventually promoting plant development (Fanai et al., 2024). Therefore, investigating the degree of ammonification in HM-tolerant bacteria can aid in gaining a better understanding of how certain bacterial strains support plants in sustaining their nitrogen metabolism under a HM stress environment (Gupta et al., 2024).

The elevated ammonia production observed in the AS3 strain, along with the moderate levels produced by the AS4 and AS11 strains, suggests its potential

application as PGP by addressing nitrogen needs, thereby contributing to improved growth in the plants. A number of studies indicate ammonia production by different strains of *Lysinibacillus* which aid in HM remediation such as- *Lysinibacillus fusiformis* 5B (Jibrin et al., 2020), *Lysinibacillus fusiformis* 5.1 and *Lysinibacillus xylanilyticus* 4.3 (Leeprasert et al., 2022), and *Lysinibacillus* sp. GY3 (Li et al., 2022). Similar kind of study was conducted by Gohil et al. (2022) where *Bacillus* sp. PG-8, a HM resistant bacterial strain, was found to be enhance growth in groundnut plant through the production of ammonia. Moreover, other species such as *Azotobacter salinestris* ASM and *Bradyrhizobium* spp. have also been associated with enhanced growth of plants such as tomato and chickpea with ammonia production (Khoso et al., 2024). Nonetheless, the existing scientific literature on Lysinibacillus is relatively sparse, particularly regarding their traits associated with PGP when compared to well-established genera of PGP-rhizobacteria (PGPR), including *Acinetobacter*, *Agrobacterium, Arthobacter, Azotobacter, Azospirillum, Burkholderia, Bradyrhizobium, Rhizobium, Frankia, Serratia, Thiobacillus, Pseudomonads*, and *Bacillus* (Cordero et al., 2023). In the context of *Staphylococcus* species, strains including *Staphylococcus pasteuri* RR1 and RR2, along with *Staphylococcus* sp., exhibited ammonia production, demonstrated HM resistance, and displayed enhanced PGP traits (Roychowdhury et al., 2017). Furthermore, urease activity has been documented in *Staphylococcus epidermidis* and *Staphylococcus aureus*, which is essential for the conversion of ammonia from urea (Vandecandelaere et al., 2017). Thus, studied bacterial strains particularly AS3 followed by AS4 and AS11 have great utility in further enhancing plant growth.

5.16. IAA production by the bacterial strains

The selected strains showed the capacity of IAA production which is an indicator of its utility as PGP microorganism. The production of indole-acetic acid (IAA) by bacteria in response to HM stress is frequently linked to increased root growth branching, which enhances the capacity of plants to absorb essential nutrients and withstand toxic HMs. For instance, IAA-producing PGPR have demonstrated a reduction in Cr stress in *Brassica juncea*, accompanied by improved growth and siderophore production (Rajkumar et al., 2005; Kangsopa et al., 2025). Furthermore, IAA has been linked to decreased oxidative damage and an increase in antioxidant

enzyme activity in *Sorghum bicolor*, leading to improved physiological performance (Bibi et al., 2025). Bacterial strain AS3 and AS4 showed very good IAA production while strain AS11 showed a limited IAA production. In contrast to PGP features found in *Staphylococcus aureus* K1, the minimal IAA generation in *Staphylococcus equorum* AS11 may be explained by a separate mechanism for HM detoxification, such as biotransformation and antioxidant regulation in the presence of HM stress (Zeng et al., 2020). Furthermore, there is not enough scientific literature that links *Staphylococcus* strains to IAA production and stimulated plant growth, whereas several studies have showed evidence of enhanced plant biomass and stimulated plant growth when amended with *Lysinibacillus* species, for instance *Lysinibacillus sphaericus* ZA9 (Sahu et al., 2018). Previous reports on *Lysinibacillus* species such as *L. fusiformis* B-CM18 showed beneficial role as PGPR in Chickpea (*Cicer arietinum L.*) plants (Singh et al., 2013). In another report, *L. fusiformis* EI20 showed several PGPR traits in ginseng (*Panax ginseng*) plant (Vendan et al., 2010).

Empirical studies have further highlighted the importance of HM tolerant bacteria isolated from different HM contaminated areas, exhibiting increased IAA synthesis, in presence of HMs such as As, Cd, Pb, Cu and Ni, thereby indicating IAA production as an adaptive mechanism for survival and plant growth promotion (Carlos et al., 2016). The present investigation thus confirmed the strains' adaptability to the HMs by demonstrating their capacity to reduce HM stress caused by As, Cd, and Pb.

Therefore, bacterial strains particularly AS3 followed by AS4 and AS11 have great utility in enhancing their plant growth through secretion of IAA which is a vital hormone for plant growth and development. Findings of IAA production capacity among the strains was found to be similar with the production of ammonia.

5.17. *Phytotoxicity assay*

Seed phytotoxicity tests are bioassays that are used to assess the toxicity of chemicals, waste, or industrial effluents by analysing the germination and development of plant seeds. This approach is often employed in ecotoxicology research (Bae et al., 2014; Balestri et al., 2019; Luo et al., 2019; Martínez-Cruz and Rojas-Valencia, 2024). The current study evaluated the toxicity of selected HMs on Mung bean seeds using phytotoxicity assays. The results showed that the inclusion of

the bacterial strains, AS3, AS4 and AS11 had a stimulating impact, whereas treatment with HMs alone had an inhibitory effect.

The phytotoxicity assay findings showed that the highest levels of GI and GVI were observed exclusively in the samples treated with bacterial strains. In addition, the use of chosen HMs in conjunction with bacterial strain resulted in greater values for both GI and GVI, in comparison to samples treated with only HMs. This suggests that the addition of the AS3, AS4 and AS11 strains have a beneficial effect on the growth of Mung bean seedlings. It also helps to reduce stress caused by HMs, leading to higher values for the GI and GVI.

A number of investigations on *Lysinibacillus* spp. have demonstrated its positive impact on plant growth and development. The observed stimulating effect of *Lysinibacillus* spp. strain AS3 strain may be attributed to its inherent hydrolytic enzymes, which aid in mitigating abiotic stress caused by HMs. This phenomenon was also observed in a study where *L. sphaericus* ZA9, which contained hydrolytic enzymes like cellulases, chitinases, and proteases, was able to increase the length of shoots in Tomato and Cucumber seeds. As a result, it had a stimulating effect on seed germination and vigour (Naureen et al., 2017). Another possible factor might be the capacity to synthesize IAA, as seen in *L. pakistanensis* PCPSMR15, which promoted the development of Mung bean plants (Lelapalli et al., 2021).

The present investigation also demonstrated the substantial contribution of siderophores in facilitating plant growth and development. Several studies on *Lysinibacillus* spp. strains that produce siderophores have reported consistent findings, such as the finding of *L. xylanilyticus* strain GIC41 (Ahsan et al., 2021) and *L. sphaericus* ZA9 (Naureen et al., 2017). The presence of biofilm can also upsurge the growth of Mung bean plants by reducing the harmful effects of HMs and promoting overall plant growth and productivity. Similar kind of findings were reported by Ahsan et al. (2021) and Rafique et al. (2024).

Further, several strains of *Staphylococcus* species have also been reported to enhance growth in seedlings affected with HM stress. In a study by Zeng et al. (2020), the introduction of *S. aureus* K1 to wheat (*Triticum aestivum*) plants under chromium (Cr) stress resulted in increased root and shoot growth, dry biomass, and decreased oxidative stress in the seedlings, all of which were evidence of lessened Cr toxicity. In

another study by Ravisankar et al. (2024), it was reported that co-cultivation of *Staphylococcus saprophyticus* with Napier grass (*Pennisetum purpureum*) and cotton (*Gossypium sp*.) in Cr contaminated soil resulted in enhanced root and shoot length as well as biomass. Previous studies involving *Lysinibacillus* and *Staphylococcus* species have shown enhanced growth in plants when these bacterial strains were introduced to plants under HM stress. The current findings represent the very first evidence from Nagaland, India, demonstrating that both bacterial species can stimulate growth in sprouts.

5.18. *Brine shrimp toxicity study*

The results indicate absence of mortality of shrimp larvae when treatments of only bacterial strain were added. Further, when bacterial strains and HMs amended treatments were used the mortality percentage were lesser as compared to HM treated samples. Further, highest mortality percentages were recorded for As^{5+} HM ions, followed by As^{3+}, Pb^{2+} and Cd^{2+}. This might be due to the harmful effects of HMs which was recorded by Duan et al. (2021), where it was observed that Pb and Cd exposure impart negative effects on the intestinal health of the shrimp, *Litopenaeus vannamei*. Moreover, As-induced mortality could also be due to the toxicity imposed by As on the brine shrimps, which was observed in a study of acute toxicity in white shrimp, *L. vannamei* when exposed to As (Valentino-Álvarez et al., 2013).

Moreover, the decrease in mortality percentage in bacterial strain amended treatment alone, or with HMs might be due to the metal detoxification mechanisms acquired by the bacterial strains through the generation of EPS, siderophore, biofilm or biotransformation of toxic arsenite to lesser toxic forms as evident from the results of biofilm, siderophore, EPS as well presence of arsenite oxidase and arsenate reductase studies. Findings of the present study are found to be consistent with the observations of previous investigations which were reported by a number of researchers where they have established that adding beneficial probiotic bacteria enhanced the shrimp survival against pathogens by boosting immunity (Pooljun et al., 2020; Wang et al., 2020; Fernandes et al., 2021). However, no studies have been reported as from North-East India till date that showed enhanced survival of shrimps against exposure to As, Cd and Pb when amended with HM resistant bacterial strain.

5.19. *Statistical analysis*

The experiments were conducted in replicates of ≥ 3, and found to be significant at $p<0.05$ indicating that the observed results were unlikely to have occurred by random chances. Thus, indicating that the treatments had a significant impact on the studied variables.

The significance at $p<0.05$ further legitimates the findings as it reflects < 5 % probability of committing Type I error (*i.e.* rejecting a null hypothesis when it is actually true), which aligns with accepted threshold for biological and experimental research, proving meaningful differences between groups. Even though, statistical findings support the validity of results, future studies are also pivotal for larger sample sizes or with field conditions.

6.1. *Summary*

The ongoing unsustainable levels of human exploitation of natural resources led to the seek for alternate methods for treating wastewater tainted with HMs. The goal of the present study was to explore indigenous bacterial species from natural stream lines of Changki range of Nagaland, India using an *in vitro* setting that was enriched with As, Cd, and Pb HM. The potential bacterial species based on the their obtained MTC and MIC values against the selected HMs *viz*. As^{3+}, As^{5+}, Cd^{2+} and Pb^{2+} were selected and identified as *Lysinibacillus* sp. AS3, *Lysinibacillus* sp. AS4 and *Staphylococcus equorum* AS11. The bacterial strain AS3 showed to be resistant to As^{3+}, As^{5+}, Cd^{2+}, and Pb^{2+} up to 1562.50 µg/mL, 125000 µg/mL, 3125 µg/mL, and 12500 µg/mL, respectively. While, AS4 showed to be resistant to As^{3+}, As^{5+}, Cd^{2+}, and Pb^{2+} up to 3125 µg/mL, 15625 µg/mL, 1562.50 µg/mL, and 6250 µg/mL, respectively. Further, AS11 showed to be resistant to As^{3+}, As^{5+}, Cd^{2+}, and Pb^{2+} up to 1562.50 µg/mL, 250000 µg/mL, 97.64 µg/mL, and 12500 µg/mL, respectively. Additionally, co-selection of antibiotic resistance has also been noted in the selected bacterial strains; which might be the outcome of the process called co-selection in the selected strains for HM tolerance. The bacterial strains demonstrated resistance to a number of broad and narrow spectrum antibiotics with a MAR value of 0.476, higher than the normal value of 0.2. Further, additional research is required to clarify the precise resistance mechanisms. The physiological profile of strains, which includes their capacity to form biofilm, siderophore production, and EPS secretion, conferring adaptations for their survival under stressful and unfavourable circumstances and establish the potential adaptability to the strains in the toxic HM polluted environments. Studies on the oxidation and reduction potential of As showed that the strains had the ability to release the enzyme arsenite oxidase, as well as arsenate reductase for detoxification of As HM. Interaction of As^{3+}, As^{5+}, Cd^{2+}, and Pb^{2+} HM ions with bacterial strains was confirmed by SEM-EDX, TEM-EDX and FT-IR analysis of the bacterial biomass, indicating adsorption and bioaccumulation of respective HM ions. The expression of stress-induced enzyme that provide resistance against HM toxicity was verified by a stress enzyme assess that includes SOD, CAT, MDA, GPx, and GR. The strains further demonstrated significant removal potential for As^{3+}, As^{5+}, Cd^{2+}, and Pb^{2+} under *in vitro* setting, indicating its utility for

bioremediation. An inhibitory effect was seen when HMs were used alone in the phytotoxicity experiment on Mung seeds, however the presence of the bacterial strain reduced the toxicity of As^{3+}, As^{5+}, Cd^{2+}, and Pb^{2+} HM ions along with boosting plant growth suggesting their possible application in the bioremediation of HM polluted agricultural fields. Similar behaviour with reduced mortality on exposure to As^{3+}, As^{5+}, Cd^{2+}, and Pb^{2+} HM ions together with bacterial strains were noted in larvicidal experiment with brine shrimp larvae, indicating the possible application of bacterial strains in reducing HM toxicity in aquacultures.

6.2. *Future perspectives*

Although the selected bacterial strains were found to be resistant to the tested HM significantly. Most of the experiments were conducted in laboratory scale conditions under optimum temperatures, pH, agitation, and other controlled environment with necessary nutrients and amendments for the proper growth of the bacterial strains. However, such conditions may not fully replicate the natural conditions, affecting external validity. Apart from the abiotic factors, behaviour of bacterial strains in natural habitat in the presence of other biotic and abiotic factors and their interactions with the pre-existing microbial populations will define their effectiveness. Capacity of the bacteria to overcome the stress caused by HM-contaminants can be measured by different biochemical pathways that bacteria employed which is under the control of different genes or operon systems. There are several natural stimuli called triggering factor, that lead to the activation of genes and their subsequent enzyme/protein driven biochemical reaction, are need to be studied for an insight understanding. Moreover, such genetic controlled differs with the bacterial species or strains. Additionally, certain strains may be employed for functional gene analysis, which can assist in determining the genes and mechanisms behind HM resistance. These investigations will contribute to better understanding about the various operon systems that are inextricably linked to HM-resistant bacteria, as well as their detoxification processes.

Certain metabolite *viz*. oxidation-reduction potential of As ions, EPS, siderophore production, biofilm production etc. are some of the major routes through which bacteria find a way to overcome or reduce the HM stress. However, to determine

their environmental application *viz*. bioremediation, factors associated with effective metabolite production need to be optimized. Further their ecological role in the environment apart from HM toxicity also required to be studied for a better understanding of their adaptive features.

Though, the association of the selected bacterial strains in the presence of test plant species is found to be have positive interaction and was supported by a number of PGP traits *viz*. IAA production, ammonia production, siderophore production, biofilm formation etc., but the actual mechanism behind the reduced phytotoxicity in the presence of test HMs compared to control need to be understand. Moreover, the interaction of the selected bacteria in the field condition required to be understand in order to determine their capacity to establish in the presence of pre-existed microflora. Besides establishing a stable population, interaction between selected bacterial with other commercially important crops needs to be evaluated in order to establish their bioremediation potentiality. Further influence of the physicochemical profile of rhizospheric environment on the selected bacterial strains required to be assessed to validate their ability to promote plant development. Determining the traits of the selected strain that promote plant growth and experimenting with commercially significant crop species to determine their potential use as growth enhancers in agricultural land effected by HMs could be another crucial component of future study. Although removal efficiency of selected HM by the bacterial strains were found to be significant. However, field trials experiment is critical in order to determine the efficiency for possible bioremediation application. In a similar manner, selected bacterial strains found to be non-toxic to brine shrimp larvae, and reduced the mortality in the presence of HM treatments. However, the mechanisms through which bacteria reduced the metallic stress in the larvae is need to be studied to establish their eco-benign nature. Further, their response towards other organisms also need to be studied to conform their ecological compatibility. Thus, future studies could pave a way to address mentioned limitations and prove the practical applicability of selected bacterial strains.

Abbas, S., Zulfiqar, S., Arshad, M., Khalid, N., Hussain, A. and Ahmed, I., 2025. Molecular characterization of heavy metal-tolerant bacteria and their potential for bioremediation and plant growth promotion. Frontiers in Microbiology, 16, p.1644466.

Abbas, S.Z., Riaz, M., Ramzan, N., Zahid, M.T., Shakoori, F.R. and Rafatullah, M., 2014. Isolation and characterization of arsenic resistant bacteria from wastewater. *Brazilian Journal of Microbiology*, *45*, pp.1309-1315.

Abd Elnabi, M.K., Elkaliny, N.E., Elyazied, M.M., Azab, S.H., Elkhalifa, S.A., Elmasry, S., Mouhamed, M.S., Shalamesh, E.M., Alhorieny, N.A., Abd Elaty, A.E. and Elgendy, I.M., 2023. Toxicity of heavy metals and recent advances in their removal: a review. *Toxics*, *11*(7), p.580.

Acosta-Rodríguez, I., Cárdenas-González, J.F., Rodríguez Pérez, A.S., Oviedo, J.T. and Martínez-Juárez, V.M., 2018. Bioremoval of different heavy metals by the resistant fungal strain Aspergillus niger. *Bioinorganic chemistry and applications*, *2018*(1), p.3457196.

Adams, M.B., Kelly, C., Kabrick, J. and Schuler, J., 2019. Temperate forests and soils. In *Developments in soil science* (Vol. 36, pp. 83-108). Elsevier.

Adimalla, N., 2020. Heavy metals pollution assessment and its associated human health risk evaluation of urban soils from Indian cities: a review. *Environmental geochemistry and health*, *42*(1), pp.173-190.

Adimalla, N., Qian, H. and Wang, H., 2019. Assessment of heavy metal (HM) contamination in agricultural soil lands in northern Telangana, India: an approach of spatial distribution and multivariate statistical analysis. *Environmental monitoring and assessment*, *191*(4), p.246.

Agarwal, M., Rathore, R.S. and Chauhan, A., 2020. A rapid and high throughput MIC determination method to screen uranium resistant microorganisms. *Methods and protocols*, *3*(1), p.21.

Agarwala, S., Bora, A., Koch, J. and Kalita, A., 2024. Isolation and identification of heavy metal tolerant (Cr, Cu, Pb) bacteria from municipal waste dumping site and

assessment of their MIC and antibiotic susceptibility. *African Journal of Biological Sciences*, 6, pp. 3182–3193.

Aguilar, N.C., Faria, M.C., Pedron, T., Batista, B.L., Mesquita, J.P., Bomfeti, C.A. and Rodrigues, J.L., 2020. Isolation and characterization of bacteria from a brazilian gold mining area with a capacity of arsenic bioaccumulation. *Chemosphere*, *240*, p.124871.

Ahemad, M., 2019. Remediation of metalliferous soils through the heavy metal resistant plant growth promoting bacteria: paradigms and prospects. Arab. J. Chem. 12 (7), 1365–1377. https://doi.org/10.1016/j.arabjc.2014.11.020

Ahsan, N., Marian, M., Suga, H. and Shimizu, M., 2021. Lysinibacillus xylanilyticus strain GIC41 as a potential plant biostimulant. *Microbes and environments*, *36*(4), p.ME21047.

Ajmal, A.W., Yasmin, H., Hassan, M.N., Khan, N., Jan, B.L. and Mumtaz, S., 2022. Heavy metal–resistant plant growth–promoting citrobacter werkmanii strain WWN1 and enterobacter cloacae strain JWM6 enhance wheat (Triticum aestivum L.) growth by modulating physiological attributes and some key antioxidants under multi-metal stress. *Frontiers in Microbiology*, *13*, p.815704.

Ajsuvakova, O.P., Tinkov, A.A., Aschner, M., Rocha, J.B., Michalke, B., Skalnaya, M.G., Skalny, A.V., Butnariu, M., Dadar, M., Sarac, I. and Aaseth, J., 2020. Sulfhydryl groups as targets of mercury toxicity. *Coordination chemistry reviews*, *417*, p.213343.

Al Salah, D.M.M., Laffite, A., Sivalingam, P. and Poté, J., 2022. Occurrence of toxic metals and their selective pressure for antibiotic-resistant clinically relevant bacteria and antibiotic-resistant genes in river receiving systems under tropical conditions. *Environmental Science and Pollution Research*, *29*(14), pp.20530-20541.

Alasmary, Z., 2025. Lead (Pb) Contamination in Soil and Plants at Military Shooting Ranges and Its Mitigation Strategies: A Comprehensive Review. *Processes*, *13*(2), p.345.

Alghamdi, S.A. and El-Zohri, M., 2024. Phytoremediation characterization of heavy metals by some native plants at anthropogenic polluted sites in Jeddah, Saudi Arabia. *Resources*, *13*(7), p.98.

Ali, S. and Ahirwar, R., 2025. Accumulation of toxic metals in vegetable crops and associated dietary exposure risks to human health. *Discover Environment*, *3*(1), pp.1-28.

Alidoosti, F., Giyahchi, M., Moien, S. and Moghimi, H., 2024. Unlocking the potential of soil microbial communities for bioremediation of emerging organic contaminants: omics-based approaches. *Microbial Cell Factories*, *23*(1), p.210.

Al-Kelani, M. and Buthelezi, N., 2024. Advancements in medical research: Exploring Fourier Transform Infrared (FTIR) spectroscopy for tissue, cell, and hair sample analysis. *Skin Research and Technology*, *30*(6), p.e13733.

Alloway, B.J. ed., 2012. *Heavy metals in soils: trace metals and metalloids in soils and their bioavailability* (Vol. 22). Springer Science & Business Media.

Almashhadany, D.A., Rashid, R.F., Altaif, K.I., Mohammed, S.H., Mohammed, H.I. and Al-Bader, S.M., 2024. Heavy metal (loid) bioaccumulation in fish and its implications for human health. *Italian Journal of Food Safety*, *14*(1), p.12782.

Ameen, F.A., Hamdan, A.M. and El-Naggar, M.Y., 2020. Assessment of the heavy metal bioremediation efficiency of the novel marine lactic acid bacterium, Lactobacillus plantarum MF042018. *Scientific reports*, *10*(1), p.314.

Amin, I., Nazir, R. and Rather, M.A., 2024. Evaluation of multi-heavy metal tolerance traits of soil-borne fungi for simultaneous removal of hazardous metals. *World Journal of Microbiology and Biotechnology*, *40*(6), p.175.

Amutha, V., Aiswarya, D., Deepak, P., Selvaraj, R., Tamilselvan, C., Perumal, P. and Balasubramani, G., 2023. Toxicity potential evaluation of ethyl acetate extract of Cymodocea serrulata against the mosquito vectors vis-a-vis zebrafish embryos and Artemia salina cysts. *South African Journal of Botany*, *152*, pp.230-239.

Anekwe, I.M.S. and Isa, Y.M., 2023. Bioremediation of acid mine drainage–Review. Alexandria Engineering Journal, 65, pp.1047-1075.

Angon, P.B., Islam, M.S., Das, A., Anjum, N., Poudel, A. and Suchi, S.A., 2024. Sources, effects and present perspectives of heavy metals contamination: Soil, plants and human food chain. *Heliyon*, *10*(7).

Anil Kumar, S., Abyaneh, M.K., Gosavi, S.W., Kulkarni, S.K., Pasricha, R., Ahmad, A. and Khan, M.I., 2007. Nitrate reductase-mediated synthesis of silver nanoparticles from AgNO3. *Biotechnology letters*, *29*(3), pp.439-445.

Aniş, I.B., Popescu, I.V., Stihi, C. and Dulama, I.D., 2024. Determination of Metal Content in Soil and Wheat Plant by Inductively Coupled Plasma Mass Spectrometry. Journal of Agricultural Chemistry and Environment, 13(3), pp.300-311.

AOAC International, 1990. Kjeldahl Nitrogen in Fertilizers, AOAC Official Method 978.02. In: K. Helrich, ed., Official Methods of Analysis of AOAC International, 15th ed. Arlington, VA: AOAC International, pp. 13-15.

Arora, N.K. and Verma, M., 2017. Modified microplate method for rapid and efficient estimation of siderophore produced by bacteria. *3 Biotech*, *7*(6), p.381.

Aryal, M., Ziagova, M. and Liakopoulou-Kyriakides, M., 2010. Study on arsenic biosorption using Fe (III)-treated biomass of Staphylococcus xylosus. Chemical Engineering Journal, 162(1), pp.178-185.

Aryal, M., Ziagova, M. and Liakopoulou-Kyriakides, M., 2011. Comparison of Cr (VI) and As (V) removal in single and binary mixtures with Fe (III)-treated Staphylococcus xylosus biomass: Thermodynamic studies. *Chemical Engineering Journal*, *169*(1-3), pp.100-106.

Aslam, A., Kanwal, F., Javied, S., Nisar, N. and Torriero, A.A.J., 2025. Microbial biosorption: A sustainable approach for metal removal and environmental remediation. *International Journal of Environmental Science and Technology*, *22*(13), pp.13245-13276.

Atykyan, N., Revin, V. and Shutova, V., 2020. Raman and FT-IR Spectroscopy investigation the cellulose structural differences from bacteria Gluconacetobacter sucrofermentans during the different regimes of cultivation on a molasses media. *Amb Express*, *10*(1), p.84.

Ayala, A., Muñoz, M.F. and Argüelles, S., 2014. Lipid peroxidation: production, metabolism, and signaling mechanisms of malondialdehyde and 4-hydroxy-2-nonenal. *Oxidative medicine and cellular longevity*, *2014*(1), p.360438.

Ayangbenro, A.S. and Babalola, O.O., 2017. A new strategy for heavy metal polluted environments: a review of microbial biosorbents. *International journal of environmental research and public health*, *14*(1), p.94.

Azeh Engwa, G., Udoka Ferdinand, P., Nweke Nwalo, F. and Unachukwu, M., 2019. *Mechanism and health effects of heavy metal toxicity in humans. Poisoning in the Modern World-New Tricks for an Old Dog? IntechOpen* [online]

Bachate, S.P., Khapare, R.M. and Kodam, K.M., 2012. Oxidation of arsenite by two β-proteobacteria isolated from soil. *Applied microbiology and biotechnology*, *93*(5), pp.2135-2145.

Badr, F.M. and El-Habit, O., 2018. Heavy metal toxicity affecting fertility and reproduction of males. In *Bioenvironmental Issues Affecting Men's Reproductive and Sexual Health* (pp. 293-304). Academic Press.

Bae, J., Mercier, G., Watson, A.K. and Benoit, D.L., 2014. Seed germination test for heavy metal phytotoxicity assessment. *Canadian Journal of Plant Science*, *94*(8), pp.1519-1521.

Baker-Austin, C., Wright, M.S., Stepanauskas, R. and McArthur, J.V., 2006. Co-selection of antibiotic and metal resistance. *Trends in microbiology*, *14*(4), pp.176-182.

Balan, B., Dhaulaniya, A.S., Varma, D.A., Sodhi, K.K., Kumar, M., Tiwari, M. and Singh, D.K., 2021. Microbial biofilm ecology, in silico study of quorum sensing receptor-ligand interactions and biofilm mediated bioremediation. *Archives of Microbiology*, *203*(1), pp.13-30.

Balestri, E., Menicagli, V., Ligorini, V., Fulignati, S., Galletti, A.M.R. and Lardicci, C., 2019. Phytotoxicity assessment of conventional and biodegradable plastic bags using seed germination test. *Ecological indicators*, *102*, pp.569-580.

Balouiri, M., Sadiki, M. and Ibnsouda, S.K., 2016. Methods for in vitro evaluating antimicrobial activity: A review. *Journal of pharmaceutical analysis*, *6*(2), pp.71-79.

Banerjee, S., Datta, S., Chattyopadhyay, D. and Sarkar, P., 2011. Arsenic accumulating and transforming bacteria isolated from contaminated soil for potential use in bioremediation. *Journal of Environmental Science and Health, Part A*, *46*(14), pp.1736-1747.

Baruah, M.K., Kotoky, P., Baruah, J., Borah, G.C. and Bora, P.K., 2003. Arsenic association and distribution in carbonaceous materials in northeastern India. *Current Science*, pp.204-208.

Basak, N., Chowdhury, A.A., Roy, T. and Islam, E., 2024. Evaluation of root plaque associated plant growth promoting Burkholderia sp. EIKU24 in metal (loid) s removal, minerals solubilization and arsenic uptake inhibition in rice seedlings. *Biocatalysis and Agricultural Biotechnology*, *58*, p.103236.

Bauer, A.W., Kirby, W.M., Sherris, J.C. and Turck, M., 1966. Antibiotic susceptibility testing by a standardized single disk method. *American journal of clinical pathology*, *45*(4_ts), pp.493-496.

Bayraktar, E.P., Isinkaralar, O. and Isinkaralar, K., 2022. Usability of several species for monitoring and reducing the heavy metal pollution threatening the public health in urban environment of Ankara. *World Journal of Advanced Research and Reviews*, *14*(3), pp.276-283.

Behera, M., Dandapat, J. and Rath, C.C., 2014. Effect of heavy metals on growth response and antioxidant defense protection in Bacillus cereus. *Journal of basic microbiology*, *54*(11), pp.1201-1209.

Benvenuto, M.A., 2016. *Metals and alloys: industrial applications*. Walter de Gruyter GmbH & Co KG.

Bera, S., Arora, R., Ateba, C.N. and Kumar, A., 2022. Microbes: A sustainable tool for healthy and climate smart agriculture. In *Relationship Between Microbes and the Environment for Sustainable Ecosystem Services, Volume 1* (pp. 197-213). Elsevier.

Bergey, D.H., 1994. *Bergey's manual of determinative bacteriology*. Lippincott Williams & Wilkins.

Bertrand, R.L., 2019. Lag phase is a dynamic, organized, adaptive, and evolvable period that prepares bacteria for cell division. *Journal of bacteriology*, *201*(7), pp.10-1128.

Beyer, W.N., Dalgarn, J., Dudding, S., French, J.B., Mateo, R., Miesner, J., Sileo, L. and Spann, J., 2004. Zinc and lead poisoning in wild birds in the Tri-State Mining District (Oklahoma, Kansas, and Missouri). *Archives of Environmental Contamination and Toxicology*, *48*(1), pp.108-117.

Bhattacharya, A. and Bhattacharya, S., 2007. Induction of oxidative stress by arsenic in Clarias batrachus: involvement of peroxisomes. *Ecotoxicology and Environmental Safety*, *66*(2), pp.178-187.

Bianucci, E., Fabra, A. and Castro, S., 2012. Involvement of glutathione and enzymatic defense system against cadmium toxicity in Bradyrhizobium sp. strains (peanut symbionts). *Biometals*, *25*(1), pp.23-32.

Bibi, A., Ullah, M.S., Mahmood, A., Shahzad, M., Javaid, M.M., Nadeem, M.A., Altihani, F.A., Hashem, M. and Qari, S.H., 2025. Indole-3-acetic acid improves growth, physiology, photosynthesis, and ion balance under cadmium stress in Sorghum bicolor. *Scientific Reports*, *15*(1), pp.1-16.

Bissen, M. and Frimmel, F.H., 2003. Arsenic—a review. Part I: occurrence, toxicity, speciation, mobility. *Acta hydrochimica et hydrobiologica*, *31*(1), pp.9-18.

Biswas, R., Vivekanand, V., Saha, A., Ghosh, A. and Sarkar, A., 2019. Arsenite oxidation by a facultative chemolithotrophic Delftia spp. BAs29 for its potential application in groundwater arsenic bioremediation. *International Biodeterioration & Biodegradation*, *136*, pp.55-62.

Botle, A., Salgaonkar, S., Tiwari, R. and Barabde, G., 2025. Heavy metal pollution in river ulhas, Maharashtra, India: Unraveling contamination dynamics through pollution indices, multivariate analysis, and health risk assessment. *International Journal of Environmental Research*, *19*(3), p.88.

Bouida, L., Rafatullah, M., Kerrouche, A., Qutob, M., Alosaimi, A.M., Alorfi, H.S. and Hussein, M.A., 2022. A review on cadmium and lead contamination: Sources, fate, mechanism, health effects and remediation methods. *Water*, *14*(21), p.3432.

Bowman, N., Patel, D., Sanchez, A., Xu, W., Alsaffar, A. and Tiquia-Arashiro, S.M., 2018. Lead-resistant bacteria from Saint Clair River sediments and Pb removal in aqueous solutions. *Applied Microbiology and Biotechnology*, *102*(5), pp.2391-2398.

Bradl, H.B., 2005. Sources and origins of heavy metals. In *Interface science and technology* (Vol. 6, pp. 1-27). Elsevier.

Brat, D. and Pathak, I.R., 2020. Impact of pollution on biodiversity: A review. *IRE J*, *4*(2), pp.11-15.

Bravo, D. and Braissant, O., 2022. Cadmium-tolerant bacteria: current trends and applications in agriculture. *Letters in Applied Microbiology*, *74*(3), pp.311-333.

Bray, R.H. and Kurtz, L.T., 1945. Determination of total, organic, and available forms of phosphorus in soils. Soil science, 59(1), pp.39-46.

Briffa, J., Sinagra, E. and Blundell, R., 2020. Heavy metal pollution in the environment and their toxicological effects on humans. Heliyon, 6(9).

Bueno, B.Y.M., Torem, M.L., Molina, F.A.L.M.S. and De Mesquita, L.M.S., 2008. Biosorption of lead (II), chromium (III) and copper (II) by R. opacus: Equilibrium and kinetic studies. *Minerals engineering*, *21*(1), pp.65-75.

Bureau of Indian Standards (BIS) (2012) *IS 10500:2012 – Drinking Water Specification*. New Delhi: BIS. Available at: https://www.services.bis.gov.in (Accessed: 1 December 2025).

Button, M., Jenkin, G.R., Bowman, K.J., Harrington, C.F., Brewer, T.S., Jones, G.D. and Watts, M.J., 2010. DNA damage in earthworms from highly contaminated soils: Assessing resistance to arsenic toxicity by use of the Comet assay. *Mutation Research/Genetic Toxicology and Environmental Mutagenesis*, *696*(2), pp.95-100.

Cai, L., Xu, Z., Ren, M., Guo, Q., Hu, X., Hu, G., Wan, H. and Peng, P., 2012. Source identification of eight hazardous heavy metals in agricultural soils of Huizhou, Guangdong Province, China. *Ecotoxicology and environmental safety*, *78*, pp.2-8.

Calatrava, V., Gonzalez-Ballester, D. and Dubini, A., 2024. Microalgae for bioremediation: advances, challenges, and public perception on genetic engineering. *BMC Plant Biology*, *24*(1), p.1261.

Campbell, P.G., 2006. Cadmium—a priority pollutant. *Environmental Chemistry*, *3*(6), pp.387-388.

Cardinal, M.J., Meghrous, J., Lacroix, C. and Simard, R.E., 1997. Isolation of Lactococcus lactis strains producing inhibitory activity against Listeria. *Food Biotechnology*, *11*(2), pp.129-146.

Caregnato, F.F., Koller, C.E., MacFarlane, G.R. and Moreira, J.C., 2008. The glutathione antioxidant system as a biomarker suite for the assessment of heavy metal exposure and effect in the grey mangrove, Avicennia marina (Forsk.) Vierh. *Marine Pollution Bulletin*, *56*(6), pp.1119-1127.

Carlos, M.H.J., Stefani, P.V.Y., Janette, A.M., Melani, M.S.S. and Gabriela, P.O., 2016. Assessing the effects of heavy metals in ACC deaminase and IAA production on plant growth-promoting bacteria. *Microbiological research*, *188*, pp.53-61.

Castro, M.C.R., Urrea, G. and Guasch, H., 2015. Influence of the interaction between phosphate and arsenate on periphyton's growth and its nutrient uptake capacity. *Science of the total environment*, *503*, pp.122-132.

Cen, T., Zhang, X., Xie, S. and Li, D., 2020. Preservatives accelerate the horizontal transfer of plasmid-mediated antimicrobial resistance genes via differential mechanisms. *Environment international*, *138*, p.105544.

Central Ground Water Board (2024) *Ground Water Quality of Nagaland*. Ministry of Jal Shakti, Government of India, New Delhi.

Central Pollution Control Board (CPCB) (2010) *Standards for Discharge of Environmental Pollutants / Industrial Effluents*. Ministry of Environment, Forest and

Climate Change, Government of India. Available at: https://cpcb.nic.in (Accessed: 1 December 2025).

Çetin, B., Usal, M., Aloğlu, H.Ş., Busch, A., Dertli, E. and Abdulmawjood, A., 2024. Characterization and technological functions of different lactic acid bacteria from traditionally produced Kırklareli white brined cheese during the ripening period. *Folia microbiologica*, *69*(5), pp.1069-1081.

Chakraborty, P. and Mandal, S., 2025. Isolation and Characterization of Streptococcus thermophilus from Traditionally Prepared Sour Curd. *Microbiology Research Journal International*, *35*(5), pp.83-92.

Chauhan, P. and Mathur, J., 2020. Phytoremediation efficiency of Helianthus annuus L. for reclamation of heavy metals-contaminated industrial soil. *Environmental Science and Pollution Research*, *27*(24), pp.29954-29966.

Checinska Sielaff, A., Urbaniak, C., Mohan, G.B.M., Stepanov, V.G., Tran, Q., Wood, J.M., Minich, J., McDonald, D., Mayer, T., Knight, R. and Karouia, F., 2019. Characterization of the total and viable bacterial and fungal communities associated with the International Space Station surfaces. *Microbiome*, *7*(1), p.50.

Chen, J., Li, J., Zhang, H., Shi, W. and Liu, Y., 2019. Bacterial heavy-metal and antibiotic resistance genes in a copper tailing dam area in northern China. *Frontiers in microbiology*, *10*, p.1916.

Chen, W., Kong, Y., Li, J., Sun, Y., Min, J. and Hu, X., 2020. Enhanced biodegradation of crude oil by constructed bacterial consortium comprising salt-tolerant petroleum degraders and biosurfactant producers. *International Biodeterioration & Biodegradation*, *154*, p.105047.

Chen, Y., Liu, X., Li, Q., Cai, X., Wu, W., Wu, Q., Yuan, W., Deng, X., Liu, Z., Zhao, S. and Wang, B., 2023. Integrated genomics and transcriptomics reveal the extreme heavy metal tolerance and adsorption potentiality of Staphylococcus equorum. *International Journal of Biological Macromolecules*, *229*, pp.388-400.

Chien, C.C., Lin, B.C. and Wu, C.H., 2013. Biofilm formation and heavy metal resistance by an environmental Pseudomonas sp. *Biochemical engineering journal*, *78*, pp.132-137.

Christensen, G.D., Simpson, W.A., Younger, J.J., Baddour, L.M., Barrett, F.F., Melton, D.M. and Beachey, E.H., 1985. Adherence of coagulase-negative staphylococci to plastic tissue culture plates: a quantitative model for the adherence of staphylococci to medical devices. *Journal of clinical microbiology*, *22*(6), pp.996-1006.

Coculescu, B.I., 2009. Antimicrobial resistance induced by genetic changes. *Journal of medicine and life*, *2*(2), p.114.

Cook, J., 1977. Environmental pollution by heavy metals. *International Journal of Environmental Studies*, *10*(4), pp.253-266.

Cordero, A.P., Vergara, D.E.M. and Mendoza, Y.A., 2023. Production of 1-aminocyclopropane-1-carboxylic acid deaminase (ACC) by Burkholderia cepacia as an indicator of cadmium contamination. Journal of Positive Psychology and Wellbeing, pp.1008-1016.

Costa, O.Y., Raaijmakers, J.M. and Kuramae, E.E., 2018. Microbial extracellular polymeric substances: ecological function and impact on soil aggregation. *Frontiers in microbiology*, *9*, p.1636.

Crapart, S., Fardeau, M.L., Cayol, J.L., Thomas, P., Sery, C., Ollivier, B. and Combet-Blanc, Y., 2007. Exiguobacterium profundum sp. nov., a moderately thermophilic, lactic acid-producing bacterium isolated from a deep-sea hydrothermal vent. *International journal of systematic and evolutionary microbiology*, *57*(2), pp.287-292.

Cristani, M., Naccari, C., Nostro, A., Pizzimenti, A., Trombetta, D. and Pizzimenti, F., 2012. Possible use of Serratia marcescens in toxic metal biosorption (removal). *Environmental Science and Pollution Research*, *19*(1), pp.161-168.

Cutler, C.P., 2018. Use of metals in our society. In *Metal Allergy: From Dermatitis to Implant and Device Failure* (pp. 3-16). Cham: Springer International Publishing.

Dai, F., Zhuang, Q., Huang, G., Deng, H. and Zhang, X., 2023. Infrared spectrum characteristics and quantification of OH groups in coal. *ACS omega*, *8*(19), pp.17064-17076.

Dalei, K., 2014. *Synthesis and characterization of cadmium sulphide nanoparticles and its utilization in removal of cadmium from aqueous solution* (Doctoral dissertation).

Dange, S., Arumugam, K. and Vijayaraghavalu, S.S., 2024. Geochemical insights into heavy metal contamination and health hazards in Palar River Basin: a pathway to sustainable solutions. *Ecological Indicators*, *166*, p.112568.

Das, K., Masud, M.A.A., Sarker, A., Arafa, R.A. and Patel, M., 2025. Unveiling the Sustainable and Biological Remediation of Heavy Metals Contaminations in Soils and Water Ecosystems Through Potential Microbes—A Review. *Sustainability*, *17*(16), p.7357.

Davis, J.J., Gerdes, S., Olsen, G.J., Olson, R., Pusch, G.D., Shukla, M., Vonstein, V., Wattam, A.R. and Yoo, H., 2016. PATtyFams: protein families for the microbial genomes in the PATRIC database. *Frontiers in microbiology*, *7*, p.118.

de Andrade, L.A., Santos, C.H.B., Frezarin, E.T., Sales, L.R. and Rigobelo, E.C., 2023. Plant growth-promoting rhizobacteria for sustainable agricultural production. *Microorganisms*, *11*(4), p.1088.

Del Giudice, I., Limauro, D., Pedone, E., Bartolucci, S. and Fiorentino, G., 2013. A novel arsenate reductase from the bacterium Thermus thermophilus HB27: its role in arsenic detoxification. *Biochimica et Biophysica Acta (BBA)-Proteins and Proteomics*, *1834*(10), pp.2071-2079.

Deng, M., Li, K., Yan, Y.J., Huang, F. and Peng, D., 2022. Enhanced cadmium removal by growing Bacillus cereus RC-1 immobilized on different magnetic biochars through simultaneous adsorption and bioaccumulation. *Environmental Science and Pollution Research*, *29*(13), pp.18495-18507.

Devy, R.A. and Vasudevan, V., 2025. Heavy Metals: Major Environmental and Organismal Health Impacts.

Dey, U., Chatterjee, S. and Mondal, N.K., 2016. Isolation and characterization of arsenic-resistant bacteria and possible application in bioremediation. *Biotechnology reports*, *10*, pp.1-7.

Diba, F., Khan, M.Z.H., Uddin, S.Z., Istiaq, A., Shuvo, M.S.R., Ul Alam, A.R., Hossain, M.A. and Sultana, M., 2021. Bioaccumulation and detoxification of trivalent arsenic by Achromobacter xylosoxidans BHW-15 and electrochemical detection of its transformation efficiency. *Scientific Reports*, *11*(1), p.21312.

Dimkpa, C., Svatoš, A., Merten, D., Büchel, G. and Kothe, E., 2008. Hydroxamate siderophores produced by Streptomyces acidiscabies E13 bind nickel and promote growth in cowpea (Vigna unguiculata L.) under nickel stress. *Canadian Journal of Microbiology*, *54*(3), pp.163-172.

Dimkpa, C.O., Merten, D., Svatoš, A., Büchel, G. and Kothe, E., 2009. Siderophores mediate reduced and increased uptake of cadmium by Streptomyces tendae F4 and sunflower (Helianthus annuus), respectively. *Journal of Applied Microbiology*, *107*(5), pp.1687-1696.

Directorate of Geology & Mining, Nagaland (n.d.) *Coal resources and status of explored mineral blocks*. Government of Nagaland. Available at: URL (Accessed: 24 November 2025).

Drewniak L, Styczek A, Majder-Lopatka M, Sklodowska A (2008) Bacteria, hypertolerant to arsenic in the rocks of an ancient gold mine, and their potential role in dissemination of arsenic pollution. Environ Pollut 156(3):1069-1074. https://doi.org/10.1016/j.envpol.2008.04.019

DRIIV (2025) *Top 10 wastewater treatment technologies driving India's water security*. Available at: https://blog.driiv.co.in/top-10-wastewater-treatment-technologies-driving-indias-water-security/ (Accessed: 2 December 2025).

Duan, Y., Wang, Y., Huang, J., Li, H., Dong, H. and Zhang, J., 2021. Toxic effects of cadmium and lead exposure on intestinal histology, oxidative stress response, and microbial community of Pacific white shrimp Litopenaeus vannamei. *Marine Pollution Bulletin*, *167*, p.112220.

Edgar, R.C., 2004. MUSCLE: multiple sequence alignment with high accuracy and high throughput. *Nucleic acids research*, *32*(5), pp.1792-1797.

Elliott, J.E., Scheuhammer, A.M., 1997. Heavy metal and metallothionein concentrations in seabirds from the Pacific coast of Canada. Mar. Pollut. Bull. 34 (10), 794–801. https://doi.org/10.1016/S0025-326X(97)00034-9.

EPA U.S., 2007. Method 3051A (SW-846): microwave assisted acid digestion of sediments, sludges, and oils, revision 1. *Washington, DC*.

Esringu, A., Kulekci, E.A., Turan, M. and Ercisli, S., 2015. Phytoremediation of some heavy metals by different tissues of roses grown in the main intersections in Erzurum city Turkey. *Fresenius Environmental Bulletin*, *24*(9), pp.2787-2791.

Fan, L. and Zhang, X., 2019. ATR-FTIR spectroscopic characterization of ferric arsenic-containing colloid and gypsum. *Desalination and Water Treatment*, *153*, pp.130-135.

Fanai, A., Bohia, B., Lalremruati, F., Lalhriatpuii, N., Lalmuanpuii, R. and Singh, P.K., 2024. Plant growth promoting bacteria (PGPB)-induced plant adaptations to stresses: An updated review. PeerJ, 12, p.e17882.

Fashola, M.O., Ngole-Jeme, V.M. and Babalola, O.O., 2016. Heavy metal pollution from gold mines: environmental effects and bacterial strategies for resistance. *International journal of environmental research and public health*, *13*(11), p.1047.

Feria-Cáceres, P.F., Penagos-Velez, L. and Moreno-Herrera, C.X., 2022. Tolerance and cadmium (Cd) immobilization by native bacteria isolated in cocoa soils with increased metal content. *Microbiology Research*, *13*(3), pp.556-573.

Fernandes, J.C. and Henriques, F.S., 1991. Biochemical, physiological, and structural effects of excess copper in plants. *The botanical review*, *57*(3), pp.246-273.

Fernandes, S., Kerkar, S., D'Costa, A., Costa, M., Mishra, A., Shyama, S.K. and Das, K.R., 2021. Immuno-stimulatory effect and toxicology studies of salt pan bacteria as probiotics to combat shrimp diseases in aquaculture. *Fish & Shellfish Immunology*, *113*, pp.69-78.

Filali, B.K., Taoufik, J., Zeroual, Y.F.A.Z., Dzairi, F.Z., Talbi, M. and Blaghen, M., 2000. Waste water bacterial isolates resistant to heavy metals and antibiotics. Current microbiology, 41(3), pp.151-156.

Fischer, E. and Koszorus, L., 1992. Sublethal effects, accumulation capacities and elimination rates of As, Hg and Se in the manure worm, Eisenia fetida(Oligochaeta, Lumbricidae). *Pedobiologia*, *36*(3), pp.172-178.

Fischer, E.R., Hansen, B.T., Nair, V., Hoyt, F.H., Schwartz, C.L. and Dorward, D.W., 2024. Scanning electron microscopy. Current Protocols, 4, e1034. https://doi.org/10.1002/cpz1.1034

Flemming, H.C. and Wingender, J., 2010. The biofilm matrix. *Nature reviews microbiology*, *8*(9), pp.623-633.

Flemming, H.C., Wingender, J., Szewzyk, U., Steinberg, P., Rice, S.A. and Kjelleberg, S., 2016. Biofilms: an emergent form of bacterial life. *Nature Reviews Microbiology*, *14*(9), pp.563-575.

Flohé, L. and Günzler, W.A., 1984. [12] Assays of glutathione peroxidase. In *Methods in enzymology* (Vol. 105, pp. 114-120). Academic Press.

Flora, S.J. and Kumar, P., 1996. Biochemical and immunotoxicological alterations following repeated gallium arsenide exposure and their recoveries by meso-2, 3-dimercaptosuccinic acid and 2, 3-dimercaptopropane 1-sulfonate administration in rats. *Environmental toxicology and pharmacology*, *2*(4), pp.315-320.

Fóris, T., Koska, P., Ilosvai, Á.M., Kristály, F., Daróczi, L., Vanyorek, L. and Viskolcz, B., 2025. An Innovative Bioremediation Approach to Heavy Metal Removal: Combined Application of Chlorella vulgaris and Amine-Functionalized MgFe2O4 Nanoparticles in Industrial Wastewater Treatment. *International Journal of Molecular Sciences*, *26*(12), p.5467.

Fu, F. and Wang, Q., 2011. Removal of heavy metal ions from wastewaters: a review. *Journal of environmental management*, *92*(3), pp.407-418.

Gadd, G.M., 2009. Biosorption: critical review of scientific rationale, environmental importance and significance for pollution treatment. *Journal of Chemical Technology & Biotechnology: International Research in Process, Environmental & Clean Technology*, *84*(1), pp.13-28.

Gadd, G.M., 2010. Metals, minerals and microbes: geomicrobiology and bioremediation. *Microbiology*, *156*(3), pp.609-643.

Gaidos, E., Lanoil, B., Thorsteinsson, T., Graham, A., Skidmore, M., Han, S.K., Rust, T. and Popp, B., 2004. A viable microbial community in a subglacial volcanic crater lake, Iceland. *Astrobiology*, *4*(3), pp.327-344.

Ganesh, J., Hewitt, K., Devkota, A.R., Wilson, T. and Kaundal, A., 2024. IAA-producing plant growth promoting rhizobacteria from Ceanothus velutinus enhance cutting propagation efficiency and Arabidopsis biomass. *Frontiers in Plant Science*, *15*, p.1374877.

Gaonkar, T. and Bhosle, S., 2013. Effect of metals on a siderophore producing bacterial isolate and its implications on microbial assisted bioremediation of metal contaminated soils. *Chemosphere*, *93*(9), pp.1835-1843.

Gardea-Torresdey, J.L., Peralta-Videa, J.R., De La Rosa, G. and Parsons, J.G., 2005. Phytoremediation of heavy metals and study of the metal coordination by X-ray absorption spectroscopy. *Coordination chemistry reviews*, *249*(17-18), pp.1797-1810.

Garelick, H., Jones, H., Dybowska, A. and Valsami-Jones, E., 2008. Arsenic pollution sources. *Reviews of environmental contamination volume 197: International perspectives on arsenic pollution and remediation*, pp.17-60.

Garrett, R.G., 2000. Natural sources of metals to the environment. *Human and ecological risk assessment*, *6*(6), pp.945-963.

George, S.E. and Wan, Y., 2023. Microbial functionalities and immobilization of environmental lead: Biogeochemical and molecular mechanisms and implications for bioremediation. *Journal of hazardous materials*, *457*, p.131738.

Ghayedi, N., Borazjani, J.M. and Jafari, D., 2019. Biosorption of arsenic ions from the aqueous solutions using Chlorella vulgaris micro algae. *Desalination and Water Treatment*, *165*, pp.188-196.

Ghosh, P., Rathinasabapathi, B., Teplitski, M. and Ma, L.Q., 2015. Bacterial ability in AsIII oxidation and AsV reduction: relation to arsenic tolerance, P uptake, and siderophore production. *Chemosphere*, *138*, pp.995-1000.

Ghosh, S., Rusyn, I., Dmytruk, O.V., Dmytruk, K.V., Onyeaka, H., Gryzenhout, M. and Gafforov, Y., 2023. Filamentous fungi for sustainable remediation of pharmaceutical compounds, heavy metal and oil hydrocarbons. *Frontiers in Bioengineering and Biotechnology*, *11*, p.1106973.

Gianì, F., Masto, R., Trovato, M.A., Malandrino, P., Russo, M., Pellegriti, G., Vigneri, P. and Vigneri, R., 2021. Heavy metals in the environment and thyroid cancer. *Cancers*, *13*(16), p.4052.

Giannakoudakis, D.A., Meili, L. and Anastopoulos, I. eds., 2022. *Novel materials for environmental remediation applications: adsorption and beyond*. Elsevier.

Gidudu, B. and Chirwa, E.M., 2022. Evaluation of the toxicity of a rhamnolipid biosurfactant for its application in the optimization of the bio-electrokinetic remediation of petrochemical contaminated soil. *Cleaner Engineering and Technology*, *9*, p.100521.

Gikas, P., Sengor, S., Ginn, T., Moberly, J. and Peyton, B., 2009. The effects of heavy metals and temperature on microbial growth and lag. *Global Nest J*, *11*(3), pp.325-32.

Gillespie, J.L., Noe, G.B., Hupp, C.R., Gellis, A.C. and Schenk, E.R., 2018. Floodplain trapping and cycling compared to streambank erosion of sediment and nutrients in an agricultural watershed. JAWRA Journal of the American Water Resources Association, 54(2), pp.565-582.

Gillieatt, B.F. and Coleman, N.V., 2024. Unravelling the mechanisms of antibiotic and heavy metal resistance co-selection in environmental bacteria. *FEMS Microbiology Reviews*, *48*(4), p.fuae017.

Giovanella, P., Cabral, L., Costa, A.P., de Oliveira Camargo, F.A., Gianello, C. and Bento, F.M., 2017. Metal resistance mechanisms in Gram-negative bacteria and their potential to remove Hg in the presence of other metals. *Ecotoxicology and environmental safety*, *140*, pp.162-169.

Girawale, S.D., Meena, S.N., Nandre, V.S., Waghmode, S.B. and Kodam, K.M., 2022. Biosynthesis of vanillic acid by Ochrobactrum anthropi and its applications. *Bioorganic & Medicinal Chemistry*, *72*, p.117000.

Gladysheva, T.B., Oden, K.L. and Rosen, B.P., 1994. Properties of the arsenate reductase of plasmid R773. *Biochemistry*, *33*(23), pp.7288-7293.

Godt, J., Scheidig, F., Grosse-Siestrup, C., Esche, V., Brandenburg, P., Reich, A. and Groneberg, D.A., 2006. The toxicity of cadmium and resulting hazards for human health. *Journal of occupational medicine and toxicology*, *1*(1), p.22.

Gogoi, B., Bharali, P., Ramachandran, D., Hazarika, B. and Debnath, P., 2025. Isolation and Characterization of an Arsenic-Resistant Bacterial Strain from Changki, Nagaland. Nature Environment and Pollution Technology, 24(4), pp.1-14.

Gogoi, B., Bharali, P., Sorhie, V. and Rudithongru, L., 2023. An Understanding of the Underlying Mechanisms Involved in the Bacterial Remediation of Arsenic, Cadmium, and Lead. In *Biohydrometallurgical Processes* (pp. 130-154). CRC Press.

Gohil, R.B., Raval, V.H., Panchal, R.R. and Rajput, K.N., 2022. Plant growth-promoting activity of Bacillus sp. PG-8 isolated from fermented panchagavya and its effect on the growth of Arachis hypogea. *Frontiers in Agronomy*, *4*, p.805454.

Gomes, A.F., Almeida, M.C., Sousa, E. and Resende, D.I., 2024. Siderophores and metallophores: Metal complexation weapons to fight environmental pollution. *Science of The Total Environment*, *932*, p.173044.

Gomez-Caminero, A., Howe, P.D., Hughes, M., Kenyon, E., Lewis, D.R., Moore, M., Aitio, A., Becking, G.C. and Ng, J., 2001. Arsenic and arsenic compounds.

Gonzaga, M.I., Santos, J.A. and Ma, L.Q., 2008. Phytoextraction by arsenic hyperaccumulator Pteris vittata L. from six arsenic-contaminated soils: repeated harvests and arsenic redistribution. Environmental Pollution, 154(2), pp.212-218.

Goswami, R., Bhagat, C., Lollen, I., Neog, N., Barache, U.B., Thakur, R., Mahlknecht, J. and Kumar, M., 2023. Potential arsenic–chromium–lead Co-contamination in the hilly terrain of Arunachal Pradesh, north-eastern India: Genesis and health perspective. *Chemosphere*, *323*, p.138067.

Goswami, R., Bhagat, C., Lollen, I., Neog, N., Barache, U.B., Thakur, R., Mahlknecht, J. and Kumar, M., 2023. Potential arsenic–chromium–lead Co-contamination in the hilly terrain of Arunachal Pradesh, north-eastern India: Genesis and health perspective. *Chemosphere*, *323*, p.138067.

Govarthanan, M., Fuzisawa, S., Hosogai, T. and Chang, Y.C., 2017. Biodegradation of aliphatic and aromatic hydrocarbons using the filamentous fungus Penicillium sp. CHY-2 and characterization of its manganese peroxidase activity. *RSC advances*, *7*(34), pp.20716-20723.

Goyal, T., Mitra, P., Singh, P., Sharma, S. and Sharma, P., 2021. Assessement of blood lead and cadmium levels in occupationally exposed workers of Jodhpur, Rajasthan. *Indian Journal of Clinical Biochemistry*, *36*(1), pp.100-107.

Graham, R.D., 2008. Micronutrient deficiencies in crops and their global significance. In *Micronutrient deficiencies in global crop production* (pp. 41-61). Dordrecht: Springer Netherlands.

Greenwood, N.N. and Earnshaw, A. (2012). *Chemistry of the Elements* (2nd ed.). Oxford: Butterworth-Heinemann.

Grinnell, J., 1931. Phillips and Lincoln on the Conservation of Waterfowl. *The Condor*, *33*(1), pp.41-43.

Grujić, S., Vasić, S., Radojević, I., Čomić, L. and Ostojić, A., 2017. Comparison of the Rhodotorula mucilaginosa biofilm and planktonic culture on heavy metal susceptibility and removal potential. *Water, Air, & Soil Pollution*, *228*(2), p.73.

Gu, X., Li, X., Zhang, R., Zheng, R., Li, M., Huang, R. and Pang, X., 2025. Isolation and characterization of a novel highly efficient bacterium Lysinibacillus boronitolerans QD4 for quantum dot biosynthesis. *Frontiers in Microbiology*, *16*, p.1521632.

Gujre, N., Rangan, L. and Mitra, S., 2021. Occurrence, geochemical fraction, ecological and health risk assessment of cadmium, copper and nickel in soils contaminated with municipal solid wastes. *Chemosphere*, *271*, p.129573.

Guo, J., Dai, X., Xu, W. and Ma, M., 2008. Overexpressing GSH1 and AsPCS1 simultaneously increases the tolerance and accumulation of cadmium and arsenic in Arabidopsis thaliana. *Chemosphere*, *72*(7), pp.1020-1026.

Gupta MK (2023) Isolation of microorganisms. In: Bhatt AK, Bhatia RK, Bhalla TC (ed) Basic Biotechniques for Bioprocess and Bioentrepreneurship, 1st edn. Academic Press, Cambridge, pp 3-21

Gupta, B.S., Jelle, B.P. and Gao, T., 2022. In vitro cell composition identification of wood decay fungi by Fourier transform infrared spectroscopy. *Royal Society Open Science*, *9*(2), p.201935.

Gupta, K., Chatterjee, C. and Gupta, B., 2012. Isolation and characterization of heavy metal tolerant Gram-positive bacteria with bioremedial properties from municipal waste rich soil of Kestopur canal (Kolkata), West Bengal, India. *Biologia*, *67*(5), pp.827-836.

Gupta, P. and Diwan, B., 2017. Bacterial exopolysaccharide mediated heavy metal removal: a review on biosynthesis, mechanism and remediation strategies. *Biotechnology Reports*, *13*, pp.58-71.

Gupta, R., Khan, F., Alqahtani, F.M., Hashem, M. and Ahmad, F., 2024. Plant growth–promoting Rhizobacteria (PGPR) assisted bioremediation of Heavy Metal Toxicity. Applied Biochemistry and Biotechnology, 196(5), pp.2928-2956.

Gupta, V., Bhaskar, P., Thoudam, J., Bisht, S., Sharma, A. and Tripathi, R., 2023. Psychrophiles as a novel and promising source of cold-adapted industrial enzymes. *The Applied Biology & Chemistry Journal*, *4*(2), pp.54-68.

Gurer, H. and Ercal, N., 2000. Can antioxidants be beneficial in the treatment of lead poisoning?. *Free Radical Biology and Medicine*, *29*(10), pp.927-945.

Gürgan, M., İrez, E.İ. and Adiloğlu, S., 2022. Understanding Bioremediation of Metals and Metalloids by Genomic Approaches. In *Omics Insights in Environmental Bioremediation* (pp. 375-392). Singapore: Springer Nature Singapore.

Haferburg, G. and Kothe, E., 2010. Metallomics: lessons for metalliferous soil remediation. *Applied microbiology and biotechnology*, *87*(4), pp.1271-1280.

Hajdu, R. and Slaveykova, V.I., 2012. Cd and Pb removal from contaminated environment by metal resistant bacterium Cupriavidus metallidurans CH34: importance of the complexation and competition effects. *Environmental Chemistry*, *9*(4), pp.389-398.

Halliwell, B. and Gutteridge, J.M., 2015. *Free radicals in biology and medicine*. Oxford university press.

Haque, M.M., Mosharaf, M.K., Haque, M.A., Tanvir, M.Z.H. and Alam, M.K., 2021. Biofilm formation, production of matrix compounds and biosorption of copper, nickel and lead by different bacterial strains. *Frontiers in Microbiology*, *12*, p.615113.

Hassan, S.H.A., Abskharon, R.N.N., Gad El-Rab, S.M.F. and Shoreit, A.A.M., 2008. Isolation, characterization of heavy metal resistant strain of Pseudomonas aeruginosa isolated from polluted sites in Assiut city, Egypt. *Journal of Basic Microbiology*, *48*(3), pp.168-176.

Hassan, S.S., Zehra, S.S., Ahmed, Z., Talpur, M.Y.Y. and Panhwar, S., 2022. Removal of arsenic contaminants from water using iron oxide nanoparticles by inductively coupled plasma mass spectrometery.

Hasselmann, C., 2003. Determination of minimum inhibitory concentrations (MICs) of antibacterial agents by broth dilution. *Clinical Microbiology and Infection*, *9*(8).

Hassen, A., Saidi, N., Cherif, M. and Boudabous, A.J.B.T., 1998. Resistance of environmental bacteria to heavy metals. *Bioresource technology*, *64*(1), pp.7-15.

Hausladen, D.M., Alexander-Ozinskas, A., McClain, C. and Fendorf, S., 2018. Hexavalent chromium sources and distribution in California groundwater. *Environmental science & technology*, *52*(15), pp.8242-8251.

He, T. and Zhang, X., 2016. Characterization of bacterial communities in deep-sea hydrothermal vents from three oceanic regions. *Marine Biotechnology*, *18*(2), pp.232-241.

Hidayati N.V., Siregar A.S., Sari L.K., Putra G.Y., Hartono, Nugraha I.P., Syakti A.D. 2014. Estimation of the level of heavy metal Pb, Cd and Cr contamination in water and sediments in Segara Anakan waters, Cilacap. Omni-Akuatika. Vol. 13(18) p. 30–39.

Hossen, S., Hanif, M.A. and Kho, K.H., 2023. Glutathione reductase, a biomarker of pollutant and stress in Pacific abalone. *Marine Pollution Bulletin*, *192*, p.115139.

Hussain, M., Jamir, L. and Singh, M.R., 2021. Assessment of physico-chemical parameters and trace heavy metal elements from different sources of water in and around institutional campus of Lumami, Nagaland University, India. *Applied Water Science*, *11*(4), p.76.

Hussain, M., Jamir, L. and Singh, M.R., 2021. Assessment of physico-chemical parameters and trace heavy metal elements from different sources of water in and around institutional campus of Lumami, Nagaland University, India. *Applied Water Science*, *11*(4), p.76.

Ianeva, O.D., 2009. Mechanisms of bacteria resistance to heavy metals. *Mikrobiolohichnyi Zhurnal (Kiev, Ukraine: 1993)*, *71*(6), pp.54-65.

Ibrahim, U.B., Yahaya, S., Yusuf, I. and Kawo, A.H., 2020. Cadmium (Cd) and lead (Pb) uptake potential and surface properties of Aeromonas spp. isolated from soil of local mining site. *Microbiol. Res. J. Int*, *30*(3), pp.36-47.

Igiri, B.E., Okoduwa, S.I., Idoko, G.O., Akabuogu, E.P., Adeyi, A.O. and Ejiogu, I.K., 2018. Toxicity and bioremediation of heavy metals contaminated ecosystem from tannery wastewater: a review. *Journal of toxicology*, *2018*(1), p.2568038.

Iimaa, T., Batmunkh, M., Dulguun, B., Dorjsuren, B., Turmunkh, T., Tserennadmid, E., Surenjav, U., Choidash, B. and Gereltuya, R., 2025. Bacterial heavy metal resistance in contaminated soil. Journal of Microbiology and Biotechnology, 35, p.e2411073.

Imanpour Namin, J. and Hajiaghaei Ghaazi Mahalleh, F., 2024. Microplastic as a vector of heavy metals and chemicals in aquatic ecosystems. *Caspian Journal of Environmental Sciences*, pp.1-13.

India TodayNE (2025) 'Nagaland University develops eco-tech to turn wastewater into clean resources', *India TodayNE*, 19 May. Available at: https://www.indiatodayne.in/nagaland/story/nagaland-university-develops-eco-tech-to-turn-wastewater-into-clean-resources-1215940-2025-05-19 (Accessed: 2 December 2025).

Iqbal, M.Z., Singh, K. and Chandra, R., 2024. Recent advances of plant growth promoting rhizobacteria (PGPR) for eco-restoration of polluted soil. *Cleaner Engineering and Technology*, *23*, p.100845.

Irlinger, F., Loux, V., Bento, P., Gibrat, J.F., Straub, C., Bonnarme, P., Landaud, S. and Monnet, C., 2012. Genome sequence of Staphylococcus equorum subsp. equorum Mu2, isolated from a French smear-ripened cheese.

Jacquet, P., Leonard, A. and Gerber, G.B., 1975. Embryonic death in mouse due to lead exposure. *Experientia*, *31*(11), pp.1312-1313.

Jamir, T.T., Devi, W.B., Singh, U.I. and Singh, R.B., 2011. Lead, iron and manganese contamination in spring, pond and well water in Nagaland, one of the Seven North-Eastern states of India: a future danger.

Janssen, D.B. and Stucki, G., 2020. Perspectives of genetically engineered microbes for groundwater bioremediation. *Environmental Science: Processes & Impacts*, *22*(3), pp.487-499.

Järup, L., 2003. Hazards of heavy metal contamination. *British medical bulletin*, *68*(1), pp.167-182.

Jibrin, A.M., Oyewole, O.A., Yakubu, J.G., Hussaini, A. and Egwim, E.C., 2020. Heavy metals biosorption by urease producing Lysinibacillus fusiformis 5B.

Jin, Y., Luan, Y., Ning, Y. and Wang, L., 2018. Effects and mechanisms of microbial remediation of heavy metals in soil: a critical review. *Applied Sciences*, *8*(8), p.1336.

Jobbágy, E.G. and Jackson, R.B., 2003. Patterns and mechanisms of soil acidification in the conversion of grasslands to forests. *Biogeochemistry*, *64*(2), pp.205-229.

Jomova, K., Alomar, S.Y., Nepovimova, E., Kuca, K. and Valko, M., 2025. Heavy metals: toxicity and human health effects. *Archives of toxicology*, *99*(1), pp.153-209.

Joshi, P.K., Swarup, A., Maheshwari, S., Kumar, R. and Singh, N., 2011. Bioremediation of heavy metals in liquid media through fungi isolated from contaminated sources. *Indian journal of microbiology*, *51*(4), pp.482-487.

Judah, L.A., Andriambololonirina, C., Rakotoarisoa, L., Barrett, L.J.P., Khaliq, M., Mihelcic, J.R. and Cunningham, J.A., 2024. Occurrence and Mitigation of Bacterial Regrowth in Stored Household Water in Eastern Coastal Madagascar. *Water*, *16*(11), p.1592.

Kafle, A., Timilsina, A., Gautam, A., Adhikari, K., Bhattarai, A. and Aryal, N., 2022. Phytoremediation: Mechanisms, plant selection and enhancement by natural and synthetic agents. *Environmental Advances*, *8*, p.100203.

Kama, R., Nabi, F., Aidara, M., Huang, P., Qadir, M., Diatta, S., Ma, C. and Li, H., 2025. Intercropping Pteris cretica and Spinacia oleracea L. with peanut enhances arsenic removal and soil remediation. *Frontiers in Plant Science*, *16*, p.1580332.

Kanamarlapudi, S.L.R.K., Chintalpudi, V.K. and Muddada, S., 2018. Application of biosorption for removal of heavy metals from wastewater. In *Biosorption*. IntechOpen.

Kang, C.H., Kwon, Y.J. and So, J.S., 2016. Bioremediation of heavy metals by using bacterial mixtures. *Ecological engineering*, *89*, pp.64-69.

Kangsopa, J., Singsopa, A. and Thawong, N., 2025. Seed Coating with Bacteria-producing Indole-3-Acetic Acid (IAA) on Germination, Seedling Growth and Nutrient

Contents of Vegetable Soybean [Glycine max (L.) Merrill]. *Legume Research: An International Journal*, *48*(7).

Ka-ot, A.L. and Joshi, S.R., 2022. Application of acid and heavy metal resistant bacteria from rat-hole coal mines in bioremediation strategy. *Journal of basic microbiology*, *62*(3-4), pp.480-488.

Kapahi, M. and Sachdeva, S., 2019. Bioremediation options for heavy metal pollution. *Journal of health & pollution*, *9*(24), p.191203.

Karagas, M.R., Gossai, A., Pierce, B. and Ahsan, H., 2015. Drinking water arsenic contamination, skin lesions, and malignancies: a systematic review of the global evidence. *Current environmental health reports*, *2*(1), pp.52-68.

Karn, R., Ojha, N., Abbas, S. and Bhugra, S., 2021, June. A review on heavy metal contamination at mining sites and remedial techniques. In *IOP Conference Series: Earth and Environmental Science* (Vol. 796, No. 1, p. 012013). IOP Publishing.

Karnwal, A. and Bhardwaj, V., 2014. Bioremediation of heavy metals (Zn and Cr) using microbial biosurfactant. *Ecoterra*, 11(1), pp. 29–33.

Kassem, A., Abbas, L., Coutinho, O., Opara, S., Najaf, H., Kasperek, D., Pokhrel, K., Li, X. and Tiquia-Arashiro, S., 2023. Applications of Fourier Transform-Infrared spectroscopy in microbial cell biology and environmental microbiology: advances, challenges, and future perspectives. *Frontiers in microbiology*, *14*, p.1304081.

Kaur, J., Sharma, V., Dhaliwal, S.S., Behera, S.K., Verma, V. and Singh, P., 2025. Comparative assessment of Brassica cultivars for genotypic variability in phytoremediation of soil exposed to lead (Pb) contamination. *International Journal of Phytoremediation*, *27*(2), pp.156-167.

Kelany, M.S., El-Sawy, M.A., El-Gendy, A.R. and Beltagy, E.A., 2023. Bioremediation of industrial wastewater heavy metals using solo and consortium Enterobacter spp. *Environmental Monitoring and Assessment*, *195*(11), p.1357.

Kenney, J.P. and Fein, J.B., 2011. Importance of extracellular polysaccharides on proton and Cd binding to bacterial biomass: a comparative study. *Chemical Geology*, *286*(3-4), pp.109-117.

Khalifa, A.M., ElBaghdady, K.Z., El Kafrawy, S.B. and El-Zeiny, A.M., 2025. Bioremediation vs. Traditional Methods: A Comparative Review of Heavy Metal Removal Techniques from Aquatic Environment. *Egyptian Journal of Aquatic Biology & Fisheries*, *29*(2).

Khalil, S. and Hassan, N.E., 2024. Review of heavy metal removal from soil: Methods and technologies. *Glob Acad J Agri Biosci*, *6*.

Khan, A., Sharaf, R., Zargham Khan, M., Kashif Saleemi, M. and Mahmood, F., 2013. Arsenic Toxicity in Broiler Chicks and its Alleviation with Ascorbic Acid: A Toxico-patho-biochemical Study. *International Journal of Agriculture & Biology*, *15*(6).

Khan, A.A., Gul, J., Naqvi, S.R., Ali, I., Farooq, W., Liaqat, R., AlMohamadi, H., Štěpanec, L. and Juchelková, D., 2022. Recent progress in microalgae-derived biochar for the treatment of textile industry wastewater. *Chemosphere*, *306*, p.135565.

Khan, I., Aftab, M., Shakir, S., Ali, M., Qayyum, S., Rehman, M.U., Haleem, K.S. and Touseef, I., 2019. Mycoremediation of heavy metal (Cd and Cr)–polluted soil through indigenous metallotolerant fungal isolates. *Environmental monitoring and assessment*, *191*(9), p.585.

Khan, Z., Elahi, A., Bukhari, D.A. and Rehman, A., 2022. Cadmium sources, toxicity, resistance and removal by microorganisms-A potential strategy for cadmium eradication. *Journal of Saudi Chemical Society*, *26*(6), p.101569.

Khanna, K., Jamwal, V.L., Gandhi, S.G., Ohri, P. and Bhardwaj, R., 2019. Metal resistant PGPR lowered Cd uptake and expression of metal transporter genes with improved growth and photosynthetic pigments in Lycopersicon esculentum under metal toxicity. *Scientific reports*, *9*(1), p.5855.

Khoso, M.A., Wagan, S., Alam, I., Hussain, A., Ali, Q., Saha, S., Poudel, T.R., Manghwar, H. and Liu, F., 2024. Impact of plant growth-promoting rhizobacteria (PGPR) on plant nutrition and root characteristics: Current perspective. *Plant Stress*, *11*, p.100341.

Khosravi-Darani, K., Rehman, Y., Katsoyiannis, I.A., Kokkinos, E. and Zouboulis, A.I., 2022. Arsenic exposure via contaminated water and food sources. *Water*, *14*(12), p.1884.

Kiani, B., Hashemi Amin, F., Bagheri, N., Bergquist, R., Mohammadi, A.A., Yousefi, M., Faraji, H., Roshandel, G., Beirami, S., Rahimzadeh, H. and Hoseini, B., 2021. Association between heavy metals and colon cancer: an ecological study based on geographical information systems in North-Eastern Iran. *BMC cancer*, *21*(1), p.414.

Kim, J.H. and Kang, J.C., 2015. The lead accumulation and hematological findings in juvenile rock fish Sebastes schlegelii exposed to the dietary lead (II) concentrations. *Ecotoxicology and environmental safety*, *115*, pp.33-39.

Kim, J.H. and Kang, J.C., 2017. Effects of sub-chronic exposure to lead (Pb) and ascorbic acid in juvenile rockfish: Antioxidant responses, MT gene expression, and neurotransmitters. *Chemosphere*, *171*, pp.520-527.

Kim, J.H., Oh, C.W. and Kang, J.C., 2017. Antioxidant responses, neurotoxicity, and metallothionein gene expression in juvenile Korean rockfish Sebastes schlegelii under dietary lead exposure. *Journal of Aquatic Animal Health*, *29*(2), pp.112-119.

Kırmusaoğlu, S., 2019. Biofilm and Screening Antibiofilm Activity of Agents. *Antimicrobials, antibiotic resistance, antibiofilm strategies and activity methods*, p.99.

Koch, A.L., 1997. Microbial physiology and ecology of slow growth. *Microbiology and molecular biology reviews*, *61*(3), pp.305-318.

Koechler, S., Farasin, J., Cleiss-Arnold, J. and Arsene-Ploetze, F., 2015. Toxic metal resistance in biofilms: diversity of microbial responses and their evolution. *Research in Microbiology*, *166*(10), pp.764-773.

Kotrba P, Mackova M, Fišer J, Macek T (2011) Biosorption and metal removal through living cells. In: Kotrba P, Mackova M, Macek T (ed) Microbial Biosorption of Metals, 1st edn. Springer, Dordrecht, pp.197-233.

Kowalkowski, T., Krakowska, A., Złoch, M., Hrynkiewicz, K. and Buszewski, B., 2019. Cadmium-affected synthesis of exopolysaccharides by rhizosphere bacteria. *Journal of Applied Microbiology*, *127*(3), pp.713-723.

Kramer, J., Özkaya, Ö. and Kümmerli, R., 2020. Bacterial siderophores in community and host interactions. *Nature Reviews Microbiology*, *18*(3), pp.152-163.

Krieg, C., Johnson, E., Peck, E., Kan, J. and Inamdar, S., 2021. After the Storm: Fate and Leaching of Particulate Nitrogen (PN) in the Fluvial Network and the Influence of Watershed Sources and Moisture Conditions. Water, 13(22), p.3182.

Kumar, A., Bisht, B.S., Joshi, V.D. and Dhewa, T., 2011. Review on bioremediation of polluted environment: a management tool. *International journal of environmental sciences*, *1*(6), pp.1079-1093.

Kumar, A., Mukherjee, G., Ahuja, V., Gupta, S., Tarighat, M.A. and Abdi, G., 2024. Biosorption and transformation of cadmium and lead by Staphylococcus epidermidis AS-1 isolated from industrial effluent. *BMC microbiology*, *24*(1), p.420.

Kumar, A., Mukherjee, G., Ahuja, V., Gupta, S., Tarighat, M.A. and Abdi, G., 2024. Biosorption and transformation of cadmium and lead by Staphylococcus epidermidis AS-1 isolated from industrial effluent. BMC microbiology, 24(1), p.420.

Kumar, S., Rahman, M.A., Islam, M.R., Hashem, M.A. and Rahman, M.M., 2022. Lead and other elements-based pollution in soil, crops and water near a lead-acid battery recycling factory in Bangladesh. *Chemosphere*, *290*, p.133288.

Kumar, V., Paul, D. and Kumar, S., 2024. Acid mine drainage from coal mines in the eastern Himalayan sub-region: Hydrogeochemical processes, seasonal variations and insights from hydrogen and oxygen stable isotopes. *Environmental Research*, *252*, p.119086.

Kumar, V., Sharma, A., Kaur, P., Sidhu, G.P.S., Bali, A.S., Bhardwaj, R., Thukral, A.K. and Cerda, A., 2019. Pollution assessment of heavy metals in soils of India and ecological risk assessment: A state-of-the-art. *Chemosphere*, *216*, pp.449-462.

Kumar, V., Sharma, A., Kumar, R., Bhardwaj, R., Kumar Thukral, A. and Rodrigo-Comino, J., 2020. Assessment of heavy-metal pollution in three different Indian water

bodies by combination of multivariate analysis and water pollution indices. *Human and ecological risk assessment: an international journal*, *26*(1), pp.1-16.

Kumari, K., Khare, A. and Dange, S., 2014. The applicability of oxidative stress biomarkers in assessing chromium induced toxicity in the fish Labeo rohita. *BioMed research international*, *2014*(1), p.782493.

Kurniawan, S.B., Ramli, N.N., Said, N.S.M., Alias, J., Imron, M.F., Abdullah, S.R.S., Othman, A.R., Purwanti, I.F. and Hasan, H.A., 2022. Practical limitations of bioaugmentation in treating heavy metal contaminated soil and role of plant growth promoting bacteria in phytoremediation as a promising alternative approach. *Heliyon*, *8*(4).

Lade, H., Park, J.H., Chung, S.H., Kim, I.H., Kim, J.M., Joo, H.S. and Kim, J.S., 2019. Biofilm formation by Staphylococcus aureus clinical isolates is differentially affected by glucose and sodium chloride supplemented culture media. *Journal of clinical medicine*, *8*(11), p.1853.

Laidlaw, M.A., Filippelli, G., Mielke, H., Gulson, B. and Ball, A.S., 2017. Lead exposure at firing ranges—a review. *Environmental Health*, *16*(1), p.34.

Langdon, C.J., Hodson, M.E., Arnold, R.E. and Black, S., 2005. Survival, Pb-uptake and behaviour of three species of earthworm in Pb treated soils determined using an OECD-style toxicity test and a soil avoidance test. *Environmental Pollution*, *138*(2), pp.368-375.

Langdon, C.J., Piearce, T.G., Meharg, A.A. and Semple, K.T., 2001. Survival and behaviour of the earthworms Lumbricus rubellus and Dendrodrilus rubidus from arsenate-contaminated and non-contaminated sites. *Soil biology and biochemistry*, *33*(9), pp.1239-1244.

Laoye, B., Olagbemide, P., Ogunnusi, T. and Akpor, O., 2025. Heavy metal contamination: Sources, health impacts, and sustainable mitigation strategies with insights from nigerian case studies. *F1000Research*, *14*, p.134.

Lata, S., Kaur, H.P. and Mishra, T., 2019. Cadmium bioremediation: a review. *Int. J. Pharm. Sci. Res*, *10*(9), pp.4120-4128.

Lavanya, M.B., Viswanath, D.S. and Sivapullaiah, P.V., 2024. Phytoremediation: An eco-friendly approach for remediation of heavy metal-contaminated soils-A comprehensive review. *Environmental Nanotechnology, Monitoring & Management*, *22*, p.100975.

Ledrich, M.L., Stemmler, S., Laval-Gilly, P., Foucaud, L. and Falla, J., 2005. Precipitation of silver-thiosulfate complex and immobilization of silver by Cupriavidus metallidurans CH34. *Biometals*, *18*(6), pp.643-650.

Lee, B.T. and Kim, K.W., 2008. Arsenic accumulation and toxicity in the earthworm Eisenia fetida affected by chloride and phosphate. *Environmental Toxicology and Chemistry*, *27*(12), pp.2488-2495.

Leeprasert, L., Chonudomkul, D. and Boonmak, C., 2022. Biocalcifying potential of ureolytic bacteria isolated from soil for biocementation and material crack repair. *Microorganisms*, *10*(5), p.963.

Lelapalli, S., Baskar, S., Jacob, S.M. and Paranthaman, S., 2021. Characterization of phosphate solubilizing plant growth promoting rhizobacterium Lysinibacillus pakistanensis strain PCPSMR15 isolated from Oryza sativa. *Current Research in Microbial Sciences*, *2*, p.100080.

Leong, Y.K. and Chang, J.S., 2020. Bioremediation of heavy metals using microalgae: Recent advances and mechanisms. *Bioresource technology*, *303*, p.122886.

Levit, S.M., 2010. A literature review of effects of ammonia on fish. *Center for Science in Public Participation, Bozeman, Montana*.

Li, B., Yu, T., Ji, W., Liu, X., Lin, K., Li, C., Ma, X. and Yang, Z., 2023. Geochemical response of surface environment to mining of Sn-Pb-Zn sulfide deposits: a case study of Dachang tin polymetallic deposit in Guangxi. Water, 15(8), p.1550.

Li, L., Zhang, B., Jiang, B., Zhao, Y., Qian, G. and Hu, X., 2022. Potentially toxic elements in weathered waste-rocks of Fushun western opencast mine: distribution, source identification, and contamination assessment. *Environmental Geochemistry and Health*, *44*(6), pp.1813-1826.

Li, W., Fishman, A. and Achal, V., 2021. Ureolytic bacteria from electronic waste area, their biological robustness against potentially toxic elements and underlying mechanisms. *Journal of Environmental Management*, *289*, p.112517.

Li, W., Fishman, A. and Achal, V., 2022. Whole cell evaluation and the enzymatic kinetic study of urease from ureolytic bacteria affected by potentially toxic elements. *Microbiological Research*, *265*, p.127208.

Li, X., Shi, F. and Vogeler, I., 2021. Salt precipitation and evaporative flux on sandy soil with saline groundwater under different evaporation demand conditions. *Soil Research*, *60*(2), pp.187-196.

Li, Y., Xin, M., Xie, D., Fan, S., Ma, J., Liu, K. and Yu, F., 2021. Variation in extracellular polymeric substances from Enterobacter sp. and their Pb2+ adsorption behaviors. *ACS omega*, *6*(14), pp.9617-9628.

Lima e Silva, A.A.D., Carvalho, M.A., de Souza, S.A., Dias, P.M.T., Silva Filho, R.G.D., Saramago, C.S., Bento, C.A. and Hofer, E., 2012. Heavy metal tolerance (Cr, Ag and Hg) in bacteria isolated from sewage. *Brazilian Journal of Microbiology*, *43*, pp.1620-1631.

Liu, C., Liu, C., Juhasz, A.L., Dong, W.J. and Ma, L.Q., 2025. Human health risks of chromium in bright-colored leather products: Speciation-based insights into dermal permeation. *Environment International*, p.109538.

Lock, J.W., Thompson, D.R., Furness, R.W. and Bartle, J.A., 1992. Metal concentrations in seabirds of the New Zealand region. *Environmental pollution*, *75*(3), pp.289-300.

Louden, B.C., Haarmann, D. and Lynne, A.M., 2011. Use of blue agar CAS assay for siderophore detection. *Journal of microbiology & biology education*, *12*(1), pp.51-53.

Lu, W.B., Shi, J.J., Wang, C.H. and Chang, J.S., 2006. Biosorption of lead, copper and cadmium by an indigenous isolate Enterobacter sp. J1 possessing high heavy-metal resistance. *Journal of hazardous materials*, *134*(1-3), pp.80-86.

Lucia, M., Andre, J.M., Gonzalez, P., Baudrimont, M., Gontier, K., Maury-Brachet, R. and Davail, S., 2009. Impact of cadmium on aquatic bird Cairina moschata. *Biometals*, *22*(5), pp.843-853.

Ludolphy, C., Kierdorf, U. and Kierdorf, H., 2022. Antlers of European roe deer (Capreolus capreolus) as monitoring units to assess lead pollution in a floodplain contaminated by historical metal ore mining, processing, and smelting in the Harz Mountains, Germany. *Environmental Pollution*, *302*, p.119080.

Ludwig, T.G. and Goldberg, H.J., 1956. The anthrone method for the determination of carbohydrates in foods and in oral rinsing. *Journal of dental research*, *35*(1), pp.90-94.

Lugtenberg, B. and Kamilova, F., 2009. Plant-growth-promoting rhizobacteria. *Annual review of microbiology*, *63*(1), pp.541-556.

Łukaszek-Chmielewska, A., Rakowska, J., Rachwał, M. and Stawarz, O., 2025. Assessment of forest soil contamination by heavy metals in the Polish National Park near Warsaw. *Scientific Reports*, *15*(1), p.4099.

Luo, Y., Liang, J., Zeng, G., Li, X., Chen, M., Jiang, L., Xing, W., Tang, N., Fang, Y. and Chen, X., 2019. Evaluation of tetracycline phytotoxicity by seed germination stage and radicle elongation stage tests: a comparison of two typical methods for analysis. *Environmental Pollution*, *251*, pp.257-263.

Ma, B., Song, W., Zhang, X., Chen, M., Li, J., Yang, X. and Zhang, L., 2023. Potential application of novel cadmium-tolerant bacteria in bioremediation of Cd-contaminated soil. *Ecotoxicology and Environmental Safety*, *255*, p.114766.

Mabaso, M.K., Chirwa, E.M. and Tichapondwa, S.M., 2025. Effectiveness of Bio-Phytoremediation on Heavy Metal Contaminated Wastewater using Vetiver Grass. *Chemical Engineering Transactions*, *118*, pp.337-342.

Mahmoud, M.E., Fekry, N.A. and Mohamed, S.M., 2022. Effective removal of Pb (II)/4-nitroaniline/E. faecalis and E. coli pollutants from water by a novel unique graphene quantum dots@ gemifloxacin@ double-layered Fe/Al nanocomposite. *Journal of Water Process Engineering*, *46*, p.102562.

Maiti, A.K., Saha, N.C. and Paul, G., 2010. Effect of lead on oxidative stress, Na+ K+ ATPase activity and mitochondrial electron transport chain activity of the brain of Clarias batrachus L. *Bulletin of Environmental Contamination and Toxicology*, *84*(6), pp.672-676.

Maity, J.P., Kar, S., Lin, C.M., Chen, C.Y., Chang, Y.F., Jean, J.S. and Kulp, T.R., 2013. Identification and discrimination of bacteria using Fourier transform infrared spectroscopy. *Spectrochimica Acta Part A: Molecular and Biomolecular Spectroscopy*, *116*, pp.478-484.

Maity, S., Sarkar, D., Poddar, K., Patil, P. and Sarkar, A., 2023. Biofilm-mediated heavy metal removal from aqueous system by multi-metal-resistant bacterial strain Bacillus sp. GH-s29. *Applied Biochemistry and Biotechnology*, *195*(8), pp.4832-4850.

Makarem, M., Lee, C.M., Kafle, K., Huang, S., Chae, I., Yang, H., Kubicki, J.D. and Kim, S.H., 2019. Probing cellulose structures with vibrational spectroscopy. *Cellulose*, *26*(1), pp.35-79.

Malgwi, O.D., Odunze, A.C., Otene, I.J.J., Oluwagbemi, C.O. and Muhammed, B., 2019. Carbon, nitrogen, and phosphorus stocks from fallow of forage legumes on alfisols of Guinea Savanna Nigeria. World Journal of Agricultural Research, 7(4), pp.119-123.

Mandal D, Das SKr, Adhikari J, et al (2024) Genome sequencing, annotation and application of a strain of Microbacterium paraoxydans – a heavy metal hypertolerant and plant growth promoting bacterium. Research Square (Research Square). https://doi.org/10.21203/rs.3.rs-3857604/v1

Mandal, A., Purakayastha, T.J., Ramana, S., Neenu, S., Bhaduri, D., Chakraborty, K., Manna, M.C. and Rao, A.S., 2014. Status on phytoremediation of heavy metals in India-a review. *International Journal of Bio-resource and Stress Management*, *5*(4), pp.553-560.

Mandal, D., Sonar, R., Saha, I., Ahmed, S. and Basu, A., 2022. Isolation and identification of arsenic resistant bacteria: a tool for bioremediation of arsenic

toxicity. *International Journal of Environmental Science and Technology*, *19*(10), pp.9883-9900.

Mangwani, N., Kumari, S. and Das, S., 2016. Bacterial biofilms and quorum sensing: fidelity in bioremediation technology. *Biotechnology and Genetic Engineering Reviews*, *32*(1-2), pp.43-73.

Mansoor, S., Ali, A., Kour, N., Bornhorst, J., AlHarbi, K., Rinklebe, J., Abd El Moneim, D., Ahmad, P. and Chung, Y.S., 2023. Heavy metal induced oxidative stress mitigation and ROS scavenging in plants. *Plants*, *12*(16), p.3003.

Martinez-Cruz, A. and Rojas-Valencia, M.N., 2024. Assessment of phytotoxicity in untreated and electrochemically treated leachates through the analysis of early seed growth and inductively coupled plasma-optical emission spectroscopy characterization. *Horticulturae*, *10*(1), p.67.

Masindi, V. and Muedi, K.L., 2018. Environmental contamination by heavy metals. *Heavy metals*, *10*(4), pp.115-133.

Masri, S., LeBrón, A.M., Logue, M.D., Flores, P., Ruiz, A., Reyes, A., Rubio, J.M. and Wu, J., 2022. Use of radioisotope ratios of lead for the identification of historical sources of soil lead contamination in Santa Ana, California. *Toxics*, *10*(6), p.304.

Mathivanan, K., Chandirika, J.U., Mathimani, T., Rajaram, R., Annadurai, G. and Yin, H., 2021a. Production and functionality of exopolysaccharides in bacteria exposed to a toxic metal environment. *Ecotoxicology and Environmental Safety*, *208*, p.111567.

Mathivanan, K., Chandirika, J.U., Vinothkanna, A., Yin, H., Liu, X. and Meng, D., 2021b. Bacterial adaptive strategies to cope with metal toxicity in the contaminated environment–A review. *Ecotoxicology and Environmental Safety*, *226*, p.112863.

Mathur, J. and Chauhan, P., 2018. Hazardous Effects of Lead (Pb) in the Environment. *Sectional Reviewer Editors*, p.45.

McClain, R.M. and Siekierka, J.J., 1975. The effects of various chelating agents on the teratogenicity of lead nitrate in rats. *Toxicology and Applied Pharmacology*, *31*(3), pp.434-442.

Men, Y., Li, L., Zhang, F., Kong, X., Zhang, W., Hao, C. and Wang, G., 2020. Evaluation of heavy metals and metabolites in the urine of patients with breast cancer. *Oncology Letters*, *19*(2), pp.1331-1337.

Mendes, W.D.C., Alves, J., Cunha, P.C.D., Silva, A.R.D., Evangelista, A.W. and Casaroli, D., 2016. Potassium leaching in different soils as a function of irrigation depths. Revista Brasileira de Engenharia Agrícola e Ambiental, 20(11), pp.972-977.

Meng, P., Zhang, T., Su, Y., Peng, D., Zhou, Q., Zeng, H., Yu, H., Lun, L., Zhang, N., Zhang, L. and Zheng, L., 2024. Cellulose-based materials in the treatment of wastewater containing heavy metal pollution: Recent advances in quantitative adsorption mechanisms. *Industrial Crops and Products*, *217*, p.118825.

Minari, G.D., Saran, L.M., Constancio, M.T.L., da Silva, R.C., Rosalen, D.L., de Melo, W.J. and Alves, L.M.C., 2020. Bioremediation potential of new cadmium, chromium, and nickel-resistant bacteria isolated from tropical agricultural soil. *Ecotoxicology and Environmental Safety*, *204*, p.111038.

Mishra, P., Ali, S., Kumar, R. and Shekhar, S., 2025. Global Lead Contamination in Soils, Sediments, and Aqueous Environments: Exposure, Toxicity, and Remediation. *Journal of Trace Elements and Minerals*, p.100259.

Mishra, S., Huang, Y., Li, J., Wu, X., Zhou, Z., Lei, Q., Bhatt, P. and Chen, S., 2022. Biofilm-mediated bioremediation is a powerful tool for the removal of environmental pollutants. *Chemosphere*, *294*, p.133609.

Mohanpuria, P., Rana, N.K. and Yadav, S.K., 2007. Cadmium induced oxidative stress influence on glutathione metabolic genes of Camellia sinensis (L.) O. Kuntze. *Environmental Toxicology: An International Journal*, *22*(4), pp.368-374.

Mohd Bahari, Z., Ali Hamood Altowayti, W., Ibrahim, Z., Jaafar, J. and Shahir, S., 2013. Biosorption of As (III) by non-living biomass of an arsenic-hypertolerant Bacillus cereus strain SZ2 isolated from a gold mining environment: equilibrium and kinetic study. *Applied biochemistry and biotechnology*, *171*(8), pp.2247-2261.

Morcillo, R.J. and Manzanera, M., 2021. The effects of plant-associated bacterial exopolysaccharides on plant abiotic stress tolerance. *Metabolites*, *11*(6), p.337.

Morgante, V., Mirete, S., de Figueras, C.G., Postigo Cacho, M. and González- Pastor, J.E., 2015. Exploring the diversity of arsenic resistance genes from acid mine drainage microorganisms. Environmental Microbiology, 17(6), pp.1910-1925.

Morung Express (2016) 'Regional coal exploration at Changki Block – A', *MorungExpress*, 15 March. Available at: https://morungexpress.com/regional-coal-exploration-changki-block?utm_source=chatgpt.com (Accessed: 24 November 2025).

Morung Express News (2024) *All water polluting industries in Nagaland have treatment plant: NPCB*, *Morung Express*, 14 February.

Mosa, K.A., Saadoun, I., Kumar, K., Helmy, M. and Dhankher, O.P., 2016. Potential biotechnological strategies for the cleanup of heavy metals and metalloids. *Frontiers in plant science*, *7*, p.303.

Motavalli, P.P., Palm, C.A., Parton, W.J., Elliott, E.T. and Frey, S.D., 1995. Soil pH and organic C dynamics in tropical forest soils: evidence from laboratory and simulation studies. *Soil biology and biochemistry*, *27*(12), pp.1589-1599.

Motta, S.S., Cluzel, P. and Aldana, M., 2015. Adaptive resistance in bacteria requires epigenetic inheritance, genetic noise, and cost of efflux pumps. PloS one, 10(3), p.e0118464.

Mounaouer, B., Nesrine, A. and Abdennaceur, H., 2014. Identification and characterization of heavy metal-resistant bacteria selected from different polluted sources. *Desalination and Water Treatment*, *52*(37-39), pp.7037-7052.

Moustakas, M., 2021. The role of metal ions in biology, biochemistry and medicine. *Materials*, *14*(3), p.549.

Mrozek Jr, E. and Funicelli, N.A., 1982. Effect of zinc and lead on germination of Spartina alterniflora Loisel seeds at various salinities. *Environmental and Experimental Botany*, *22*(1), pp.23-32.

Muangphra, P. and Gooneratne, R., 2011. Comparative genotoxicity of cadmium and lead in earthworm coelomocytes. *Applied and Environmental Soil Science*, *2011*(1), p.218929.

Muhammad, S.M. and Jega, B.G., 2024. A Review on Environmental Impacts and Risks of Beneficial Microorganisms. *Innovative Research in Applied, Biological and Chemical Sciences*, *2*(1), pp.13-20.

Muller, D., Médigue, C., Koechler, S., Barbe, V., Barakat, M., Talla, E., Bonnefoy, V., Krin, E., Arsène-Ploetze, F., Carapito, C. and Chandler, M., 2007. A tale of two oxidation states: bacterial colonization of arsenic-rich environments. *PLoS genetics*, *3*(4), p.e53.

Mushtaq, Z., Liaquat, M., Nazir, A., Liaquat, R., Iftikhar, H., Anwar, W. and Itrat, N., 2022. Potential of plant growth promoting rhizobacteria to mitigate chromium contamination. *Environmental Technology & Innovation*, *28*, p.102826.

Nagajyoti, P.C., Lee, K.D. and Sreekanth, T.V.M., 2010. Heavy metals, occurrence and toxicity for plants: a review. *Environmental chemistry letters*, *8*(3), pp.199-216.

Naik, M.M. and Dubey, S.K., 2011. Lead-enhanced siderophore production and alteration in cell morphology in a Pb-resistant Pseudomonas aeruginosa strain 4EA. *Current microbiology*, *62*(2), pp.409-414.

Nain, S. and Smits, J.E., 2012. Pathological, immunological and biochemical markers of subchronic arsenic toxicity in rats. *Environmental toxicology*, *27*(4), pp.244-254.

Nakos, G., 1979. Fate of lead in the soil and its effects on Pinus halepensis. *Plant and soil*, *53*(4), pp.427-443.

Nam, I.H., Murugesan, K., Ryu, J. and Kim, J.H., 2019. Arsenic (As) removal using Talaromyces sp. KM-31 isolated from as-contaminated mine soil. *Minerals*, *9*(10), p.568.

Naureen, Z., Rehman, N.U., Hussain, H., Hussain, J., Gilani, S.A., Al Housni, S.K., Mabood, F., Khan, A.L., Farooq, S., Abbas, G. and Harrasi, A.A., 2017. Exploring the potentials of Lysinibacillus sphaericus ZA9 for plant growth promotion and biocontrol activities against phytopathogenic fungi. *Frontiers in microbiology*, *8*, p.1477.

Nazir, R., Ganai, B.A., Rahi, P., Rehman, S., Farooq, S., Dar, R., Parray, J.A., Al, A.B.F.A.A., Tabassum, B. and Abd_Allah, E.F., 2020. MALDI-TOF-MS and 16S rRNA characterization of lead tolerant metallophile bacteria isolated from saffron soils

of Kashmir for their sequestration potential. *Saudi Journal of Biological Sciences*, *27*(8), pp.2047-2053.

NCBI (2012) *Lysinibacillus* sp. L1 16S ribosomal RNA gene, partial sequence. GenBank accession JX402789.1. Available at: https://www.ncbi.nlm.nih.gov/nuccore/JX402789.1/ (Accessed: 11 January 2026).

NCBI (2019) *Lysinibacillus sp. strain R2-3-2 16S ribosomal RNA gene, partial sequence*. GenBank accession no. **MN696519.1**. Available at: https://www.ncbi.nlm.nih.gov/nuccore/MN696519.1/ (Accessed: 11 January 2026).

Nedjimi, B., 2021. Phytoremediation: a sustainable environmental technology for heavy metals decontamination. *SN Applied Sciences*, *3*(3), p.286.

Needleman, H., 2004. Lead Poisoning. *Annual Review of Medicine*, *55*(1), pp.209-222.

Neidhardt, F.C., Ingraham, J.L. and Schaechter, M., 1990. *Physiology of the bacterial cell: a molecular approach* (Vol. 20). Sunderland, MA: Sinauer associates.

Nies, D.H., 1999. Microbial heavy-metal resistance. *Applied microbiology and biotechnology*, *51*(6), pp.730-750.

Nikaido, H., 2001, June. Preventing drug access to targets: cell surface permeability barriers and active efflux in bacteria. In *Seminars in cell & developmental biology* (Vol. 12, No. 3, pp. 215-223). Academic Press.

Niu, Z., Guo, P., Wang, Z., Wang, H. and Li, X., 2025. Study on the Potential of Malic Acid and Tartaric Acid Assisted in Improving the Phytoextraction of Cadmium and Lead by Sunflower (Helianthus Annuus L.). *Soil and Sediment Contamination: An International Journal*, pp.1-18.

Nnaji, N.D., Anyanwu, C.U., Miri, T. and Onyeaka, H., 2024. Mechanisms of heavy metal tolerance in bacteria: A review. *Sustainability*, *16*(24), p.11124.

Nnaji, N.D., Onyeaka, H., Miri, T. and Ugwa, C., 2023. Bioaccumulation for heavy metal removal: a review. *SN Applied Sciences*, *5*(5), p.125.

Nocelli N, Bogino PC, Banchio E, Giordano W (2016) Roles of extracellular polysaccharides and biofilm formation in heavy metal resistance of rhizobia. Materials 9(6):418. https://doi.org/10.3390/ma9060418

Nover L (2022) Inducers of HSP synthesis: heat shock and chemical stressors. In: Nover L (ed) Heat shock response, 1st edn. CRC Press, Boca Raton, pp. 5-40

Nwosu, I.G., Abu, G.O. and Agwa, K.O., 2019. Isolation, screening and characterization of exopolysaccharide producing bacteria. *Microbiol. Res. J. Int*, *29*, pp.1-9.

Obayori, O.S, Ilori, M.O., Adebusoye, S.A, Oyetibo, G.O, Amund, O., 2009. Degradation of hydrocarbons and biosurfactant production by Pseudomonas sp. strain LP1, World Journal of Microbiology and Biotechnology, 25 (9), pp. 1615-1623.

Ohiagu, F.O., Chikezie, P.C., Ahaneku, C.C. and Chikezie, C.M., 2022. Human exposure to heavy metals: toxicity mechanisms and health implications. *Material Science & Engineering International Journal*, *6*(2), pp.78-87.

Ojuederie, O.B. and Babalola, O.O., 2017. Microbial and plant-assisted bioremediation of heavy metal polluted environments: a review. *International journal of environmental research and public health*, *14*(12), p.1504.

Okorondu, J., Umar, N.A., Ulor, C.O., Onwuagba, C.G., Diagi, B.E., Ajiere, S.I. and Nwaogu, C., 2022. Anthropogenic Activities as Primary Drivers of Environmental Pollution and Loss of Biodiversity A Review. *Int. J. Trend Sci. Res. Dev*, *6*, pp.621-643.

Okpara-Elom, I.A., Onochie, C.C., Elom, M.O., Ezaka, E. and Elom, O., 2024. Bioremediation of heavy metal polluted soil using plant growth promoting bacteria: an assessment of response. *Bioremediation Journal*, *28*(1), pp.34-53.

Oladimeji, T.E., Oyedemi, M., Emetere, M.E., Agboola, O., Adeoye, J.B. and Odunlami, O.A., 2024. Review on the impact of heavy metals from industrial wastewater effluent and removal technologies. *Heliyon*, *10*(23).

Oladimeji, T.E., Oyedemi, M.O., Odunfa, M.K., Agboola, O., Adeoye, J.B., Oke, M.A. and Akindele, O.O., 2025. From origin to oversight: properties, impacts and management of heavy metals. *Discover Applied Sciences*, *7*(11), p.1353.

Olszewska-Słonina, D.M., Mątewski, D., Czajkowski, R., Olszewski, K.J., WoŸniak, A., Odrowąż-Sypniewska, G., Lis, K., Musiałkiewicz, D. and Kowaliszyn, B., 2011. The concentration of thiobarbituric acid reactive substances (TBARS) and paraoxonase activity in blood of patients with osteoarthrosis after endoprosthesis implantation. *Medical science monitor: international medical journal of experimental and clinical research*, *17*(9), p.CR498.

Omoregie, A.I., Kan, F.K., Basri, H.F., Silini, M.O.E. and Rajasekar, A., 2025. Enhanced MICP for soil improvement and heavy metal remediation: insights from landfill leachate-derived ureolytic bacterial consortium. *Microorganisms*, *13*(1), p.174.

Omoregie, A.I., Ouahbi, T., Kan, F.K., Sirat, Q.A., Raheem, H.O. and Rajasekar, A., 2025. Advancing Slope Stability and Hydrological Solutions Through Biocementation: A Bibliometric Review. *Hydrology*, *12*(1), p.14.

Ondov, B.D., Treangen, T.J., Melsted, P., Mallonee, A.B., Bergman, N.H., Koren, S. and Phillippy, A.M., 2016. Mash: fast genome and metagenome distance estimation using MinHash. *Genome biology*, *17*(1), p.132.

Ondrasek, G., Shepherd, J., Rathod, S., Dharavath, R., Rashid, M.I., Brtnicky, M., Shahid, M.S., Horvatinec, J. and Rengel, Z., 2025. Metal contamination–a global environmental issue: sources, implications & advances in mitigation. *RSC advances*, *15*(5), pp.3904-3927.

Pal, A.K. and Sengupta, C., 2019. Isolation of cadmium and lead tolerant plant growth promoting rhizobacteria: Lysinibacillus varians and Pseudomonas putida from Indian Agricultural Soil. *Soil and Sediment Contamination: An International Journal*, *28*(7), pp.601-629.

Pan, X.R., Chen, L., Zhang, L.P. and Zuo, J.E., 2023. Characteristics of antibiotic resistance gene distribution in rainfall runoff and combined sewer

overflow. *Environmental Science and Pollution Research*, *30*(11), pp.30766-30778. https://doi.org/10.1007/s11356-022-24257-1

Pande, V., Pandey, S.C., Sati, D., Bhatt, P. and Samant, M., 2022. Microbial interventions in bioremediation of heavy metal contaminants in agroecosystem. *Frontiers in microbiology*, *13*, p.824084.

Pande, V., Pandey, S.C., Sati, D., Bhatt, P. and Samant, M., 2022. Microbial interventions in bioremediation of heavy metal contaminants in agroecosystem. *Frontiers in microbiology*, *13*, p.824084.

Pandey, N. and Bhatt, R., 2015. Arsenic resistance and accumulation by two bacteria isolated from a natural arsenic contaminated site. *Journal of basic microbiology*, *55*(11), pp.1275-1286.

Pandey, N. and Keshavkant, S., 2019. Characterization of arsenic resistant plant-growth promoting indigenous soil bacteria isolated from Center-East regions of India. *Journal of Basic Microbiology*, *59*(8), pp.807-819.

Parikh, S.J. and Chorover, J., 2006. ATR-FTIR spectroscopy reveals bond formation during bacterial adhesion to iron oxide. *Langmuir*, *22*(20), pp.8492-8500.

Parsoya, S. and Perwej, A., 2022. Current needs of making changes in transportation and energy policies to mitigate the bad and harmful impacts of environmental pollution an Indian perspective. *An Indian Perspective*, *10*.

Parvej, M.R., Brandt, D., Myers, R., Nelson, K., Singh, G. & Reinbott, T. (2025) Soil organic matter and soil health. University of Missouri Extension. Available at: https://extension.missouri.edu/publications/g9071 (Accessed: 20 September 2025).

Patil, A., Chakraborty, S., Yadav, Y., Sharma, B., Singh, S. and Arya, M., 2025. Bioremediation strategies and mechanisms of bacteria for resistance against heavy metals: a review. *Bioremediation Journal*, *29*(4), pp.448-480.

Patra, S. and Ghosh, P.K., 2025. Assessing severity in groundwater contamination by arsenic, iron and manganese and deciphering its heterogeneity in a sub-tropical monsoon region. *Environmental Pollution*, p.126325.

Pavez, V.B., Pacheco, N., Castro-Severyn, J., Pardo-Esté, C., Álvarez, J., Zepeda, P., Krüger, G., Gallardo, K., Melo, F., Vernal, R. and Aranda, C., 2023. Characterization of biofilm formation by Exiguobacterium strains in response to arsenic exposure. *Microbiology spectrum*, *11*(6), pp.e02657-23.

Pavithra, K.G., SundarRajan, P., Kumar, P.S. and Rangasamy, G., 2023. Mercury sources, contaminations, mercury cycle, detection and treatment techniques: A review. *Chemosphere*, *312*, p.137314.

Payne, S.M., 1993. Iron acquisition in microbial pathogenesis. *Trends in microbiology*, *1*(2), pp.66-69.

Pena-Castro, J.M., Martınez-Jerónimo, F., Esparza-Garcıa, F. and Canizares-Villanueva, R.O., 2004. Heavy metals removal by the microalga Scenedesmus incrassatulus in continuous cultures. *Bioresource technology*, *94*(2), pp.219-222.

Peters, K., Staehlke, S., Rebl, H., Jonitz-Heincke, A. and Hahn, O., 2024. Impact of metal ions on cellular functions: a focus on mesenchymal stem/stromal cell differentiation. *International journal of molecular sciences*, *25*(18), p.10127.

Pham, V.H.T., Kim, J., Chang, S. and Chung, W., 2022. Bacterial biosorbents, an efficient heavy metals green clean-up strategy: prospects, challenges, and opportunities. *Microorganisms*, *10*(3), p.610.

Piotrowska-Seget, Z., Cycoń, M. and Kozdroj, J., 2005. Metal-tolerant bacteria occurring in heavily polluted soil and mine spoil. *Applied Soil Ecology*, *28*(3), pp.237-246.

Poddar, N., Badilla, C., Maghool, S., Osborne, T.H., Santini, J.M. and Maher, M.J., 2021. Structural and functional investigation of the periplasmic Arsenate-binding protein ArrX from Chrysiogenes arsenatis. *Biochemistry*, *60*(6), pp.465-476.

Poli, A., Di Donato, P., Abbamondi, G.R. and Nicolaus, B., 2011. Synthesis, production, and biotechnological applications of exopolysaccharides and polyhydroxyalkanoates by archaea. *Archaea*, *2011*(1), p.693253.

Pooljun, C., Daorueang, S., Weerachatyanukul, W., Direkbusarakom, S. and Jariyapong, P., 2020. Enhancement of shrimp health and immunity with diets supplemented with combined probiotics: application to Vibrio parahaemolyticus infections. *Diseases of Aquatic Organisms*, *140*, pp.37-46.

Prabhu, S.G., Srinikethan, G. and Hegde, S., 2019. Spontaneous Cr (VI) and Cd (II) biosorption potential of native pinnae tissue of Pteris vittata L., a tropical invasive pteridophyte. *International journal of phytoremediation*, *21*(4), pp.380-390.

Pradel, P., Hernández, C., Tello, M., Villarroel, M.P., Corsini, G. and González, A., 2013. Staphylococcus equorum isolated from seabed as potential biotool to Cr (VI) remediation. Advanced Materials Research, 825, pp.524-527.

Prasad, K.S., Srivastava, P., Subramanian, V. and Paul, J., 2011. Biosorption of As (III) ion on Rhodococcus sp. WB-12: biomass characterization and kinetic studies. *Separation Science and Technology*, *46*(16), pp.2517-2525.

Prasath, B.B., 2025. Heavy Metal Pollution in Groundwater: Environmental and Health Concerns in Gujarat, India. In *Groundwater Resource Management Planning Strategies: A Geospatial Approach: Volume 1* (pp. 155-172). Cham: Springer Nature Switzerland.

Press, F. and Siever, R. (1994) *Fundamentals of Geology*. New York: W.H. Freeman and Company.

Prinzi, A. and Rohde, R., 2023. The role of bacterial biofilms in antimicrobial resistance. *American Society for Microbiology*.

Priti, P. and Paul, B., 2016. Assessment of heavy metal pollution in water resources and their impacts: A review. *Journal of Basic and Applied Engineering Research*, *3*(8), pp.671-675.

Priyadarshanee, M. and Das, S., 2021. Bioremediation potential of biofilm forming multi-metal resistant marine bacterium Pseudomonas chengduensis PPSS-4 isolated from contaminated site of Paradip Port, Odisha. *Journal of Earth System Science*, *130*(3), p.125.

Qi, M., Wu, Y., Zhang, S., Li, G. and An, T., 2023. Pollution profiles, source identification and health risk assessment of heavy metals in soil near a non-ferrous metal smelting plant. International Journal of Environmental Research and Public Health, 20(2), p.1004.

Qin, H., Wang, Z., Sha, W., Song, S., Qin, F. and Zhang, W., 2024. Role of plant-growth-promoting rhizobacteria in plant machinery for soil heavy metal detoxification. *Microorganisms*, *12*(4), p.700.

Quilès, F., Humbert, F. and Delille, A., 2010. Analysis of changes in attenuated total reflection FTIR fingerprints of Pseudomonas fluorescens from planktonic state to nascent biofilm state. *Spectrochimica Acta Part A: Molecular and Biomolecular Spectroscopy*, *75*(2), pp.610-616.

Radzki, W., Gutierrez Mañero, F.J., Algar, E., Lucas García, J.A., García-Villaraco, A. and Ramos Solano, B., 2013. Bacterial siderophores efficiently provide iron to iron-starved tomato plants in hydroponics culture. *Antonie Van Leeuwenhoek*, *104*(3), pp.321-330.

Rafique, M., Naveed, M., Mumtaz, M.Z., Niaz, A., Alamri, S., Siddiqui, M.H., Waheed, M.Q., Ali, Z., Naman, A., Rehman, S.U. and Brtnicky, M., 2024. Unlocking the potential of biofilm-forming plant growth-promoting rhizobacteria for growth and yield enhancement in wheat (Triticum aestivum L.). *Scientific Reports*, *14*(1), p.15546.

Rahman, A., Nahar, N., Nawani, N.N., Jass, J., Desale, P., Kapadnis, B.P., Hossain, K., Saha, A.K., Ghosh, S., Olsson, B. and Mandal, A., 2014. Isolation and characterization of a Lysinibacillus strain B1-CDA showing potential for bioremediation of arsenics from contaminated water. *Journal of Environmental Science and Health, Part A*, *49*(12), pp.1349-1360.

Rahman, I., Kode, A. and Biswas, S.K., 2006. Assay for quantitative determination of glutathione and glutathione disulfide levels using enzymatic recycling method. *Nature protocols*, *1*(6), pp.3159-3165.

Rahman, Z., Thomas, L. and Singh, V.P., 2019. Biosorption of heavy metals by a lead (Pb) resistant bacterium, Staphylococcus hominis strain AMB-2. Journal of Basic Microbiology, 59(5), pp.477-486.

Rajendran, S., Priya, T.A.K., Khoo, K.S., Hoang, T.K., Ng, H.S., Munawaroh, H.S.H., Karaman, C., Orooji, Y. and Show, P.L., 2022. A critical review on various remediation approaches for heavy metal contaminants removal from contaminated soils. *Chemosphere*, *287*, p.132369.

Rajkumar, M., Ae, N., Prasad, M.N.V. and Freitas, H., 2010. Potential of siderophore-producing bacteria for improving heavy metal phytoextraction. *Trends in biotechnology*, *28*(3), pp.142-149.

Rajkumar, M., Lee, K.J., Lee, W.H. and Banu, J.R., 2005. Growth of Brassica juncea under chromium stress: influence of siderophores and indole 3 acetic acid producing rhizosphere bacteria. *Journal of Environmental Biology*, *26*(4), pp.693-699.

Rajkumar, V., Lee, V.R. and Gupta, V. (2023) *Heavy metal toxicity*. In: StatPearls [Internet]. Treasure Island (FL): StatPearls Publishing; 2025–. Available at: https://www.ncbi.nlm.nih.gov/books/NBK560920/ (Accessed: 1 December 2025).

Raju, N.J., 2022. Arsenic in the geo-environment: A review of sources, geochemical processes, toxicity and removal technologies. *Environmental research*, *203*, p.111782.

Ramteke, P.W., 1997. Plasmid Mediated Co-transfer of Antibiotic Resistance and Heavy Metal Tolerance in Coliforms. *Indian Journal of Microbiology*, *37*, pp.177-181.

Rani, A., Souche, Y.S. and Goel, R., 2009. Comparative assessment of in situ bioremediation potential of cadmium resistant acidophilic Pseudomonas putida 62BN and alkalophilic Pseudomonas monteilli 97AN strains on soybean. *International Biodeterioration & Biodegradation*, *63*(1), pp.62-66.

Rani, R., Sharma, P., Kumar, R. and Hajam, Y.A., 2022. Effects of heavy metals and pesticides on fish. In *Bacterial fish diseases* (pp. 59-86). Academic Press.

Raud, M., Lember, E., Jõgi, E. and Kikas, T., 2013. Nitrosomonas sp. based biosensor for ammonium nitrogen measurement in wastewater. *Biotechnology and bioprocess engineering*, *18*(5), pp.1016-1021.

Ravisankar, V., Joshua, R.E. and Rajkumar, D., 2024. Synergistic effects of microbes and plant for remediation of chromium contaminated soil. *Global NEST Journal*, *26*(1).

Refaey, M., Abdel-Azeem, A.M., Abo Nahas, H.H., Abdel-Azeem, M.A. and El-Saharty, A.A., 2021. Role of fungi in bioremediation of soil contaminated with heavy metals. In *Industrially Important Fungi for Sustainable Development: Volume 1: Biodiversity and Ecological Perspectives* (pp. 509-540). Cham: Springer International Publishing.

Retamal-Morales, G., Mehnert, M., Schwabe, R., Tischler, D., Zapata, C., Chávez, R., Schlömann, M. and Levicán, G., 2018. Detection of arsenic-binding siderophores in arsenic-tolerating Actinobacteria by a modified CAS assay. *Ecotoxicology and environmental safety*, *157*, pp.176-181.

Roberts, P.B., 1983. Interactions between cadmium and radiation in the killing of Escherichia coli. *Environmental Research*, *31*(1), pp.221-228.

Rodriguez, M.G., Rivera, B.H., Ventura-Juárez, J. and Muñoz-Ortega, M.H., 2013. Cadmium toxicity evaluation in the earthworm Eisenia foetida: behavior and histopathological effects. *Trends Comp Biochem Physiol*, *17*, p.S0304423810002578.

Rom, W.N., 1976. Effects of lead on the female and reproduction: a review. *The Mount Sinai journal of medicine, New York*, *43*(5), pp.542-552.

Romaniuk, A., Lyndin, M., Sikora, V., Lyndina, Y., Romaniuk, S. and Sikora, K., 2017. Heavy metals effect on breast cancer progression. *Journal of Occupational Medicine and Toxicology*, *12*(1), p.32.

Roncero, M.I.G., 1984. Enrichment method for the isolation of auxotrophic mutants of Mucor using the polyene antibiotic N-glycosyl-polifungin. *Carlsberg research communications*, *49*(7), pp.685-690.

Rosariastuti, R. and Astuti, H.A., 2022, April. Study of potential plant of Biduri (Calotropis gigantea) with combination of bacteria, organic matter, and inorganic fertilizer for bioremediation of lead (Pb) contaminated soil. In *IOP Conference Series: Earth and Environmental Science* (Vol. 1016, No. 1, p. 012016). IOP Publishing.

Roskova, Z., Skarohlid, R. and McGachy, L., 2022. Siderophores: an alternative bioremediation strategy?. *Science of the Total Environment*, *819*, p.153144.

Roy, V., Saha, B.K., Adhikary, S., Chaki, M.G., Sarkar, M. and Pal, A., 2024. Isolation, characterization, identification, genomics and analyses of bioaccumulation and biosorption potential of two arsenic-resistant bacteria obtained from natural environments. *Scientific Reports*, *14*(1), p.5716.

Roychowdhury, R., Zaman, S. & Roy, M., 2017. Isolation and characterization of heavy metal resistant and plant growth promoting *Staphylococcus* sp. from fly ash dump site", *International Journal of Advanced Research*, 5(3), pp. 95–103.

Rubio, J.M., Masri, S., Torres, I.R., Sun, Y., Villegas, K., Flores, P., Logue, M.D., Reyes, A., LeBrón, A.M. and Wu, J., 2022. Use of historical mapping to understand sources of soil-lead contamination: Case study of Santa Ana, CA. *Environmental Research*, *212*, p.113478.

Sabater, S. & Admiraal, W. (2005) Periphyton as biological indicators in managed aquatic ecosystems. In: Azim, M.E., Verdegem, M.C.J., van Dam, A.A. & Beveridge, M.C.M. (eds.) Periphyton: Ecology, Exploitation and Management. London: CABI Publishing, pp. 159–177.

Sabry, S.A., Ghozlan, H.A. and Abou-Zeid, D.M., 1997. Metal tolerance and antibiotic resistance patterns of a bacterial population isolated from sea water. *Journal of applied Microbiology*, *82*(2), pp.245-252.

Sahmoune, M.N., 2016. The role of biosorbents in the removal of arsenic from water. *Chemical Engineering & Technology*, *39*(9), pp.1617-1628.

Sahu, P.K., Shivaprakash, M.K., Mallesha, B.C., Subbarayappa, C.T. and Brahmaprakash, G.P., 2018. Effect of bacterial endophytes Lysinibacillus sp. on plant

growth and fruit yield of tomato (Solanum lycopersicum). *Int J Curr Microbiol Appl Sci*, *7*, pp.3399-3408.

Saidon, N.B., Szabó, R., Budai, P. and Lehel, J., 2024. Trophic transfer and biomagnification potential of environmental contaminants (heavy metals) in aquatic ecosystems. *Environmental pollution*, *340*, p.122815.

Saikia, V., 2015. *Biochemical characterization and mechanistic study of heavy metal detoxification in the metal resistant bacteria* (Doctoral dissertation, Tezpur University).

Salam, M., Varma, A., Chaudhary, D. and Aggarwal, H., 2020. Novel arsenic resistant bacterium Sporosarcina luteola M10 having potential bioremediation properties. *J. Microbiol. Exp*, *8*, pp.213-218.

Sanders, E.R., 2012. Aseptic laboratory techniques: plating methods. *Journal of Visualized Experiments (JoVE)*, (63), p.e3064.

Sankarammal, M., Thatheyus, A. and Ramya, D., 2014. Bioremoval of cadmium using Pseudomonas fluorescens. *Open J. Water Pollut. Treat*, *1*, pp.92-100.

Saraeva, I., Tolordava, E., Sheligyna, S., Nastulyavichus, A., Khmelnitskii, R., Pokryshkin, N., Khmelenin, D., Kudryashov, S., Ionin, A. and Akhmatkhanov, A., 2023. FT-IR analysis of P. aeruginosa bacteria inactivation by femtosecond IR laser radiation. *International Journal of Molecular Sciences*, *24*(6), p.5119.

Sarma, U., Hoque, M.E., Thekkangil, A., Venkatarayappa, N. and Rajagopal, S., 2024. Microalgae in removing heavy metals from wastewater–An advanced green technology for urban wastewater treatment. *Journal of Hazardous Materials Advances*, *15*, p.100444.

Sarter, S., Nguyen, H.N.K., Lazard, J. and Montet, D., 2007. Antibiotic resistance in Gram-negative bacteria isolated from farmed catfish. Food control, 18(11), pp.1391-1396.

Sarvepalli, M., Velidandi, A. and Korrapati, N., 2023. Optimization of siderophore production in three marine bacterial isolates along with their heavy-metal chelation and seed germination potential determination. *Microorganisms*, *11*(12), p.2873.

Schindler, B.D. and Kaatz, G.W., 2016. Multidrug efflux pumps of Gram-positive bacteria. *Drug Resistance Updates*, *27*, pp.1-13.

Schweitzer, P.A., 2003. *Metallic materials: physical, mechanical, and corrosion properties* (Vol. 19). CRC press.

Schwyn, B. and Neilands, J., 1987. Universal chemical assay for the detection and determination of siderophores. *Analytical biochemistry*, *160*(1), pp.47-56.

Seiler, C. and Berendonk, T.U., 2012. Heavy metal driven co-selection of antibiotic resistance in soil and water bodies impacted by agriculture and aquaculture. *Frontiers in microbiology*, *3*, p.399.

Semy, K. and Singh, M.R., 2021a. Assessment of soil physico-chemical properties and heavy metals bioaccumulation on plants at a coal mining affected forest of Changki, Nagaland. Environment and Ecology, 39(1A), pp.192-199.

Semy, K. and Singh, M.R., 2021b. Quality assessment of Tsurang River water affected by coal mining along the Tsurangkong Range, Nagaland, India. Applied Water Science, 11(7), p.115.

Sencan, A., Kilic, S. and Kaya, H., 2024. Stimulating effect of biogenic nanoparticles on the germination of basil (Ocimum basilicum L.) seeds. *Scientific Reports*, *14*(1), p.1715.

Seok, S.H., Baek, M.W., Lee, H.Y., Kim, D.J., Na, Y.R., Noh, K.J., Park, S.H., Lee, H.K., Lee, B.H., Ryu, D.Y. and Park, J.H., 2007. Arsenite-induced apoptosis is prevented by antioxidants in zebrafish liver cell line. *Toxicology in vitro*, *21*(5), pp.870-877.

Sevak, P.I., Pushkar, B.K. and Kapadne, P.N., 2021. Lead pollution and bacterial bioremediation: A review. Environmental Chemistry Letters, 19(6), pp.4463-4488.

Shabaan, A.M., Embaby, M.S. and Reyad, A.M., 2025. Potential application of Staphylococcus devriesei MS as a biosorbent agent for manganase, chromium, and cadmium heavy metals in contaminated water. *Scientific Reports*, *15*(1), p.9774.

Shakya, S., Pradhan, B., Smith, L., Shrestha, J. and Tuladhar, S., 2012. Isolation and characterization of aerobic culturable arsenic-resistant bacteria from surfacewater and

groundwater of Rautahat District, Nepal. *Journal of Environmental Management*, *95*, pp.S250-S255.

Shamim, S. and Rehman, A., 2015. Antioxidative enzyme profiling and biosorption ability of Cupriavidus metallidurans CH34 and Pseudomonas putida mt2 under cadmium stress. *Journal of basic microbiology*, *55*(3), pp.374-381.

Sharma, A., Dev, K., Sourirajan, A. and Choudhary, M., 2021. Isolation and characterization of salt-tolerant bacteria with plant growth-promoting activities from saline agricultural fields of Haryana, India. *Journal of Genetic Engineering and Biotechnology*, *19*(1), p.99.

Sharma, P., 2022. Role and significance of biofilm-forming microbes in phytoremediation-a review. *Environmental technology & innovation*, *25*, p.102182.
Sharma, P., 2022. Role and significance of biofilm-forming microbes in phytoremediation-a review. *Environmental technology & innovation*, *25*, p.102182.

Sharma, P., Pandey, A.K., Udayan, A. and Kumar, S., 2021. Role of microbial community and metal-binding proteins in phytoremediation of heavy metals from industrial wastewater. *Bioresource technology*, *326*, p.124750.

Sharma, S., Mohler, J., Mahajan, S.D., Schwartz, S.A., Bruggemann, L. and Aalinkeel, R., 2023. Microbial biofilm: a review on formation, infection, antibiotic resistance, control measures, and innovative treatment. *Microorganisms*, *11*(6), p.1614.

Sharma, S., Pathania, S., Bhagta, S., Kaushal, N., Bhardwaj, S., Bhatia, R.K. and Walia, A., 2024. Microbial remediation of polluted environment by using recombinant E. coli: a review. *Biotechnology for the Environment*, *1*(1), p.8.

Shaw, D.R. and Dussan, J., 2018. Transcriptional analysis and molecular dynamics simulations reveal the mechanism of toxic metals removal and efflux pumps in Lysinibacillus sphaericus OT4b. 31. *International Biodeterioration & Biodegradation*, *127*, pp.46-61.

Sheng, G.P., Yu, H.Q. and Li, X.Y., 2010. Extracellular polymeric substances (EPS) of microbial aggregates in biological wastewater treatment systems: a review. *Biotechnology advances*, *28*(6), pp.882-894.

Sheng, G.P., Yu, H.Q. and Yue, Z.B., 2005. Production of extracellular polymeric substances from Rhodopseudomonas acidophila in the presence of toxic substances. *Applied microbiology and biotechnology*, *69*(2), pp.216-222.

Sheng, X.F., Xia, J.J., Jiang, C.Y., He, L.Y. and Qian, M., 2008. Characterization of heavy metal-resistant endophytic bacteria from rape (Brassica napus) roots and their potential in promoting the growth and lead accumulation of rape. *Environmental pollution*, *156*(3), pp.1164-1170.

Shi, H., Sun, J., Han, R., Ding, C., Hu, F. and Yu, S., 2020. The strategy for correcting interference from water in Fourier transform infrared spectrum based bacterial typing. *Talanta*, *208*, p.120347.

Shiomi, N., 2015. An assessment of the Causes of Lead Pollution and the Efficiency of Bioremediation by Plants and Microorganisms. *Advances in Bioremediation of Wastewater and Polluted Soil.: InTech*, pp.247-274.

Shrestha, R., Ban, S., Devkota, S., Sharma, S., Joshi, R., Tiwari, A.P., Kim, H.Y. and Joshi, M.K., 2021. Technological trends in heavy metals removal from industrial wastewater: A review. *Journal of Environmental Chemical Engineering*, *9*(4), p.105688.

Shukla, D. and Vankar, P.S., 2014. Role of Trichoderma species in bioremediation process: biosorption studies on hexavalent chromium. In *Biotechnology and biology of Trichoderma* (pp. 405-412). Elsevier.

Shukla, J., Singh, S., Dixit, S., Kushwaha, A.S., Mohd, S., Saji, J. and Kumar, M., 2025. Efficient removal of arsenic from the environment by endophytic fungus *Serendipita indica* through bio-accumulation in cells and adsorption on the cell wall. *Environmental Technology & Innovation*, *39*, p.104229.

Sikorski, E.E., Burns, L.A., Stern, M.L., Luster, M.I. and Munson, A.E., 1991. Splenic cell targets in gallium arsenide-induced suppression of the primary antibody response. *Toxicology and applied pharmacology*, *110*(1), pp.129-142.

Singh, A., Pal, D.B., Mohammad, A., Alhazmi, A., Haque, S., Yoon, T., Srivastava, N. and Gupta, V.K., 2022. Biological remediation technologies for dyes and heavy metals in wastewater treatment: New insight. *Bioresource Technology*, *343*, p.126154.

Singh, A.L. and Sarma, P.N., 2010. Removal of arsenic (III) from waste water using Lactobacillus acidophilus. *Bioremediation Journal*, *14*(2), pp.92-97.

Singh, J.S., Abhilash, P.C., Singh, H.B., Singh, R.P. and Singh, D.P., 2011. Genetically engineered bacteria: an emerging tool for environmental remediation and future research perspectives. *Gene*, *480*(1-2), pp.1-9.

Singh, N., Gupta, S., Marwa, N., Pandey, V., Verma, P.C., Rathaur, S. and Singh, N., 2016. Arsenic mediated modifications in Bacillus aryabhattai and their biotechnological applications for arsenic bioremediation. *Chemosphere*, *164*, pp.524-534.
Singh, N., Gupta, S., Marwa, N., Pandey, V., Verma, P.C., Rathaur, S. and Singh, N., 2016. Arsenic mediated modifications in Bacillus aryabhattai and their biotechnological applications for arsenic bioremediation. *Chemosphere*, *164*, pp.524-534.

Singh, R., 2014. Microorganism as a tool of bioremediation technology for cleaning environment: a review. *Proceedings of the International Academy of Ecology and Environmental Sciences*, *4*(1), p.1.

Singh, R.K., Kumar, D.P., Solanki, M.K., Singh, P., Srivastva, A.K., Kumar, S., Kashyap, P.L., Saxena, A.K., Singhal, P.K. and Arora, D.K., 2013. Optimization of media components for chitinase production by chickpea rhizosphere associated Lysinibacillus fusiformis B-CM18. *Journal of basic microbiology*, *53*(5), pp.451-460.

Sodhi, K.K., Mishra, L.C., Singh, C.K. and Kumar, M., 2022. Perspective on the heavy metal pollution and recent remediation strategies. *Current Research in Microbial Sciences*, *3*, p.100166.

Sohlenkamp, C. and Geiger, O., 2016. Bacterial membrane lipids: diversity in structures and pathways. *FEMS microbiology reviews*, *40*(1), pp.133-159.

Soleimanpour Moghadam, N. and Azadmehr, A., 2025. The environmental effects of coal and pollution control techniques for green coal mining. *Journal of Environment and Sustainable Mining*, *1*(1), pp.44-59.

Soltan, E.S.M., 2001. Isolation and characterization of antibiotic and heavy metal-resistant pseudomonas aeruginosa from different polluted waters in sohag district, egypt. *Journal of microbiology and biotechnology*, *11*(1), pp.50-55.

Spain, A. and Alm, E., 2003. Implications of microbial heavy metal tolerance in the environment. *Reviews in Undergraduate Research*, 2, pp. 1–6.

Stamatakis, A., 2014. RAxML version 8: a tool for phylogenetic analysis and post-analysis of large phylogenies. *Bioinformatics*, *30*(9), pp.1312-1313.

Stamatakis, A., Hoover, P. and Rougemont, J., 2008. A rapid bootstrap algorithm for the RAxML web servers. *Systematic biology*, *57*(5), pp.758-771.

Steunou, A.S., Babot, M., Bourbon, M.L., Tambosi, R., Durand, A., Liotenberg, S., Krieger-Liszkay, A., Yamaichi, Y. and Ouchane, S., 2020. Additive effects of metal excess and superoxide, a highly toxic mixture in bacteria. *Microbial biotechnology*, *13*(5), pp.1515-1529.

Stohs, S.J. and Bagchi, D., 1995. Oxidative mechanisms in the toxicity of metal ions. *Free radical biology and medicine*, *18*(2), pp.321-336.

Su, K., Zhang, Q., Chen, A., Wang, X., Zhan, L., Rao, Q., Wang, J. and Yang, H., 2025. Heavy metals concentrations in commercial organic fertilizers and the potential risk of fertilization into soils. Scientific Reports, 15(1), p.1230.

Suhani, I., Sahab, S., Srivastava, V. and Singh, R.P., 2021. Impact of cadmium pollution on food safety and human health. *Current opinion in toxicology*, *27*, pp.1-7.

Sun, R., Gao, Y. and Yang, Y., 2022. Leaching of heavy metals from lead-zinc mine tailings and the subsequent migration and transformation characteristics in paddy soil. *Chemosphere*, *291*, p.132792.

Sundseth, K., Pacyna, J.M., Pacyna, E.G., Pirrone, N. and Thorne, R.J., 2017. Global sources and pathways of mercury in the context of human health. *International journal of environmental research and public health*, *14*(1), p.105.

Szumińska, D., Czapiewski, S., Szopińska, M. and Polkowska, Ż., 2018. Analysis of air mass back trajectories with present and historical volcanic activity and anthropogenic compounds to infer pollution sources in the South Shetland Islands (Antarctica). *Bulletin of Geography. Physical Geography Series*, (15), pp.111-137.

Tabatabaei Khodadadei, M., Mansouri, H. and Salari, H., 2025. Investigating the Removal of Arsenic (III) from Water Using a Biosorbent Containing Chlorella Sorokiniana Microalgae. *Water, Air, & Soil Pollution*, *236*(15), p.962.

Tamura, K., Stecher, G. and Kumar, S., 2021. MEGA11: molecular evolutionary genetics analysis version 11. *Molecular biology and evolution*, *38*(7), pp.3022-3027.

Tandon, H.L.S., 2009. Methods of analysis of soils, plants, waters and fertilizers. 2nd ed. New Delhi: Fertiliser Development and Consultation Organisation (FDCO), pp. 64–66.

Tang, H., Xiang, G., Xiao, W., Yang, Z. and Zhao, B., 2024. Microbial mediated remediation of heavy metals toxicity: mechanisms and future prospects. *Frontiers in Plant Science*, *15*, p.1420408.

Tangaromsuk, J., Pokethitiyook, P., Kruatrachue, M. and Upatham, E.S., 2002. Cadmium biosorption by Sphingomonas paucimobilis biomass. *Bioresource Technology*, *85*(1), pp.103-105.

Tarfeen, N., Nisa, K.U., Hamid, B., Bashir, Z., Yatoo, A.M., Dar, M.A., Mohiddin, F.A., Amin, Z., Ahmad, R.A.A. and Sayyed, R.Z., 2022. Microbial remediation: a promising tool for reclamation of contaminated sites with special emphasis on heavy metal and pesticide pollution: a review. *Processes*, *10*(7), p.1358.

Tatung, M. and Deb, C.R., 2024. Screening and characterization of heavy metal tolerant rhizobacteria from wild Musa rhizosphere from coal mining area of Changki,

Nagaland, India and assessment of their growth promoting potential under Cd/Cu contaminated conditions. *South African Journal of Botany*, *165*, pp.217-227.

Tchounwou, P.B., Yedjou, C.G., Patlolla, A.K. and Sutton, D.J., 2012. Heavy metal toxicity and the environment. *Molecular, clinical and environmental toxicology: volume 3: environmental toxicology*, pp.133-164.

Teitzel, G.M. and Parsek, M.R., 2003. Heavy metal resistance of biofilm and planktonic Pseudomonas aeruginosa. *Applied and environmental microbiology*, *69*(4), pp.2313-2320.

Timková, I., Maliničová, L., Nosáľová, L., Kolesárová, M., Lorková, Z., Petrová, N., Pristaš, P. and Kisková, J., 2024. Genomic insights into the adaptation of Acinetobacter johnsonii RB2-047 to the heavy metal-contaminated subsurface mine environment. *Biometals*, *37*(2), pp.371-387.

Timková, I., Sedláková-Kaduková, J. and Pristaš, P., 2018. Biosorption and bioaccumulation abilities of actinomycetes/streptomycetes isolated from metal contaminated sites. *Separations*, *5*(4), p.54.

Timofeeva, A.M., Galyamova, M.R. and Sedykh, S.E., 2022. Bacterial siderophores: classification, biosynthesis, perspectives of use in agriculture. *Plants*, *11*(22), p.3065.

Tiquia-Arashiro, S.M., 2018. Lead absorption mechanisms in bacteria as strategies for lead bioremediation. *Applied microbiology and biotechnology*, *102*(13), pp.5437-5444.

Titah, H.S., Abdullah, S.R.S., Idris, M., Anuar, N., Basri, H., Mukhlisin, M., Tangahu, B.V., Purwanti, I.F. and Kurniawan, S.B., 2018. Arsenic resistance and biosorption by isolated rhizobacteria from the roots of Ludwigia octovalvis. *International journal of microbiology*, *2018*(1), p.3101498.

Tolins, M., Ruchirawat, M. and Landrigan, P., 2014. The developmental neurotoxicity of arsenic: cognitive and behavioral consequences of early life exposure. *Annals of global health*, *80*(4), pp.303-314.

Tournay, R.J., Firrincieli, A., Parikh, S.S., Sivitilli, D.M. and Doty, S.L., 2023. Effect of arsenic on EPS synthesis, biofilm formation, and plant growth-promoting abilities of the endophytes pseudomonas PD9R and Rahnella laticis PD12R. *Environmental Science & Technology*, *57*(23), pp.8728-8738.

Türkmen, D., Bakhshpour, M., Akgönüllü, S., Aşır, S. and Denizli, A., 2022. Heavy metal ions removal from wastewater using cryogels: A review. Frontiers in Sustainability, 3, p.765592.

U.S. Environmental Protection Agency (EPA). (2014). Method 6020B: Inductively Coupled Plasma–Mass Spectrometry (ICP-MS). Washington, DC: United States Environmental Protection Agency.

Ukkund, S.J., Adarsh, D.P., Nair, H., Manasa, J., Krishna, S., Naveen, R., Jacob, S., Shettar, A.B., Badiuddin, A.F. and Nellerichale, A., 2021. Antimicrobial coating of fabric by biosynthesized silver nanoparticles from Panchakavya. *Nano Express*, *2*(1), p.010033.

Umana, I.M., Neji, P.A. and Agwupuye, J.A., 2022. Assessment of underground water quality in Okobo local government area of Akwa Ibom State, Nigeria. *Applied Water Science*, *12*(5), p.106.

UNEP (2022) *Cadmium*. United Nations Environment Programme. Available at: https://www.unep.org/topics/chemicals-and-pollution-action/pollution-and-health/heavy-metals/cadmium (Accessed: 1 December 2025).

United Nations Environment Programme (UNEP) (2025) *Heavy metals*. Available at: https://www.unep.org/topics/chemicals-and-pollution-action/chemicals-management/pollution-and-health/heavy-metals-0 (Accessed: 1 December 2025).

United Nations General Assembly (2015) *Transforming our world: The 2030 Agenda for Sustainable Development (A/RES/70/1)*. New York: United Nations. Available at: https://docs.un.org/en/A/RES/70/1 (Accessed: 5 November 2025).

Upadhyay, M.K., Yadav, P., Shukla, A. and Srivastava, S., 2018. Utilizing the potential of microorganisms for managing arsenic contamination: a feasible and sustainable approach. *Frontiers in environmental Science*, *6*, p.24.

Upadhyay, S.K., Rani, N., Kumar, V., Mythili, R. and Jain, D., 2023. A review on simultaneous heavy metal removal and organo-contaminants degradation by potential microbes: current findings and future outlook. *Microbiological Research*, *273*, p.127419.

Uqab, B., Nazir, R., Ahmad Ganai, B., Rahi, P., Rehman, S., Farooq, S., Dar, R., Parray, J.A., Fahad Al-Arjani Al-Arjani, A.B., Tabassum, B. and Fathi Abd_Allah, E., 2020. MALDI-TOF-MS and 16S rRNA characterization of lead tolerant metallophile bacteria isolated from saffron soils of Kashmir for their sequestration potential. Saudi J Biol Sci 27 (8): 2047–2053.

Usoltsev, D., Sitnikova, V., Kajava, A. and Uspenskaya, M., 2019. Systematic FTIR spectroscopy study of the secondary structure changes in human serum albumin under various denaturation conditions. *Biomolecules*, *9*(8), p.359.

Vadeo, K., Chang, C.N. and Walling, T., 2023. Impact of Coal Mining on the Tzuong River System of Mokokchung, Nagaland. *Current World Environment*, *18*(1), p.223.

Valentino-Álvarez, J.A., Núñez-Nogueira, G. and Fernández-Bringas, L., 2013. Acute toxicity of arsenic under different temperatures and salinity conditions on the white shrimp Litopenaeus vannamei. *Biological trace element research*, *152*(3), pp.350-357.

Van Houdt, R. and Michiels, C.W., 2010. Biofilm formation and the food industry, a focus on the bacterial outer surface. *Journal of applied microbiology*, *109*(4), pp.1117-1131.

Vandecandelaere, I., Van Nieuwerburgh, F., Deforce, D. and Coenye, T., 2017. Metabolic activity, urease production, antibiotic resistance and virulence in dual species biofilms of Staphylococcus epidermidis and Staphylococcus aureus. *PLoS One*, *12*(3), p.e0172700.

Vats, P., Kaur, U.J. and Rishi, P., 2022. Heavy metal-induced selection and proliferation of antibiotic resistance: a review. *Journal of applied microbiology*, *132*(6), pp.4058-4076.

Vendan, R.T., Yu, Y.J., Lee, S.H. and Rhee, Y.H., 2010. Diversity of endophytic bacteria in ginseng and their potential for plant growth promotion. *The Journal of Microbiology*, *48*(5), pp.559-565.

Ventura-Lima, J., Sandrini, J.Z., Cravo, M.F., Piedras, F.R., Moraes, T.B., Fattorini, D., Notti, A., Regoli, F., Geracitano, L.A., Marins, L.F. and Monserrat, J.M., 2007. Toxicological responses in Laeonereis acuta (Annelida, Polychaeta) after arsenic exposure. *Environment international*, *33*(4), pp.559-564.

Verma, L., Ekka, A., Banjara, R.A., Ambade, B., Kumar, A. and Gautam, S., 2025. A Review on Bacterial Exopolysaccharides for Heavy Metal Remediation: Mechanisms, Challenges, and Sustainable Applications. *Water Environment Research*, *97*(10), p.e70184.

Vetillard, A., Bailhache, T., 2005. Cadmium: an endocrine disrupter that affects gene expression in the liver and brain of juvenile rainbow trout. Biol. Reprod. 72 (1), 119–126. https://doi.org/10.1095/biolreprod.104.029520

Vijayanand, S., Divyashree, M., 2015. Bioremediation of heavy metals using biosurfactant producing microorganisms. International Journal of Pharma Sciences and Research,. 6(5), pp. 840-847.

Vishnoi, N., Dixit, S. and Singh, D.P., 2014. Surface binding and intracellular uptake of arsenic in bacteria isolated from arsenic contaminated site. *Ecological engineering*, *73*, pp.569-578.

Voica, D.M., Bartha, L., Banciu, H.L. and Oren, A., 2016. Heavy metal resistance in halophilic bacteria and archaea. FEMS Microbiology Letters, 363(14), p.146.

Vullo, D. L., Ceretti, H. M., Daniel, M. A., Ramı´rez, S. A. M., Zalts, A., 2008. Cadmium, zinc and copper biosorption mediated by Pseudomonas veronii 2E, Bioresource Technology, 99, pp. 5574–5581

Walkley, A. and Black, I.A., 1934. An examination of the Degtjareff method for determining soil organic matter, and a proposed modification of the chromic acid titration method. Soil science, 37(1), pp.29-38.

Walsh, C., 2000. Molecular mechanisms that confer antibacterial drug resistance. *Nature*, *406*(6797), pp.775-781.

Wan, Y., Liu, J., Zhuang, Z., Wang, Q. and Li, H., 2024. Heavy metals in agricultural soils: Sources, influencing factors, and remediation strategies. Toxics, 12(1), p.63.

Wang, H.T., Zhu, D., Li, G., Zheng, F., Ding, J., O'Connor, P.J., Zhu, Y.G. and Xue, X.M., 2019. Effects of arsenic on gut microbiota and its biotransformation genes in earthworm Metaphire sieboldi. *Environmental science & technology*, *53*(7), pp.3841-3849.

Wang, J. and Chen, C., 2009. Biosorbents for heavy metals removal and their future. *Biotechnology advances*, *27*(2), pp.195-226.

Wang, J., Zhao, F.J., Meharg, A.A., Raab, A., Feldmann, J. and McGrath, S.P., 2002. Mechanisms of arsenic hyperaccumulation in Pteris vittata. Uptake kinetics, interactions with phosphate, and arsenic speciation. *Plant physiology*, *130*(3), pp.1552-1561.

Wang, R., Guo, Z., Tang, Y., Kuang, J., Duan, Y., Lin, H., Jiang, S., Shu, H. and Huang, J., 2020. Effects on development and microbial community of shrimp Litopenaeus vannamei larvae with probiotics treatment. *Amb Express*, *10*(1), p.109.

Wang, Y., Branicky, R., Noë, A. and Hekimi, S., 2018. Superoxide dismutases: Dual roles in controlling ROS damage and regulating ROS signaling. *Journal of Cell Biology*, *217*(6), pp.1915-1928.

Wang, Y.C., Chaung, R.H. and Tung, L.C., 2004. Comparison of the cytotoxicity induced by different exposure to sodium arsenite in two fish cell lines. *Aquatic Toxicology*, *69*(1), pp.67-79.

Wang, Z., Deng, G., Hu, C., Hou, X., Zhang, X., Fan, Z., Zhao, Y. and Peng, M., 2025. Microbial diversity and community assembly in heavy metal-contaminated soils: insights from selenium-impacted mining areas. *Frontiers in Microbiology*, *16*, p.1561678.

Watanabe, T. and Hirano, S., 2013. Metabolism of arsenic and its toxicological relevance. *Archives of toxicology*, *87*(6), pp.969-979.

Wätjen, W., Haase, H., Biagioli, M. and Beyersmann, D., 2002. Induction of apoptosis in mammalian cells by cadmium and zinc. *Environmental Health Perspectives*, *110*(Suppl 5), p.865.

Wei, W., Wang, Q., Li, A., Yang, J., Ma, F., Pi, S. and Wu, D., 2016. Biosorption of Pb (II) from aqueous solution by extracellular polymeric substances extracted from Klebsiella sp. J1: Adsorption behavior and mechanism assessment. *Scientific reports*, *6*(1), p.31575.

Wei, Z., Niu, S., Wei, Y., Liu, Y., Xu, Y., Yang, Y., Zhang, P., Zhou, Q. and Wang, J.J., 2024. The role of extracellular polymeric substances (EPS) in chemical-degradation of persistent organic pollutants in soil: A review. *Science of The Total Environment*, *912*, p.168877.

Wen, Q., Yang, X., Yan, X. and Yang, L., 2022. Evaluation of arsenic mineralogy and geochemistry in gold mine-impacted matrices: Speciation, transformation, and potential associated risks. *Journal of Environmental Management*, *308*, p.114619.

Weydert, C.J. and Cullen, J.J., 2010. Measurement of superoxide dismutase, catalase and glutathione peroxidase in cultured cells and tissue. *Nature protocols*, *5*(1), pp.51-66.

WHO (2022) *Guidelines for Drinking-water Quality, 4th edition incorporating the 1st addendum*. Geneva: World Health Organization. Available at: https://www.who.int/publications/i/item/9789241548151 (Accessed: 1 December 2025).

Widawati, S., 2020, September. Isolation of Indole Acetic Acid (IAA) producing Bacillus siamensis from peat and optimization of the culture conditions for maximum IAA production. In *IOP Conference Series: Earth and Environmental Science* (Vol. 572, No. 1, p. 012025). IOP Publishing.

Wiegand, I., Hilpert, K. and Hancock, R.E., 2008. Agar and broth dilution methods to determine the minimal inhibitory concentration (MIC) of antimicrobial substances. *Nature protocols*, *3*(2), pp.163-175.

William, V.U. and Magpantay, H.D., 2023. Arsenic and microorganisms: genes, molecular mechanisms, and recent advances in microbial arsenic bioremediation. *Microorganisms*, *12*(1), p.74.

Wojcik, M. and Tukiendorf, A., 2004. Phytochelatin synthesis and cadmium localization in wild type of Arabidopsis thaliana. *Plant Growth Regulation*, *44*(1), pp.71-80.

Wróblewski, M., Miłek, J., Godlewski, A. and Wróblewska, J., 2025. The Impact of Arsenic, Cadmium, Lead, Mercury, and Thallium Exposure on the Cardiovascular System and Oxidative Mechanisms in Children. *Current Issues in Molecular Biology*, *47*(7), p.483.

Wu, W., Tang, W., He, Z. and Wang, L., 2024. Archaea, bacteria and protists share a depth–decay relationship of community similarity in deep oceans. *Journal of Plankton Research*, *46*(4), pp.398-402.

Wu, X., Cobbina, S.J., Mao, G., Xu, H., Zhang, Z. and Yang, L., 2016. A review of toxicity and mechanisms of individual and mixtures of heavy metals in the environment. *Environmental Science and Pollution Research*, *23*(9), pp.8244-8259.

Wu, X., Wu, X., Shen, L., Li, J., Yu, R., Liu, Y., Qiu, G. and Zeng, W., 2019. Whole genome sequencing and comparative genomics analyses of Pandoraea sp. XY-2, a new species capable of biodegrade tetracycline. *Frontiers in Microbiology*, *10*, p.33.

Wu, Y., Song, Q., Wu, J., Zhou, J., Zhou, L. and Wu, W., 2021. Field study on the soil bacterial associations to combined contamination with heavy metals and organic contaminants. *Science of the Total Environment*, *778*, p.146282.

Wu, Z., Zhang, D., Xia, T. and Jia, X., 2022. Characteristics, sources and risk assessments of heavy metal pollution in soils of typical chlor-alkali residue storage sites in northeastern China. *Plos one*, *17*(9), p.e0273434.

Wuana, R.A. and Okieimen, F.E., 2011. Heavy metals in contaminated soils: a review of sources, chemistry, risks and best available strategies for remediation. *International Scholarly Research Notices*, *2011*(1), p.402647.

Xing, L., 2022. Determination of Toxic Elements in Food by ICP-MS Using AOAC Method 2015.01. *Spectroscopy*, 37(10), pp. 7–12.

Xu, C., He, S., Liu, Y., Zhang, W. and Lu, D., 2017. Bioadsorption and biostabilization of cadmium by Enterobacter cloacae TU. *Chemosphere*, *173*, pp.622-629.

Xu, J.L., Herrero-Langreo, A., Lamba, S., Ferone, M., Scannell, A.G., Caponigro, V. and Gowen, A.A., 2021. Characterisation and classification of foodborne bacteria using reflectance FTIR microscopic imaging. *Molecules*, *26*(20), p.6318.

Xu, P., Tu, X., An, Z., Mi, W., Wan, D., Bi, Y. and Song, G., 2024. Cadmium-induced physiological responses, biosorption and bioaccumulation in Scenedesmus obliquus. *Toxics*, *12*(4), p.262.

Yan, L., Yin, H., Zhang, S., Leng, F., Nan, W. and Li, H., 2010. Biosorption of inorganic and organic arsenic from aqueous solution by Acidithiobacillus ferrooxidans BY-3. *Journal of Hazardous Materials*, *178*(1-3), pp.209-217.

Yan, T., Zhao, W., Yu, X., Li, H., Gao, Z., Ding, M. and Yue, J., 2022. Evaluating heavy metal pollution and potential risk of soil around a coal mining region of Tai'an City, China. *Alexandria Engineering Journal*, *61*(3), pp.2156-2165.

Yang, W., Li, J. and Hekimi, S., 2007. A measurable increase in oxidative damage due to reduction in superoxide detoxification fails to shorten the life span of long-lived mitochondrial mutants of Caenorhabditis elegans. *Genetics*, *177*(4), pp.2063-2074.

Yang, Z., Shi, W., Yang, W., Liang, L., Yao, W., Chai, L., Gao, S. and Liao, Q., 2018. Combination of bioleaching by gross bacterial biosurfactants and flocculation: A potential remediation for the heavy metal contaminated soils. *Chemosphere*, *206*, pp.83-91.

Yani, A., Hutasoit, L.R., Rohman, F., Irfandi, R., Rijal, S., Jayanegara, A. and Amin, A.M., 2025. Bioremediation of cadmium polluted water using a novel indigenous bacteria Bacillus albus Isolated from Tempe Lake, Indonesia. *Applied Water Science*, *15*(9), p.238.

Yin, W., Wang, Y., Liu, L. and He, J., 2019. Biofilms: the microbial "protective clothing" in extreme environments. *International journal of molecular sciences*, *20*(14), p.3423.

Yu, H.S., Liao, W.T. and Chai, C.Y., 2006. Arsenic carcinogenesis in the skin. *Journal of biomedical science*, *13*(5), pp.657-666.

Yu, L., Zhang, T., Yang, J., Zhang, R., Zhou, J., Ding, F., Shao, C. and Guo, R., 2023. Isolation of a novel multiple-heavy metal resistant Lampropedia aestuarii GYF-1 and investigation of its bioremediation potential. *BMC microbiology*, *23*(1), p.330.

Yu, M.H. and Tsunoda, H., 2004. *Environmental toxicology: biological and health effects of pollutants*. CRC Press.

Yu, S., Wang, X., Zhang, R., Chen, R. and Ma, L., 2023. A review on the potential risks and mechanisms of heavy metal exposure to Chronic Obstructive Pulmonary Disease. *Biochemical and Biophysical Research Communications*, *684*, p.149124.

Yue, T., Yang, Y., Chen, S., Yao, J., Liang, H., Jia, L., Fu, K. and Wang, Z., 2023. In situ prepared Chlorella vulgaris–supported nanoscale zero-valent iron to remove arsenic (III). *Environmental Science and Pollution Research*, *30*(38), pp.89676-89689.

Žaltauskaitė, J., Kniuipytė, I. and Kugelytė, R., 2020. Lead impact on the earthworm Eisenia fetida and earthworm recovery after exposure. *Water, Air, & Soil Pollution*, *231*(2), p.49.

Zeng, F., Zahoor, M., Waseem, M., Anayat, A., Rizwan, M., Ahmad, A., Yasmeen, T., Ali, S., El-Sheikh, M.A., Alyemeni, M.N. and Wijaya, L., 2020. Influence of metal-resistant Staphylococcus aureus strain K1 on the alleviation of chromium stress in wheat. *Agronomy*, *10*(9), p.1354.

Zeng, W., Li, F., Wu, C., Yu, R., Wu, X., Shen, L., Liu, Y., Qiu, G. and Li, J., 2020. Role of extracellular polymeric substance (EPS) in toxicity response of soil bacteria Bacillus sp. S3 to multiple heavy metals. *Bioprocess and biosystems engineering*, *43*(1), pp.153-167.

Zhang, H., Wang, K., Liu, X., Yao, L., Chen, Z. and Han, H., 2024. Exopolysaccharide-producing bacteria regulate soil aggregates and bacterial communities to inhibit the uptake of cadmium and lead by lettuce. *Microorganisms*, *12*(11), p.2112.

Zhang, J., Noor, Z.Z., Baharuddin, N.H., Setu, S.A., Hamzah, M.A.A.M. and Zakaria, Z.A., 2024. Uptake of lead, cadmium and copper by heavy metal-resistant Pseudomonas aeruginosa strain DR7 isolated from soil. *World Journal of Microbiology and Biotechnology*, *40*(12), p.387.

Zhang, Q., Jia, S., Ding, Y., Li, D., Ding, Y. and Zhou, X., 2022. Antibacterial activity and mechanism of malondialdehyde against Staphylococcus xylosus and Lactiplantibacillus plantarum isolated from a traditional Chinese dry-cured fish. Frontiers in Microbiology, 13, p.979388.

Zhang, S., Deng, Z., Borham, A., Ma, Y., Wang, Y., Hu, J., Wang, J. and Bohu, T., 2023. Significance of soil siderophore-producing bacteria in evaluation and elevation of crop yield. *Horticulturae*, *9*(3), p.370.

Zhang, Y., Zhou, J. and Chen, H., 2025. Global Trajectories of Forest Soil Acidification: A Scientometric Synthesis of Drivers, Impacts and Sustainable Solutions. *Forests*, *16*(5), p.733.

Zhang, Y., Zhou, J., Lei, Z., Ren, H. and Chen, H., 2024. Effect of Acid Production from Forest Litter on the Availability of Heavy Metals in Soil. *Forests*, *15*(12), p.2097.

Zhitkovich, A., 2011. Chromium in drinking water: sources, metabolism, and cancer risks. *Chemical research in toxicology*, *24*(10), pp.1617-1629.

Zhou, T., Wang, Z., Christie, P. and Wu, L., 2021. Cadmium and lead pollution characteristics of soils, vegetables and human hair around an open-cast lead-zinc mine. *Bulletin of Environmental Contamination and Toxicology*, *107*(6), pp.1176-1183.

Zhu, Y.G., Yoshinaga, M., Zhao, F.J. and Rosen, B.P., 2014. Earth abides arsenic biotransformations. *Annual Review of Earth and Planetary Sciences*, *42*(1), pp.443-467.

Zolgharnein, H., Karami, K., Assadi, M.M. and Sohrab, A.D., 2010. Investigation of heavy metals biosorption on *Pseudomonas aeruginosa* strain MCCB 102 isolated from the Persian Gulf. *Asian Journal of Biotechnology*, 2(2), pp. 99–109. https://doi.org/10.3923/ajbkr.2010.99.109

Zouagui, R., Zouagui, H., Aurag, J., Ibrahimi, A. and Sbabou, L., 2024. Functional analysis and comparative genomics of Rahnella perminowiae S11P1 and Variovorax sp. S12S4, two plant growth-promoting rhizobacteria isolated from Crocus sativus L.(saffron) rhizosphere. *BMC genomics*, *25*(1), p.289.

APPENDIX-I

REAGENTS AND CHEMICALS USED

A. *Reagents, Solutions and Buffers*

(i) Molybdate Reagent

Sl. No.	Ingredient	Composition per litre
1.	Ammonium molybdate	10 g
2.	Concentrated sulphuric acid (H_2SO_4)	250 mL
3.	Distilled water	Adjusted to 1 L

Preparation of the reagent

The molybdate reagent was prepared by dissolving 10 g of ammonium molybdate in about 400 mL of distilled water. To this solution, 250 mL of concentrated sulphuric acid was slowly added with constant stirring (acid to water). After cooling, the volume was made up to 1 litre with distilled water, mixed thoroughly, and stored in a clean reagent bottle.

(ii) EDTA (Ethylenediaminetetraacetic acid)

Sl. No.	Ingredient	Composition per litre
1.	EDTA disodium salt ($Na_2EDTA \cdot 2H_2O$)	186.1 g
2.	Sodium hydroxide (NaOH)	As required (for pH adjustment)
3.	Distilled water	Adjusted to 1 L

Preparation of the EDTA solution

EDTA solution was prepared by dissolving 186.1 g of disodium EDTA in about 800 mL of distilled water with continuous stirring and gentle heating. Sodium hydroxide pellets or solution are added gradually to adjust the pH to 8.0, which facilitates complete dissolution of EDTA. After the EDTA is fully dissolved, the volume was made up to 1 litre with distilled water, mixed thoroughly, and sterilized.

(iii) TBE (Tris-Borate-EDTA) buffer

Sl. No.	Ingredient	Composition per litre
1.	Tris base	10.8 g
2.	Boric acid	5.5 g
3.	EDTA (0.5 M, pH 8.0)	2 mL
4.	Distilled water	Adjusted to 1 L

Preparation of the TBE buffer

TBE buffer was prepared by dissolving 10.8 g of Tris base and 5.5 g of boric acid in approximately 800 mL of distilled water. To this, 2 mL of 0.5 M EDTA (pH 8.0) was added and mixed thoroughly. The volume was adjusted to 1 litre with distilled water, and the buffer was stored at room temperature for use.

(iv) Bacterial Lysis buffer for total protein extraction

Sl. No.	Ingredient	Final concentration (per litre)
1.	Tris–HCl (pH 7.5–8.0)	50 mM
2.	NaCl	150 mM
3.	EDTA	1 mM
4.	SDS	1 % (w/v)
5.	Triton X-100	1 % (v/v)
6.	Protease inhibitor cocktail	As required
7.	Distilled water	Adjusted to 1 L

Preparation of the bacterial lysis buffer

Bacterial lysis buffer was prepared by dissolving Tris–HCl, sodium chloride, and EDTA in about 800 mL of distilled water. SDS and Triton X-100 are then added slowly with gentle stirring to ensure uniform mixing. After complete dissolution, the volume was adjusted to 1 litre with distilled water. Protease inhibitor cocktail was added freshly before use, and the buffer is stored at 4 °C.

(v) Loading buffer for gel electrophoresis

Ingredient	Concentration (%)	Volume for 10 mL
Bromophenol blue	0.25	0.025 g
Xylene cyanol FF	0.25	0.025 g
Glycerol in water	30	3.0 mL

Preparation of bromophenol blue dye (loading dye)

Bromophenol blue loading dye was prepared by dissolving bromophenol blue (0.25%, w/v) in a buffer containing 40 % (v/v) glycerol and 50 mM Tris–HCl (pH 7.5). The solution was mixed thoroughly until complete dissolution and stored at 4 °C until

use. The dye was added to samples prior to electrophoresis to increase sample density and to monitor the progress of migration during gel running.

(vi) PCR (Polymerase Chain Reaction) master mixture

Reaction Mixture	**Quantity (µL)**
PCR buffer (10x)	5.0 µL
dNTPs mixture	5.0 µL
Taq DNA polymerase	1.0 µL
Forward primer (20 p mol/ µL)	2.0 µL
Reverse primer (20 p mol/ µL)	2.0 µL
Sterile distilled water	31.0 µL
Template DNA (100 µg/1 µL)	2.0 µL
$MgCl_2$ (25mM)	2.0 µL
Total PCR mix volume	50.0 µL

(vii) PCR reaction scheme for 16s rRNA sequencing

Step	**Temperature (º C)**	**Duration**
I (Initial denaturation)	94	5 minutes
II (Denaturation)	94	1 minute
III (Annealing)	55	1 minute
IV (Extension)	72	1 minute 30 seconds
V (Final extension)	72	7 minutes
Holding	4	∞

(viii) Phosphate-Buffered Saline (PBS, 1X)

Sl. No.	**Ingredient**	**Composition per litre**
1.	Sodium chloride (NaCl)	8 g
2.	Potassium chloride (KCl)	0.2 g
3.	Disodium hydrogen phosphate (Na_2HPO_4)	1.44 g
4.	Potassium dihydrogen phosphate (KH_2PO_4)	0.24 g
5.	Distilled water	Adjusted to 1 L
6.	pH	7.4 ± 0.1

Preparation of PBS

To prepare PBS, 8 g of sodium chloride was dissolved with 0.2 g of potassium chloride, 1.44 g of disodium hydrogen phosphate, and 0.24 g of potassium dihydrogen phosphate in about 800 mL of distilled water. The pH was adjusted to 7.4 using HCl or NaOH if needed. Then, the volume was made up to 1 litre with distilled water and mixed thoroughly. The solution was sterilized by autoclaving at 121 °C for 15 minutes.

(ix) Crystal violet (0.1%) solution

To prepare 0.1% crystal violet solution, 1 g of crystal violet dye was dissolved in about 800 mL of distilled water with continuous stirring until fully dissolved. Then, the volume was adjusted to 1 litre with distilled water and mixed thoroughly. The solution was stored in a dark, tightly closed bottle at room temperature to prevent photodegradation.

(x) CAS reagent

Sl. No.	**Ingredient**	**Composition per litre**
1.	Chrome Azurol S (CAS)	60.5 mg
2.	Ferric chloride ($FeCl_3 \cdot 6H_2O$)	10 mg
3.	Hexadecyltrimethylammonium bromide (HDTMA / CTAB)	72.9 mg
4.	Distilled water	Adjusted to 1 L

Preparation of CAS reagent

To prepare CAS reagent, 60.5 mg of Chrome Azurol S was dissolved with 10 mg of ferric chloride in 50 mL of distilled water. In a separate container, 72.9 mg of HDTMA (CTAB) was dissolved in 40 mL of distilled water. Slowly HDTMA solution was mixed with the CAS–$FeCl_3$ solution while stirring. The final volume was adjusted to 100 mL with distilled water. The solution was stored in a dark bottle at room temperature.

(xi) Preparation of 1mM silver nitrate ($AgNO_3$) solution

To prepare 1 mM $AgNO_3$ solution, 0.1699 g of silver nitrate was dissolved in approximately 800 mL of distilled water with stirring until fully dissolved. The volume

was made up to 1 litre with distilled water and mixed thoroughly. The solution was stored in a brown (amber) bottle away from light to prevent photodecomposition.

(xii) Potassium pyrophosphate buffer

Sl. No.	Ingredient	Composition per litre
1.	Dipotassium hydrogen pyrophosphate ($K_2H_2P_2O_7$)	0.2 M (≈ 44.1 g)
2.	Potassium dihydrogen phosphate (KH_2PO_4)	0.2 M (≈ 27.6 g)
3.	Distilled water	Make up to 1 L
4.	pH	Adjusted to 7.8–8.0

Preparation of the Buffer

To prepare potassium pyrophosphate buffer, 44.1 g of $K_2H_2P_2O_7$ and 27.6 g of KH_2PO_4 was dissolved in about 800 mL of distilled water with stirring. The pH was adjusted to 7.8–8.0 using 1 M HCl or 1 M KOH as needed. Then, the volume was made up to 1 litre with distilled water and mixed thoroughly. The buffer was stored at room temperature or 4 °C for long-term use.

(xiii) Nessler's reagent

Sl. No.	Ingredient	Composition per litre
1.	Potassium iodide (KI)	10 g
2.	Mercuric chloride ($HgCl_2$)	2 g
3.	Sodium hydroxide (NaOH, 10%)	25 mL
4.	Distilled water	Adjusted to 1 L

Preparation of the Nessler's reagent

To prepare Nessler's reagent, first 2 g of mercuric chloride was dissolved in about 50 mL of distilled water. In a separate container, 10 g of potassium iodide was dissolved in 50 mL of distilled water. After that, the two solutions were mixed carefully; a brown precipitate may form initially. The precipitate was dissolved by adding 25 mL of 10% sodium hydroxide slowly with constant stirring. Then, the final

volume was made upto to 1 litre with distilled water, mixed thoroughly, and stored in a dark glass bottle at room temperature.

(xiv) Preparation of L-Tryphtophan (100 mg/mL)

To prepare a 100 mg/mL L-Tryptophan stock solution, at first 10 g of L-Tryptophan was weighed and dissolved it in approximately 80 mL of distilled water with constant stirring. If needed, the pH was adjusted to about 7.0 using 1 M NaOH or HCl to aid dissolution. The final volume was made up to 100 mL with distilled water and mixed thoroughly. Then, the solution was sterilized by filtration through a 0.22 µm membrane filter and store in an amber bottle at 4 °C to prevent degradation.

(xv) Salkowski reagent

Sl. No.	Ingredient	Composition per litre
1.	Concentrated Sulfuric Acid (H_2SO_4)	50 mL
2.	Ferric chloride ($FeCl_3$) solution (0.5 M)	1 mL
3.	Distilled water	Adjusted to 1 L

Preparation of the reagent

Salkowski reagent was prepared by carefully adding 50 mL of concentrated sulfuric acid to about 950 mL of distilled water with constant stirring (acid to water). Then, 1 mL of 0.5 M ferric chloride solution was added slowly with mixing. The reagent was stored in a dark, tightly closed bottle at room temperature.

(xvi) MTT reagent

Sl. No.	Ingredient	Final concentration / Notes
1.	MTT powder	5 mg/mL in PBS or culture medium (without phenol red)
2.	Phosphate-buffered saline (PBS) or cell culture medium	Adjusted to desired volume
3.	Storage	Protect from light; store at 4 °C

Preparation of the reagent

To prepare MTT reagent, 50 mg of MTT powder was weighed and dissolved in 10 mL of sterile PBS to make a 5 mg/mL solution. It was mixed gently until fully

dissolved. The solution was filter sterilized using a 0.22 µm membrane filter if required. The reagent was stored at 4 °C for short-term use (usually up to 1–2 weeks).

(xvii) Hydrogen peroxide solution for catalase test

3 % hydrogen peroxide solution: 3 mL of 30 % (v/v) H_2O_2 in 27 mL of distilled water.

(xviii) Molisch's reagent for carbohydrate test

Molisch's test is a universal assay for all carbohydrates. Molisch's reagent is prepared by dissolving 3.75 g of α-naphthol in 99 % (v/v) ethanol. Concentrated sulfuric acid converts the specified carbohydrate into furfural or its derivatives.

B. *Microbiological media*

(i) Composition of Luria Bertani Broth medium

Sl. No.	Ingredient	Composition per litre
1.	Tryptone	10 g
2.	Yeast extract	5 g
3.	Sodium chloride	10 g
4.	Distilled water	Adjusted to 1 L

Preparation of the medium:

Luria–Bertani broth was prepared by dissolving 10 g of tryptone, 5 g of yeast extract, and 10 g of sodium chloride in approximately 800 mL of distilled water. The solution was mixed thoroughly, the volume was made up to 1 litre with distilled water, and the pH was adjusted to 7.0 if required. The medium was then sterilized by autoclaving at 121 °C for 15 minutes and allowed to cool before use.

(ii) Composition of Luria Bertani Agar

Sl. No.	Ingredient	Composition per litre
1.	Tryptone	10 g
2.	Yeast extract	5 g
3.	Sodium chloride	10 g
4.	Agar	15 g
5.	Distilled water	Adjusted to 1 L

Preparation of the medium:

Luria–Bertani agar was prepared by dissolving 10 g of tryptone, 5 g of yeast extract, 10 g of sodium chloride, and 15 g of agar in about 800 mL of distilled water with continuous heating and stirring. The volume was adjusted to 1 litre with distilled water and the pH was set to 7.0 if required. The medium was sterilized by autoclaving at 121 °C for 15 minutes, cooled to about 45–50 °C, and then poured into sterile Petri plates under aseptic conditions.

(iii) Composition of Nutrient Broth medium

Sl. No.	Ingredient	Composition per litre
1.	Peptone	5 g
2.	Beef extract	3 g
3.	Sodium chloride	5 g
4.	Distilled water	Adjusted to 1 L

Preparation of the medium:

Nutrient broth was prepared by dissolving 5 g of peptone, 3 g of beef extract, and 5 g of sodium chloride in approximately 800 mL of distilled water with gentle heating and stirring. The volume was adjusted to 1 litre with distilled water and the pH was adjusted to 7.2–7.4 if required. The medium was then sterilized by autoclaving at 121 °C for 15 minutes and cooled before use.

(iv) Composition of Mueller–Hinton (MH) agar

Sl. No.	Ingredient	Composition per litre
1.	Beef extract	2 g
2.	Acid hydrolysate of casein	17.5 g
3.	Starch	1.5 g
4.	Agar	17 g
5.	Distilled water	Adjusted to 1 L

Preparation of MH agar

MH agar was prepared by dissolving beef extract, acid hydrolysate of casein, starch, and agar in approximately 900 mL of distilled water with continuous stirring. The pH was adjusted to 7.3 ± 0.1 if needed. The volume was made up to 1 litre with

distilled water. The medium was sterilized by autoclaving at 121 °C for 15 minutes, cooled to about 45–50 °C, and poured into sterile Petri plates under aseptic conditions. Plates were allowed to solidify and stored at 4 °C until use.

(v) Composition of Tryptic Soy Broth (TSB)

Sl. No.	Ingredient	Composition per litre
1.	Tryptone	17 g
2.	Soy peptone	3 g
3.	Dextrose (glucose)	2.5 g
4.	Sodium chloride (NaCl)	5 g
5.	Dipotassium phosphate (K_2HPO_4)	2.5 g
6.	Distilled water	Adjusted to 1 L

Preparation of TSB

Tryptic Soy Broth was prepared by dissolving tryptone, soy peptone, dextrose, sodium chloride, and dipotassium phosphate in approximately 800 mL of distilled water with continuous stirring. The volume is then adjusted to 1 litre with distilled water. The pH was checked and adjusted to 7.3 ± 0.2 if necessary. The medium was sterilized by autoclaving at 121 °C for 15 minutes and cooled before use.

(vi) Composition of peptone broth

Sl. No.	Ingredient	Composition per litre
1.	Peptone	10 g
2.	Sodium chloride (NaCl)	5 g
3.	Distilled water	Adjusted to 1 L
4.	pH	7.0–7.2

Preparation of the peptone broth medium

Peptone broth was prepared by dissolving 10 g of peptone and 5 g of sodium chloride in approximately 800 mL of distilled water with gentle stirring. The pH was adjusted to 7.0–7.2 if required. The volume was then made up to 1 litre with distilled water and mixed thoroughly. The medium was sterilized by autoclaving at 121 °C for 15 minutes and allowed to cool before use.

(vii) Indole Test (Tryptone Broth)

Sl. No.	Ingredients	Composition per litre
1	Tryptone	10
2	Sodium Chloride	5

Preparation of the medium

Each component was dissolved in distilled water, and the final volume was set up to 1 L. The medium underwent sterilization via autoclaving at 121 °C for 15 minutes. After incubating the test organisms, Kovac's reagent was introduced to identify indole production.

(viii) Methyl Red (MR) Test

Sl. No.	Ingredients	Composition per litre
1	Peptone	7
2	Glucose	5
3	Dipotassium phosphate	5

Preparation of the medium

Each component was solubilized in distilled water, and the final volume was set up to 1 litre. The medium underwent sterilization *via.,* autoclaving at 121 °C for 15 minutes. After incubating the test organisms, methyl red indicator solution was introduced, which was made by dissolving 0.04 g of methyl red in 300 mL of 95 % (v/v) ethanol and thereafter diluting to a final volume of 500 mL with distilled water.

(ix) Voges–Proskauer (MR–VP) Medium

Sl. No.	Ingredients	Composition per litre
1	Peptone	7
2	Glucose	5
3	Dipotassium phosphate	5

Preparation of the medium

Each component was solubilized in distilled water, and the final volume was set to 1 litre. The medium underwent sterilization via autoclaving at 121 °C for 15 minutes. In the Voges–Proskauer (VP) test, after incubation, Barritt's reagents were introduced: Reagent A, consisting of 5 g of α-naphthol dissolved in 100 mL of pure ethanol, and Reagent B, comprising 40 g of potassium hydroxide dissolved in 100 mL of distilled water.

(x) Citrate Utilization Medium (Simmons' Citrate Agar)

Sl. No.	Ingredients	Composition per litre
1	Sodium citrate	2
2	Ammonium dihydrogen phosphate	1
3	Dipotassium phosphate	1
4	Sodium chloride	5
5	Magnesium sulfate	0.2
6	Bromothymol blue	0.08
7	Agar	15

Preparation of the medium

Each component was solubilized in distilled water, and the final volume was set up to 1 litre. The pH of the medium was calibrated to 6.9 ± 0.2, and the media was sterilized using autoclaving at 121 °C for 15 minutes. The liquid was thereafter dispensed into tubes and permitted to harden at an inclined angle.

(xi) Motility Test Medium

Sl. No.	Ingredients	Composition per litre
1	Peptone	10
2	Sodium Chloride	5
3	Agar	4
4	pH	± 0.2

Preparation of the medium

Each component was solubilized in distilled water, and the final volume was set up to 1 litre. The pH of the media was modified to 7.3 ± 0.2. The produced medium was subsequently sterilized *via.,* autoclaving at 121 °C for 15 minutes. The medium was formulated as a semi-solid to enable the movement of motile bacteria.

(xii) Hydrogen Sulfide (H_2S) Test — SIM Medium

Sl. No.	Ingredients	Composition per litre
1	Peptone	30
2	Beef extract	3
3	Ferrous ammonium sulfate	0.2
4	Sodium thiosulfate	0.025
5	Agar	3

Preparation of the medium

Each component was solubilized in distilled water, and the final volume was set up to 1 litre. The medium's pH was calibrated at 7.3 ± 0.2 and sterilized using autoclaving at 121 °C for 15 minutes. The SIM medium was formulated as a semi-solid to facilitate concurrent assessment of hydrogen sulfide generation, indole synthesis, and motility.

APPENDIX-II

ABBREVIATIONS AND DATA

I. Abbreviations of units/symbols

Sl No.	Units/symbols	Abbreviations
1	g	Gram
2	mL	Millilitres
3	±	Plus–Minus Sign
4	rpm	Revolutions Per Minute
5	w/v	Weight Per Volume
6	mg	Milligrams
7	N	Normal
8	%	Percentage
9	°C	Degree Centigrade
10	cm	Centimetre
11	µL	Microliter
12	µm	Micrometre
13	µg/L	Microgram Per Litre
14	X	Multiplication
15	+	Addition
16	=	Equals
17	kg/ha	Kilogram Per Hectare
18	v/cm	Volts Per Centimeter
19	ppm	Parts Per Million
20	v/v	Volume Per Volume
21	U/mL	Units Per Millilitre
22	U/mg	Units Per Milligram
23	bp	Base Pairs
24	≤	Less Than Equals To
25	HM	Heavy Metal
26	EPS	Exopolysaccharides
27	SOD	Superoxide Dismutase
28	MDA	Malondialdehyde
29	GR	Glutathione Reductase
30	GPx	Glutathione Peroxidase
31	CAT	Catalase
32	MBPs	Metal Binding Proteins
33	SDGs	Sustainable Development Goals
34	GM	Genetically Modified
35	As	Arsenic
36	Cd	Cadmium
37	Pb	Lead
38	Hg	Mercury
39	Cr	Chromium
40	Ni	Nickel

II. FASTA sequence of *Lysinibacillus* sp. strain AS3 (16s rRNA sequencing)

>OQ202230.1 Lysinibacillus sp. strain AS3 16S ribosomal RNA gene, partial sequence

TTTTGTTCGTGGAAGGGGAGTACCAGATACCTGCAAGTCGTGCGAAGCGT
AGCCAAGTAACTTGCTCCTTTGACGTTAGGCGGCGGACGGGTGAGTAACA
CGTGGGCAACCTACCTTATAGTTTGGGATAACTCCGGGAAACCGGGGCTA
ATACCGAATAATCTGTTTCACCTCATGGTGAAATATTGAAAGACGGTTTCG
GCTGTCGCTATAGGATGGGCCCGCGGCGCATTAGCTAGTTGGTGAGGTAAC
GGCTCACCAAGGCGACGATGCGTAGCCGACCTGAGAGGGTGATCGGCCA
CACTGGGACTGAGACACGGCCCAGACTCCTACGGGAGGCAGCAGTAGGG
AATCTTCCACAATGGGCGAAAGCCTGATGGAGCAACGCCGCGTGAGTGAA
GAAGGATTTCGGTTCGTAAAACTCTGTTGTAAGGGAAGAACAAGTACAGT
AGTAACTGGCTGTACCTTGACGGTACCTTATTAGAAAGCCACGGCTAACTA
CGTGCCAGCAGCCGCGGTAATACGTAGGTGGCAAGCGTTGTCCGGAATTA
TTGGGCGTAAAGCGCGCGCAGGTGGTTTCTTAAGTCTGATGTGAAAGCCC
ACGGCTCAACCGTGGAGGGTCATTGGAAACTGGGAGACTTGAGTGCAGA
AGAGGATAGTGGAATTCCAAGTGTAGCGGTGAAATGCGTAGAGATTTGGA
GGAACACCAGTGGCGAAGGCGACTATCTGGTCTGTAACTGACACTGAGGC
GCGAAAGCGTGGGGAGCAAACAGGATTAGATACCCTGGTAGTCCACGCCG
TAAACG

III. FASTA sequence of *Lysinibacillus* sp. strain AS4 (16s rRNA sequencing)

>OQ202231.1 Lysinibacillus sp. strain AS4 16S ribosomal RNA gene, partial sequence

TTTTTTTGATGCGGCCTTGCATGATACGTGGCAAGGTCGAGCGAAGCGATA
GCCAAGTAACTTGCTCCTTCGGACGTTAGCGGCGGACGGGTGAGTAACAC
GTGGGCAACCTACCTTATAGTTTGGGATAACTCCGGGAAACCGGGGCTAAT
ACCGAATAATCTGTTTCACCTCATGGTGAAACACTGAAAGACGGTTTCGG
CTGTCGCTATAGGATGGGCCCGCGGCGCATTAGCTAGTTGGTGAGGTAACG
GCTCACCAAGGCGACGATGCGTAGCCGACCTGAGAGGGTGATCGGCCAC
ACTGGGACTGAGACACGGCCCAGACTCCTACGGGAGGCAGCAGTAGGGA
ATCTTCCACAATGGGCGAAAGCCTGATGGAGCAACGCCGCGTGAGTGAAG
AAGGATTTCGGTTCGTAAAACTCTGTTGTAAGGGAAGAACAAGTACAGTA

GTAACTGGCTGTACCTTGACGGTACCTTATTAGAAAGCCACGGCTAACTAC
GTGCCAGCAGCCGCGGTAATACGTAGGTGGCAAGCGTTGTCCGGAATTATT
GGGCGTAAAGCGCGCGCAGGTGGTTTCTTAAGTCTGATGTGAAAGCCCAC
GGCTCAACCGTGGAGGGTCATTGGAAACTGGGAGACTTGAGTGCAGAAA
AGGATAGTGGAATTCCAAGTGTAGCGGTGAAATGCGTAGAGATTTGAGGA
ACACCAGTGGCGAAGGCGACTGTCTGGTCTGTAACTGACACTGAGGCGC
GAAAGCGTGGGGAGCAAACAGGAT

IV. List of databases, tools and software used

Sl. No.	Name of Tools/Software
1.	NCBI BLAST
2.	MEGA software (version 11.0)
3.	Origin 2021
4.	Microsoft Excel 2021
5.	Microsoft PowerPoint 2021
6.	SPSS
7.	Google Earth Pro Version 7.3
8	https://scholar.google.com/

APPENDIX-III

LIST OF PUBLICATIONS

List of Paper Publications/Book Chapters

a) Paper published as first author

1. **Gogoi**, **B**., Bharali, P. and Paul, A., 2025. Unveiling the Plant Growth-Promoting Potential of an Arsenic-Resistant Isolate: A Natural Ally for Sustainable Agriculture. Environment and Ecology, 43(2), pp.475-488.

2. **Gogoi**, **B**., Bharali, P., Ramachandran, D., Hazarika, B. and Debnath, P., 2025. Isolation and Characterization of an Arsenic-Resistant Bacterial Strain from Changki, Nagaland. *Nature Environment and Pollution Technology*, *24*(4), pp.1-14.

3. **Gogoi**, **B**., Acharjee, S.A., Bharali, P., Sorhie, V. and Walling, B., 2024. A critical review on the ecotoxicity of heavy metal on multispecies in global context: A bibliometric analysis. *Environmental Research*, *248*, p.118280.

b) Paper published as co-author

1. Acharjee, S.A., Bharali, P., Ramachandran, D., Kanagasabai, V., Hazarika, S., Koch, P.J., Dutta, N., Maadurshni, G.B., Manivannan, J., Kumari, S. and **Gogoi**, **B**., 2025. Bacterial cell factories for sustainable production of green polyesters using saccharides: unlocking the potential to mitigate microplastic pollution. *Journal of Polymer Research*, *32*(7), pp.1-22.

2. Walling, B., Borah, A., Hazarika, S., Bharali, P., Ramachandran, D., Kanagasabai, V., Dutta, N., Maadurshni, G.B., Manivannan, J., Mudoi, P. and Kaman, P.K., Sorhie, V., **Gogoi**, **B**., Alemtoshi, Acharjee, S.A., Vishwakarma, V., and Nath, P.D., 2025. Production of bacterial nanocellulose as green adsorbent matrix using distillery wastes for dye removal: a combined approach for waste management and pollution mitigation. *Biomass Conversion and Biorefinery*, *15*(5), pp.7265-7281.

3. Walling, B., Bharali, P., Ramachandran, D., Kanagasabai, V., Dutta, N., Hazarika, S., Maadurshni, G.B., Manivannan, J., Kumari, S., Acharjee, S.A. and **Gogoi**, **B**., 2024. Bacterial valorization of agricultural-waste into a nano-sized cellulosic matrix for mitigating emerging pharmaceutical pollutants: An eco-benign approach. *International Journal of Biological Macromolecules*, *277*, p.133684.

4. Acharjee, S.A., Bharali, P., Ramachandran, D., Kanagasabai, V., **Gogoi**, **B**., M., Hazarika, S., Koch, P.J., Dutta, N., Maadurshni, G.B., Manivannan, J. and Kumari, S.,

2024. Polyhydroxybutyrate (PHB)-Based sustainable bioplastic derived from Bacillus sp. KE4 isolated from kitchen waste effluent. *Sustainable Chemistry and Pharmacy*, *39*, p.101507.

5. Acharjee, S.A., **Gogoi**, **B**., Bharali, P., Sorhie, V. and Alemtoshi, B.W., 2024. Recent trends in the development of Polyhydroxyalkanoates (PHAs) based biocomposites by blending with different bio-based polymers. *Journal of Polymer Research*, *31*(4), p.98.

6. Boro, B., Boruah, J.S., Devi, C., **Gogoi**, **B**., Bharali, P., Reddy, P.V.B., Chowdhury, D. and Kalita, P., 2024. A novel route to fabricate ZnO nanoparticles using Xanthium indicum ethanolic leaf extract: Green nanosynthesis perspective towards photocatalytic and biological applications. *Journal of Molecular Structure*, *1300*, p.137227.

7. Bharali, P., **Gogoi**, **B**., Sorhie, V., Acharjee, S.A., Walling, B., Alemtoshi, Vishwakarma, V. and Shah, M.P., 2024. Autochthonous psychrophilic hydrocarbonoclastic bacteria and its ecological function in contaminated cold environments. *Biodegradation*, *35*(1), pp.1-46.

8. Kulnu, A.S., Acharjee, S.A., Humtsoe, R.N., Kuotsu, R., Limasenla, Walling, B., Bharali, P., Alemtoshi, **Gogoi**, **B**. and Sorhie, V., 2024. Ethnoecological insights on wild fodder bioresources and their geospatial perspectives on sustainable piggery in Wokha and Zunheboto districts of Nagaland, India. *Genetic Resources and Crop Evolution*, *71*(2), pp.691-720.

9. Walling, B., Bharali, P., Giridharan, B., **Gogoi**, **B**., Sorhie, V. and Mani, S.K., 2023. Bacterial nanocellulose: A novel nanostructured bio-adsorbent for green remediation technology. *Acta Ecologica Sinica*, *43*(6), pp.946-967.

10. Walling, B., Bharali, P., Ramachandran, D., Viswanathan, K., Hazarika, S., Dutta, N., Mudoi, P., Manivannan, J., Kamath, S.M., Kumari, S. .., **Gogoi**, **B**., and Vishwakarma, V., 2023. In-situ biofabrication of bacterial nanocellulose (BNC)/graphene oxide (GO) nano-biocomposite and study of its cationic dyes adsorption properties. *International Journal of Biological Macromolecules*, *251*, p.126309.

11. Acharjee, S.A., Bharali, P., **Gogoi**, B., Sorhie, V., Walling, B. and Alemtoshi, 2023. PHA-based bioplastic: a potential alternative to address microplastic pollution. *Water, Air, & Soil Pollution*, *234*(1), p.21.

c) Book chapter published as first author

1. **Gogoi**, **B**., Bharali, P., Sorhie, V. and Rudithongru, L., 2023. An Understanding of the Underlying Mechanisms Involved in the Bacterial Remediation of Arsenic, Cadmium, and Lead. In *Biohydrometallurgical Processes* (pp. 130-154). CRC Press.
2. **Gogoi**, **B**., Bharali, P., Walling, B., Acharjee, S.A. and Vishwakarma, V., 2025. An insight into the ecological toxicity triggered by anthropogenically driven heavy metal micropollutants on biotic community. *Development in Waste Water Treatment Research and Processes*, pp.615-632.
3. **Gogoi**, **B**. and Bharali, P., 2025. Nature's Cleanup Crew: Microbial Innovations in Bioremediation. In *Global Perspectives of Toxic Metals in Bio Environs: Volume 2: Biotransformation, Remediation and Technological Advances* (pp. 161-190). Cham: Springer Nature Switzerland.

d) Book chapter published as co-author

1. Sudharsan, P., Vijayakumar, T.S., Bupesh, G., **Gogoi**, **B**. and Mathiyazhagan, M., 2023. Employment of Phytal Mediated Metallic Nanoparticles for the Effective Remediation of Wastewater Particulates. *Wastewater Treatment Using Green Synthesis*, pp.153-160.
2. Bharali, P., **Gogoi**, **B**. and Giridharan, B., 2022. Psychrophiles survival strategies: insights into the comprehensive adaptive behavioral approaches in cold-habituated bacteria. *Extremophiles: A Paradox of Nature with Biotechnological Implications*, *1*, p.197.

e) <u>Patents</u>

1. **Patent Office, Government of India**

   Patent Title: Polyhydroxybutyrate (PHB)-based Sustainable Bioplastic derived from *Bacillus* sp. KE4 isolated from kitchen waste effluent

   Patent no: 568503

   Application no: 202431045242

   Date of filing: 12/06/2024

   Name of Inventor: Shiva Aley Acharjee, Pranjal Bharali, Bendangtula Walling, **Bhagyudoy Gogoi**, Viphrezolie Sorhie, Alemtoshi

2. Patent Application Publication: India

Application no: 202431045240 A

Date of filing: 12/06/2024

Publication date: 21/06/2024

Patent Title: Bacterial Nanocellulose Green Adsorbent matrix using Distillery wastes for Dye removal and Waste Management

Name of Inventor: Bendangtula Walling, Pranjal Bharali, Shiva Aley Acharjee, **Bhagyudoy Gogoi**, Alemtoshi, Viphrezolie Sorhie

3. Patent Application Publication: India

Application no: 202431049557 A

Date of filing: 28/06/2024

Publication date: 05/07/2024

Patent Title: Bio-fabrication of Bacterial Nanocellulose (BNC)/ Graphene Oxide (GO) Nano- Biocomposite

Name of Inventor: Bendangtula Walling, Pranjal Bharali, Shiva Aley Acharjee, **Bhagyudoy Gogoi**, Alemtoshi, Viphrezolie Sorhie

Prepublished copy

Nature Environment & Pollution Technology

This is a peer-reviewed prepublished version of the paper

Isolation and Characterization of an Arsenic Resistant Bacterial Strain from Changki, Nagaland

Bhagyudoy Gogoi[1], Pranjal Bharali[1], D. Ramachandran[2], Bhrigupoti Hazarika[3] and Palash Debnath[4]

[1]Applied Environmental Microbial Biotechnology Laboratory, Department of Environmental Science, Nagaland University, Lumami, Zunheboto-798627, Nagaland, India;

[2]Centre for Nanoscience & Nanotechnology, Sathyabama Institute of Science and Technology, Jeppiaar Nagar, Rajiv Gandhi Road, Chennai-600119, Tamil Nadu, India;

[3]Department of Life Science & Bioinformatics, Assam University, Diphu Campus, Diphu-782462, Assam, India;

[4]Department of Plant Pathology, Assam Agricultural University, Jorhat-785013, Assam, India

†Corresponding author: Dr. Pranjal Bharali; prangenetu@gmail.com

Bhagyudoy Gogoi: https://orcid.org/0000-0003-4159-9008; Pranjal Bharali: https://orcid.org/0000-0001-5657-8993; D. Ramachandran: https://orcid.org/0000-0002-9302-3820; Bhrigupoti Hazarika: https://orcid.org/0009-0005-9195-7418 ; Palash Debnath: https://orcid.org/0000-0002-7225-5497

Key Words	Heavy metal, Arsenic, Resistant, Bacterium, Nagaland, Bioremediation
DOI	https://doi.org/10.46488/NEPT.2025.v24i04.B4310 (DOI will be active only after the final publication of the paper)
Citation for the Paper	Gogoi, B., Bharali, P., Ramachandran, D., Hazarika, B. and Debnath, P., 2025. Isolation and characterization of an arsenic resistant bacterial strain from Changki, Nagaland. *Nature Environment and Pollution Technology*, 24(4), p. B4310. https://doi.org/10.46488/NEPT.2025.v24i04.B4310

ABSTRACT

The present study focused on isolating arsenic (As) resistant bacteria from acid mine tailings of Changki, Nagaland and evaluating their bioremediation potential. The isolation was performed using enrichment culture approach and was further characterized using standard procedures. The obtained bacterial strain AS3 was found to be resistant to As^{3+} and As^{5+} ions up to 1562 µg/mL and 125000 µg/mL, respectively. The 16S rRNA gene sequence of the strain was found to be identical to Lysinibacillus sp. The growth behaviour of the strain in the presence of selected heavy-metals (HMs) showed a prolonged lag phase, especially in As^{5+}. Moreover, the strain appeared to be resistant to several antibiotics. SEM and EDX analyses, revealed the presence of HM ions on the outer surface of AS3 strain. Available functional groups on the surface of the AS3 strain cells engaged in the metal-binding process were identified using FTIR, suggesting their active participation in adsorption. AAS showed that the strain had the potential to remove As^{3+} and As^{5+} ions with removal efficiencies of 99.94% and 99.49% respectively. Based on the findings, strain exhibits intriguing biotechnological potential for HM bioremediation.

Environment and Ecology 43 (2) : 475—488, April—June 2025
Article DOI: https://doi.org/10.60151/envec/NUBN8247
ISSN 0970-0420

Unveiling the Plant Growth-Promoting Potential of an Arsenic-Resistant Isolate: A Natural Ally for Sustainable Agriculture

Bhagyudoy Gogoi, Pranjal Bharali, Asosii Paul

Received 16 March 2025, Accepted 25 April 2025, Published on 30 May 2025

ABSTRACT

This study utilizes a bacterial strain, *Lysinibacillus* sp. AS3 which was previously found resistant to arsenic (As). The strain was studied for exopolysaccharides (EPS), biofilm, siderophore, Indole-3-acetic acid (IAA) producing ability in presence of arsenate (As^{5+}) and arsenite (As^{3+}) heavy metal (HM) ions, which would help to determine its plant growth promoting activity. The study was done through both qualitative and quantitative assessment to observe the significant changes in exposure to As HMs. Moreover, phytotoxicity assay was performed on *Vigna radiata* seeds in presence of the both the HM ions. The results indicated enhanced production of biofilm, IAA and EPS in presence of both HM ions. While, reduced production of siderophore was recorded in presence of As^{3+} HM ions. Further, it was observed that employing AS3 strain on *V. radiata* seeds showed stimulating effect on the growth of the seedlings albeit arsenic stress, along with enhanced growth of the seedlings as compared to control. Thus, present study shows that this AS3 strain could be a potent strain in agriculture applications.

Keywords Heavy metal, Arsenic, Bacterium, Siderophore, Bioremediation, Exopolysaccharides (EPS), Biofilm.

Bhagyudoy Gogoi[1], Pranjal Bharali[2]*, Asosii Paul[3]

[1,2]Assistant Professor

[1,2]Applied Environmental Microbial Biotechnology Laboratory, Department of Environmental Science, Nagaland University, Head quarter-Lumami, Zunheboto 798627, Nagaland, India

[3]Department of Botany, Nagaland University, Head quarter-Lumami, Zunheboto 798627, Nagaland, India

Email: pranganetu@gmail.com
*Corresponding author

INTRODUCTION

Arsenic (As) contamination is a persistent environmental issue affecting globally humans, plants animals and microbes. This metalloid, once if it enters into the ecosystems through human activity or natural origins can cause significant damages to biological functions in different living organisms (Fatoki and Badmus 2022). In plants, it is often reported to hinder useful biochemical pathways (Martínez-Castillo *et al.* 2022), reduced growth and development (Emamverdian *et al.* 2023) or induce oxidative stress (Sharma 2012). While, in humans chronic exposure to arsenic can been to cause severe health issues such as cancer and damages to the organs (Speer *et al.* 2023). Addressing arsenic pollution, requires human interventions and among many techniques to tackle as pollution, utilizing arsenic-resistant bacterial isolates

क्रम सं/SL No :0331388031

INTELLECTUAL PROPERTY INDIA

पेटेंट कार्यालय,भारत सरकार
पेटेंट प्रमाण पत्र |
(पेटेंट नियमावली का नियम 74)

The Patent Office, Government Of India
Patent Certificate
(Rule 74 of The Patents Rules)

पेटेंट सं. / Patent No.	:	568503
आवेदन सं. / Application No.	:	202431045242
फाइल करने की तारीख / Date of Filing	:	12/06/2024
पेटेंटी / Patentee	:	Nagaland University
आविष्कारकों का नाम /Name of Inventor(s)	:	1.Shiva Aley Acharjee 2.Pranjal Bharali 3.Bendangtula Walling 4.Bhagyudoy Gogoi 5.Viphrezolie Sorhie 6.Alemtoshi

प्रमाणित किया जाता है कि पेटेंटी को, उपरोक्त आवेदन में यथाप्रकटित *Polyhydroxybutyrate (PHB)-based Sustainable Bioplastic derived from Bacillus sp. KE4 isolated from kitchen waste effluent* नामक आविष्कार के लिए, पेटेंट अधिनियम, 1970 के उपबंधों के अनुसार आज तारीख जून 2024 के बारहवें दिन से बीस वर्ष की अवधि के लिए पेटेंट अनुदत्त किया गया है।

It is hereby certified that a patent has been granted to the patentee for an invention entitled *Polyhydroxybutyrate (PHB)-based Sustainable Bioplastic derived from Bacillus sp. KE4 isolated from kitchen waste effluent* as disclosed in the above mentioned application for the term of 20 years from the 12th day of June 2024 in accordance with the provisions of the Patents Act,1970.

अनुदान की तारीख : 08/07/2025
Date of Grant :

पेटेंट नियंत्रक
Controller of Patents

टिप्पणी - इस पेटेंट के नवीकरण के लिए फीस, यदि इसे बनाए रखा जाना है, जून 2026 के बारहवें दिन को और उसके पश्चात प्रत्येक वर्ष में उसी दिन देय होगी।

Note. - The fees for renewal of this patent, if it is to be maintained, will fall / has fallen due on 12th day of June 2026 and on the same day in every year thereafter.

(12) PATENT APPLICATION PUBLICATION
(19) INDIA
(22) Date of filing of Application :12/06/2024

(21) Application No.202431045240 A
(43) Publication Date : 21/06/2024

(54) Title of the invention : Bacterial Nanocellulose Green Adsorbent Matrix using Distillery Wastes for Dye Removal and Waste Management

(51) International classification :C02F1/28, C12P19/04, B01J20/24, B01J20/30
(86) International Application No :NA
Filing Date :NA
(87) International Publication No : NA
(61) Patent of Addition to Application Number :NA
Filing Date :NA
(62) Divisional to Application Number :NA
Filing Date :NA

(71)**Name of Applicant :**
1)Nagaland University
Address of Applicant :Nagaland University, Lumami, Zunheboto-798627, Nagaland, India Zunheboto ---------- ----------
Name of Applicant : NA
Address of Applicant : NA
(72)**Name of Inventor :**
1)Bendangtula Walling
Address of Applicant :Applied Environmental Microbial Biotechnology Laboratory, Department of Environmental Science, Nagaland University, Lumami, Zunheboto-798627, Nagaland, India Zunheboto ---------- ----------
2)Pranjal Bharali
Address of Applicant :Applied Environmental Microbial Biotechnology Laboratory, Department of Environmental Science, Nagaland University, Lumami, Zunheboto-798627, Nagaland, India Zunheboto ---------- ----------
3)Shiva Aley Acharjee
Address of Applicant :Applied Environmental Microbial Biotechnology Laboratory, Department of Environmental Science, Nagaland University, Lumami, Zunheboto-798627, Nagaland, India Zunheboto ---------- ----------
4)Bhagyudoy Gogoi
Address of Applicant :Applied Environmental Microbial Biotechnology Laboratory, Department of Environmental Science, Nagaland University, Lumami, Zunheboto-798627, Nagaland, India Zunheboto ---------- ----------
5)Alemtoshi
Address of Applicant :Applied Environmental Microbial Biotechnology Laboratory, Department of Environmental Science, Nagaland University, Lumami, Zunheboto-798627, Nagaland, India Zunheboto ---------- ----------
6)Viphrezolie Sorhie
Address of Applicant :Applied Environmental Microbial Biotechnology Laboratory, Department of Environmental Science, Nagaland University, Lumami, Zunheboto-798627, Nagaland, India Zunheboto ---------- ----------

(57) Abstract :
The invention is usage of rice beer stillage as a carbon source to produce bacterial nanocellulose (BNC). A method of production of Bacterial Nanocellulose (BNC) comprising the steps of: preparation of carbon source from rice beer stillage; and production and purification of BNC. The BNC made using rice beer stillage has excellent thermostability (up to 380 °C), a dense nano-fibrous network with cellulose I type properties, and a high crystallinity index (86.23%). It demonstrated a high water-holding capacity (97.53 g g−1) and a robust tensile strength (68.044 MPa). BNC also demonstrated its recyclable nature by going through several cycles of sorption and desorption. According to this invention, waste distillery stillage may be efficiently used as a sustainable raw material to produce BNC that is safe for the environment and has a wide range of uses.

No. of Pages : 25 No. of Claims : 7

(12) PATENT APPLICATION PUBLICATION
(19) INDIA
(22) Date of filing of Application :28/06/2024

(21) Application No.202431049557 A
(43) Publication Date : 05/07/2024

(54) Title of the invention : Bio-fabrication of Bacterial Nano-Cellulose (BNC) /Graphene Oxide (GO) Nano-Biocomposite

(51) International classification :C02F0101300000, C12P0019040000, C02F0001280000, B01J0020280000, B01J0020260000
(86) International Application No :NA
Filing Date :NA
(87) International Publication No : NA
(61) Patent of Addition to Application Number :NA
Filing Date :NA
(62) Divisional to Application Number :NA
Filing Date :NA

(71)**Name of Applicant :**
1)Nagaland University
Address of Applicant :Nagaland University, Lumami Headquarters, Zunheboto district, Nagaland Zunheboto ---------- ----------
Name of Applicant : NA
Address of Applicant : NA
(72)**Name of Inventor :**
1)Bendangtula Walling
Address of Applicant :Applied Environmental Microbial Biotechnology Laboratory, Department of Environmental Science, Nagaland University, Lumami, Zunheboto-798627, Nagaland, India Zunheboto ---------- ----------
2)Pranjal Bharali
Address of Applicant :Applied Environmental Microbial Biotechnology Laboratory, Department of Environmental Science, Nagaland University, Lumami, Zunheboto-798627, Nagaland, India Zunheboto ---------- ----------
3)Shiva Aley Acharjee
Address of Applicant :Applied Environmental Microbial Biotechnology Laboratory, Department of Environmental Science, Nagaland University, Lumami, Zunheboto-798627, Nagaland, India Zunheboto ---------- ----------
4)Bhagyudoy Gogoi
Address of Applicant :Applied Environmental Microbial Biotechnology Laboratory, Department of Environmental Science, Nagaland University, Lumami, Zunheboto-798627, Nagaland, India Zunheboto ---------- ----------
5)Alemtoshi
Address of Applicant :Applied Environmental Microbial Biotechnology Laboratory, Department of Environmental Science, Nagaland University, Lumami, Zunheboto-798627, Nagaland, India Zunheboto ---------- ----------
6)Viphrezolie Sorhie
Address of Applicant :Applied Environmental Microbial Biotechnology Laboratory, Department of Environmental Science, Nagaland University, Lumami, Zunheboto-798627, Nagaland, India Zunheboto ---------- ----------

(57) Abstract :
In this invention, a time-dependent technique is used to synthesize Bacterial Nanocellulose/Graphene Oxide Nano-Biocomposites (BNC-GO-NBCs) by Komagataeibacter saccharivorans NUWB1. The dried BNC-GO-NBC exhibited great tensile strength (84.72 MPa), enhanced thermostability (up to 380°C), high crystallinity (74.21%), and a porous structure with embedded GO layers, according to physicochemical examination. A mesoporous structure with a significant adsorption capacity for cationic dyes is shown by the N2 adsorption-desorption isotherm. Additionally, the substance demonstrated the ability to regenerate and shown non-cytotoxic qualities in tests for oxidative stress, cell cytotoxicity, and antibacterial activity. These results point to BNC-GO-NBC's intriguing potential for environmental applications, including dye adsorption.

No. of Pages : 20 No. of Claims : 7

APPENDIX-IV

CONFERENCES/WORKSHOPS/SEMINARS

Lists of Conferences/Seminars/Webinars/Workshop Attended

(i) **Oral Presentations**:

1. Isolation and characterization of arsenite (As^{3+}) and arsenate (As^{5+}) resistant bacteria from Changki, Nagaland; "Interational Conference on "Bioresources and Bioeconomy (ICBB-2022)", Department of Botany, Nagaland University, HQ: Lumami, Nagaland, September 19-21, 2022.
2. Characterization of an arsenic resistant bacterial strain and its susceptibility against antibiotics; National Conference on "Reviving Traditional Knowledge for Biodiversity Conservation", Department of Zoology, Nagaland University, HQ: Lumami, Nagaland, 31st March, 2023.
3. Antibiotic susceptibility of an Arsenic Resistant Bacteria from Changki, Nagaland; International Conference on "Challenges and Prospects of Bioresource Conservation in Eastern Himalaya- with special reference to UN-Sustainable Development Goals", Department of Zoology, Gauhati University, Assam, India, 3-4 May, 2023.

(ii) Workshops webinar and certifications

1. Participated in the workshop 'Research Ethics, Paper Writing & IPR' organized by Department of Botany and Advance Level Institutional Biotech Hub, Nagaland University, Lumami on November 14-15, 2019.
2. Participated in the International Webinar on 'Application of Molecular and Bioinformatics tools in Crop Protection' organized by the Department of Plant Pathology, AAU, Jorhat on 1-3 March, 2021.
3. Completed E-Shodh Sindhu Web of Series Certification Series on June 15, 2020.

NMHS SPONSORED NATIONAL CONFERENCE
On REVIVING TRADITIONAL KNOWLEDGE FOR BIODIVERSITY CONSERVATION (RTKBC-23)

CERTIFICATE OF PARTICIPATION

This is to certify that Prof./Dr./Mr./Ms. Bhagyudoy Gogoi of Dept. of Environmental Science, NU, Lumami participated/presented a paper (Key Note Talk/Invited Talk/Presentation Talk) titled Characterization of an arsenic resistant bacterial strain and its susceptibility against antibiotics in the NMHS sponsored National Conference on "Reviving Traditional Knowledge for Biodiversity Conservation" organized by the Department of Zoology, Nagaland University, Lumami, Nagaland held on 31st March 2023.

Dr. Lobeno Mozhui
Organizing Secretary
RTKBC-2023

Prof. M. S. Rawat
Dean
School of Sciences

Prof. Bendang Ao
Convener
RTKBC-2023

International Conference on 'Bioresources & Bioeconomy' (ICBB-2022)
Organized By
Department of Botany, Nagaland University, Lumami 798627, Nagaland, India
In Collaboration With
Nagaland Forest Management Project, Department of Environment, Forest and Climate Change, Govt. of Nagaland, India.
September 19-21, 2022

CERTIFICATE OF PRESENTATION

This is to certify that

Mr./Miss/Dr. Bhagyudoy Gogoi of Nagaland University, India
has presented a paper (Oral/poster) titled
'Isolation and Characterization of Arsenite (As3+) and Arsenate (As5+) Resistant Bacteria from Changki, Nagaland'
in the ICBB-2022 organized by the Department of Botany, Nagaland University, Lumami 798627, Nagaland, India, held on September 19-21, 2022.

(Prof. M. S. Rawat)
Dean, School of Sciences

(Prof. Chitta Ranjan Deb)
Convener cum Organizing Secretary
ICBB-22

International Conference
on
Challenges & Prospects of Bioresource Conservation in Eastern Himalaya
-with special reference to UN-Sustainable Development Goals

Aaranyak

Certificate of Participation

This is to certify that

Prof./Dr./Mr./Ms. Bhagyudoy Gogoi

has successfully presented (Oral/ Poster)/ participated in the ***International Conference on Challenges & Prospects of Bioresource Conservation in Eastern Himalaya -with special reference to UN-Sustainable Development Goals*** held on 3-4 May, 2023 at Department of Zoology, Gauhati University, India. The Conference has been organized by the Department of Zoology, GU in collaboration with Pollution Control Board Assam, Assam Science Technology & Environmental Council, Aaranyak & Zoological Society of Assam.

Prof. Pratap Jyoti Handique
Vice Chancellor
Gauhati University

Prof. Jogen Chandra Kalita
President
ICCPBC

Dr. Malabika Kakati Saikia
Convenor
ICCPBC